

ECONOMIC GEOLOGY OF THE JONES CAMP
IRON DEPOSIT, SOCORRO COUNTY, NEW MEXICO

by

David A. Bickford

Submitted in Partial Fulfillment
of the Requirements for the Degree of
Master of Science in Geology

New Mexico Institute of Mining and Technology

Socorro, New Mexico

1980

ABSTRACT

The Jones Camp Iron Deposit occurs along the N75°W trending Jones Camp Dike. The petrology of the dike, a composite intrusive, varies from that of a quartz diorite to a granodiorite. It dips between 82°S and vertical, averages 575 feet (175 m) in width, and crops out for approximately 11 miles (17.7 km). A later pyroxene syenodiorite intrusive, referred to as a diabase, forms sills and dikes parallel with the Jones Camp Dike.

Magnetite mineralization of economic importance occurs as discrete pods along the length of the Jones Camp Dike. The distribution of these pods is controlled by zones of secondary permeability along the dike. The intrusion of diabase has enhanced secondary permeability along the dike, apparently causing concentration of ore in these areas during mineralizing events. As ore fluids migrated upward most of the ore was localized along favorable limestone-sandstone contacts in the Yeso Formation.

Results of a combined geological and geophysical analysis of the property indicate 1,117,940 tons of probable reserves and 1,575,630 tons of possible reserves.

A preliminary feasibility study of the deposits suggests that a profitable open pit mine can be operated on the property. Discounted Cash Flow Return on Investment (DCFROI) and payback period analyses indicate that a Return on Investment (ROI) of 40.29% and a payback period of 3.56 years may be achieved on an initial investment of \$3,000,000 as of spring 1980.

TABLE OF CONTENTS

	Page
Abstract	ii
List of Plates and Overlays.	v
List of Figures and Tables	vi
Acknowledgements	vii
Introduction	1
Methodology.	4
Geological	4
Geophysical.	5
Geologic Setting	7
Stratigraphy	10
Yeso Formation	10
Torres Member.	10
Cañas Member	11
Joyita Member.	11
Glorieta Formation	12
San Andres Formation	12
Igneous Rocks.	14
Jones Camp Dike.	14
Diabase.	15
Alteration	16
Mineralization	18
Mineralogy	18
Mode of Occurrence	18
Structure.	21
Folding.	23

Faulting	24
Geophysical Data	25
Characteristic Magnetic Anomalies of Rock Types in the Study Area	25
Magnetic Contour Maps.	27
Direction and Intensity of Remanent Magnetism.	29
Geologic Summary	30
Controls on Mineralization	30
Formation of the Deposit	37
Intrusion of the Jones Camp Dike	37
Geophysical Summary.	39
Interpretation Concepts.	39
Qualitative Analysis of the Magnetic Data.	45
Economic Geology	48
Grade and Tenor of the Ore	51
Ore Reserve Estimates.	51
References	53
Appendices	56
I - Total Field Magnetic Data	56
II - Preliminary Feasibility Study of the Jones Camp Deposit.	200
III - Thin Section Descriptions	218

LIST OF PLATES AND OVERLAYS

Plate	See Pocket
1) Geologic map of the Jones Camp Deposit (1:12,000)	"
2) Measured Sections.	"
3) Geologic map of the Section 17 Prospect (1:2400)	"
4) Geologic map of the Section 19 Prospect (1:2400)	"
Overlay	
1) Location of areas mapped at 1:2400 scale, and sites of previous mining activity	"
2) Location of magnetic profiles.	"
3) Magnetic contour map of profiles 1-66.	"
4) Magnetic contour map of profiles 65-112.	"
5) Magnetic contour map of filtered profiles 11-18.	"
6) Magnetic contour map of filtered profiles 91-112	"

LIST OF FIGURES AND TABLES

Figure	Page
1) Location of the Jones Camp Deposit, Socorro County, New Mexico.	2
2) Generalized stratigraphic column of Permian and Pennsylvanian sediments in eastern Socorro County, New Mexico.	8
3) Example of magnetite replacing limestone (thin section L-0).	19
4) Structural contour map of the study area and surrounding regions (after Kelley and Thompson, 1964)	22
5) Hand fitted approximation of the magnetic anomaly of the Jones Camp Dike.	26
6) Example of well developed magnetite anomaly	28
7) Chilled margin of a diabase intrusive (dark area) in contact with the Jones Camp Dike (thin section Db-11)	31
8) Schematic sketch of the convection cell model for the deposition of the Cornwell magnetite deposits (after Eugster and Chou, 1979)	32
9) Magnetite localized in faulted limestone beds near the Jones Camp Dike.	34
10) Range of magnetic susceptibilities (emu) for the Jones Camp Dike, the diabase, and magnetite ore	42
11) Examples of the variation of horizontal (ΔH), vertical (Δz), and total (ΔT) magnetic anomalies as a function of the dip and the direction of magnetism in the body (after Parasnis, 1971).	43
12) Generalized cross section across profile 59, showing the relationship of rock type and magnetic anomalies.	46
 Table	 Page
1) Summary of proposed drill hole lengths and dips for the Section 17 Prospect	49
2) Summary of proposed drill hole lengths for the Section 19 Prospect.	50

ACKNOWLEDGEMENTS

I would like to acknowledge the efforts of all the people who helped with this project, especially my thesis committee members, Dr. George Austin, Dr. Allan Sanford, and in particular Dr. Clay T. Smith for his endless patience.

I would also like to thank Mr. Ed Bottinelli and the Aweco Co. for their financial support.

INTRODUCTION

Economic grade magnetite mineralization is associated with diabasic intrusions in and along a N75°W striking quartz diorite-granodiorite dike in eastern Socorro County, New Mexico. The steeply dipping (82°S) dike is exposed over an 11 mile (17.7 km) length and averages 575 feet (175 m) in width. It constitutes a prominent geologic feature on Chupadera Mesa, approximately 7 miles (11.3 km) east of Bingham; the dike cuts sediments of the Lower Permian Yeso Formation in Sections 11-13 inclusive, T5S, R6E, Sections 14-18 inclusive, Sections 23, 24, T5S, R7E, and Sections 19, 29, 30, T5S, R8E New Mexico Base and Meridan (Fig. 1).

The Jones Camp occurrence offers an excellent opportunity for an integrated geophysical and geological study of the economic potential of the area. The present data suggest structural as well as stratigraphic controls on magnetite mineralization.

Access to the study area is possible on rough roads extending eastward from Bursum's Adobe Ranch headquarters or by following the old Socorro-Carrizozo highway eastward from U. S. Route 380 at Bingham, New Mexico (Fig. 1). The roads are passable for most vehicles but become difficult in wet weather; locally 4-wheel drive may be necessary to negotiate steep slopes.

The early history and descriptions of the prospect have been documented by Jones (1904), Keyes (1904), Emmens (1906), and more accurately by Lindgren (1908). Extensive trenching and sampling in the Jones Camp area by the U. S. Bureau of Mines (Grantham and Soule, 1947) was utilized by V. C. Kelley (1949) in his mapping and evaluation of the property.

Prior to the inception of production in 1964, Cleveland Cliffs Iron Co. drilled several holes in 1963, but records of the results are not

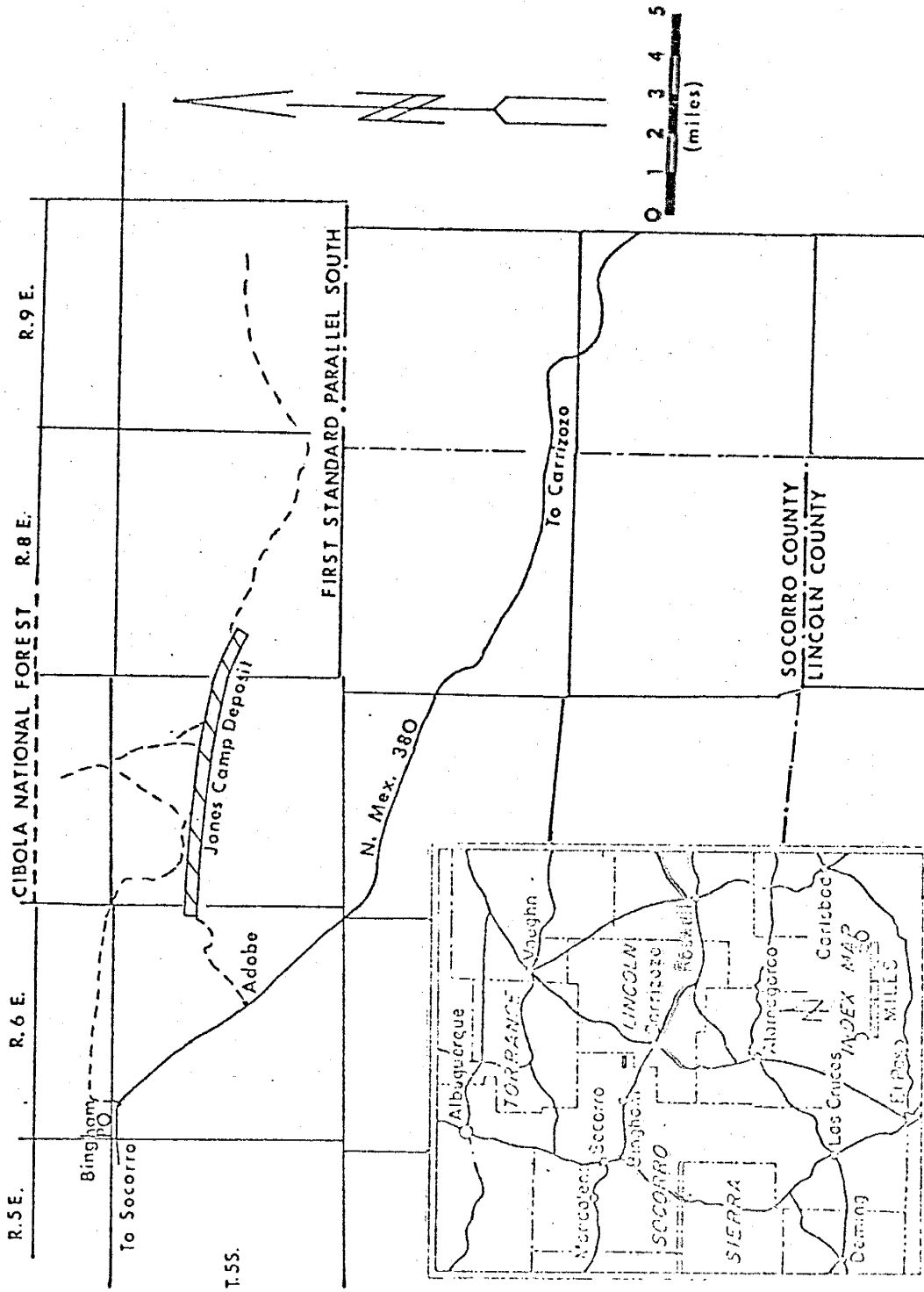


Figure 1. Location map of the Jones Camp Deposit, Socorro County, New Mexico.

available. Nogueira (1917) in an unpublished M.S. thesis studied the mineralogy and geochemistry of the deposit and supplemented Kelley's mapping (1949) with greater detail.

Kelley (1949) estimated 643,000 tons of probable and possible iron ore reserves for the 7000 feet of strike length along the dike sampled by the U. S. Bureau of Mines in Sections 14, 23, and 24, T5S, R7E. The 100,000 tons of production from 1964 to 1973 came from surface exposures and pits less than 35 feet deep and is confined to the area of Kelley's study (1949). In 1978 approximately 5000 tons were recovered from the East-pit area in Section 24, T5S, R7E (Clay T. Smith personal communication, 1979). Present production goals are 10,000 to 20,000 tons per month by 1982.

METHODOLOGY

Geological

Geologic data is plotted on enlarged portions of the U. S. Geological Survey 15' Bingham and Broken Back Crater Quadrangles at a scale of 1:12,000; Bureau of Land Management aerial photographs aided in geologic mapping. Detailed maps of two mineralized areas mapped using a plane table and telescopic alidade are plotted at a scale of 1:2400 (see overlay 1 for locations).

Stratigraphic units in the study area include the San Andres Formation, the Glorieta Formation, and the Torres, Cañas, and Joyita Members of the Yeso Formation. Three igneous rock types are also delineated. The first two are an undifferentiated diorite and a diabase (pyroxene syenodiorite). The third is a quartz diorite which is only recognized on the Section 19, 1:2400 map (plate 4).

A detailed well-exposed stratigraphic section (MS-1) was measured along the western slope of Chupadera Mesa three-quarters of a mile south of the study area. Three other, less detailed sections were measured within the study area (see plate 1 for the location of all measured sections).

Representative rock samples were collected throughout the study area for petrographic analysis. Igneous rocks are classified according to Johannsen (1937) and thin sections of sedimentary rocks are classified according to Folk (1974). Megascopic hand specimens of sedimentary rocks observed while mapping and measuring stratigraphic sections are classified according to Travis (1955).

Ore reserves are estimated in a two step process. First, observed geologic controls on the mineralization are used to identify potential

host rocks. Second, through the combined use of the magnetic contour maps and observed mineralization, the strike length of mineralized host rock is determined. Tonnages are calculated for mineralization depths of 75 feet (22.9 m) and 100 feet (30.5 m) with an average ore horizon thickness of 6 feet (1.8 m) and 8.83 feet (2.7 m) respectively. The total mineralized strike length used in the calculation is 13,732 feet (4.19 km) of which 4850 feet (1.48 km) is inferred from the magnetic data. Five hundred thousand tons estimated by Kelley (1949) for Sections 14, 23 and 24, T5S, R7E is contained in each probable reserve estimate. Possible ore reserves are calculated in a similar manner. Potential ore horizons in the Torres member of the Yeso Formation are summarized, and assumed to be mineralized along the same strike-length used to calculate probable reserves.

Geophysical

Total field magnetic measurements were made with a Geometrics G-816 Proton Magnetometer. Each magnetic measurement is spaced approximately 50 feet (15 m) apart (paced intervals), along a profile flagged roughly perpendicular to the Jones Camp Dike. Overlay 2 shows the location of each magnetometer profile. Control points for profiles 1 through 20 and 67 through 112 were identified and plotted on a 1:12,000 scale topographic map. Control for lines 21 through 66 was established by a plane table survey.

Each magnetic measurement is an average of three magnetic readings. Signal to noise ratios were also observed; if the signal to noise ratio fell to 4 or less, more than three readings were taken to obtain the average.

A separate base station reading was taken at the beginning and end

of each day. As profiles were being run, the first profile measurement of the day was repeated after every two profiles.

Each magnetic measurement is normally corrected (Grant and West, 1965) using the average value of the base station measurements (51,764 gammas). Magnetic profile data from the study area is tabulated in Appendix I.

Two types of contour maps were constructed from the magnetic data. The first (overlays 3 and 4) is contoured from the corrected data. The second (overlays 5 and 6) is contoured from data generated with a low-frequency filtering process suggested by Allan Sanford (A. Sanford, personal communication, 1979). Areas were selected for the filtering process on the basis of their economic potential. Each profile from the chosen area was fitted with a hand drawn approximation of the magnetic anomaly of the Jones Camp Dike (Appendix I). The difference between the hand fitted curves and each corresponding data point was then tabulated to construct the second contour map.

Magnetic susceptibilities (K) of the rock samples plotted in figure 6 are calculated from two empirically derived formulas. The first is $K = (2.6 \times 10^{-3}) V^{1.33}$ where V is the volume percent of magnetite in the rock. It is valid for $0.1 < V < 10$ (Balsley and Buddington, 1958). The second formula, $K = (1.16 \times 10^{-3}) V^{1.39}$, is valid for $V > 10$ (Bath, 1962). Measurement of the direction and intensity of remanent magnetism followed a procedure described by Keyes (1971).

GEOLOGIC SETTING

The study area occupies a narrow east-west strip, approximately 1 mile (1.61 km) wide and 8 miles (12.9 km) long across the southern portion of Chupadera Mesa. Chupadera Mesa is part of the structural Chupadera platform described by Kelley and Thompson (1964). The platform extends from the southwestern end of the Estancia basin, 45 miles (72.4 km) south to the Oscura Uplift, and is 10 to 15 miles (16-24 km) wide between the Chupadera fault to the east and the Chupadera anticline to the west (Kelley and Thompson, 1946). Figure 2 is a generalized stratigraphic column of Permian and Pennsylvanian sediments which crop out in the region surrounding the study area. Tertiary age dikes crop out on the platform in sediments assigned to the Yeso, Glorieta, and San Andres Formations. The largest of these dikes is the Jones Camp Dike which averages 575 feet (175.2 m) in width and is exposed for approximately 11 miles (17.7 km). It dips between 82°S and vertical, and strikes N75°W, paralleling the nearby Iron Horse Dike (Sec. 9, T6S, R7E). In Sections 15, 16 and 17, T5S, R7E the dike is sporadically capped by the Yeso Formation (commonly sandstone), but it generally forms a prominent ridge across the study area recognizable by its bouldery outcrops. East of the study area the dike is covered by sediments of the San Andres Formation. A gentle anticlinal arching of the San Andres Formation marks the position of the dike for 1.6 miles (2.57 km) east of the mapped area before it curves ESE and eventually loses all topographic expression after 1.15 miles (1.85 km). At its western end the dike gradually disappears beneath the Yeso Formation, extending at least 3 miles (4.83 km) west of the study area. Between Sections 30, T5S, R8E and Section 16, T5S, R7E the valley on the south side of the dike is 50 feet (15 m) to 100 feet (30.5 m) lower than

P e r m i a n	San Andres Formation 140'		Sediments cropping out in the study area
	Glorieta Formation 50'		
	Yeso Formation 1630'	Joyita Member 140'	
		Canas Member 140'	
		Torres Member 1000'	
	Mesita Blanca Member 350'		
Abo Formation 740'			
P e n n s y l v a n i a n	Bursum Formation 210'		
	Madera Formation 765'		
	Sandia Formation 15'-625'		
Precambrian			

Figure 2. Generalized stratigraphic column of Permian and Pennsylvanian sediments in eastern Socorro County, New Mexico (not to scale).

the valley on the north side. Strata along both sides of the Jones Camp Dike are typically folded back from the contact. Occasionally there are small anticlinal or synclinal folds paralleling the dike. The overall effect is a broad anticlinal arching of sediments centered along the dike.

Intruded after the Jones Camp Dike are a number of diabase (pyroxene syenodiorite) sills and dikes. Most of these intrusions occur close to the dike's contact or along the hillsides south of it. Some of the diabase sills extend for over one-half mile.

Magnetite mineralization occurs in discontinuous pods usually localized within 100 feet (30.5 m) of the Jones Camp Dike or at the contact of diabase intrusives.

STRATIGRAPHY

Yeso Formation

The Yeso Formation was first named by Lee (1909) for Mesa Del Yeso which lies 12 miles (19.3 km) north east of Socorro, New Mexico. It has since been redescribed and subdivided by Needham and Bates (1943); from base to top it is divided into the Mesita Blanca member, the Torres member, the Canas member, and the Joyita member. Only the upper three members crop out in the study area.

Torres Member

The Torres Member, whose lower contact is not exposed in the study area, is a succession of interbedded limestone, gypsum, siltstone, and silty sandstone layers. Prominent in the Torres Member are three limestone units varying from 0 to 30 feet (0-9.1 m) in thickness. Physiographically they form ridges and cap small cuestas. Stratigraphically they correlate well in terms of thickness, lithology and spacial relationships with three limestone units measured by Wilpot and Wanek (1951). The stratigraphic sequence in the Torres Member is rhythmic. In measured Section 1, three cycles are present, varying in thickness from 20 to 60 feet (6.1-18.3 m). A typical cycle begins with thickly-bedded limestone grading upward into thin discontinuous laminations of limestone interbedded with thickly laminated gypsum. The gypsum is interbedded with several thin to thickly bedded siltstones and sandstones. Discontinuous sandstones are typically found at the top of each cycle. These sands grade laterally into gypsum and are in sharp contact with an overlying limestone. Most of the gypsum measured in the Torres Member is nodular although bedded gypsum is present. Two hundred feet (61 m) of the Torres Member is present in MS-1 (plate 2). The contact between the Torres

member and the overlying Cañas Member is gradational. It is placed at the top of the thickest of the prominent limestones.

Cañas Member

Similar to the Torres Member, The Cañas Member is a rhythmic limestone, gypsum, sandstone sequence. The major difference between the two members is the abundance of gypsum in the Cañas Member and lack of interbedded siltstones and silty sandstones. Distinct limestone layers from 2 to 4 feet (0.6-1.2 m) thick mark the beginning of each Cañas cycle. Both nodular and laminated gypsum are present in the Cañas Member in approximately equal amounts. These two types of gypsum grade laterally and vertically into each other. A few siltstones and silty sandstones are interbedded with the gypsum. Like the Torres Member, sandstones occur at the top of each cycle in sharp contact with an overlying limestone. These sandstones are typically 1 to 2 feet (0.3-0.6 m) thick, thinly bedded and fine to very fine-grained. Eighty to one hundred feet (24.4-30.5 m) of the Cañas Member is present in MS-2 and MS-3 (plate 2). These thicknesses agree well with the 80 feet (24.4 m) measured by Kelley (1949). One hundred and forty feet (42.7 m) of the Cañas Member is present in MS-1. The contact between the Cañas Member and the overlying Joyita Member is sharp and conformable.

Joyita Member

The Joyita Member lies conformably above the Cañas Member. The contact is sharp and poorly exposed except on steep slopes. The Joyita Member is dominated by red, fine-grained, poorly-sorted, discontinuous massive to thinly bedded sandstone. Two gypsum units are interbedded with the Joyita Member. The first is a 6 to 8 foot (1.8-2.4m) thick bed of nodular and thickly laminated gypsum occurring 8 to 20 feet (2.44-6.10 m)

above the base. This unit is in sharp contact with the surrounding sandstone. The second gypsum unit is a 6 to 8 feet (1.8-5.5 m) thick nodular and laminated gypsum bed occurring at the top of the Joyita Member. At the base of this gypsum bed is a gray 1 to 2 foot (0.30-0.6 m) thick discontinuous limestone bed (see thin section L-11, Appendix III). One hundred and six feet (32.3 m) of the Joyita Member is present in MS-3 (plate 2), while 140 feet (42.7 m) is present in MS-1. The contact between the Joyita Member and the overlying Glorieta Formation is sharp and conformable.

Glorieta Formation

Keyes (1915) first described the Glorieta Formation, but he did not give a type locality for his description. The Glorieta is commonly included as a basal member of the San Andres Formation (Read and Andrews, 1944) but has been given formational status in this thesis.

Resting conformably on the Yeso Formation, the Glorieta Formation generally forms poor outcrops although it can be well-exposed on the steeper slopes of the study area. It consists of reddish orange-buff, fine-grained, thinly bedded, sandstone. The base may contain up to 3% limonite. The Glorieta Formation thins to the east in the study area. Fifty six feet (17.1 m) of the Glorieta Formation are present in MS-1 (plate 2), and Kelley (1949) measured 50 feet (15.2 m) of Glorieta in the Jones Camp Area (Sec. 14, T5S, R7E). The upper contact of the Glorieta Formation is sharp and conformable with the overlying San Andres Formation.

San Andres Formation

The San Andres Formation was originally described by Lee (1909) for a location in the San Andres Mountains of Socorro County, New Mexico.

The contact of the San Andres with the Glorieta is marked by the contrast between the buff sandstone of the Glorieta and the gray medium to thickly bedded, cliff-forming limestones of the San Andres. Discontinuous horizons of erosion resistant nodules (1-12 inches; 2.5-30 cm) crop out in the limestone beds. A 10 to 20 foot (3-6.1 m) thick sandstone unit occurs between 12 feet (3.7 m) and 25 feet (7.6 m) above the Glorieta Formation contact. This sandstone is lithologically very similar to the Glorieta Formation. This unit thins eastward until it pinches out in Section 29, T5S, R8E. Gypsum occurs in several areas outside of the study area. Erosion has truncated the San Andres Formation. A maximum of 140 feet (42.3 m) of San Andres is exposed in MS-2 (plate 2).

IGNEOUS ROCKS

Two groups of igneous rocks crop out in the study area. Most abundant are those of the Jones Camp Dike. The Jones Camp Dike is a composite dike which varies from quartz diorite at its margins to granodiorite in its center (Nogueira, 1971). The second rock group is comprised of pyroxene syenodiorites. Two previous authors, Kelley (1949) and Nogueira (1971), have described this second group of rocks as diabase. Because of variation in texture and composition this term is only locally correct. The rock type is actually a pyroxene syenodiorite, but the term diabase is retained as a convenient field designation to maintain continuity with previous work by Kelley (1949) and Nogueira (1971) in the study area.

Jones Camp Dike

On the basis of mineralogical, textural, and spacial variations in the Jones Camp Dike, Nogueira (1971) divided it into four facies. In the Jones Camp area (Sec. 14, T5S, R7E), these facies occur symmetrically within the dike. The continuance of this relationship outside of the Jones Camp Area is unknown. Situated on either side of the dike is a quartz diorite known as the mottled border facies (M.B.F.) (Nogueira, 1971). This facies typically weathers to a light green or gray mottled surface. It varies between 50 feet (15.2 m) and 150 feet (45.7 m) in thickness and is characterized by a distinct vertical layering oriented roughly parallel to the dike contact. The bands are from 1 to 6 inches (2.5-15.2 cm) thick, and are typically fine-grained. They grade laterally into coarse-grained, massive, lensoidal pods and then back into fine-grained layered zones. The coarse-grained, massive zones are compositionally similar to the adjacent outer intermediate hornblende facies (Nogueira, 1971). The M.B.F. is the only dike facies to contain

veinlets of magnetite but no primary magnetite (Nogueira, 1971). The contact of the M.B.F. with the adjacent facies is typically sharp. Locally the M.B.F. appears to have been intruded by tongues of the adjacent facies (Kelley, 1964). Inward from the M.B.F. there are the outer-intermediate hornblende facies (O.H.F.) and the inner-intermediate pyroxene facies (I.P.F.) respectively (Nogueira, 1971). Both of these facies are syenodiorite in composition. They are distinguished primarily by their relative abundances of hornblende and pyroxene. Contacts between the two facies are irregular and typically gradational. The contact between the I.P.F. and the central dike facies (C.F.) is similar to the O.H.F. and I.P.F. contact. Nogueira (1971) separated the C.F. into two subfacies, a syenodiorite and a granodiorite. The syenodiorite is the more abundant of the two, with the granodiorite forming small elliptical patches in the syenodiorite (Nogueira, 1971).

Based on estimates of the molten dikes composition and the water vapor pressure in the melt, Nogueira (1971) estimated that the dike was emplaced at temperatures between 800°C and 900°C. Nogueira (1971) also estimated that sediments in contact with the dike during its intrusion reached 600°C by evaluating the dikes thickness, temperature of emplacement, and the lithologies of the intruded sediments.

Diabase

The diabase intrusives described by Kelley (1949) and Nogueira (1971) are actually pyroxene syenodiorites. They form dikes and sills striking roughly parallel to the Jones Camp Dike, and range from less than 1 foot (0.3 m) to over 75 feet (22.9 m) in thickness and up to one half mile (0.8 km) in length. The sills occur at several stratigraphic horizons and sometimes form tongue-like bodies fed from nearby dikes or

small intrusives. Surrounding most of the diabase is a 1 to 3 foot (0.3-0.9 m) thick chilled margin. Locally the chilled margin has a well developed diabasic texture. This may be the source for Kelley's (1949) original use of the term. Locally inclusions of the Jones Camp Dike are present in the diabase where it is in contact with the dike. A close spatial association occurs between the diabase intrusives and magnetite mineralization. Magnetite is commonly found at the contact between diabase and intruded sediments, especially limestone. The relationship is best observed along the sills intruded south of the dike (plate 1). Magnetite can also be found as high grade pods in the diabase or as a low grade mixture of diabase and ore.

Alteration

Alteration in the Jones Camp Dike is characterized by epidotization, sericitization and kaolinitization of the feldspars, sometimes in excess of 30% (Nogueira, 1971). The pyroxene and amphiboles are altered to a combination of magnetite and chlorite. Nogueira (1971) reported the presence of deuteric alteration in the dike also. Thin sections, cut from the diabase, indicate that sericite (1-2%) is concentrated in the calcic cores of plagioclase laths. A trace of kaolinite is present in both the alkali and plagioclase feldspars. Pyroxenes are typically replaced by uralite and actinolite-tremolite, some of the pyroxenes have altered to a combination of carbonate and magnetite. Hornblende typically alters to a combination of magnetite, carbonate and chlorite or sometimes biotite. Chlorite also occurs fringing a few biotites.

Surrounding both the dike and the diabase is a narrow irregular contact metamorphic aureole belonging to the albite-epidote-hornfels facies (Nogueira, 1971). Mineralogically it contains actinolite,

tremolite, epidote, andradite, cordierite, talc and acmite (Nogueira, 1971). The aureole appears to be best developed in the mottled border facies. Kelley (1949) felt that this was especially true near areas of mineralization.

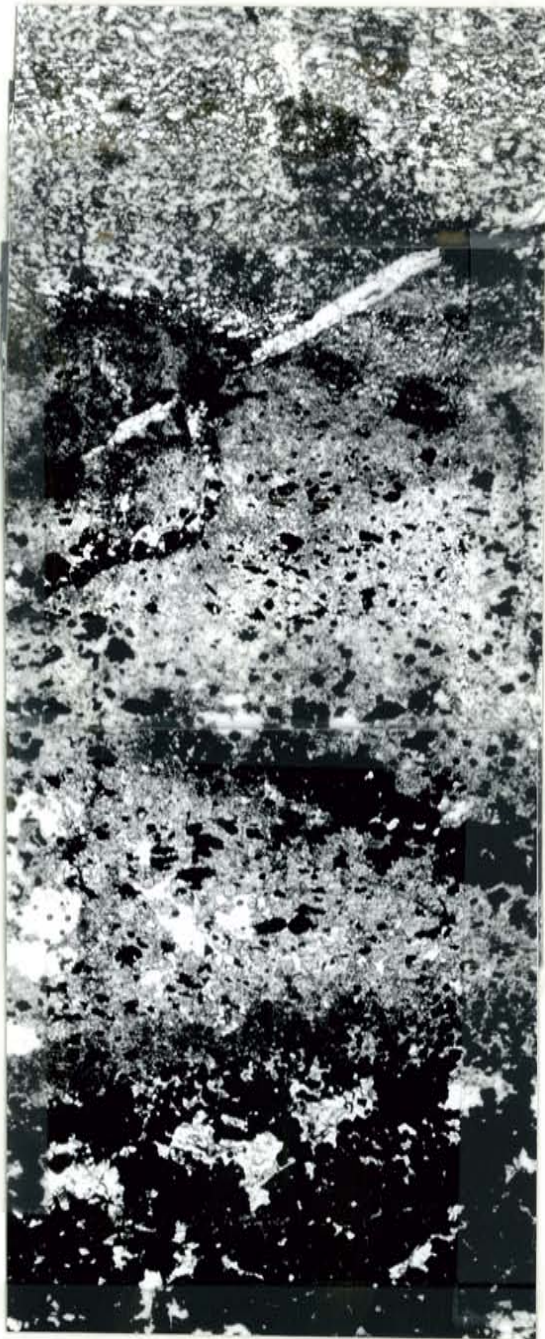
MINERALIZATION

Mineralogy

Mineralization in the study area is overwhelmingly magnetite and hematite; magnetite comprises more than 90% of most samples (Clay T. Smith, personal communication, 1979). Minor amounts of sulphides, mostly pyrite, are present. The presence of trace amounts of malachite and azurite suggests the presence of copper sulphides. Goethite and limonite are present on weathered surfaces of most ore bodies.

Mode of Occurrence

The most common geologic occurrence of the mineralization is as conformable pods. Individual pods range in strike length from several feet to over 1200 feet (365.8 m) and some may exceed this when fully developed. Thicknesses vary from 1 to 30 feet (0.3-0.1 m) averaging about 6 feet (1.8 m). A typical down dip extent has yet to be established because of a lack of drilling information. The pods are located at several stratigraphic horizons. Usually they are in limestone (Fig. 3) or at limestone-sandstone contacts, particularly the cyclic contacts of the Torres Member of the Yeso Formation. A few pods are located in sandstone and rarely they occur in gypsum. Interestingly the largest exposed pod, known as the East-pit ore body (SE $\frac{1}{4}$, NE $\frac{1}{4}$, Sec. 24, T5S, R7E), appears to be localized in gypsum. Many of the pods are directly underlain by diabase or are spacially close to it. This is particularly evident along the hillside south of the dike. Kelley (1949) mapped several ore bodies in the Jones Camp area which are isolated in diabase. (Much of the geology in the Jones Camp area has been obscured by mining operations.) Another ore occurrence is as irregular masses mixed with diabase. A few magnetite veins up to 1 foot (0.3 m) thick are exposed



unreplaced limestone

replacement zone

magnetite ore

Figure 3. Example of magnetite replacing limestone (thin section L-0).

in open pits of the Jones Camp area. Both the M.B.F. and the diabase contain small veinlets of magnetite. Slickensides are present in some ore outcrops. No placer deposits are known to exist in the area, but several placer claims have been staked north of Jones Camp (Clay T. Smith, personal communication, 1979).

Based on geochemical data and ore mineral stability fields, Nogueira (1971) estimated that the ore was emplaced under oxidizing conditions at temperatures between 450°C and 550°C.

STRUCTURE

Chupadera Mesa is part of the Chupadera Platform (Kelley and Thompson, 1964), which lies between the Estancia Basin to the north and the Oscura uplift to the south (Fig. 4). It covers an area 45 miles (72.4 km) long (N-S) and 10 to 15 miles (16.1-24.1 km) wide (E-W), and slopes slightly to the east and southeast (Kelley and Thompson, 1964). The position of the northern and southern boundaries is somewhat arbitrary. To the east it is separated from the Claunch Sag by the Chupadera Fault, which is downthrown to the east. Along its western side is the northerly plunging Chupadera anticline which separates the Jornada Del Muerto Basin from the platform. The Chupadera Anticline begins just south of the western most Jones Camp Dike outcrop and continues north for about 22 miles (35.4 km) along the eastern edge of the Jornada Del Muerto Basin.

The central feature of the study area is the Jones Camp Dike. It strikes approximately N75°W and varies in dip between 82°S and vertical. The strike of the Jones Camp Dike parallels that reported by Kelley (1949) for the nearby Iron Horse Dike (Sec. 9, T6S, R7E). The Iron Horse Dike is also associated with magnetite mineralization in the Yeso Formation. At its eastern most exposure the Jones Camp Dike plunges beneath the Glorieta Formation. To the west, after cutting the western escarpment of Chupadera mesa, it is gradually concealed by either the Torres or the Mesita Blanca members of the Yeso Formation. In Sections 15, 16, and 17, T5S, R7E, the Jones Camp Dike is capped by a thin veneer of sediments which are usually sandstone (plate 1). In Section 30, T5S, R7E a diabase dike parallels the Jones Camp Dike enclosing a narrow trough of sediments between the two. A similar occurrence is found north

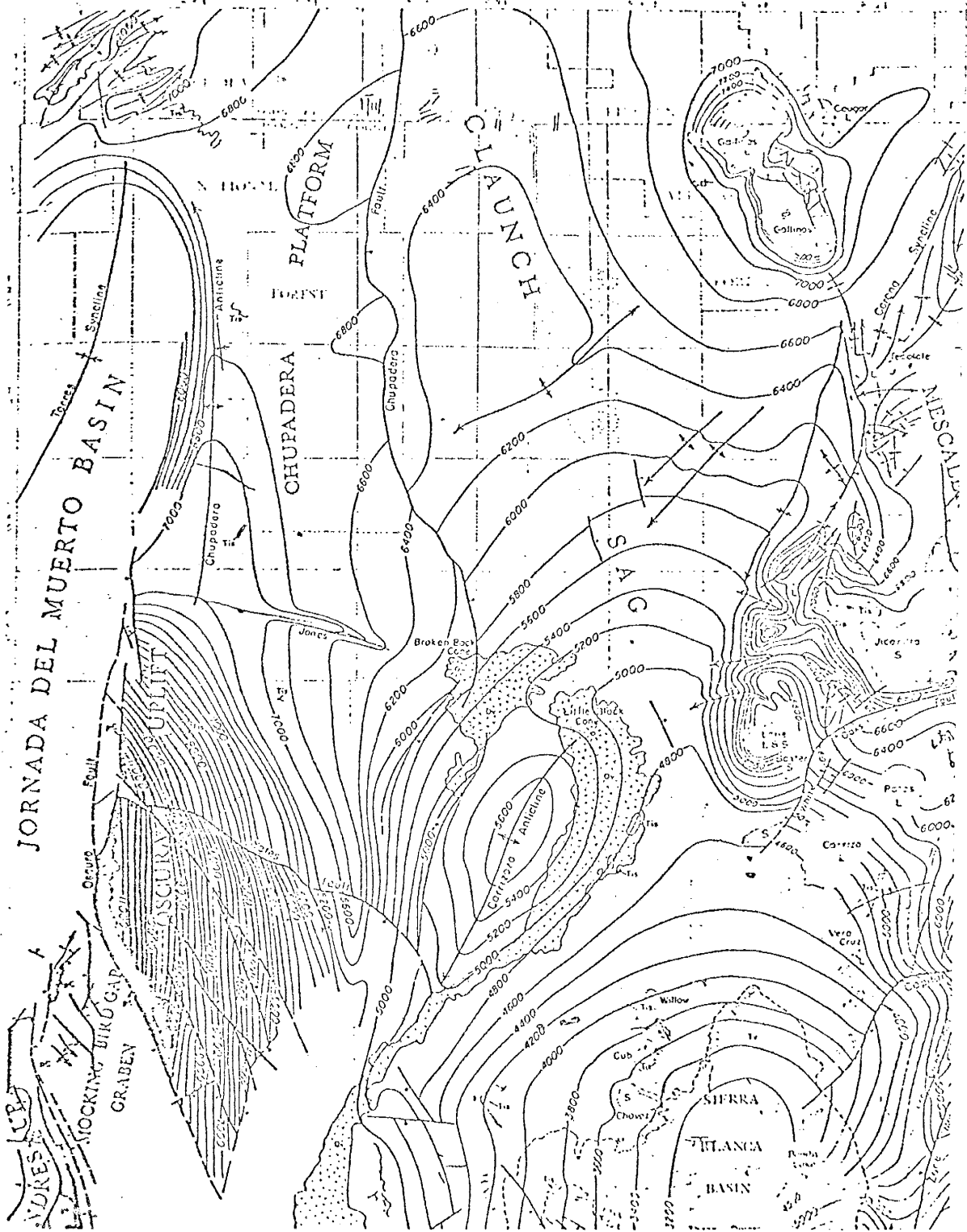


Figure 4. Structural contour map of the study area and surrounding regions (after Kelley and Thompson, 1964).

of the dike extending west from Section 15, T5S, R7E into Section 16. Here the diabase becomes increasingly concordant westward until it forms a sill. On either side of the Jones Camp dike there are many additional diabase sills and dikes. Some of the dikes feed tongue-like sills which extend outward for distances of up to one-half mile (0.8 km). The stratigraphic horizon which is most persistently intruded by diabase is the contact between the Glorieta Formation and the San Andres Formation on the south side of the dike. Diabase intrusives crop out along nearly 80% of this horizon between Section 30, T5S, R8E and Section 16, T5S, R7E. In Section 16, T5S, R7E and further westward, these intrusives are no longer exposed. Only two small diabase intrusives crop out beyond the dike contact west of Section 16.

Folding

East of Section 29, T5S, R8E strata of the San Andres Formation are anticlinally arched along the strike of the Jones Camp Dike for 1.6 miles (2.6 km) beyond its last exposure. The arching bends east south east for an additional 1.2 miles (1.9 km) before the topographic ridge and dip reversals cannot be recognized. Roughly parallel to both dike contacts are small discontinuous asymmetrical synclinal and anticlinal folds. In Section 17, T5S, R7E a series of alternating synclinal and anticlinal folds extend outward from the north side of the dike. In several cases the anticlinal limb closest to the the dike will dip gently into it. Most of the folds occur within 50 to 100 feet (15.2-30.5 m) of the dike and few are further than 200 feet (61 m) from the contact. Kelley (1949) mapped several occurrences of magnetite localized in the crests of anticlinal folds close to the dike. Cross section H-H' in plate 3 shows what may be an occurrence similar to those mapped by Kelley (1949). Strata

along the contacts of the Jones Camp Dike are tilted away from the dike with dips ranging from 30° to slightly overturned. Dips lessen to between 0° and 10° at a distance of 3000 feet (609.6 m) north or south of the contact.

Faulting

Much of the faulting in the study area is obscured by alluvium. Aerial photographs suggested a NW trending lineament in Section 16, T5S, R7E, but a field check could not confirm its existence. Where the Jones Camp Dike plunges beneath the Glorieta Formation in Section 29, T5S, R8E two small south-dipping (70°) normal faults cut the Glorieta Formation and the San Andres Formation. The faults have a combined displacement of 30 feet (9.1 m) and strike roughly parallel to the dike, but they are traceable for only a few feet along strike. Roughly perpendicular to the dike contact are small strike-slip and normal faults (see plates 3 & 4). More of these faults are probably present but are obscured by alluvium.

Comparison of MS-2, 3 and 4 with MS-1 shows an average shortening of 37 feet (11.3 m) in the Canas Member and 56 feet (17.1 m) in the Joyita Member of the Yeso Formation.

GEOPHYSICAL DATA

Characteristic Magnetic Anomalies of Rock Types in the Study Area

The magnetic anomaly of the Jones Camp Dike commonly extends north-south between 2000 feet (609 m) and 3000 feet (914 m). In most profiles the complete anomaly has not been surveyed. Its magnitude ranges from approximately 550 gammas where covered in Section 20, T5S, R8E to several thousand gammas where exposed. In every profile (see Appendix I) the anomaly is consistently asymmetric from north to south. The solid line in figure 5 is a hand fitted approximation of the dike's theoretical magnetic anomaly. It shows the typical negative region north of the dike, the high shifted towards the south side of the dike, and the gentle south slope which approaches zero asymptotically.

Erratic peaks with magnitudes of several hundred gammas occur in the real data of figure 5. Similar peaks centered over the Jones Camp Dike are present in most of the profiles. Two exceptions to this occurrence are profiles 1 and 2 (Appendix I). These profiles are from an area where the dike is completely covered by sediments.

The diabase intrusives do not have a characteristic magnetic anomaly. The magnitude, symmetry, and breadth of their anomalies are quite variable. When the diabase and the Jones Camp Dike are in contact they may form only one anomaly instead of two separate ones.

Magnetite mineralization can form very distinct magnetic anomalies. Discrete pods of magnetite have very sharp narrow, large magnitude, asymmetric anomalies (Fig. 6). Anomaly breadths vary with the pod's size, but typically they range from 30 feet (9.1 m) to 100 feet (30.5 m). The broadest anomaly which occurs over the East-pit (profiles 44-54 on overlay 3) is 300 feet (91.4 m) wide. Anomaly magnitudes also

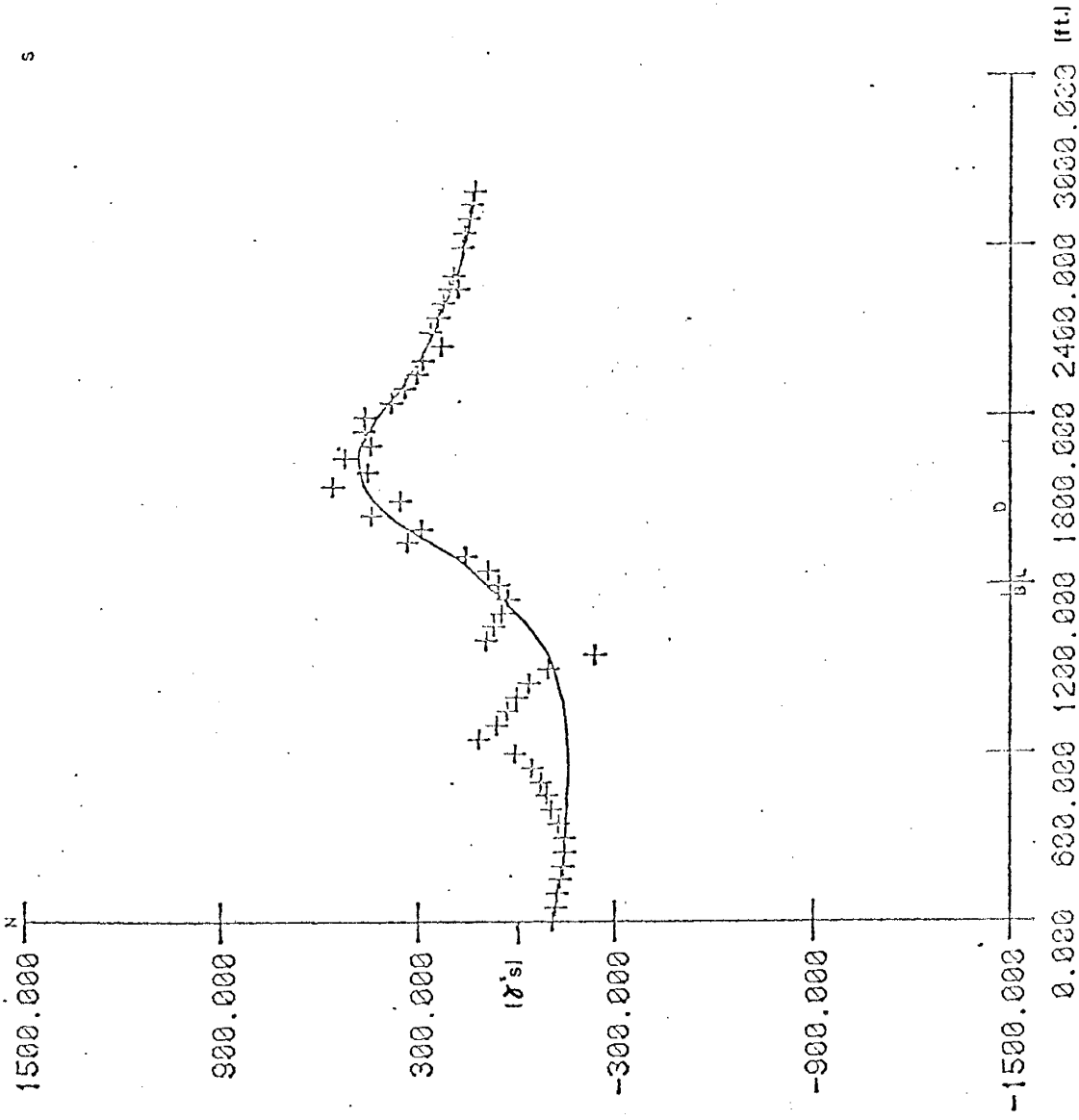


Figure 5. Hand fitted approximation of the magnetic anomaly of the Jones Camp Dike.

vary with each pod, but are typically from 2000 to 3000 gammas. A maximum anomaly of 5000 gammas was recorded (profile 28, Appendix I). The symmetry of magnetite anomalies is the same as the Jones Camp Dike, negative on the north side changing to positive on the south side. Figure 6 is an example of a magnetite anomaly. It shows the characteristic sharpness, large magnitude and symmetry.

Magnetic anomalies formed by sediments in the study area are ignored because of the sediment's low magnetic susceptibilities.

Magnetic Contour Maps

Data used to construct overlays 3 and 4 has undergone a normal correction of 51,764 gammas. The data has a broad negative to positive trend from north to south along the entire study area. The zero line of the trend is located on the north side of the Jones Camp Dike. On either side of the zero line there are irregularly shaped regions of magnetic highs and lows oriented roughly parallel to the Jones Camp Dike. The regions have magnitudes of 500 to 1500 gammas and range spatially from 3,000 to 10,000 feet (0.91-3.05 km) in length and 200 to 1,000 feet (61.-304.8 m) in width. The negative regions are typically located north of the zero line, and the positive ones south of it. The major exception to this positioning is a positive region located north of the dike between profiles 97 and 104. Within all of the regions there are smaller more linear and typically larger anomalies. These anomalies usually correlate with either the Jones Camp Dike or areas of magnetite mineralization.

North of the baseline between profiles 20 and 45 the magnetic anomalies become irregular and less extensive compared to anomalies of similar magnitude. Near profile 60 there is a prominent bulge in the

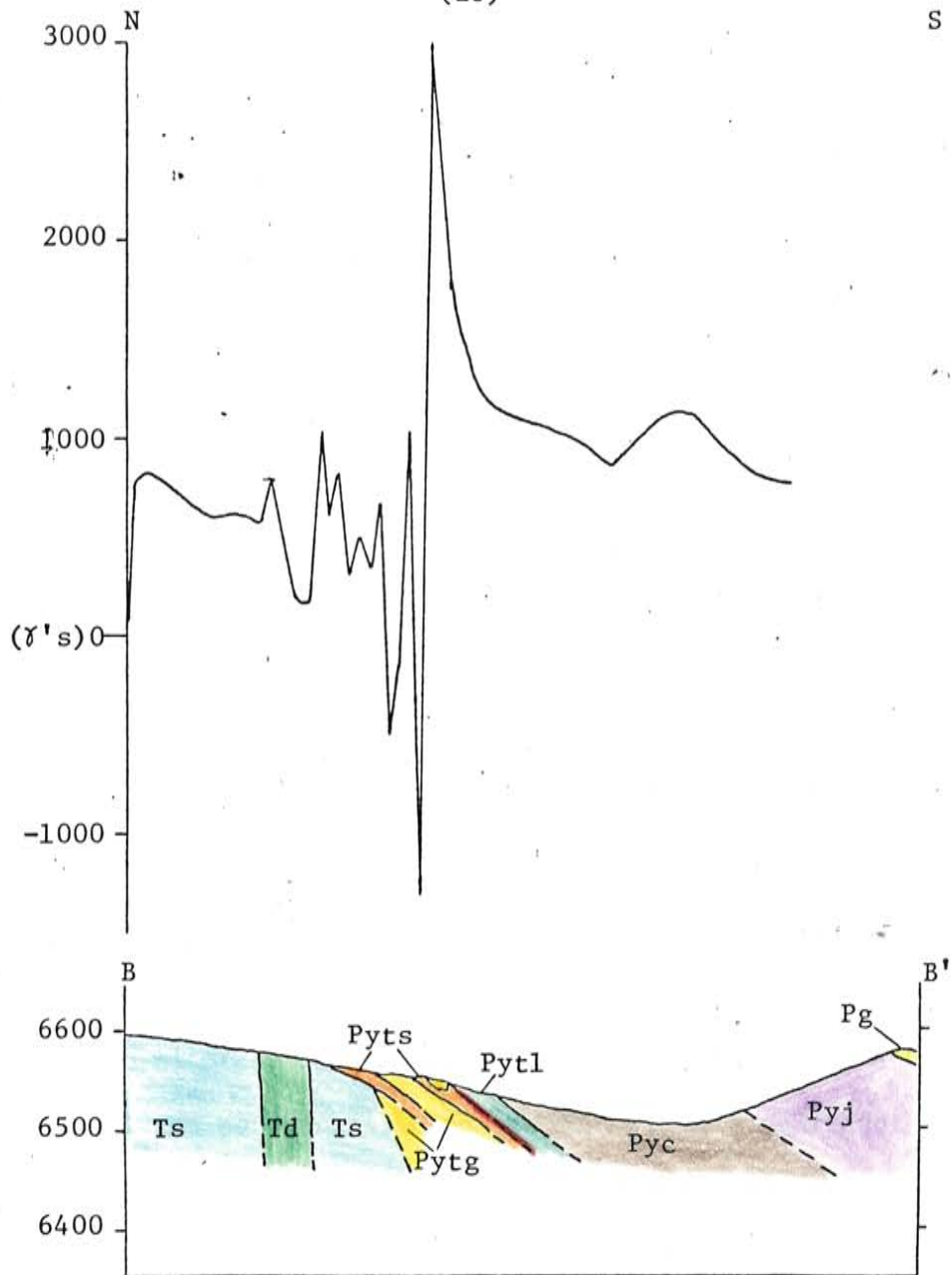


Figure 6. Example of a well developed magnetite anomaly along cross section B-B' of the Section 19 Prospect. (See plate no. 4)

	Magnetite ore
	Td Diabase intrusive
	Ts Jones Camp Dike "undifferentiated"
	Pg Glorieta Formation
	Pyj Joyita member
	Pyc Canas member
	Pytl Torres member (limestone)
	Pyts Torres member (sandstone)
	Pytg Torres member (gypsum)

Scale: 1 inch = 200 feet

contours south of the dike which appears to be related to mining activity in that area. Negative anomalies located at the south end of profiles 4 to 86 correlate with diabase intrusives in these areas.

Overlays 5 and 6 are constructed from data generated with the low frequency filtering process described previously (see page 6). The anomalies of plates 5 and 6 are more distinct and better developed than the original data. They do not have the north-south trend present in overlays 3 and 4. In overlay 5 the anomalies are parallel to the unfiltered data except for an anomaly 500 feet (152.4 m) north of the baseline on profile 12. This anomaly trends NE-SE across the dike and correlates with a mineralized diabase intrusive in that area.

Overlay 6 covers profiles 91 to 112 at the west end of the study area. Its central features are two large negative regions located between profiles 91 to 97 and 98 to 107. Within both of these lows, large magnitude anomalies correlate with areas of significant magnetite mineralization. Several other occurrences of mineralization covered by overlay 6 have little or no expression on the map. Most significant is the Section 17 Prospect which shows up strongly for only 900 feet (274 m) between profiles 94 and 97.

Direction and Intensity of Remanent Magnetism

The direction and intensity of remanent magnetism was measured in one ore sample from the Section 19 Prospect. The direction of remanent magnetism is between due north and N10°E (geographical). It is inclined between 55° and 65° below the horizontal. The ratio of the intensity of remanent magnetism (Ir) to induced magnetism (Ii) is 2.16:1.

GEOLOGIC SUMMARY

Controls on Mineralization

Several factors control mineralization in the study area. Enhancement of effective porosity during diabase intrusion appears to be an important control of mineralization on a large scale. Locally, stratigraphy plays an important role in localizing ore.

Data gathered in the study area places the broad sequence of intrusive and mineralizing events as follows:

- 1) Intrusion of the Jones Camp Dike,
- 2) Diabase intrusion,
- 3) Magnetite mineralization.

Nogueira (1971) stated that the diabase intrusives predate the Jones Camp Dike based on cross-cutting relationships. Contrary to this conclusion, cross-cutting relationships between the Jones Camp Dike and diabase indicate that the diabase is post dike (Fig. 7). Neither was evidence found to confirm the presence of two separate ages of diabase reported by Nogueira (1971), but the diabase has not been studied enough to eliminate this possibility.

The close spacial relationship between the diabase intrusives and magnetite mineralization in the study area suggests that some control is exerted by the diabase. The exact nature of this relationship is not fully understood. In the Cornwall District of Pennsylvania a direct genetic link has been proposed between diabase intrusives and magnetite ore (Eugster and Chou, 1979). Geologically these deposits are similar to the Jones Camp Deposits. Magnetite occurs as replacement bodies at the contact of Triassic diabase intruded into Paleozoic limestones (Hickok, 1933). Eugster and Chou (1979) have proposed a convection-cell model for the origin of these deposits. Figure 8 is a schematic

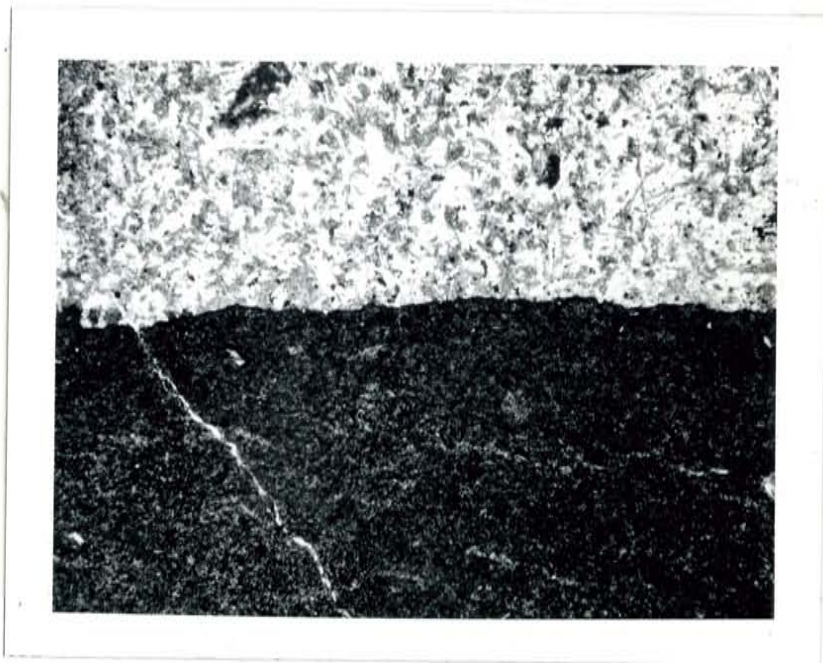


Figure 7. Chilled margin of a diabase intrusive (dark area) in contact with the Jones Camp Dike (thin section Db-11).

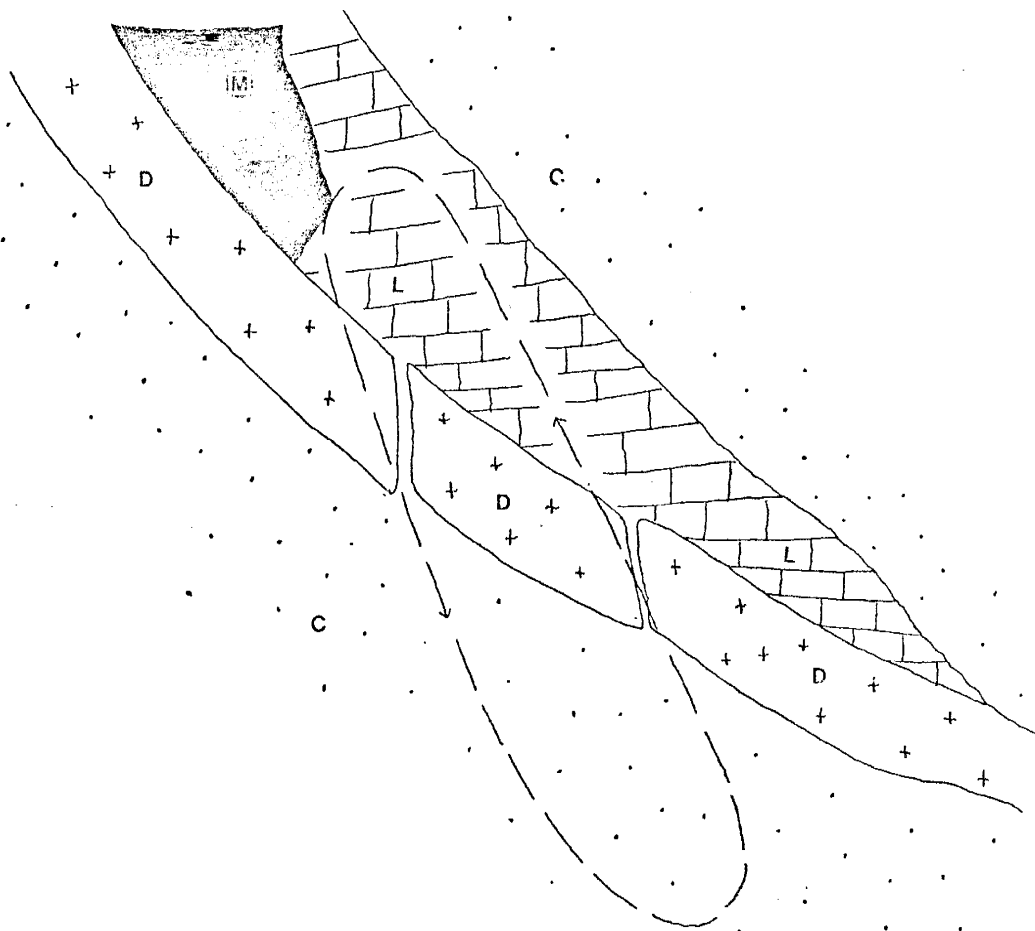


Figure 8. Schematic sketch of the convection cell model for the deposition of the Cornwall Magnetite Deposits (after Eugster and Chou, 1979). M = magnetite, L = limestone, D = diabase, C = country rock.

representation of this model. In it, a convection cell, powered by temperature gradients set up by the diabase, carries iron from an unknown source to the limestone host. Some of the iron may be supplied by the diabase. In the Jones Camp District, the ore and diabase do not appear to be genetically linked as has been suggested for the Cornwall District. The ore-diabase relationship appears to be more of a secondary nature than primary.

A regional comparison of several geologically similar iron deposits gives an insight into the role of the diabase at the Jones Camp Deposit. At the Iron Horse Deposit (Sec. 9, T6S, R7E) and the Blackington and Harris Deposit (Sec. 20, T1N, R6E) magnetite occurs as replacement bodies in the Yeso Formation along the contacts of dikes which are compositionally similar to the Jones Camp Dike (Kelley, 1949). They are distinguished from the Jones Camp Deposit by the lack of a later diabase intrusive. The fact that there is significant mineralization at these deposits but no diabase seems to preclude a direct genetic link between the diabase and the ore. Nogueira (1971) concluded the ore in the Jones Camp Deposit was carried by hydrothermal fluids rising along zones of secondary permeability in the form of fractured and brecciated sediments developed during intrusion of the Jones Camp Dike. The fact that mineralization is localized along faulted sediments near the dike (Fig. 9) and that it is difficult to maintain circulation in drill holes close to the dike indicates the presence of secondary permeability. A later intrusion by the diabase could have enhanced the total effective porosity by increasing the secondary permeability already present. If so, it would have probably concentrated ore near the diabase by facilitating ore fluid movement to these areas. Thus it seems probable that the ore-diabase



Figure 9. Magnetite localized in faulted limestone beds near the Jones Camp Dike.

relationship can be explained by the enhancement of effective porosity in areas of diabase intrusion. This relationship is compatible with the occurrence of ore at the Iron Horse and Blackington and Harris deposits since it does not preclude the occurrence of ore beyond areas of diabase intrusion. It only suggests that ore is more likely to be localized near the diabase.

The author realizes that this idea is predicated on the existence of a hydrothermal fluid of unknown origin, and that it is possible to invoke a convection cell model such as proposed by Eugster and Chou (1979) in which the Jones Camp Dike is the heat source and not the diabase. But neither the Yeso nor the San Andres Formations contain enough iron within a reasonable distance of the deposit to supply the iron present; nor is there any evidence of iron having been leached from either of these formations. The closest sedimentary source with any potential for supplying the necessary iron, is the Abo Formation underlying the Yeso Formation. The Abo contains approximately 1% iron (Clay T. Smith, personal communication, 1980). This would require the leaching of approximately 2.7×10^9 cubic feet (7.6×10^7 m³) of Abo to supply the nearly 2.7 million tons (combined probable and possible reserves) estimated to be in the Jones Camp Deposit. This corresponds to a block of Abo 8 miles (12.9 km) long, 740 feet (226 m) thick, and extending 43.2 feet (13.2 m) from either side of the Jones Camp Dike being completely leached.

Even if the Abo Formation is the source, the ore fluids would have to migrate upward to the Yeso Formation. Thus the basic premise for the formation of the deposits in the study area would be correct.

Locally, stratigraphy and structure play a large role in controlling

mineralization. Nogueira (1971) concluded that limestone is chemically the most favorable host rock. Support for this conclusion comes from the abundance of ore bodies in limestone. Interestingly the largest exposed ore body (the East-pit ore body) apparently occurs in gypsum. This can be explained by the complete replacement of an original limestone host and the migration of ore fluids into surrounding gypsum. Drilling near the ends of the pod should provide the answer.

The most commonly mineralized stratigraphic horizons are limestone-sandstone contacts. Of particular importance are those in the Torres member of the Yeso Formation. Three of these horizons are present in MS-1 (plate 2). Three others, lower in the section, have been identified in a section measured by Wilpolt and Wanek (1951) south of the study area.

From scattered outcrops and cross sections constructed by Kelley (1949) it is apparent that ore can be conformable along these horizons for several tens of feet. The reasons for this appear to be two-fold. First, the limestones provided an excellent host rock. Secondly the underlying sandstones must have been permeable enough to have allowed the migration of ore fluids beneath the host rock.

Although no permeability data is available, the porosity of sediments is suggestive of its presence. Point counts in sandstones of the Torres Member indicate porosities up to 9% (see thin Section S-7, Appendix III). Some secondary permeability may have also developed along bedding plane faults as the sediments were structurally deformed during intrusive events.

Ore replacement is least selective in the immediate vicinity of diabase intrusives. Field observations indicate that ore may replace any

rock type with which it comes in contact. In thin sections of diabase magnetite replaces both feldspar and ferromagnesian minerals. Veinlets of carbonate and magnetite cut some of the samples. The magnetite veinlets crosscut the carbonate veinlets suggesting that they are a later stage of mineralization. Thin sections S-7, S-12a, and S-12B are taken from unmineralized, weakly mineralized, and strongly mineralized areas of a sandstone outcrop, respectively. Comparison of point counts from each sample suggests that the order of replacement in the samples is feldspar grains and then quartz grains.

Formation of Deposit

In summary the author believes that the Jones Camp ore deposits were formed by hydrothermal fluids. These fluids probably migrated upward along zones of secondary permeability close to the Jones Camp Dike. Host rocks in contact with the dike were mineralized and ore spread into those favorable stratigraphic zones which were encountered during the upward migration of the fluids. The concentration of much of the ore near diabase intrusives probably reflects the enhancement of effective porosity in areas of diabase intrusion.

Intrusion of the Jones Camp Dike

Both Nogueira (1971) and Smith (Clay T. Smith, personal communication, 1978) have suggested that the Jones Camp Dike is emplaced along a fault. The linear form of the dike over an 11 mile (17.7 km) length does suggest this. Faulting is suspected in the Cañas member of measured sections MS-2 and MS-3, but they are not considered reliable for determining the existence of a predike fault. Geologic mapping does show that the top of the Torres member of the Yeso Formation is approximately 20 to 30 feet (6.1-9.1 m) lower on the south side of the dike than on

the north side in Section 17, T5S, R7E. This corresponds with the direction of displacement of two normal faults (70°S) in sediments above the dike at the east end of the study area. This evidence could reflect a predike fault, but it could also have developed during intrusion of the dike.

Interpretation Concepts

As an exploration tool the magnetic data is most useful qualitatively. To interpret the data effectively it is necessary to understand what factors control the character of a magnetic anomaly, and how geology influences each factor. Once these relationships are understood a good qualitative analysis of the data can be made by correlating it with the geology.

The character of every magnetic anomaly is a function of several complexly interrelated factors. Five of these are:

- 1) The lateral magnetic susceptibility contrast between a body and its surroundings.
- 2) The direction and intensity of remanent magnetism in the body.
- 3) The direction and intensity of the earth's magnetic field relative to the body.
- 4) The size and shape of the body
- 5) The depth of burial of the body

To achieve meaningful quantitative results each factor must be estimated with a good degree of accuracy. As the number of factors which can be estimated decreases, the results of the study become less meaningful. The problem is essentially one of uniqueness of interpretation. The difficulty stems from the fact that for a given body there is an unique anomaly, but for a given anomaly there are an infinite number of bodies which can form the anomaly. Geology usually places restraints on the number of reasonable causes of the anomaly. However, even within the geologic limits there still exists a large variation in the number of possible interpretations. Thus a quantitative analysis is difficult to interpret

when a limited amount of geologic data is available because of the variability in the results. A qualitative analysis is easier to perform for two reasons. First, it is possible to reduce the number of factors involved by combining the first three into one. Secondly, it is generally necessary to speak only in terms of relative values and not exact numbers when evaluating the effects of geology on each factor.

The direction and intensity of magnetism in the body (It) is the most complex of all the factors to be considered. A change in its position relative to a body will alter the anomalies character. Likewise, a change in its magnitude will change the anomalies magnitude in direct proportion. It is a vector quantity made up of two components, Ir which is the direction and intensity of remanent magnetism, and Ii which is the direction and intensity of induced magnetism in the body. The direction of the remanent component is controlled by the orientation of the earth's magnetic field at the time the component was acquired, and by subsequent tectonic movement which may have changed the position of the body. Complications caused by post emplacement movement of intrusives and ore in the study area should be minimal since little faulting was observed in these rocks. The magnitude of remanent magnetism probably varies throughout the study area as a function of the amount of magnetic minerals in the rock, and the magnetizing or demagnetizing processes which have affected the rock since its emplacement. A measurement of the direction and intensity of remanent magnetism in the Section 19 ore body indicated that the magnetism is oriented almost parallel to the earth's present magnetic field, and that it has an intensity approximately 2.16 times the earth's field. Ignoring this fact in a quantitative analysis would cause a significant overestimate of the size of the body forming the

anomaly.

The direction of induced magnetism is controlled by the present orientation of the earth's magnetic field. Its intensity is a product of the strength of the earth's field and the magnetic susceptibility contrast of the body with its surroundings. Because the earth's field is essentially constant throughout the study area, measureable variations in the intensity of induced magnetism are caused by lateral magnetic susceptibility contrasts between the rock types present. Figure 10 gives an example of how the susceptibility contrast can affect an interpretation. In figure 10 it is apparent that the susceptibilities of the Jones Camp Dike and the diabase overlap considerably. This indicates that the dike and the diabase can be magnetically indistinguishable although they are petrographically distinct. This circumstance has its greatest impact on the filtered magnetic data, since it allows the simultaneous removal of both the dike and the diabase anomalies. This is based on the assumption that the bodies are in contact, and that their remanent magnetism vectors are the same.

The combined effects of these two vectors is shown in figure 11. The horizontal rows show how an anomaly varies as the body changes dip while it is fixed. The vertical columns show how the anomaly changes as it rotates and the body remains fixed. An increase or decrease in the magnitude of it will change the anomalies magnitude proportionally.

The second factor to be considered is the size of a body. An anomaly will change in direct proportion to an increase or decrease in the size of the body. This effect is most noticeable when comparing the anomalies of the Jones Camp Dike and magnetite ore. Because of the large size of the Jones Camp Dike it typically forms a broad, high magnitude

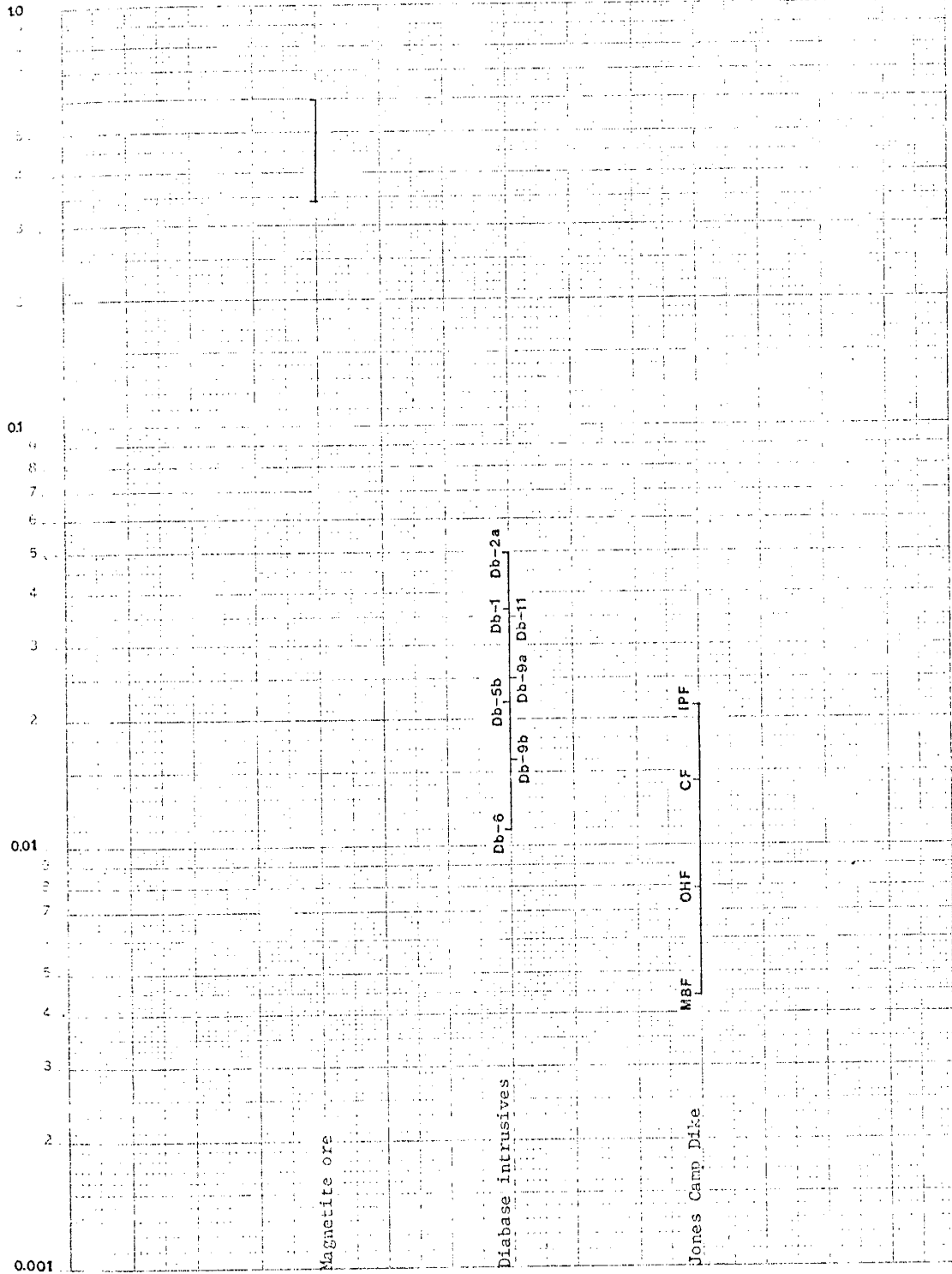


Figure 10, Range of the magnetic susceptibilities for the Jones Camp Dike, the diabase intrusives, and magnetite ore. (emu)

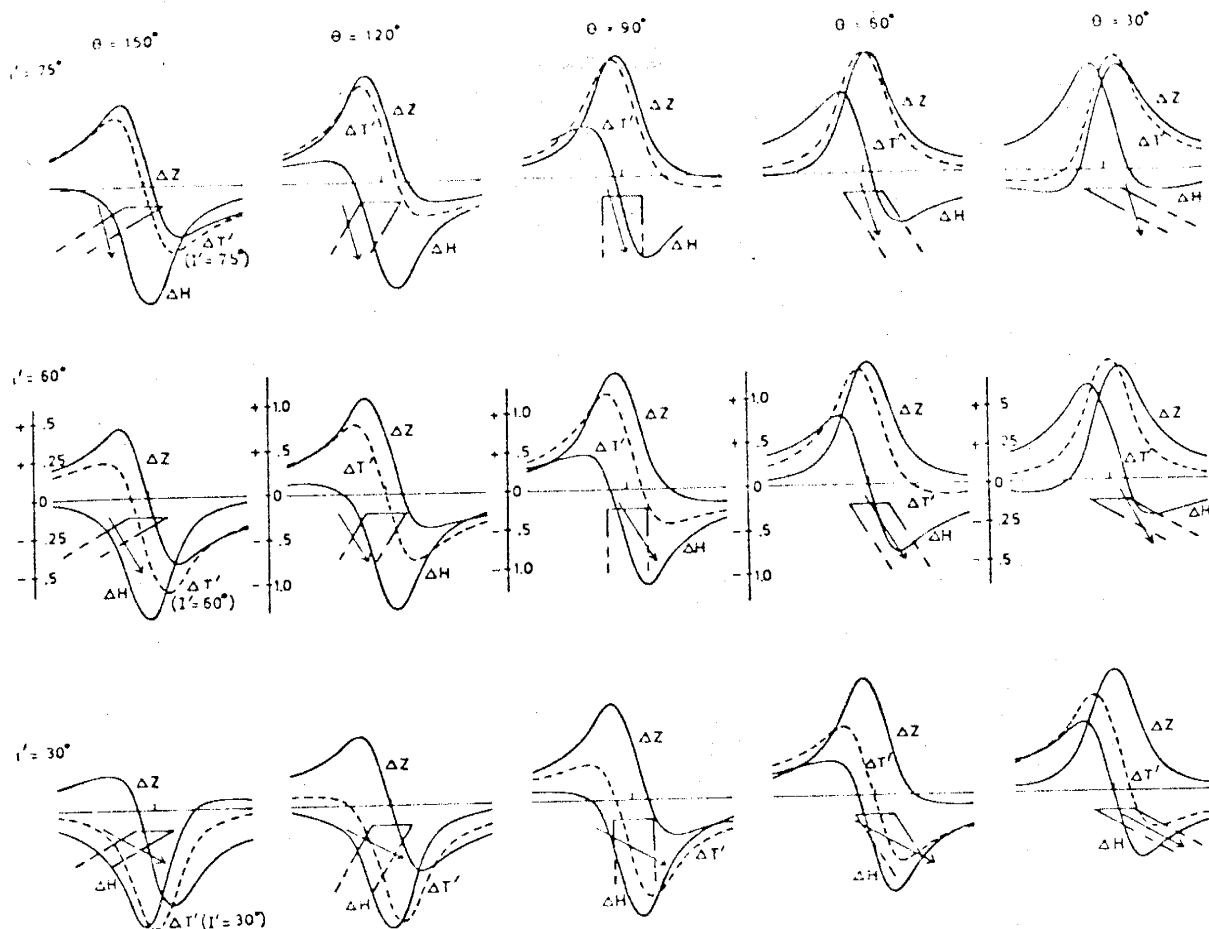


Figure 11. Examples of the variation of horizontal (ΔH), vertical (ΔZ), and total (ΔT) magnetic anomalies as a function of the dip and the direction of magnetism in the body (after Parasnis, 1971). θ = inclination of the body from the horizontal, i' = inclination of magnetism from the horizontal (both measured clockwise from the abscissa).

anomaly. In comparison, ore bodies usually form a narrow anomaly because of their small width, but one of large magnitude because of their high magnetic susceptibility. The diabase intrusives cannot be characterized on this basis because of the variability in their size.

The third factor to be considered is the depth of burial of the body. Unlike the previous factors, as the depth of burial increases, the magnitude of an anomaly decreases. The decrease in magnitude is accompanied by an attenuation in the anomalies sharpness. The relationship between a body's depth of burial and the sharpness of its anomaly is frequently used as a qualitative indication of a body's depth.

A fourth factor to be considered, unrelated to those controlling the character of an anomaly, is the effect of lightning strokes. Lightning-caused anomalies can cover areas up to several hundred square feet and have magnitudes of 1000 gammas or more (Grant, 1965). In the study area they are probably concentrated along the Jones Camp Dike, and account for many of the erratic peaks located over the dike.

From this discussion it should be clear that a magnetic anomaly is not constituted solely on the basis of magnitude, but that it is necessary to consider all of the factors involved when judging an anomaly's significance. It should also be clear that the simplest way to do this is by correlating the magnetic and geologic data.

Qualitative Analysis of the Magnetic Data

Most of the magnetic profiles in the study area reveal composite anomalies. They reflect the super-position of anomalies from two or more discrete bodies. Figure 12 is a typical profile. Each anomaly along the profile is correlatable with a body of rock plotted on the cross-section. Even within each discrete body there is some irregularity in the anomaly caused by variations of magnetic susceptibility in the body itself (Fig. 10).

The primary use of the magnetic data in this study is to expand the strike length of known ore bodies. Roughly 35% of the total mineralized strike length or 4,850 feet (1.48 km) is inferred this way. In addition three areas are targeted for further study.

The largest expansion of an ore body is at the East-pit. It lies on the north side of the dike between profiles 44 and 50. Here a large continuous magnetic anomaly correlates well with the geology and extends 1,300 feet (396 m) east of the last ore outcrop. Between profiles 44 and 45 the anomaly is displaced 350 feet (107 m) north along what may be a left lateral fault.

The three areas targeted for further study are:

- 1) north of the Jones Camp Dike between profiles 21 and 28
- 2) south of the dike between profiles 91 and 95, and
- 3) north of the dike between profiles 101 and 105.

Profiles 21 and 28 lie approximately 600 feet east of the East-pit. These anomalies may reflect an extension of the East-pit, but their irregular and complex character suggest a difference between the two areas. Increased sampling along these profiles may account for some of the complexity, but a comparison of the south end of the profiles with more

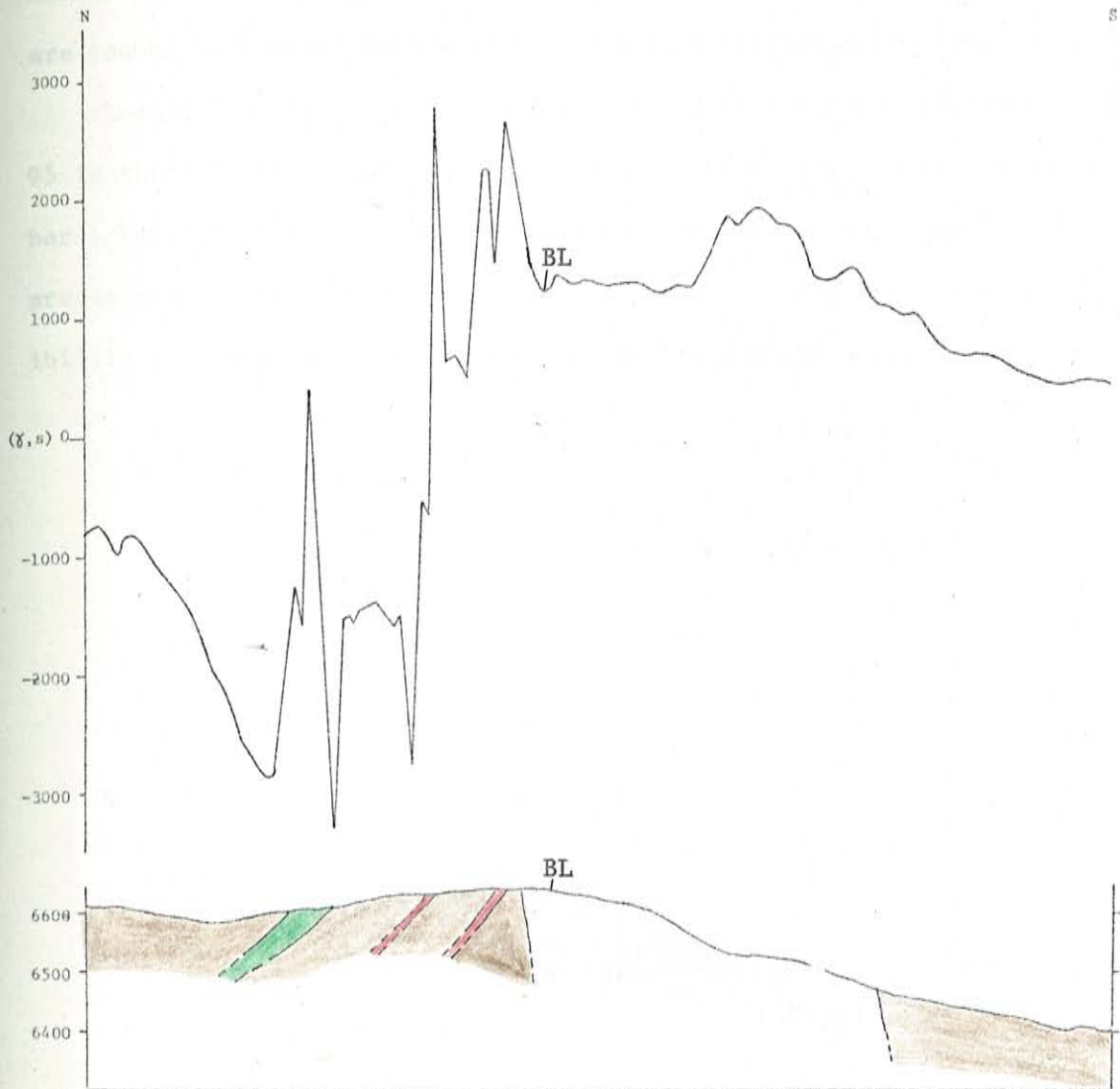




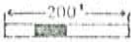


Figure 12. Generalized cross section across profile 59, showing the relationship of rock types and magnetic anomalies. (Magnetic measurements were made at 10 foot intervals.)

-  Magnetite ore
 -  Jones Camp Dike "undifferentiated"
 -  Diabase intrusive
 -  Sediments
- Baseline point (Bl.)
- Scale: 

broadly sampled regions suggests that this is only part of the reason. Because of the character of the anomalies the author believes that they are caused by mineralization which is structurally complicated.

Located southeast of the Section 17 Prospect between profiles 91 and 95 is the second area of interest. Only a trace of magnetite is exposed here, but the character and lateral extent of the anomaly suggest the presence of a significant ore body. Geologic mapping indicates the possibility of potential host rocks close to the surface also.

ECONOMIC GEOLOGY

The results of the preliminary feasibility study presented in Appendix II suggest that a profitable open pit mine can be operated in the study area. Since the original study's completion, a new market has emerged for gypsum overburden. If the major additional costs of loading and trucking the gypsum can be minimized, the operation should benefit from this new market. Using operating costs from Appendix II, the raw gypsum must have a market value of 5 to 6 dollars per ton to make a profit.

Currently the Jones Camp Deposit is in the early stages of development drilling at one of two locations along the dike. The Section 17 Prospect (plate 3), where drilling has begun is located in T5S, R7E, and the Section 19 Prospect (plate 4) is located in T5S, R8E. (Overlay 1 shows the exact location of each prospect.) A detailed drilling plan is presented for both prospects. Ore intercepts along each drill hole are shown on cross sections accompanying the geologic maps. Some of the ore intercepts will change position as the drilling data develops a more accurate picture of the subsurface structure. Tables 1 and 2 summarize the length and inclination of each drill hole.

Through analysis of the magnetic data four areas have been targeted for future study. They are:

- 1) directly east and west of the East-pit ore body,
- 2) south of the dike between profiles 91 and 95 in Section 17, T5S, R7E, and
- 3) north of the dike between profiles 101 and 105 in Section 18, T5S, R7E.

(The details of each area are discussed in the geophysical summary.)

Profile	Hole #	Angle from horizontal (degrees)	Length
A-A'	1	20	175'
	2	40	180'
	3	65	180'
B-B'	1	20	220'
	2	35	170'
C-C'	1	20	240'
	2	40	190'
D-D'	1	25	175'
	2	20	220'
	3	30	230'
E-E'	1	15	235'
	2	28	250'
	3	45	290'
F-F'	1	20	180'
	2	30	270'
	3	20	270'
G-G'	1	20	175'
	2	35	185'
	3	48	210'
H-H'	1	40	160'
	2	60	210'
	3	74	255'
I-I'	1	20	200'
	2	50	250'
	3	68	220'
	4	77	280'
J-J'	1	35	150'
	2	60	210'
	3	70	220'
K-K	1	20	170'
	2	48	220'
	3	68	215'

Table 1. Summary of proposed drill hole lengths and dips for the Section 17 Prospect.

Profile	Hole #	Angle from horizontal (degrees)	Length
A-A'	1	20	285'
	2	40	260'
	3	70	240'
B-B'	1	20	230'
	2	55	215'
	3	70	180'
C-C'	1	20	215'
	2	70	330'
	3	70	340'
	4	70	340'
D-D'	1	20	170'
	2	50	190'
	3	70	270'
	4	70	260'
E-E'	1	20	180'
	2	45	175'
	3	50	210'
	4	70	255'
F-F'	1	20	180'
	2	70	245'
	3	70	320'
	4	70	370'
	5	75	365'

Table 2. Summary of proposed drill hole lengths and dips for the Section 19 Prospect.

Based on this study, the author recommends that future drilling programs focus on intercepting favorable stratigraphic horizons (limestone-sandstone contacts) of the Torres member of the Yeso Formation near areas of diabase intrusion along the Jones Camp Dike. This target offers the most potential per dollar spent because of its predictable location and known favorability.

Grade and Tenor of Ore

Grantham and Soule (1947) reported an average ore grade of 55.82% Fe with a range from 41.96% to 62.04%, based on 235 samples taken from 19 ore bodies by the U. S. Bureau of Mines in 1947. The best replacement ores are likely to occur in limestone. Ores from the East-pit and others containing significant amounts of gypsum will have milling problems. Sulphides which commonly occur with these ores can also cause metallurgical problems. Ores occurring in sandstone and some diabase bodies will have higher than average silica contents. Near surface weathering has improved the quality of ores replacing limestone and gypsum (Kelley, 1949).

Ore Reserve Estimates

A deficiency of drilling information in the study area causes a large variation in ore reserve estimates. The greatest uncertainty is in estimating the down dip extent of mineralization. A maximum of 1,712,535 tons of probable reserves and 3,091,736 tons of possible reserves is estimated for the deposit. These figures are based on an average ore horizon thickness of 8.83 feet (2.69 m) (Kelley, 1949) and a 100 foot (30.48 m) down dip extent of mineralization. The author prefers a more conservative estimate of 1,117,940 tons of probable reserves and 1,575,630 tons of possible reserves, based on an average

ore horizon thickness of 6 feet (1.83 m) and a 75 foot (22.86 m) down dip extension of mineralization.

REFERENCES

- Balsley, J. R. and Buddington, A. F., 1958, Iron-titanium oxide minerals, rocks, and aeromagnetic anomalies of the Adirondack Area, New York: Economic Geology, vol. 53, p. 777-805.
- Bath, G. D., 1962, Magnetic anomalies and magnetizations of the Biwabik Iron Formation, Mesabi area, Minnesota: Geophysics, vol. 27, p. 627-650.
- Dobrin, M. B. 1960, Introduction to geophysical prospecting: McGraw-Hill, Toronto, p. 308-311.
- Dreyer, R. M. 1978, Principle of evaluation of lateritic ores: Mining Engineering, vol. 30, no. 8, p. 1201-1202.
- Emmens, N. W. 1906, The Jones Iron Fields of New Mexico: Mining Magazine, vol. 13, p. 109-116.
- Eugster, H. P. and Chou, I., 1979, A model for the deposition of Cornwall-type magnetite deposits, Economic Geology, vol 74, p. 763-774.
- Folk, R. L., 1974, Petrology of sedimentary rocks: Hemphill Pub. Co., Austin, Texas, 182 p.
- Grant, F. S. and West G. F., 1965, Interpretation theory in applied geophysics: McGraw-Hill, p. 355-381.
- Grantham, R. M. and Soule, J. H., 1947, Jones iron deposit, Socorro Country, New Mexico: U. S. Bureau of Mines, Report of Investigation 4010, 4 p.
- Green, R., 1960, Remanent magnetism and the interpretation of magnetic anomalies: Geophysical Prospecting, vol. 8, p. 98-110.
- Gupta, V. K. and Fitzpatrick, M. M., 1971, Evaluation of terrain effects in ground magnetic surveys: Geophysics, vol. 36, no. 2, p. 582-589.

- Johannsen, A., 1937, A descriptive petrography of the igneous rocks, Volumes I, II, and III: The Univ. of Chicago Press, Chicago, Illinois.
- Jones, F. A., 1904, New Mexico mines and minerals: The New Mexico Printing Co., Santa Fe, N. M., p. 102-103.
- Kelley, V. C., 1949, Geology and economics of New Mexico iron ore deposits: The Univ. of New Mexico Press, Albuquerque, N. M., p. 213-223.
- Kelley, V. C. and Thompson, T. B., 1964, Tectonics and general geology of the Ruidoso-Carrizozo Region, central New Mexico: New Mexico Geological Society Guidebook, 15th Field Conference, p. 110-121.
- Keyes, C. R., 1904, Iron deposits of Chupadera Mesa: The Engineering and Mining Journal, p. 632.
- Keyes, C. R., 1915, Foundations of exact geologic correlation: Iowa Acad. Sci., Pr., vol. 22, p. 249-267.
- Lee, W. B., 1909, The Manzano group of the Rio Grande Valley, New Mexico: U. S. Geological Survey, Bull, 380, p. 141.
- Lindgren, W., Graton, L. C. and Gordon, C. H., 1910, U. S. Geological Survey Prof. Paper no. 68: p. 203-204.
- Muehlberger, W. R. and Baldwin, B., 1958, Field method for determining direction of magnetization as applied to late Cenozoic basalts, Northeastern New Mexico: Journal of Geophysical, Res. 63, p. 353.
- Needham, C. E. and Bates, R. L., 1943, Permian type sections in central New Mexico: Geol. Soc. Am. Bull., vol. 54, p. 1653-1668.
- Nettleton, L. L., 1976, Gravity and magnetics in oil prospecting: McGraw-Hill, p. 464

- Nogueira, A. C., 1971, Mineralogy and geochemistry of contact metasomatic iron deposits at Jones Camp, Socorro County, New Mexico: Unpub. Master of Science thesis, New Mexico Institute of Mining and Technology, 86 p.
- Parasnis, D. S., 1971, Principles of applied geophysics: Chapman and Hall, London, 214 p.
- Parasnis, D. S., 1975, Mining geophysics 2nd edition: Elsevier Scientific Pub. Co., 388 p.
- Park, P. E., 1973, Cost engineering analysis: John Wiley & Sons, 308 p.
- Peters, W. C., 1978, Exploration and mining geology: John Wiley & Sons, 696 p.
- Read, C. B. and Andrews, D. A., 1944, U. S. Geological Survey Oil and Gas Investigations, preliminary map 8: U. S. Geological Survey.
- Strangeway, D. W., 1961, Magnetic prospecting of diabase dikes: Journal of Geophysical Research, vol. 66, p. 3021-3032.
- Telford, W. M., Geldart, L. P., Sheriff, R. E. and Keys, D. A., 1976 Applied geophysics: Cambridge Univ. Press, Cambridge Mass., p. 105-216.
- Travis, R. B., 1955, Classification of rocks: Quarterly of the Colorado School of Mines, vol. 50, no. 1, 98 p.
- Wilpolt, R. H. and Wanek, A. A., 1951, U. S. Geological Survey Oil and gas investigations, map OM 121: U. S. Geological Survey

APPENDIX I

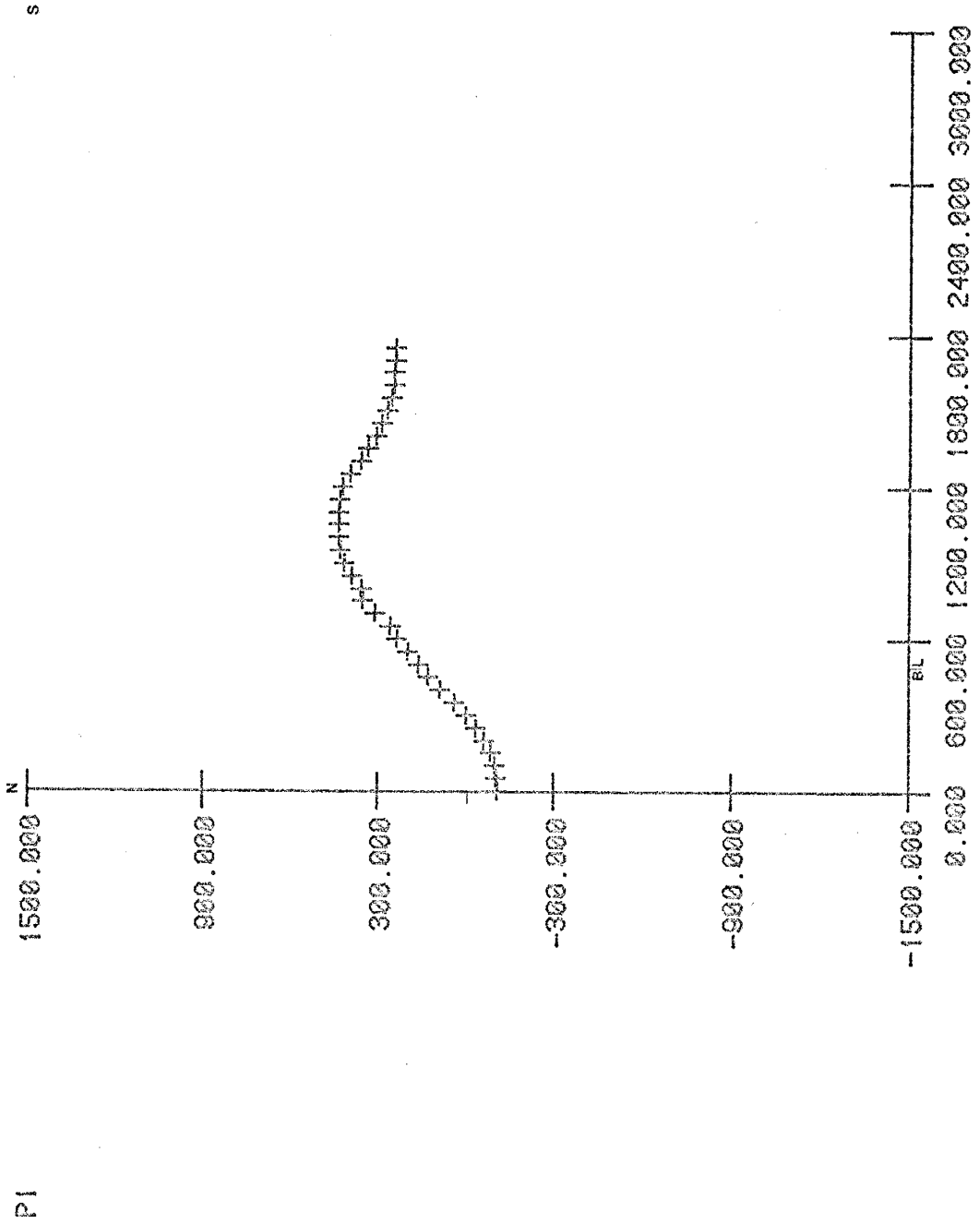
Total Field Magnetic Data

Table of Contents	Page
A) Profiles of normally corrected magnetic data	57
B) Profiles of normally corrected magnetic data with hand fitted approximations of the magnetic anomaly of the Jone Camp Dike	170

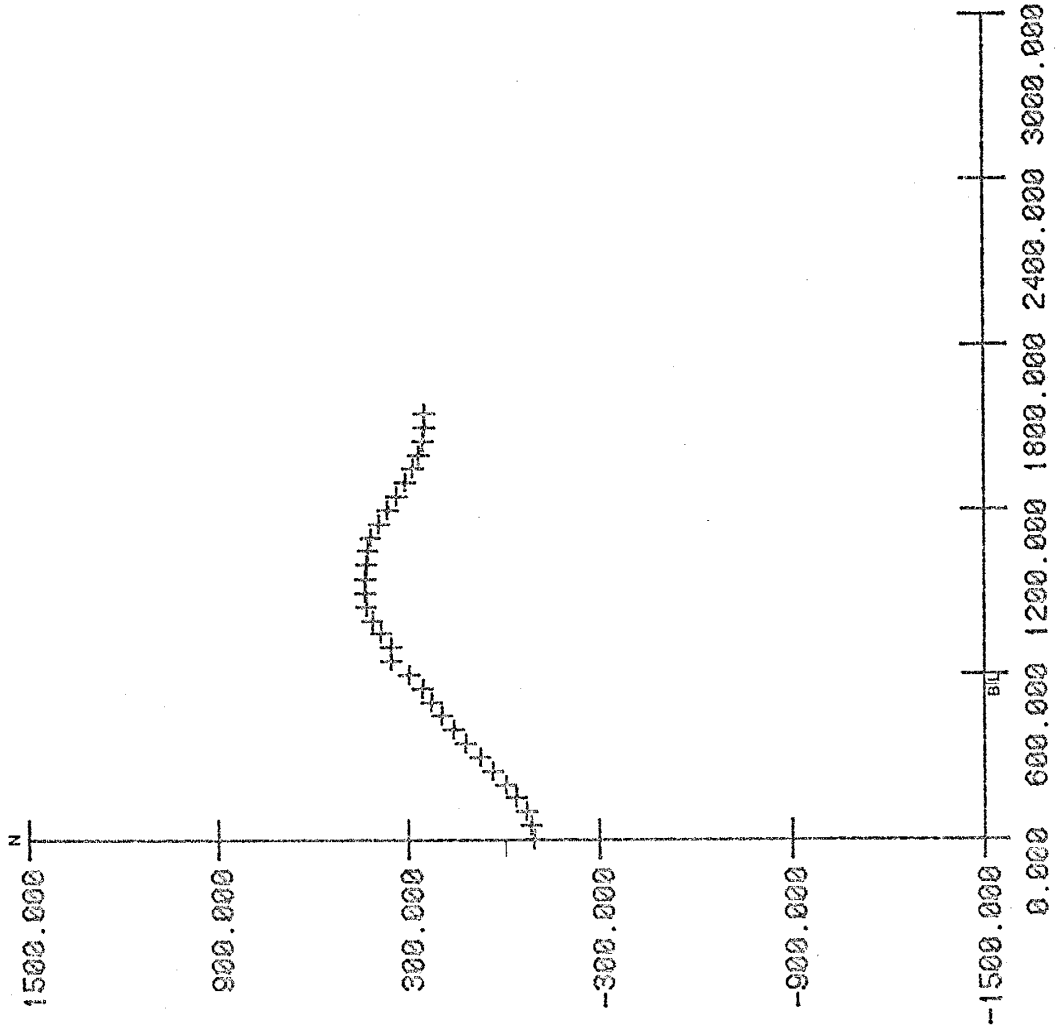
Explanation of abbreviations

BL: baseline
D: Jones Camp Dike
Db: diabase
S: sediments

Ordinates are in units of gammas.
Abcissas are in units of feet.



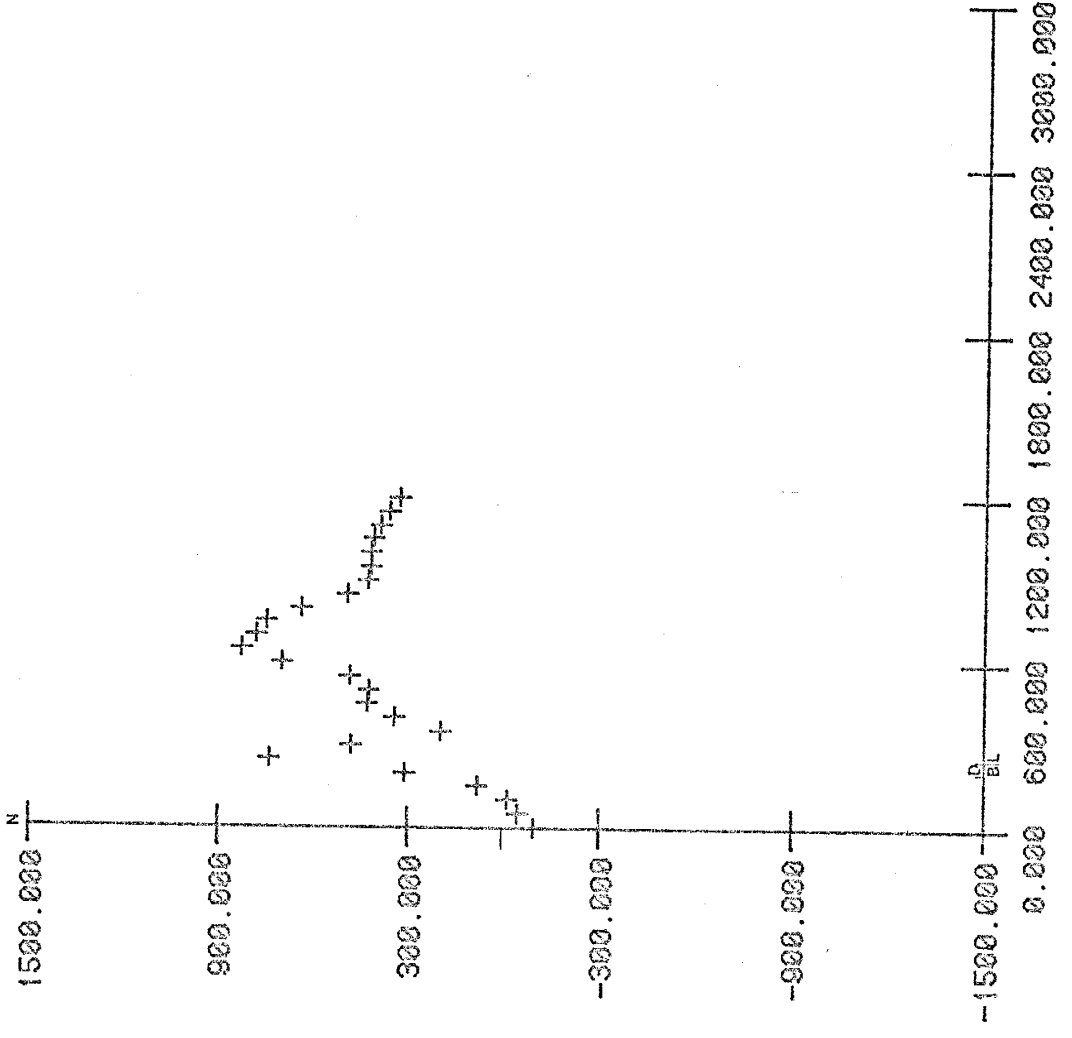
S



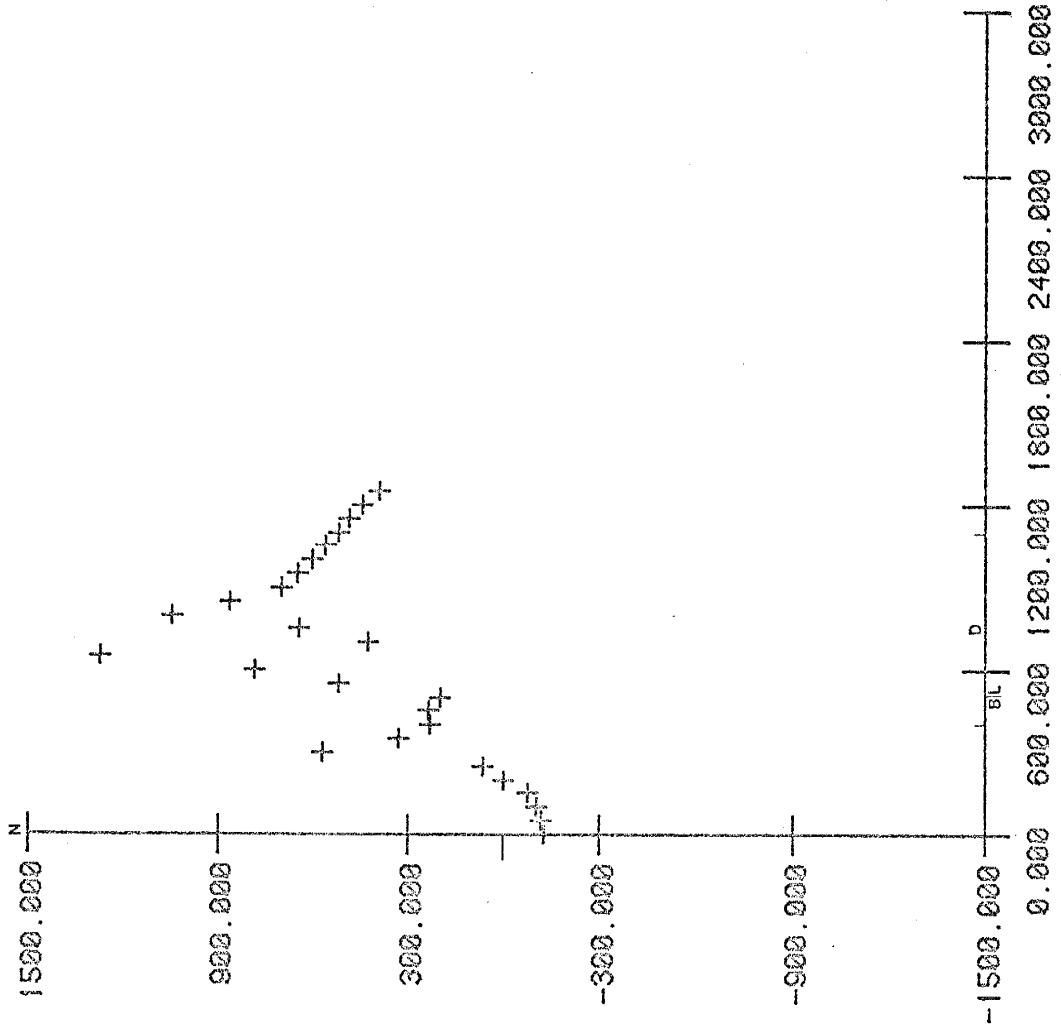
P2

P3

s

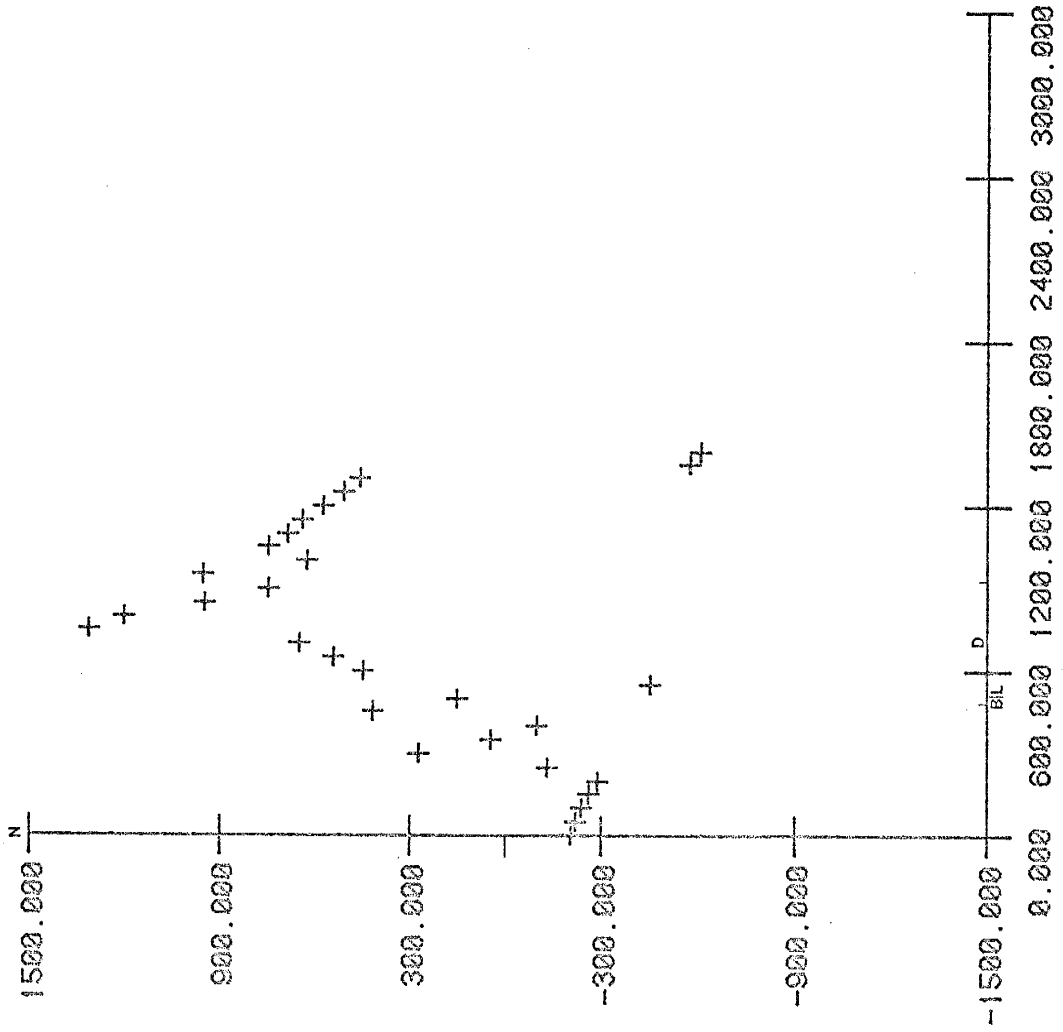


S



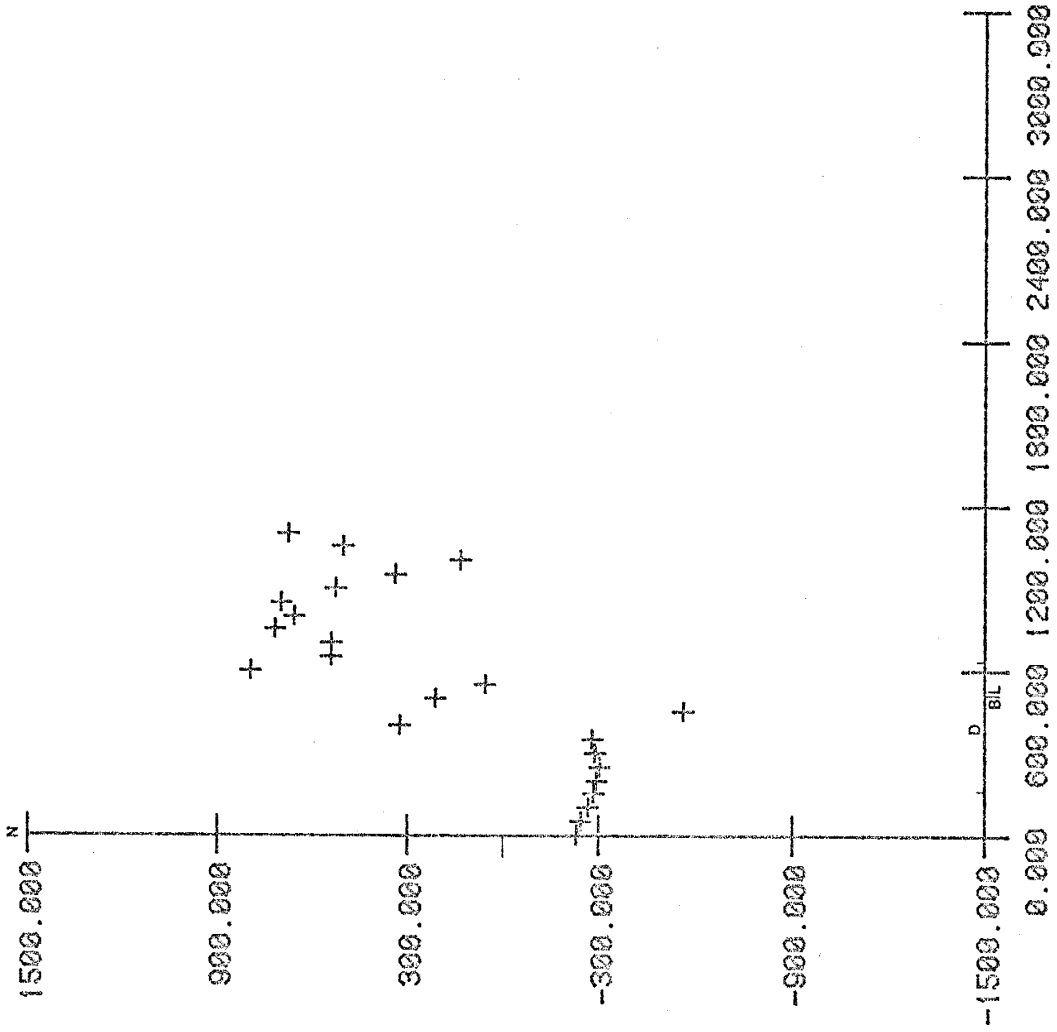
P4

s

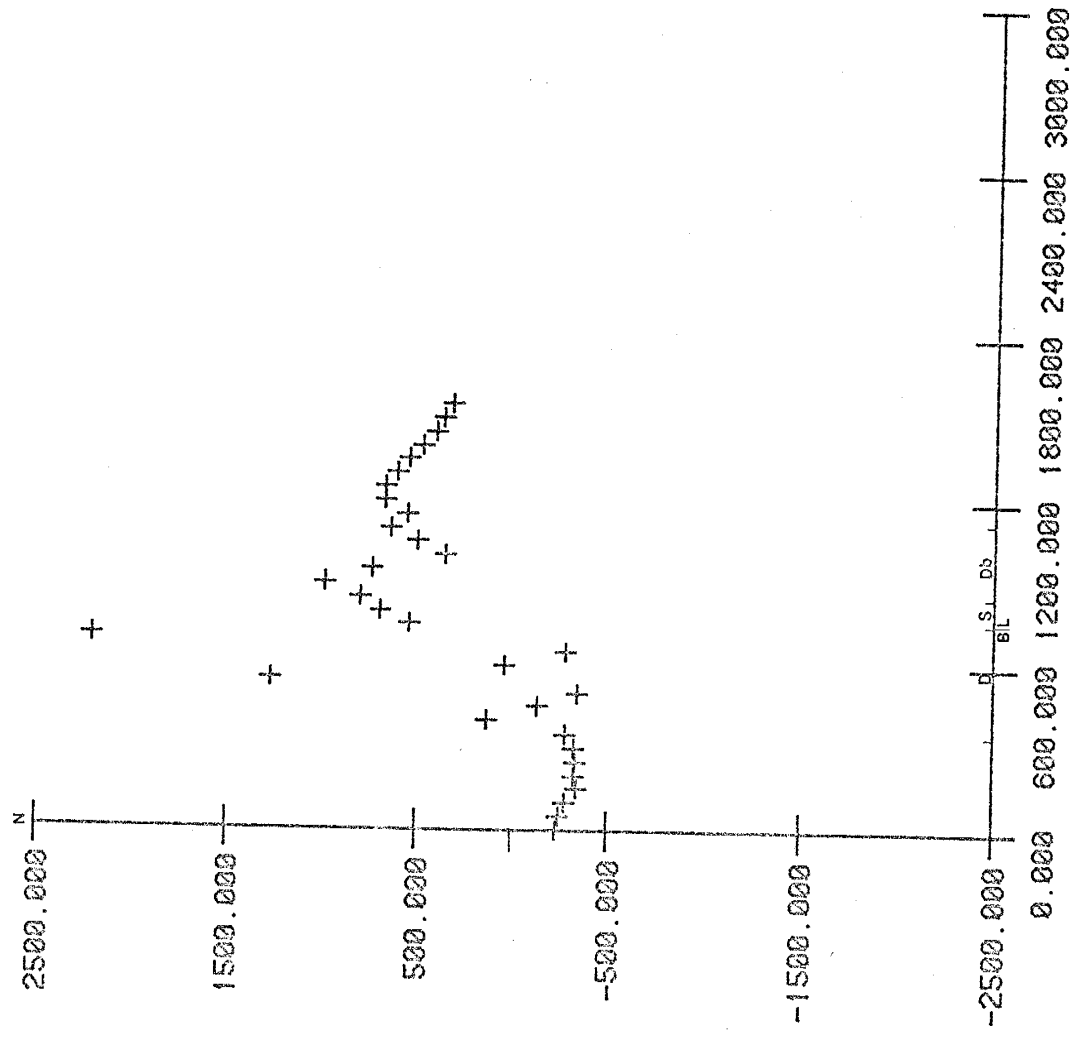


P5

s

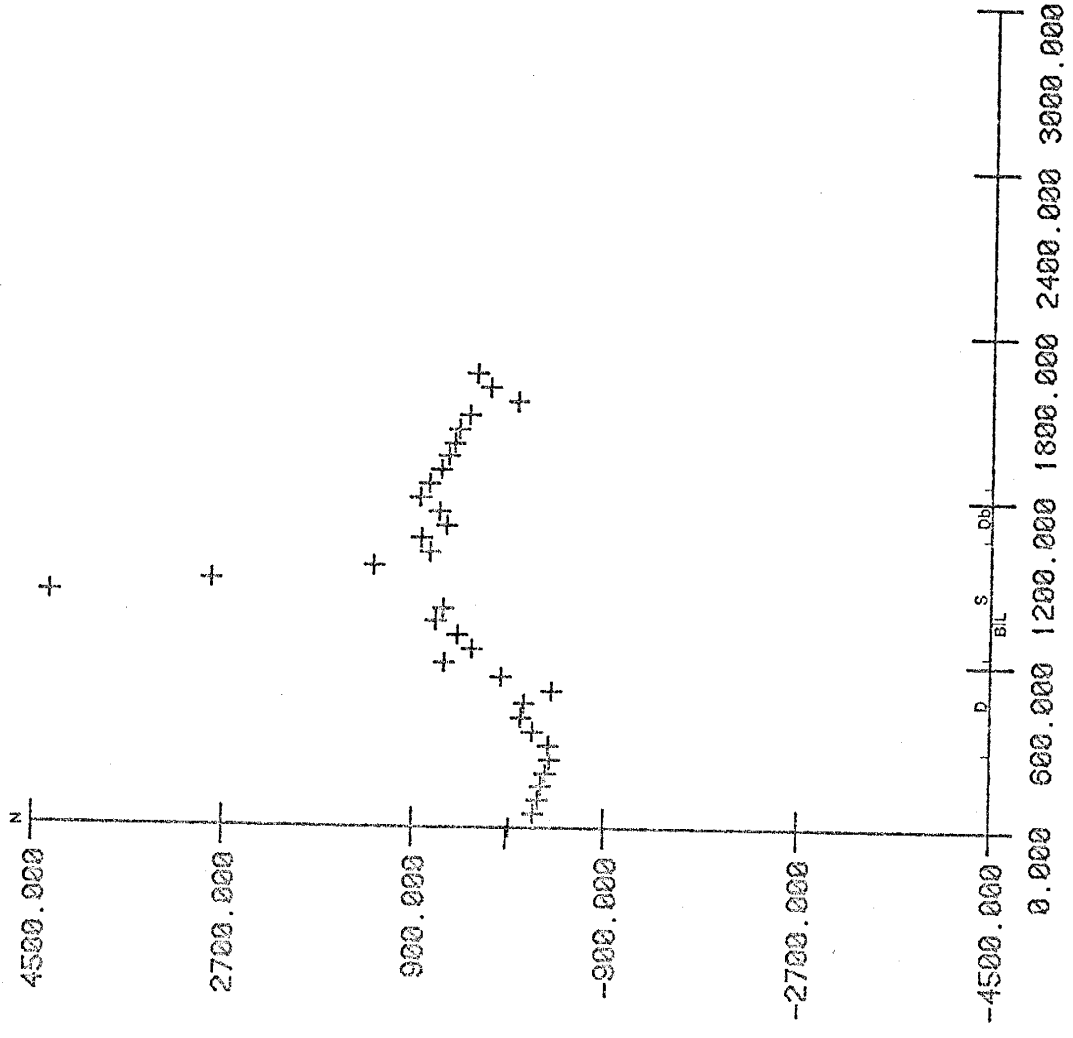


S



P7

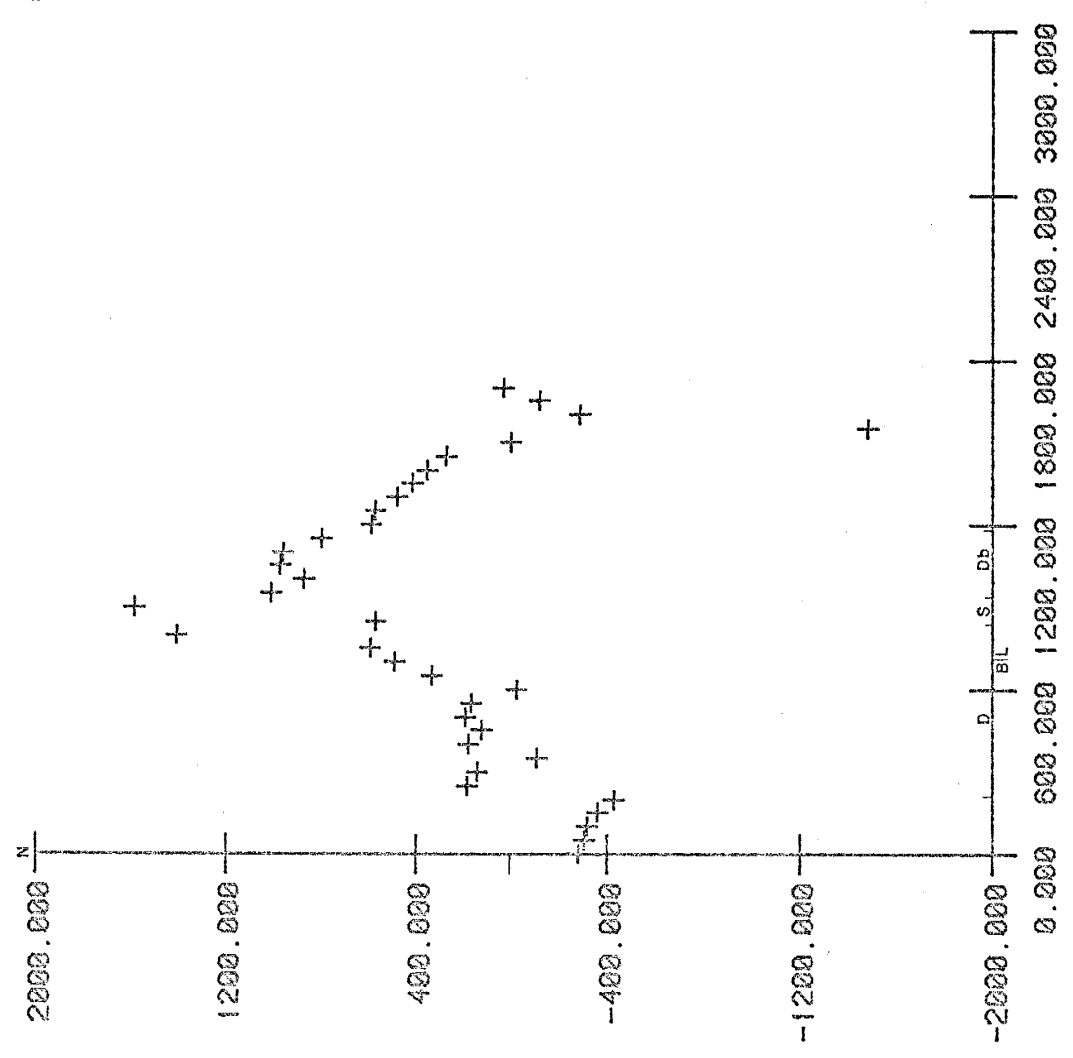
S

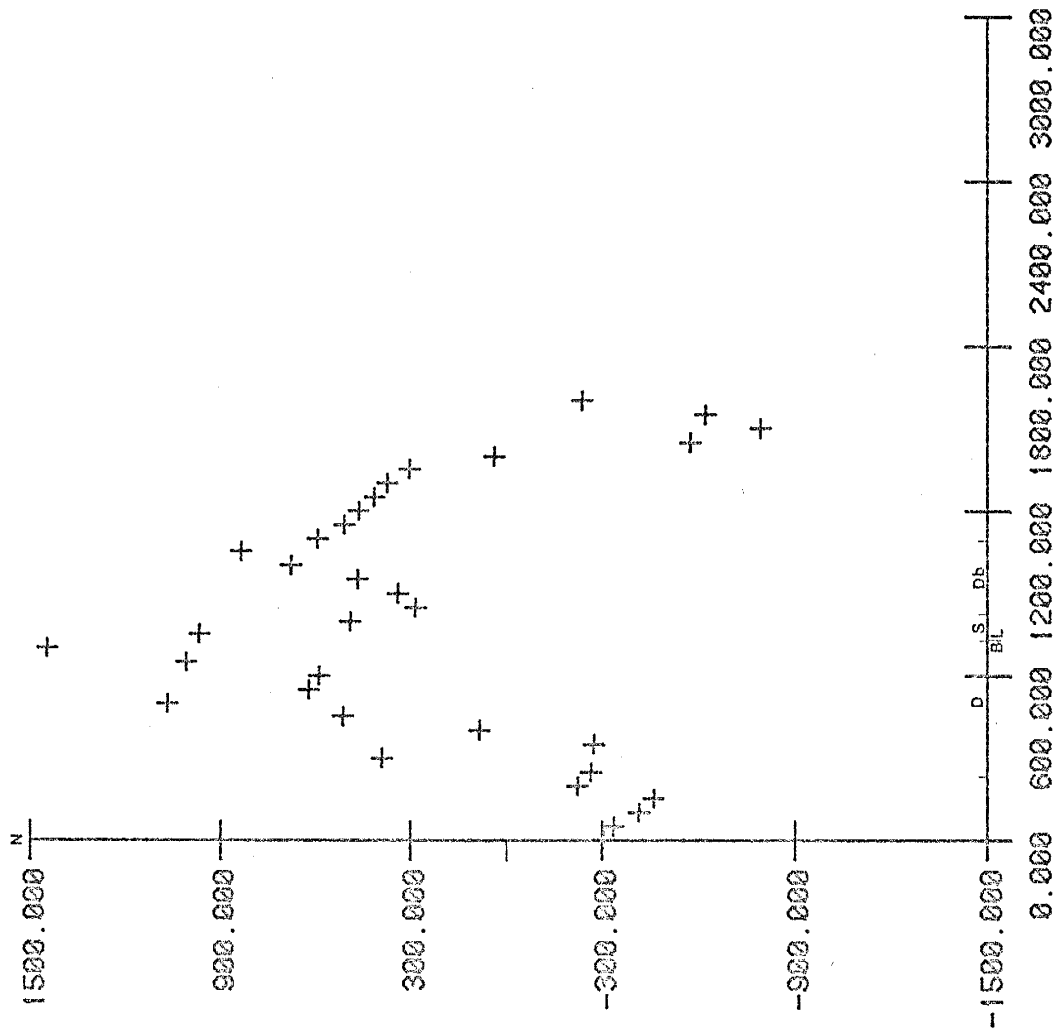


P8

P9

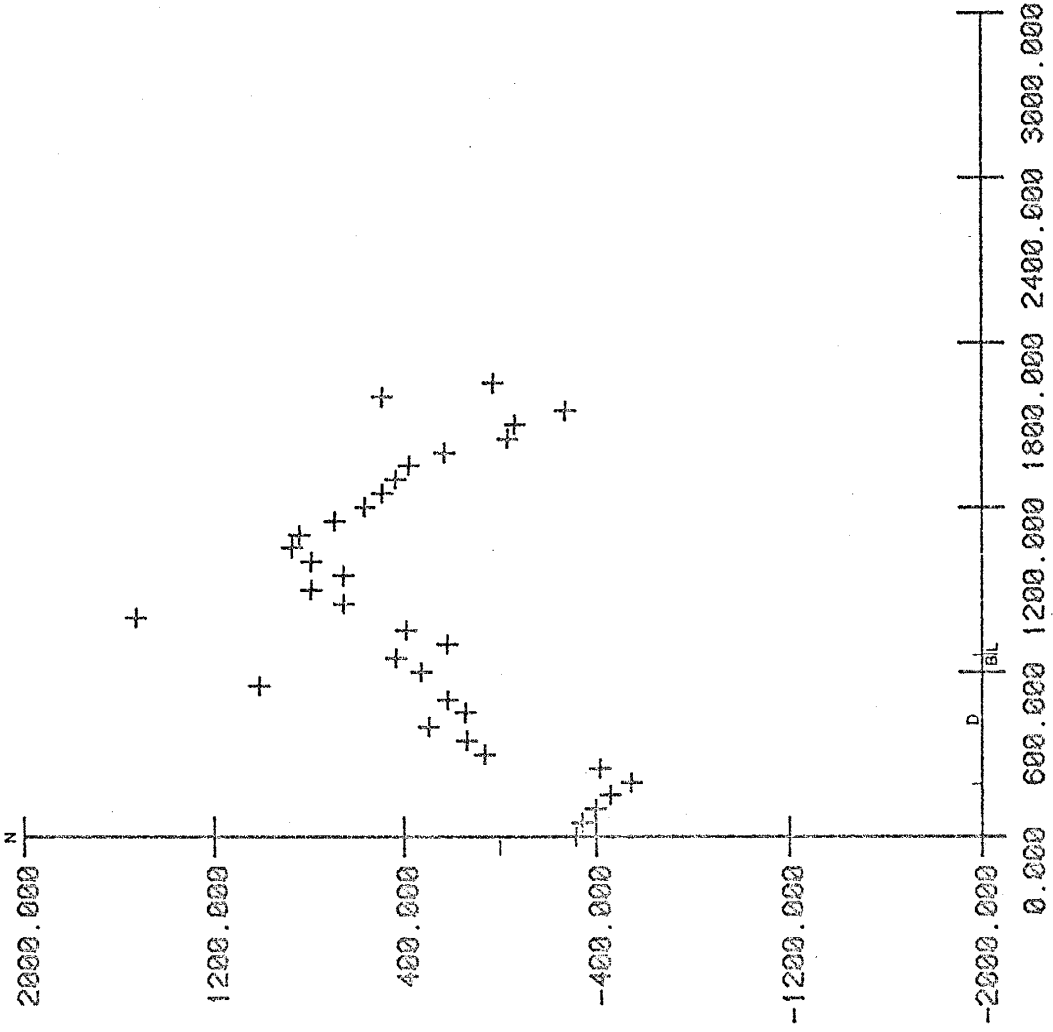
S





P10

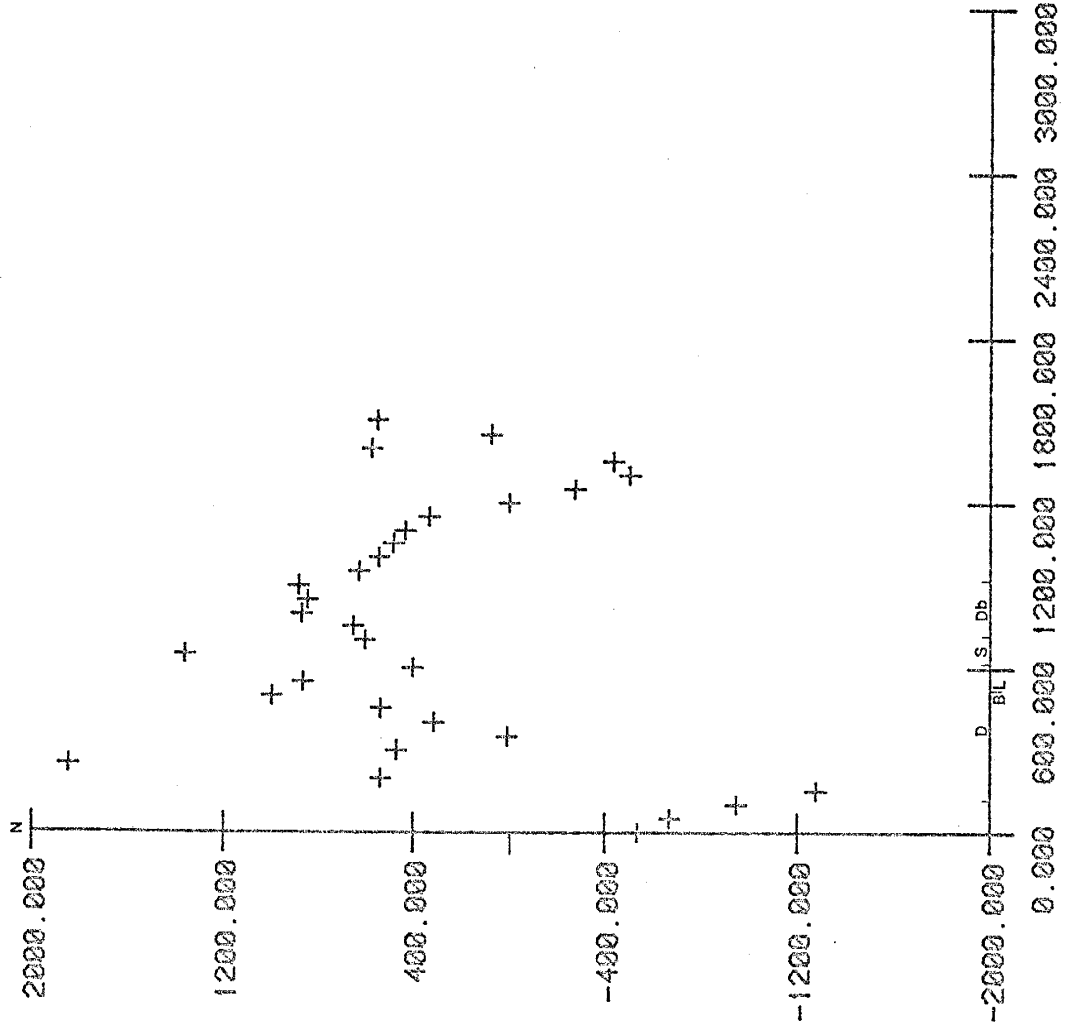
S



P11

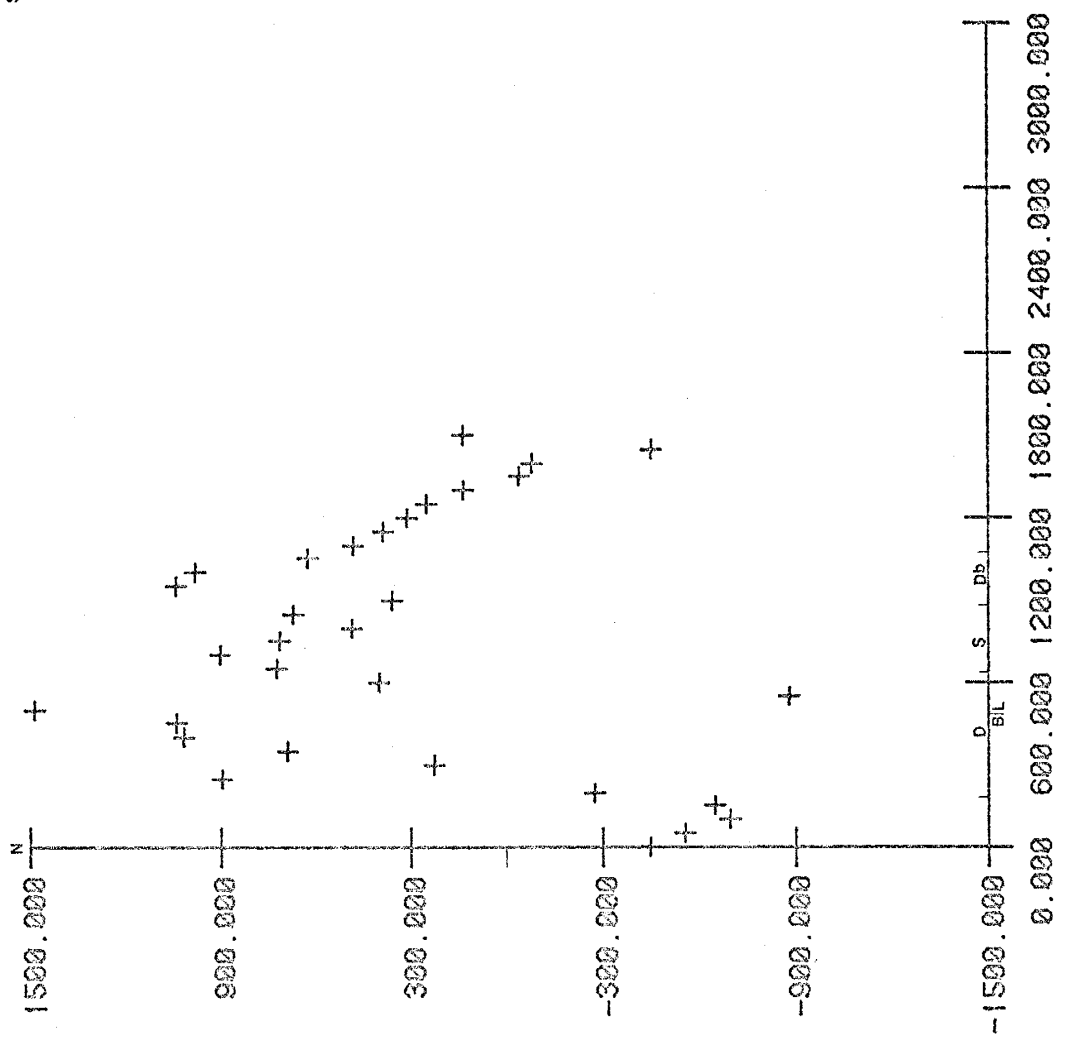
P12

S

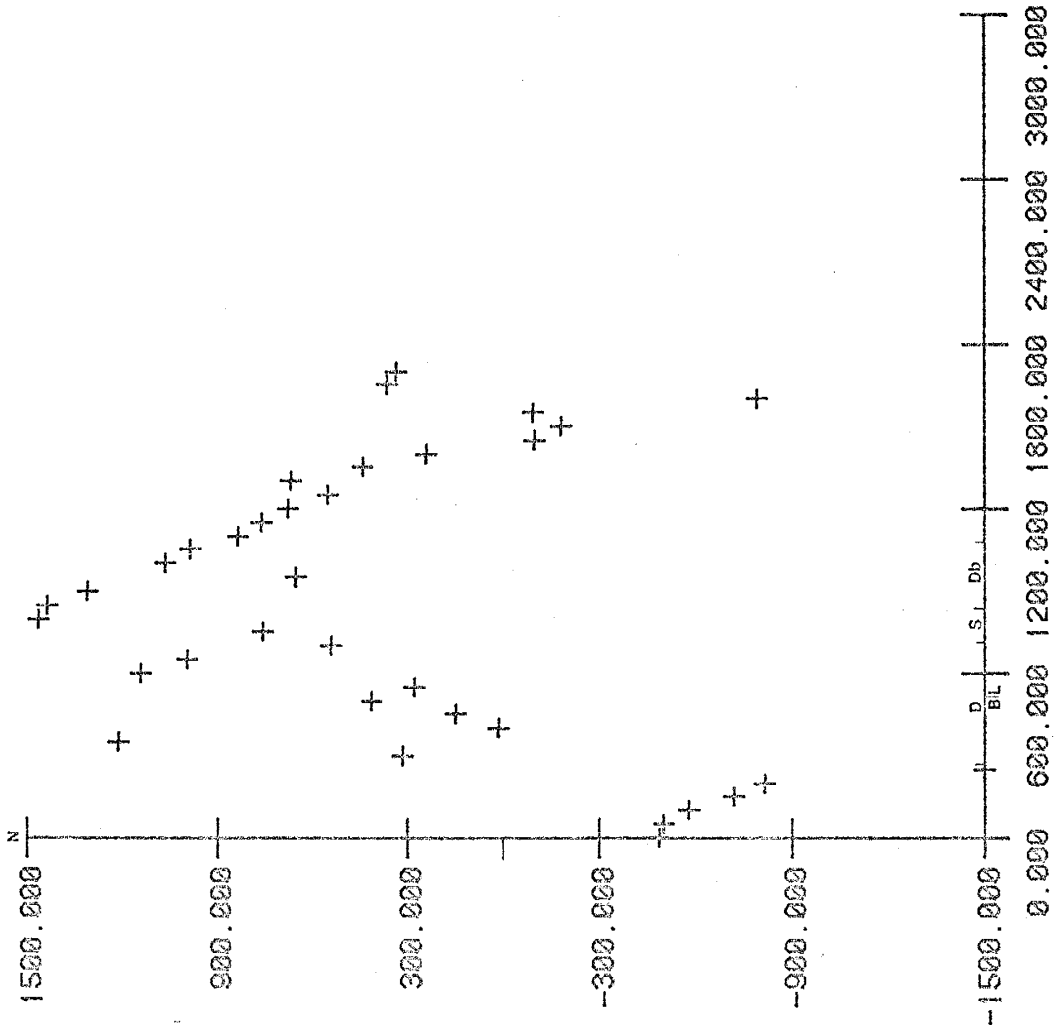


5

P13

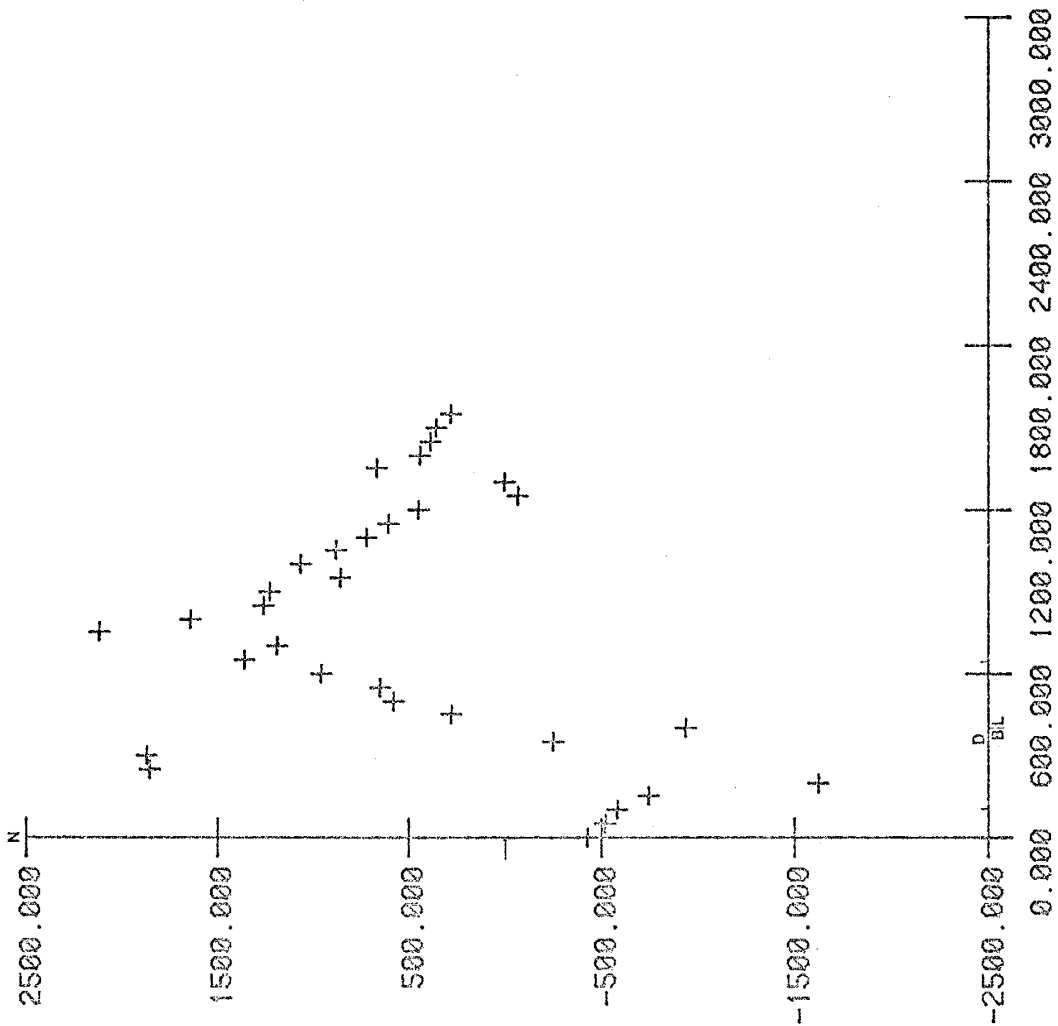


S



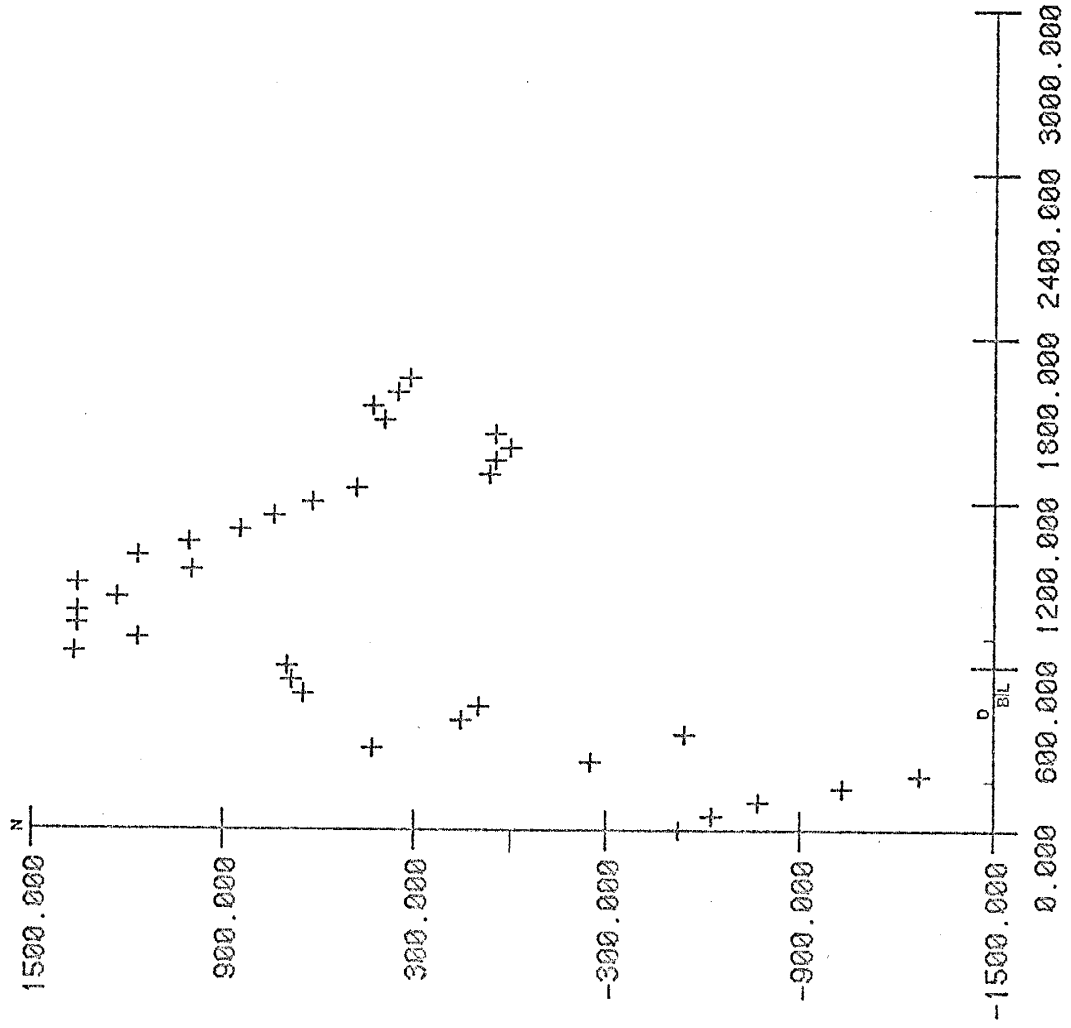
P14

s

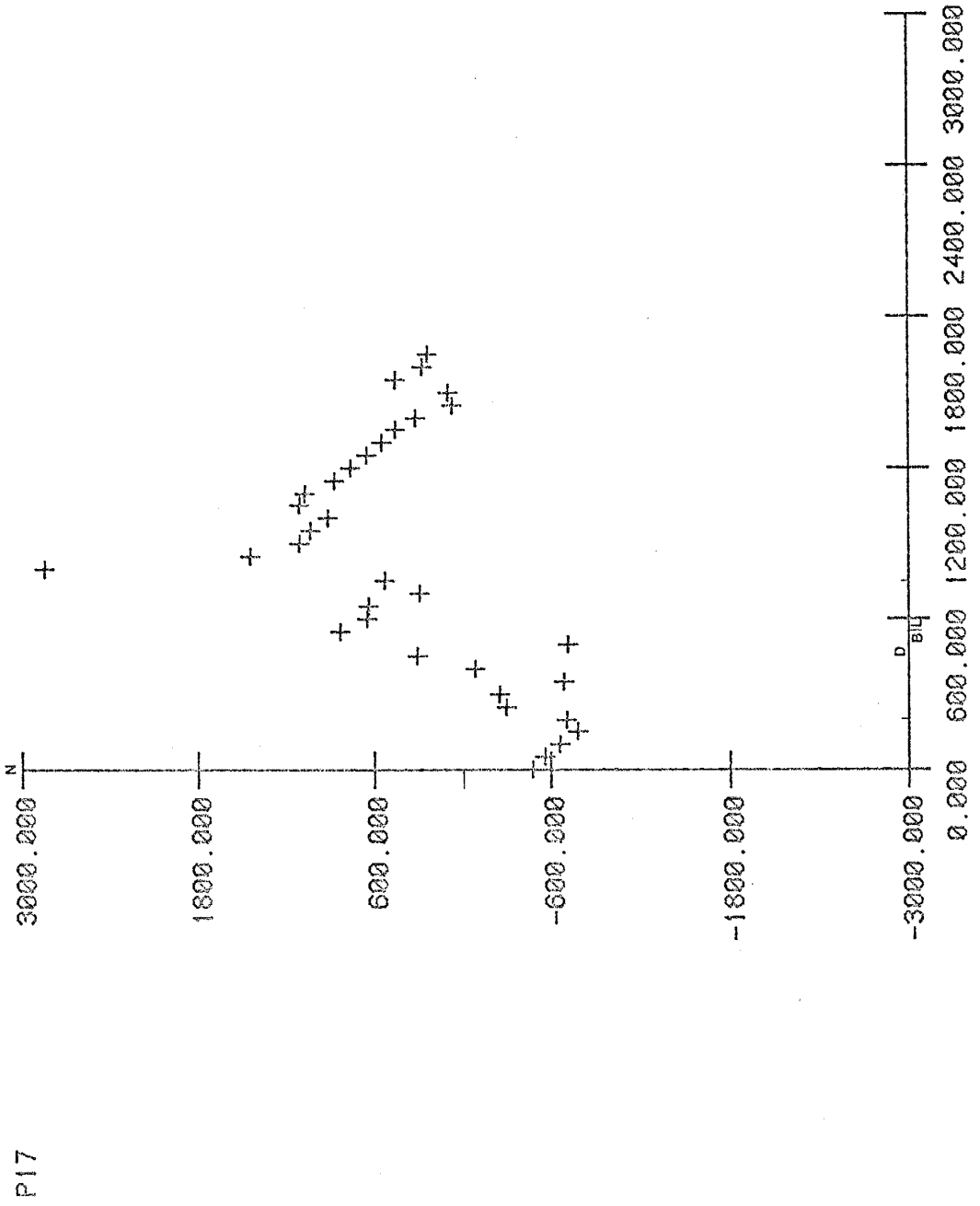


P16

S

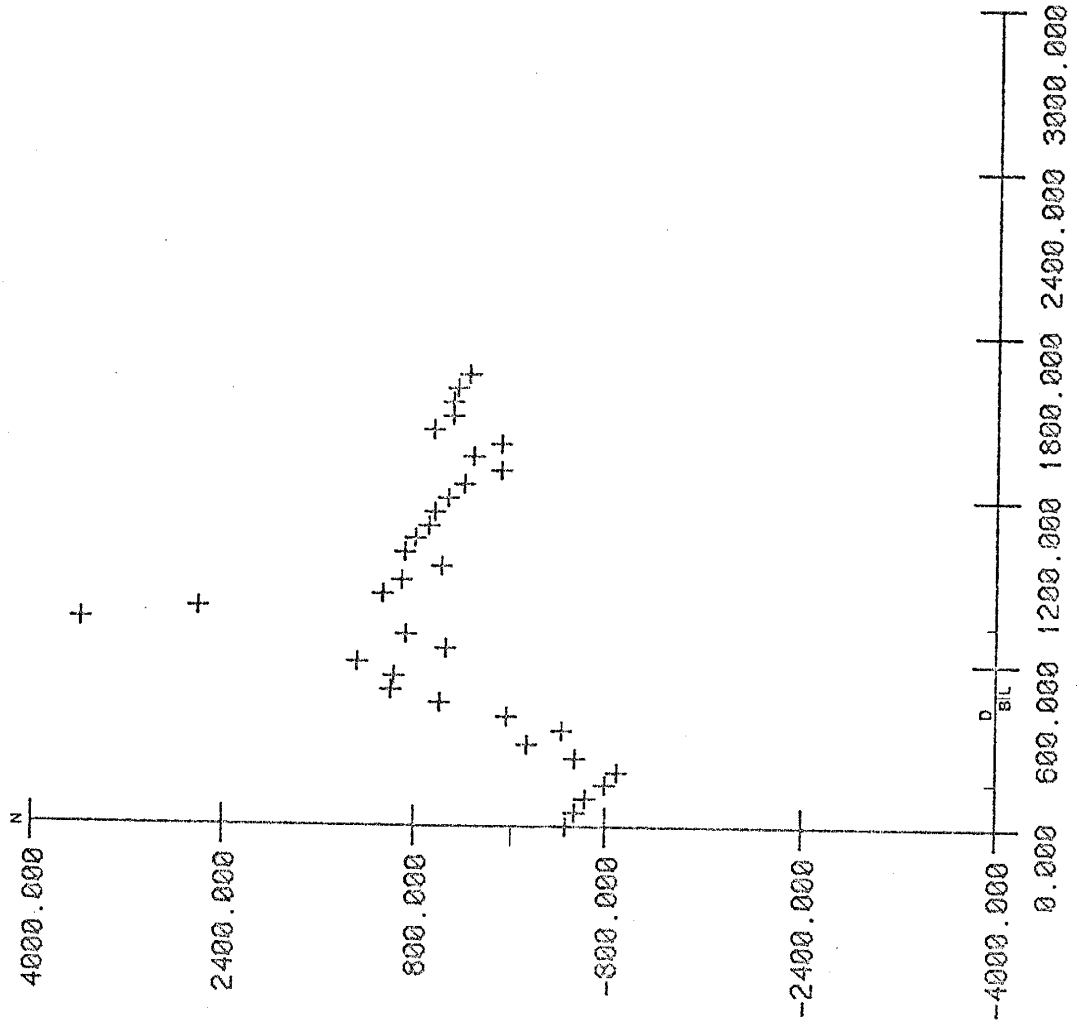


5

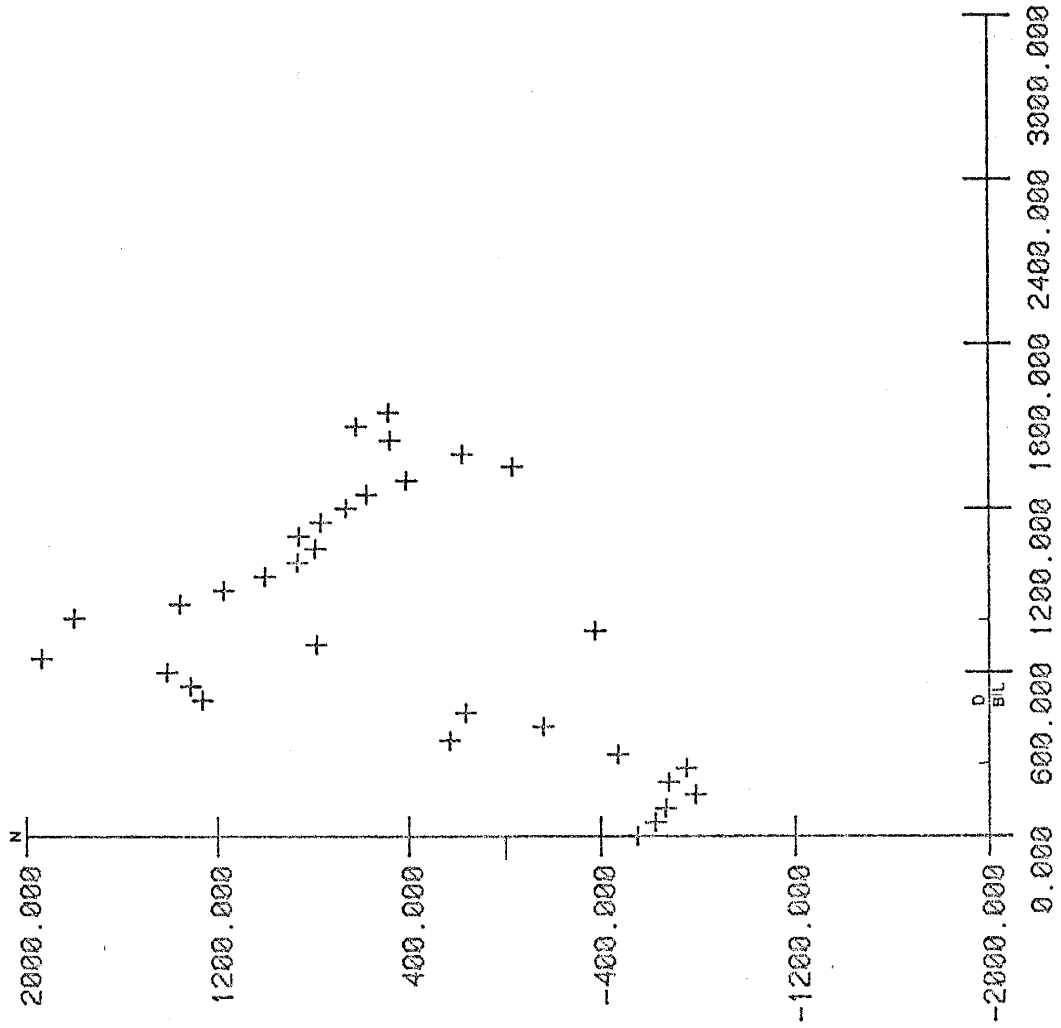


P18

5

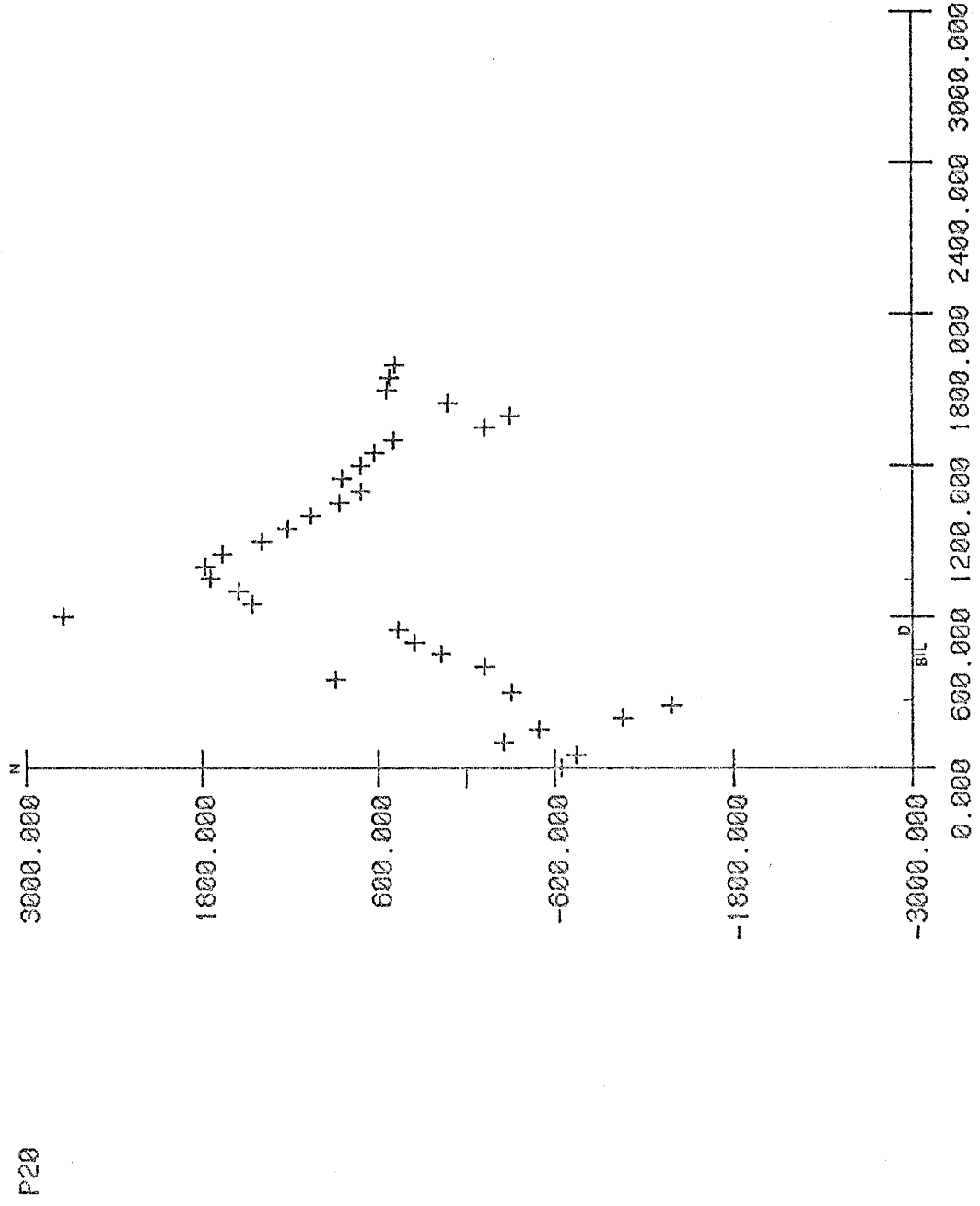


S

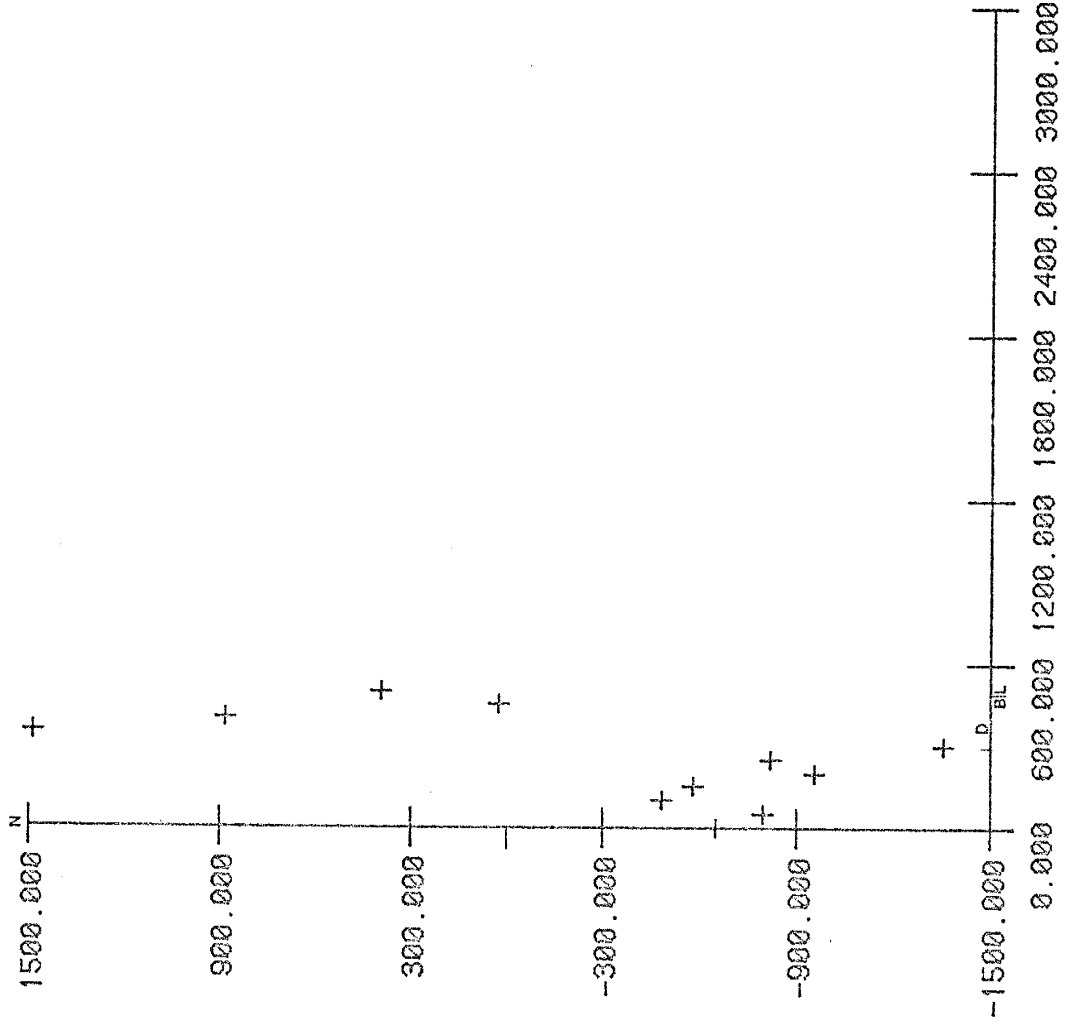


P19

S

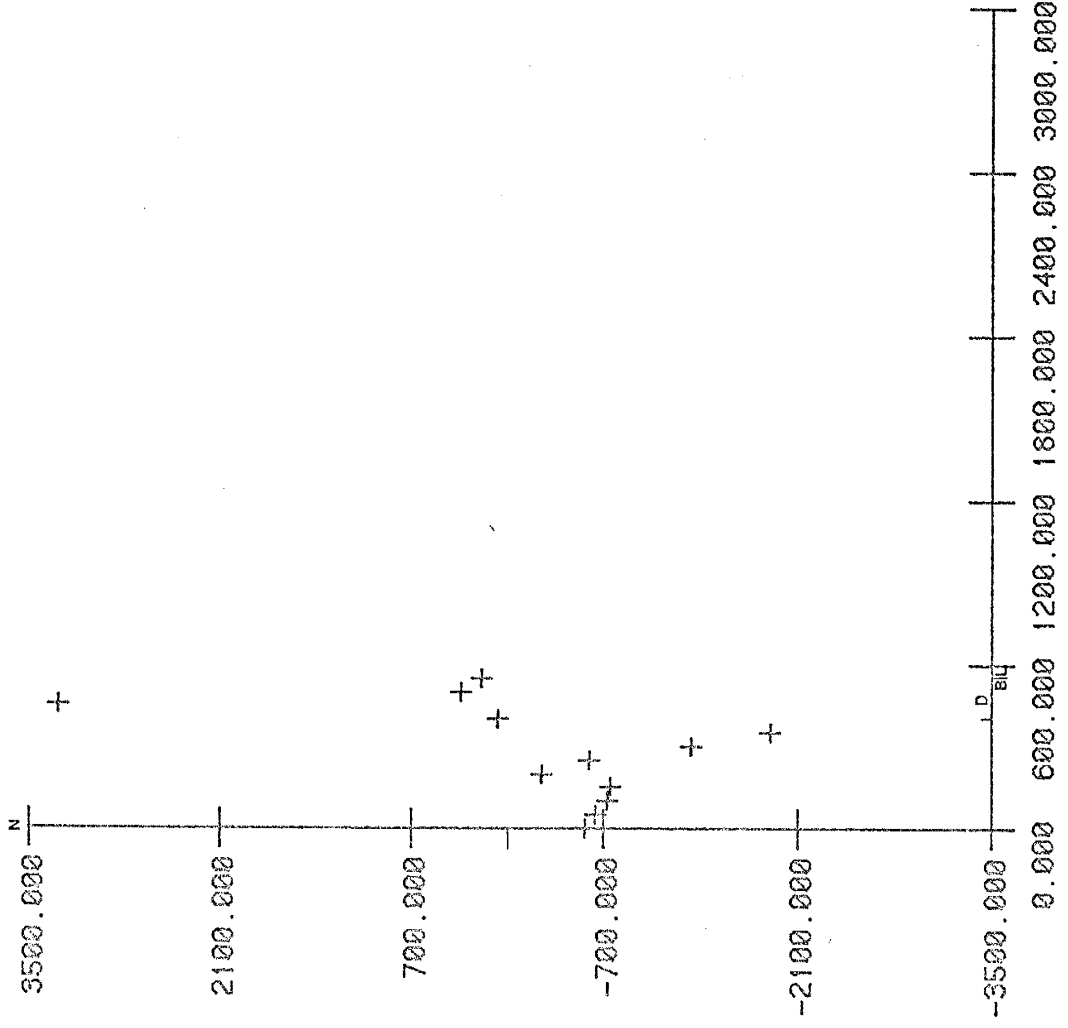


S



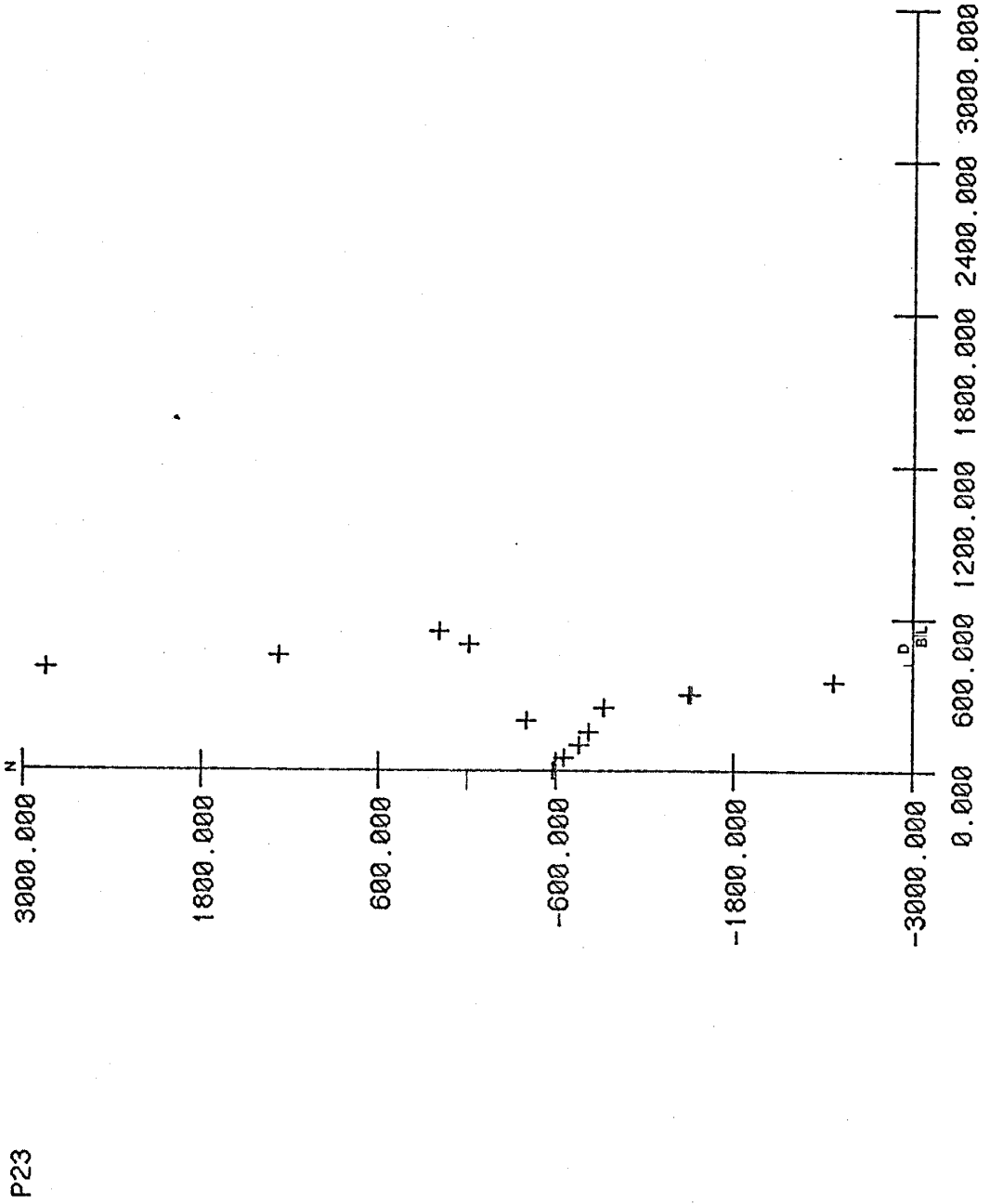
P21

s



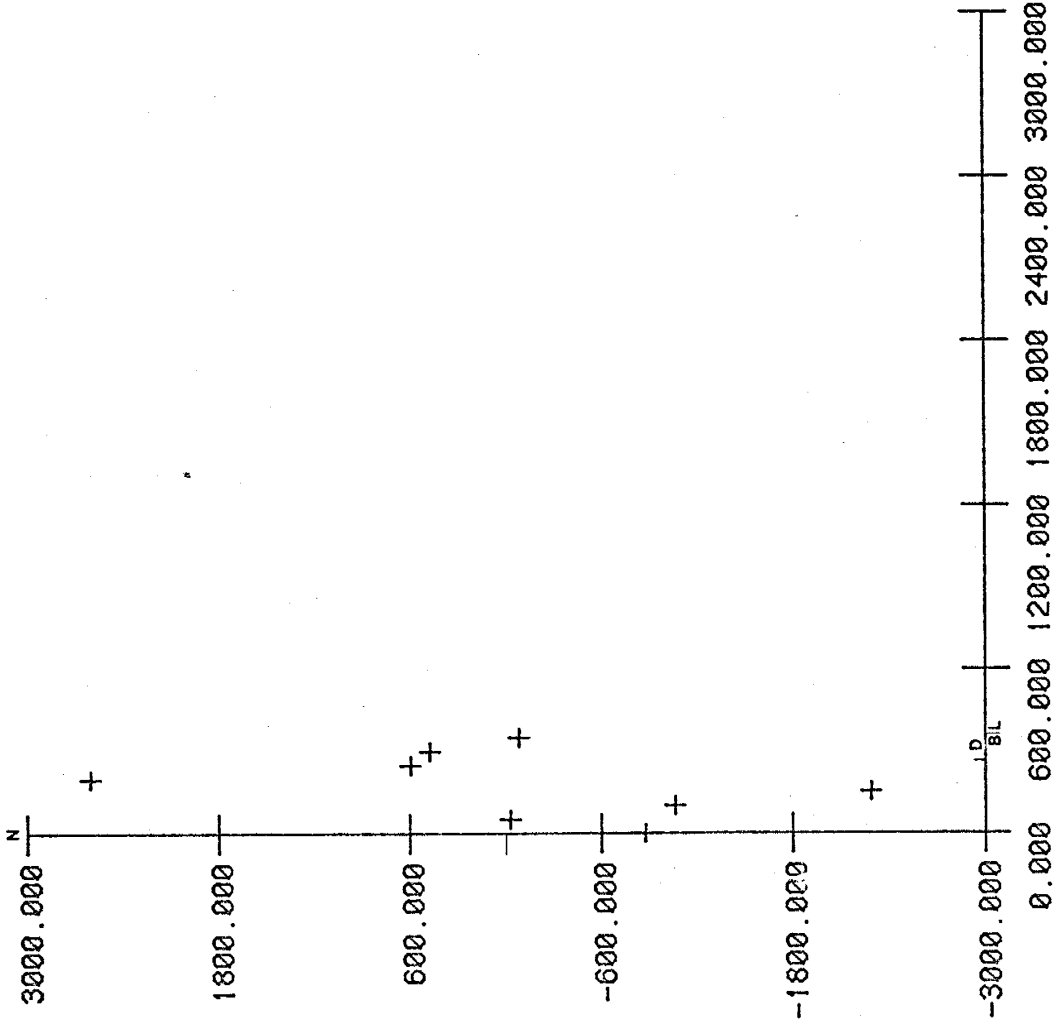
P22

S

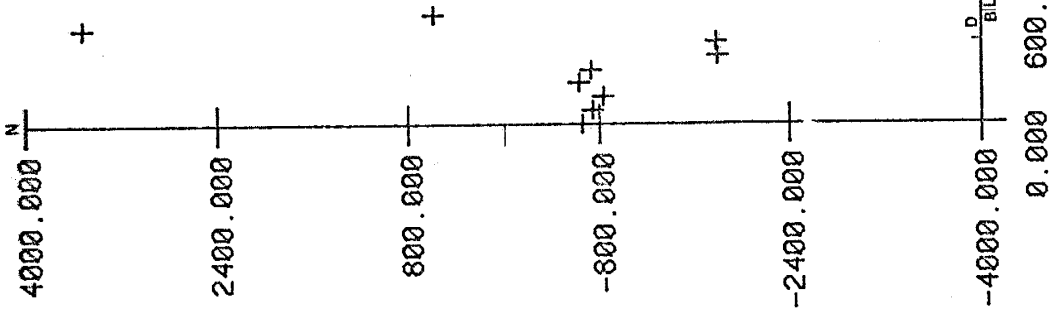


S

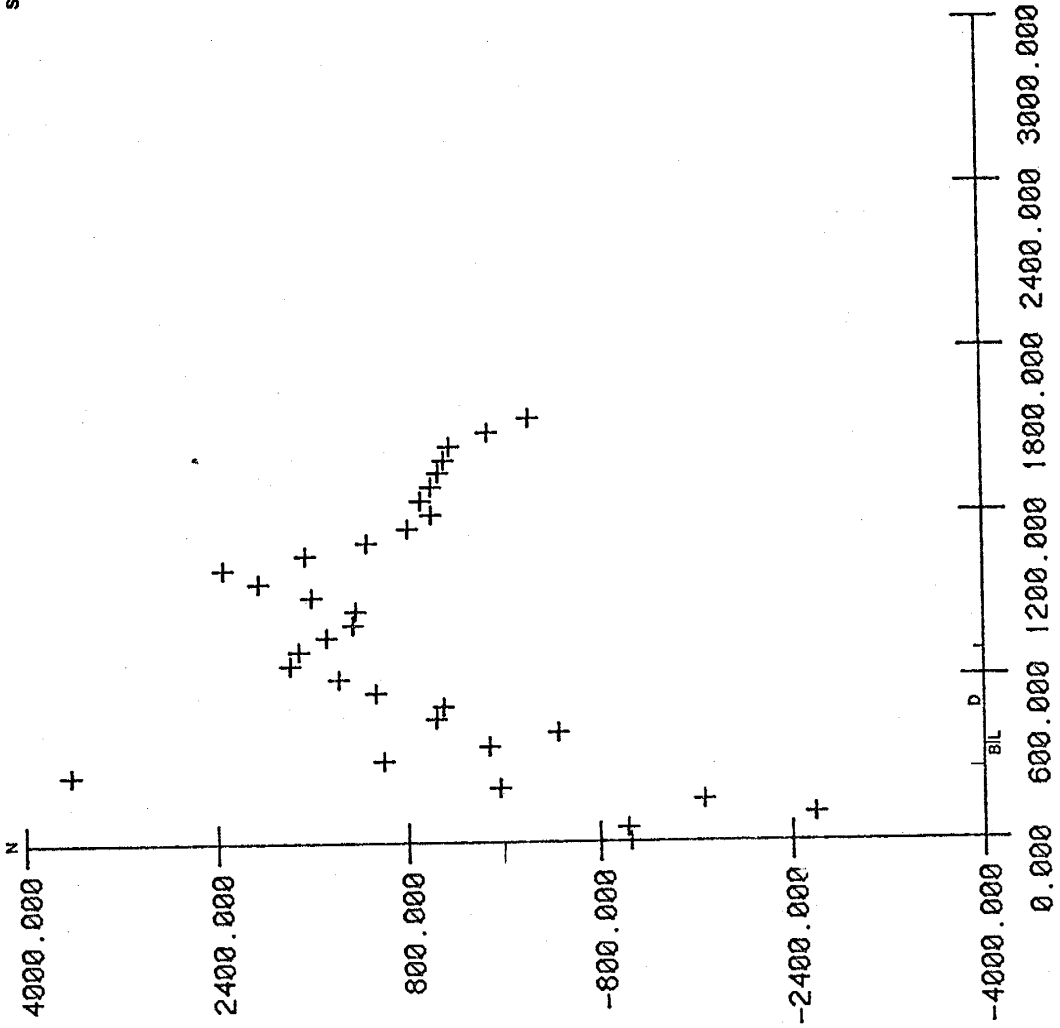
P24



P25

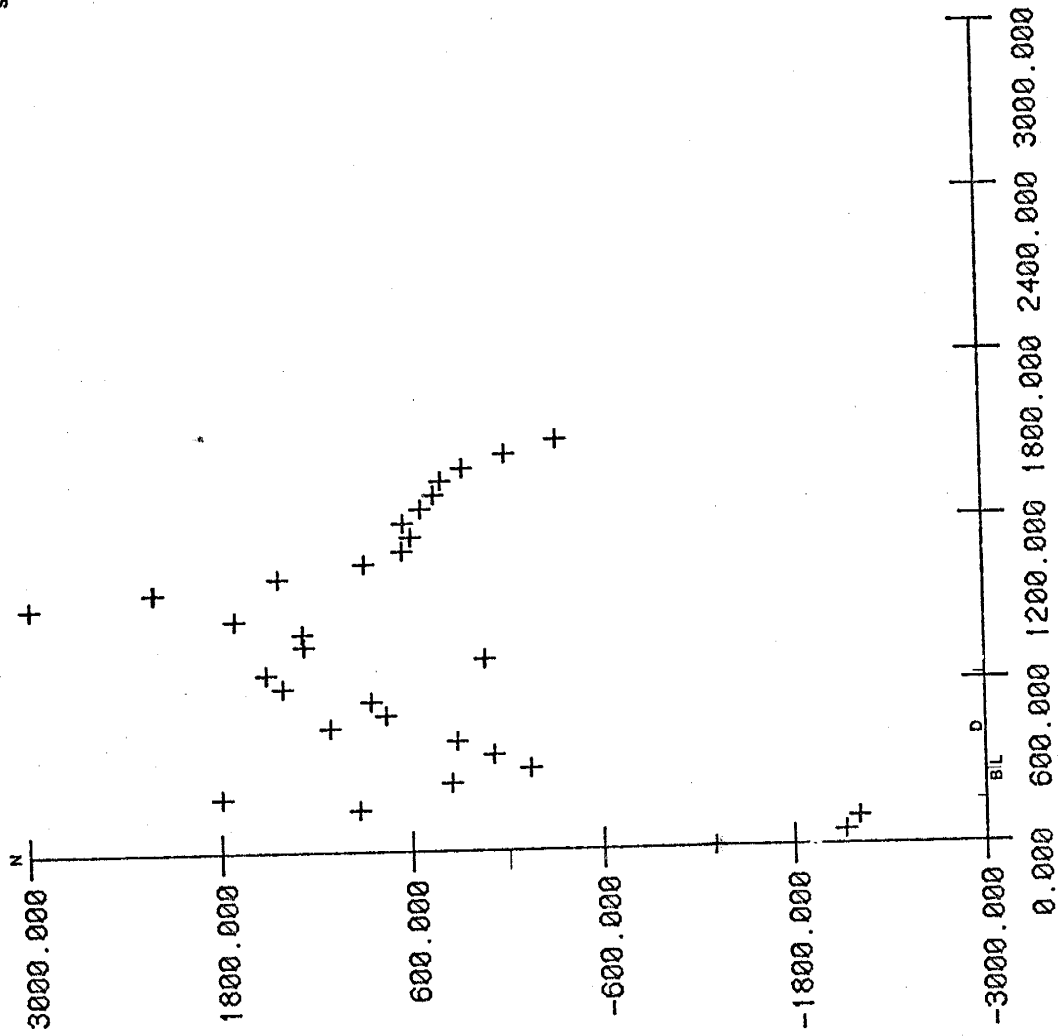


S



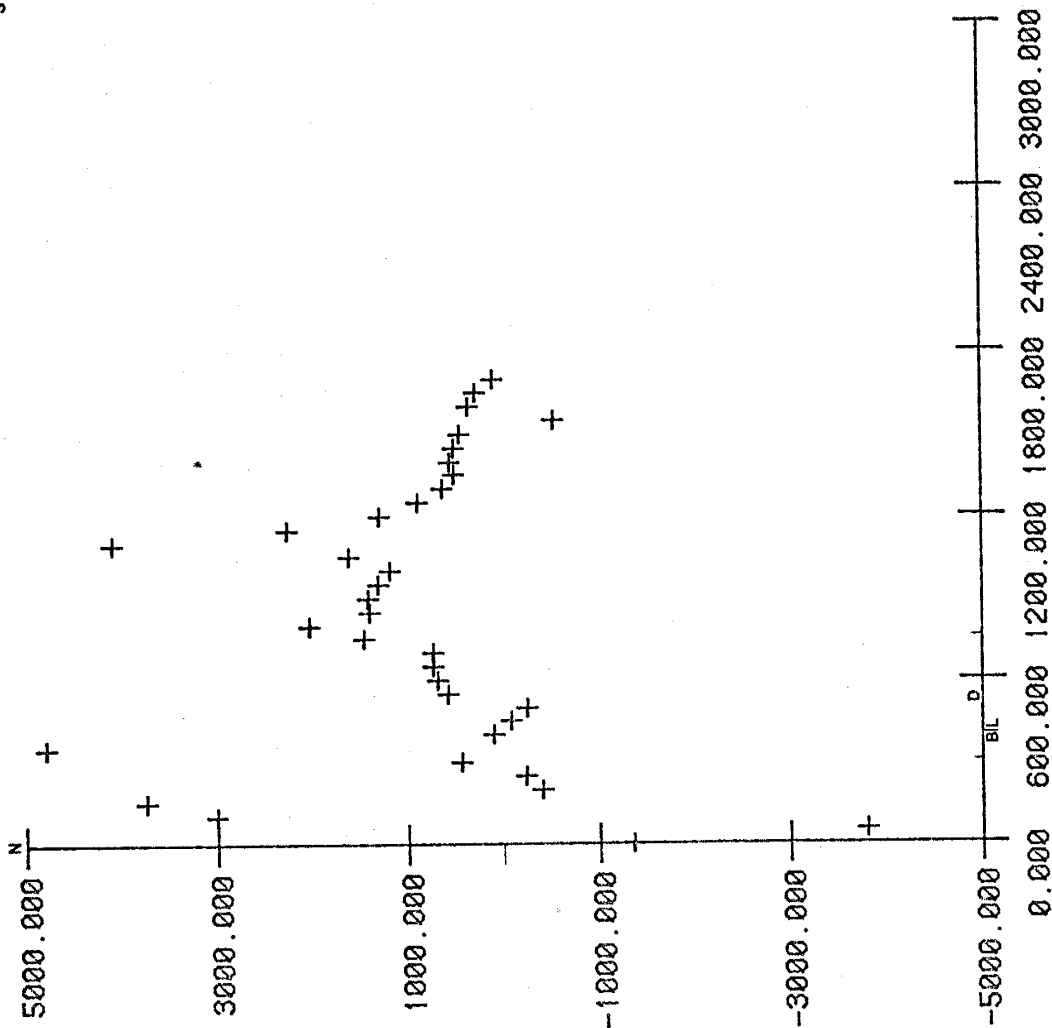
P26

s



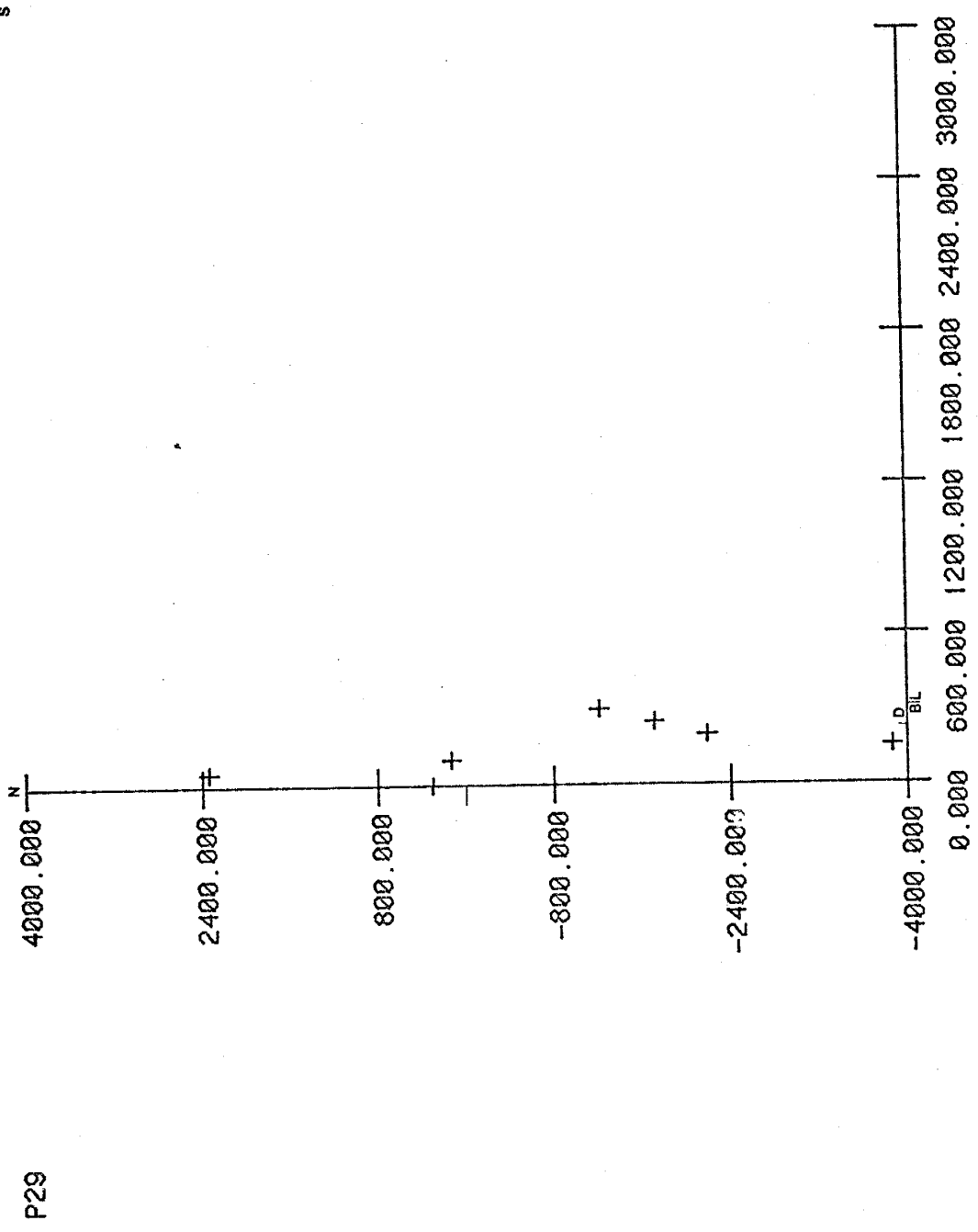
P27

s



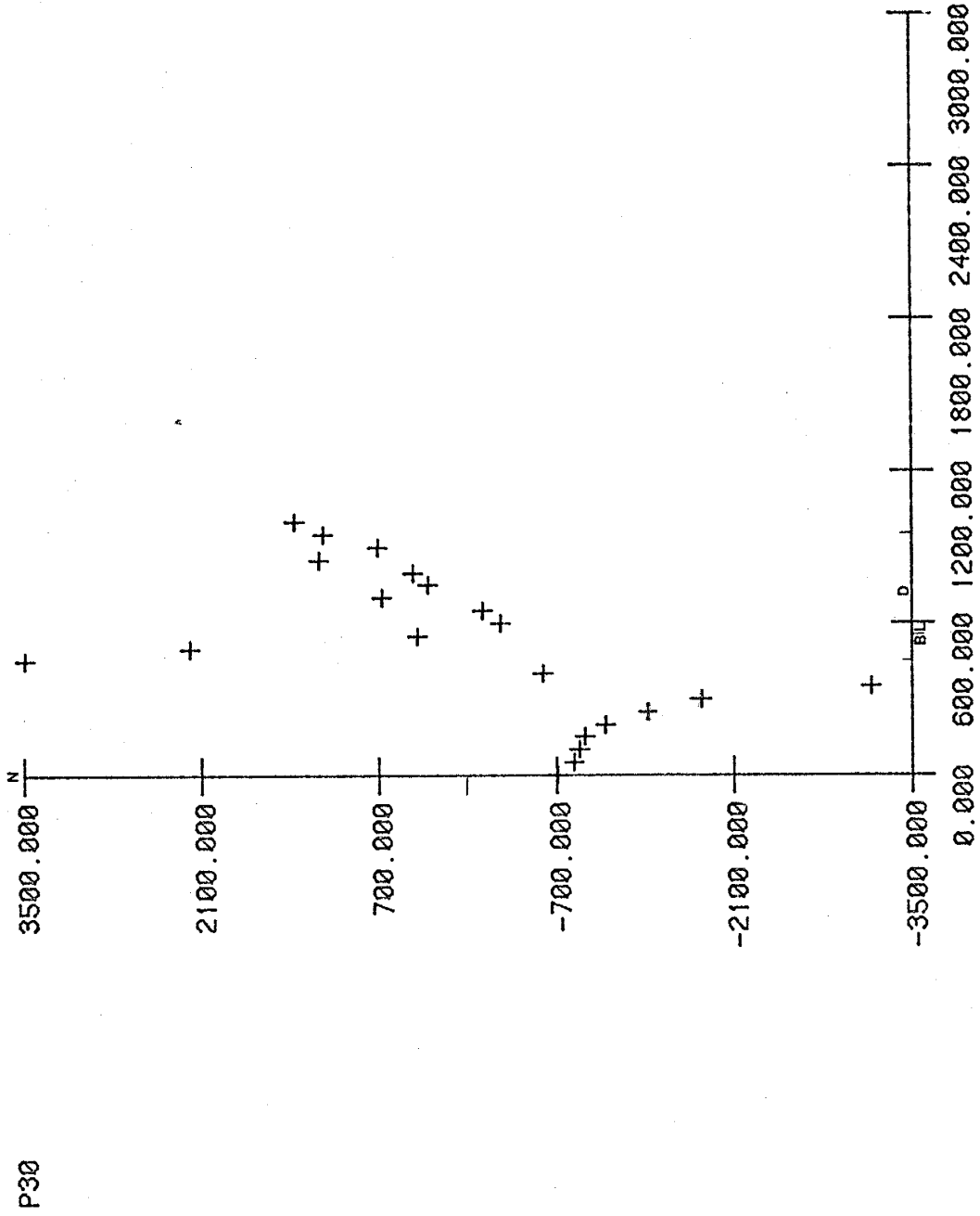
P28

6

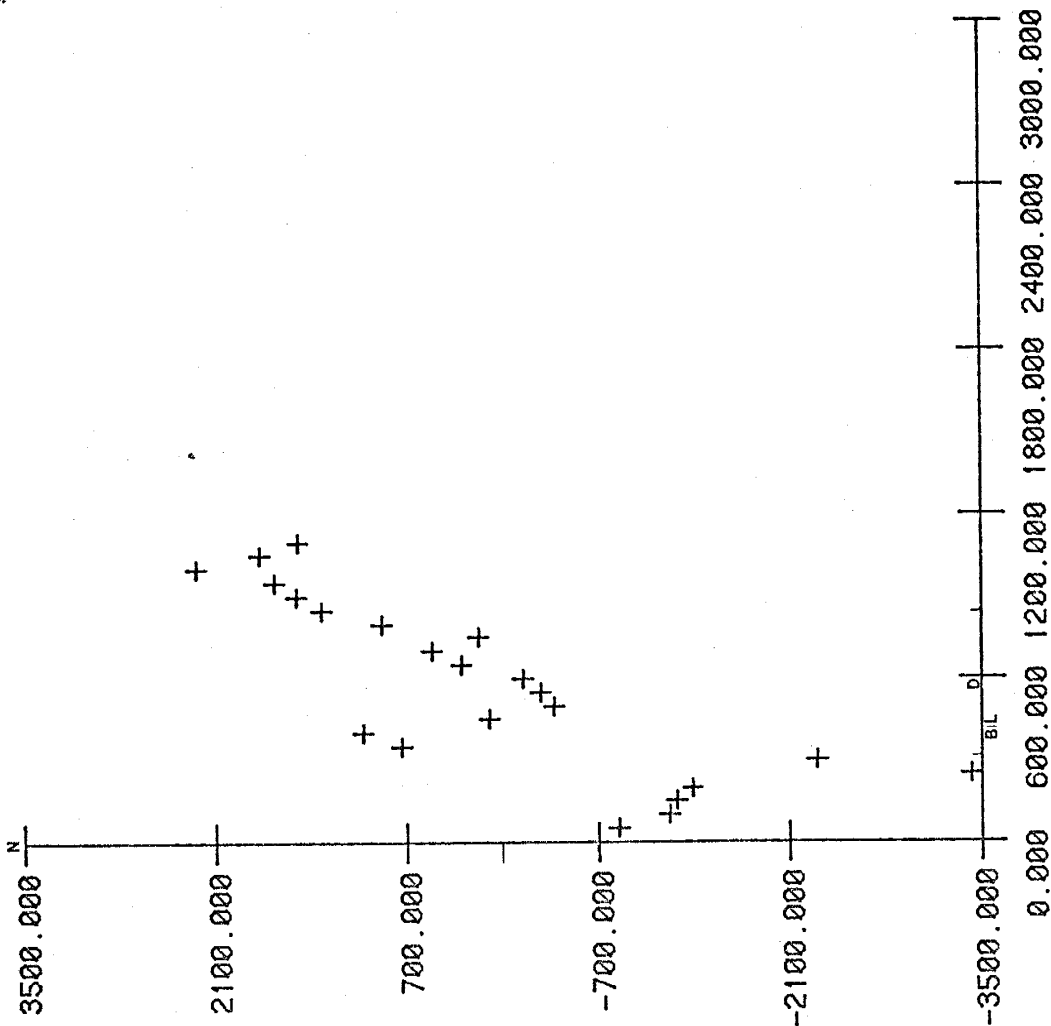


P29

s

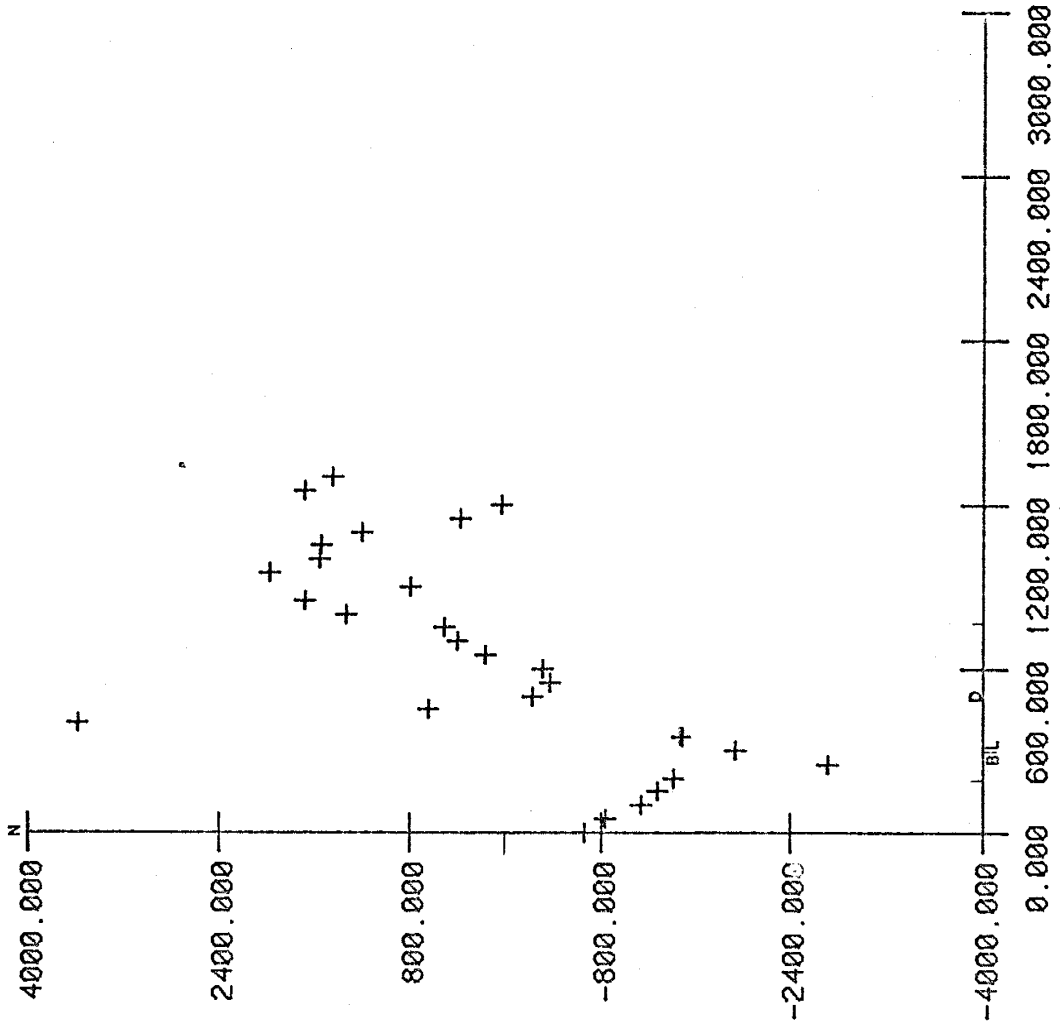


S



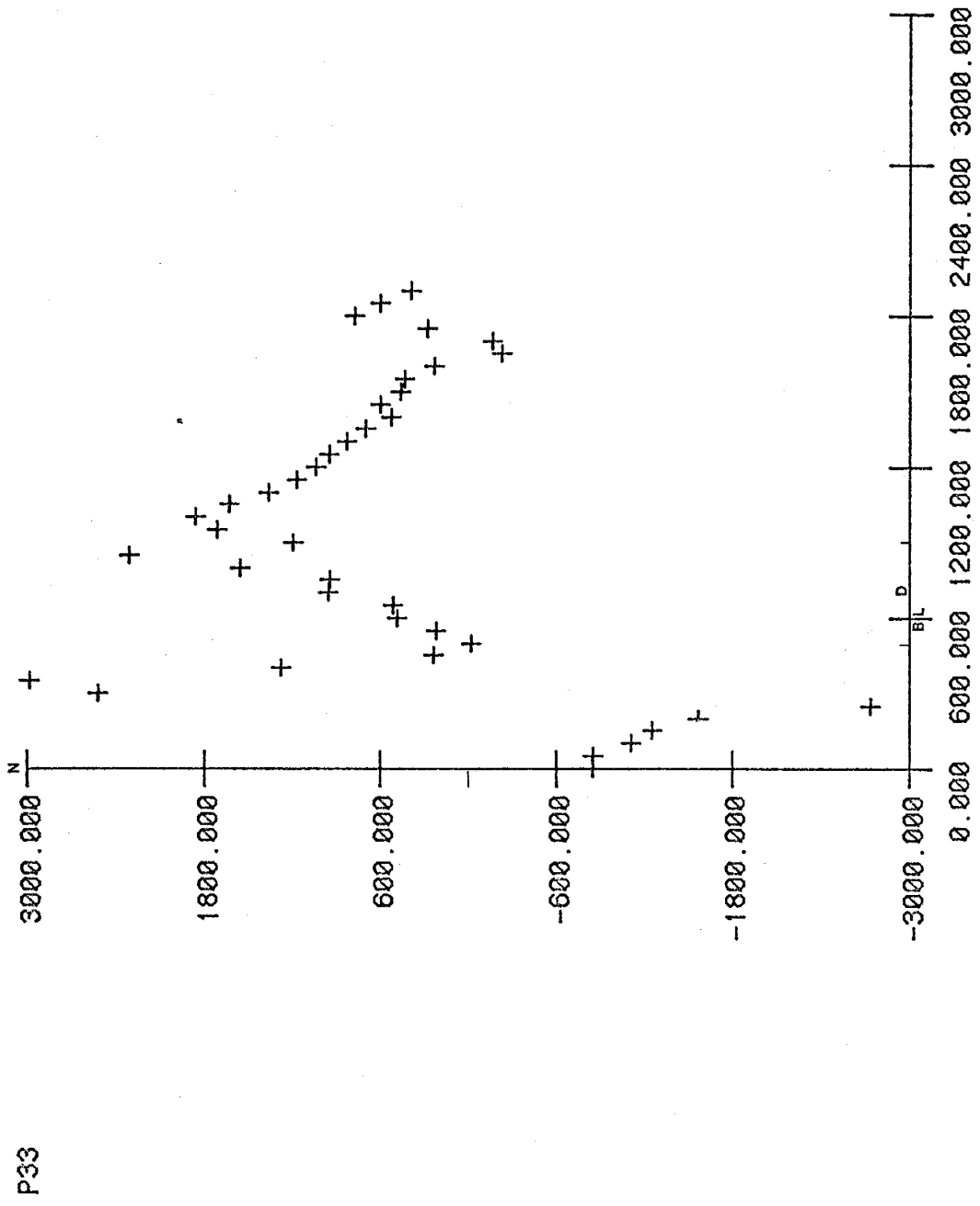
P31

s

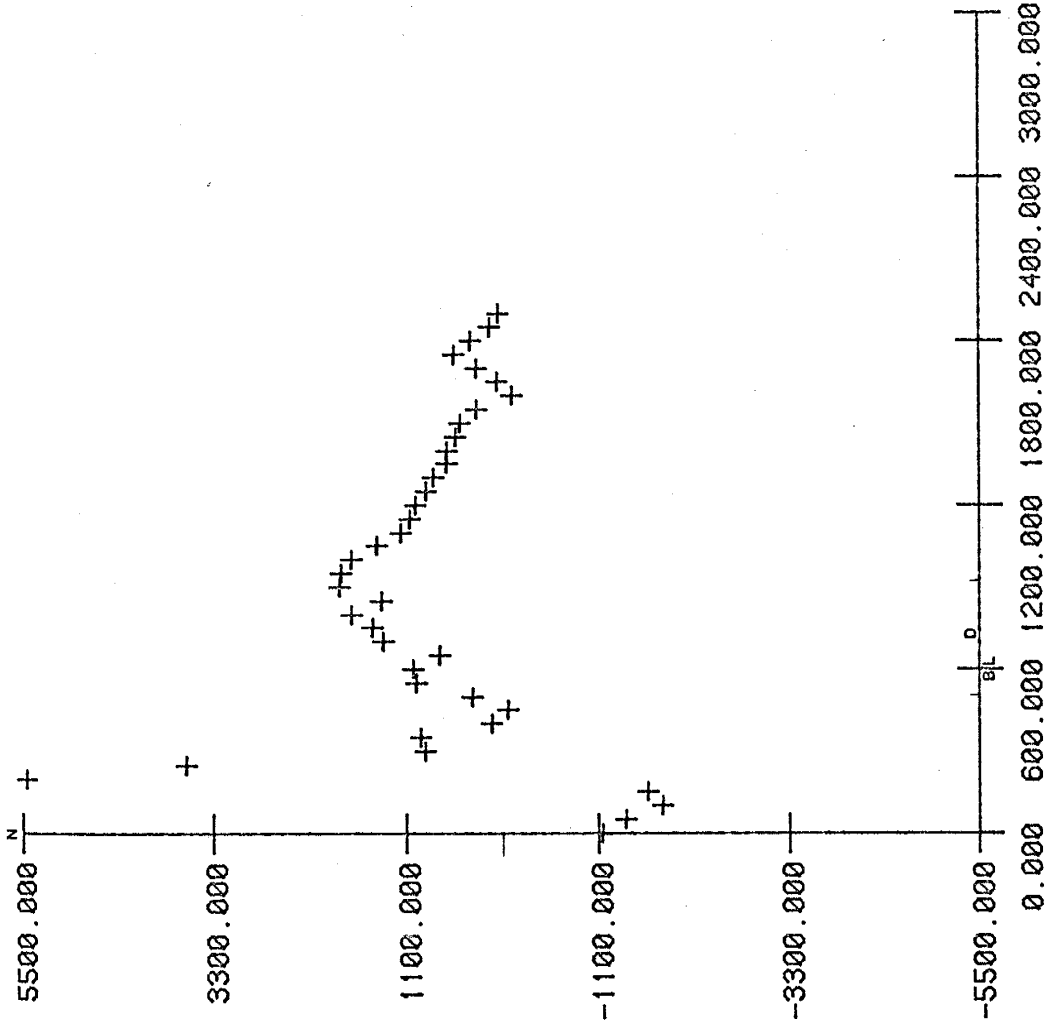


P32

S

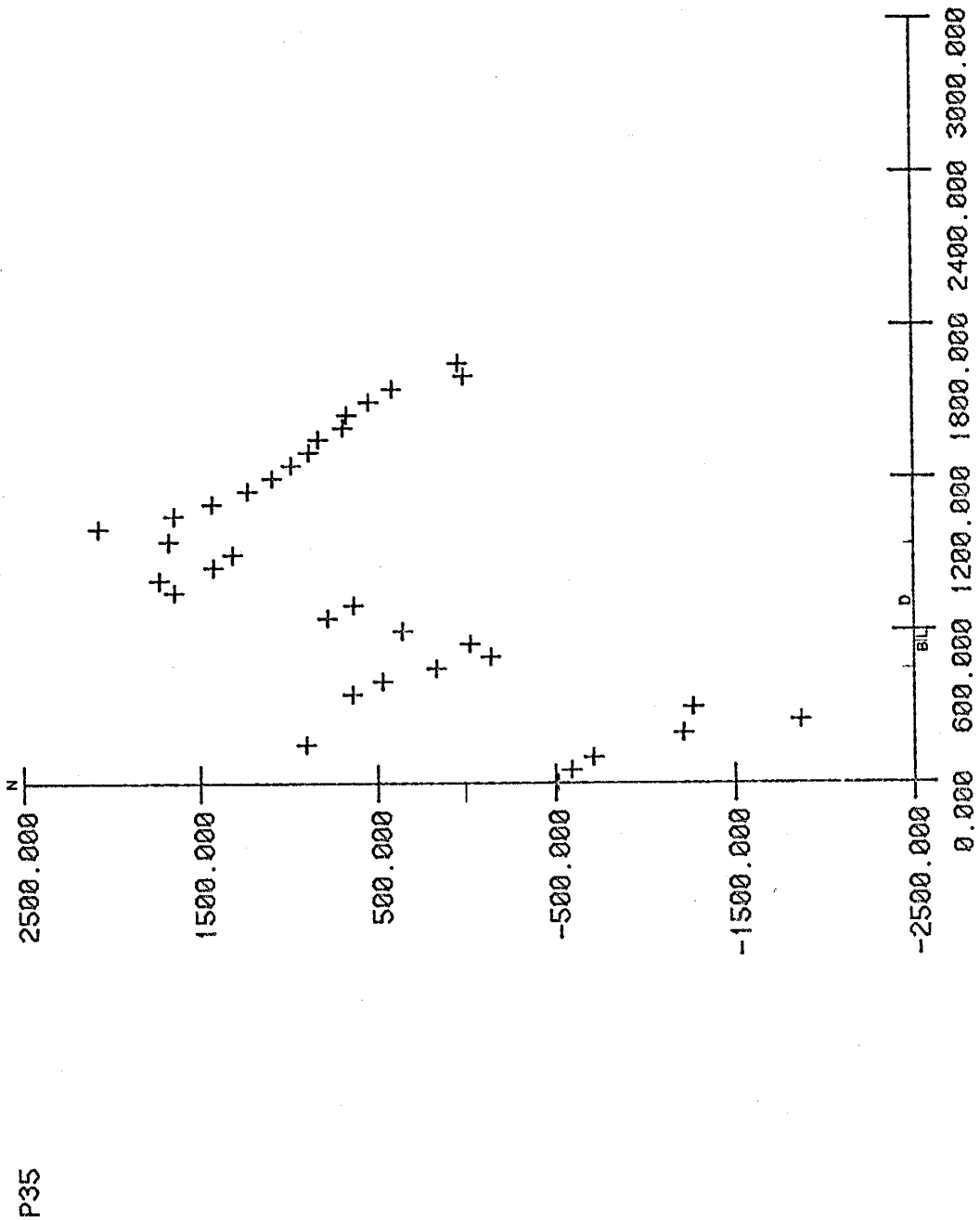


s

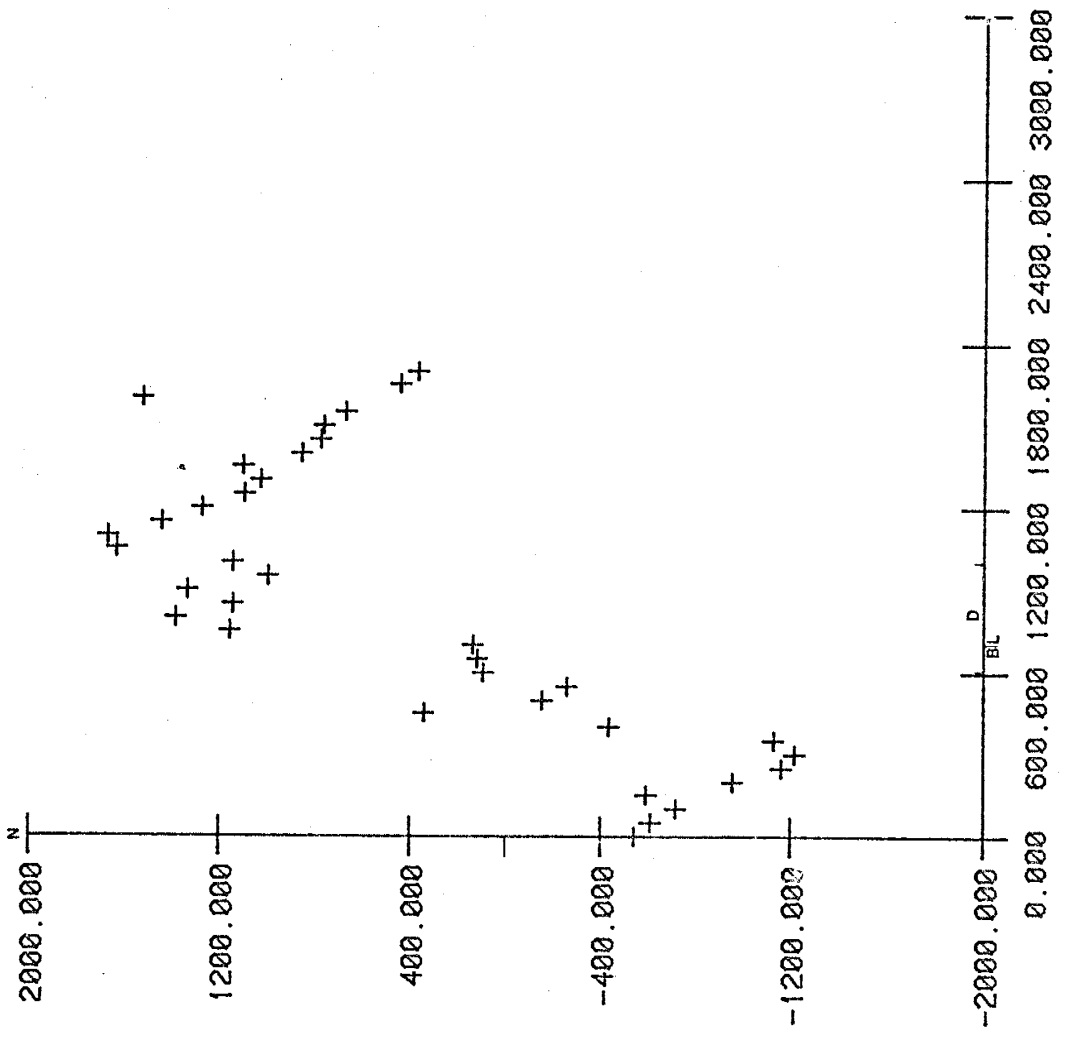


P34

5



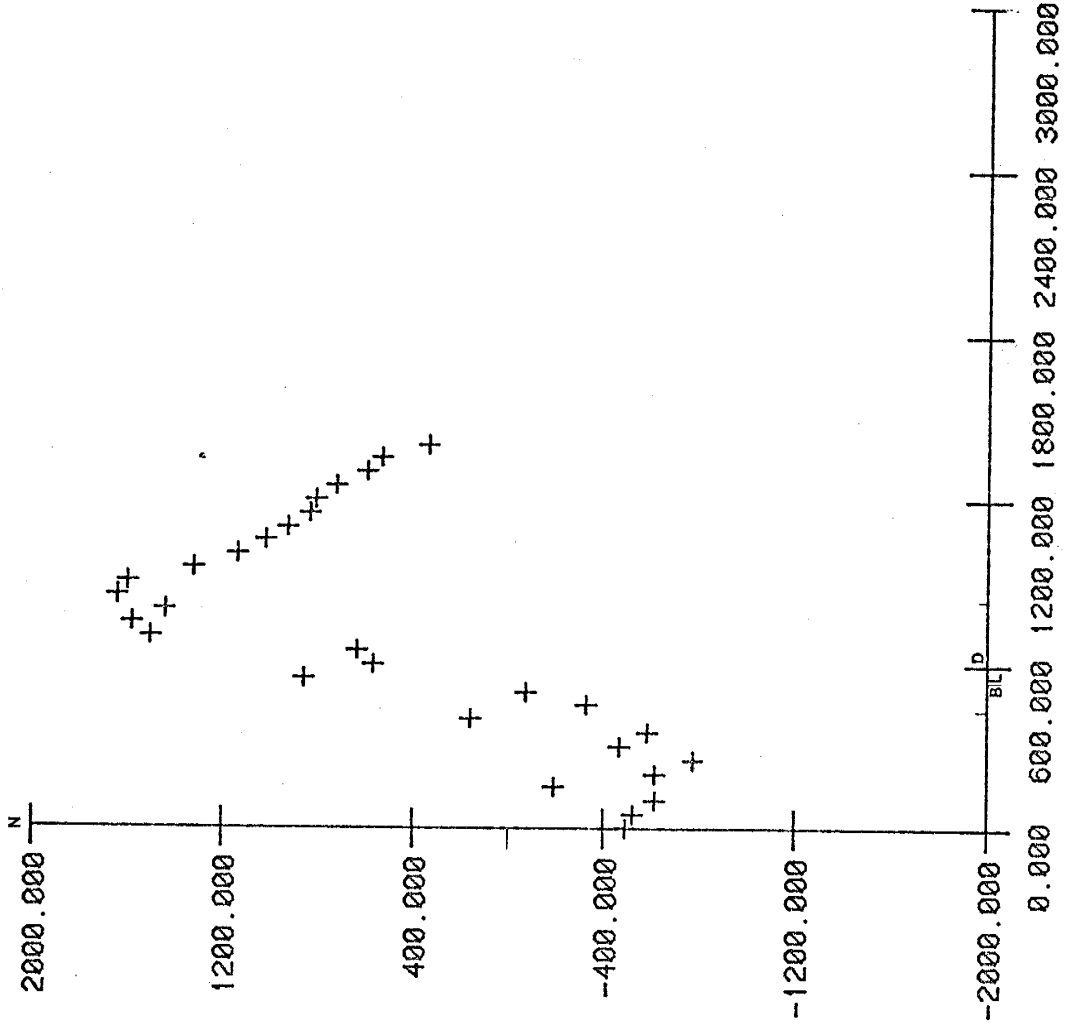
s



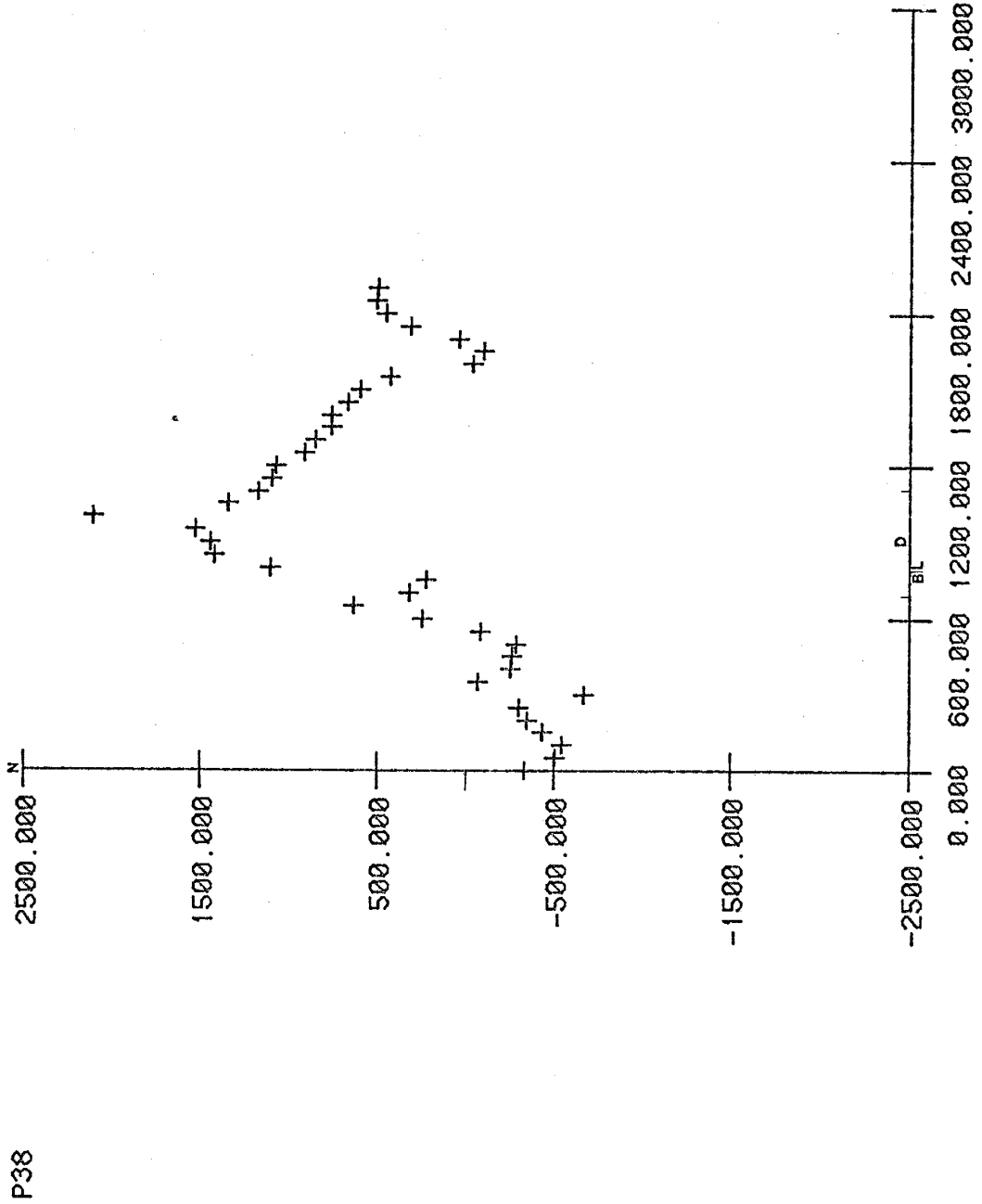
P36

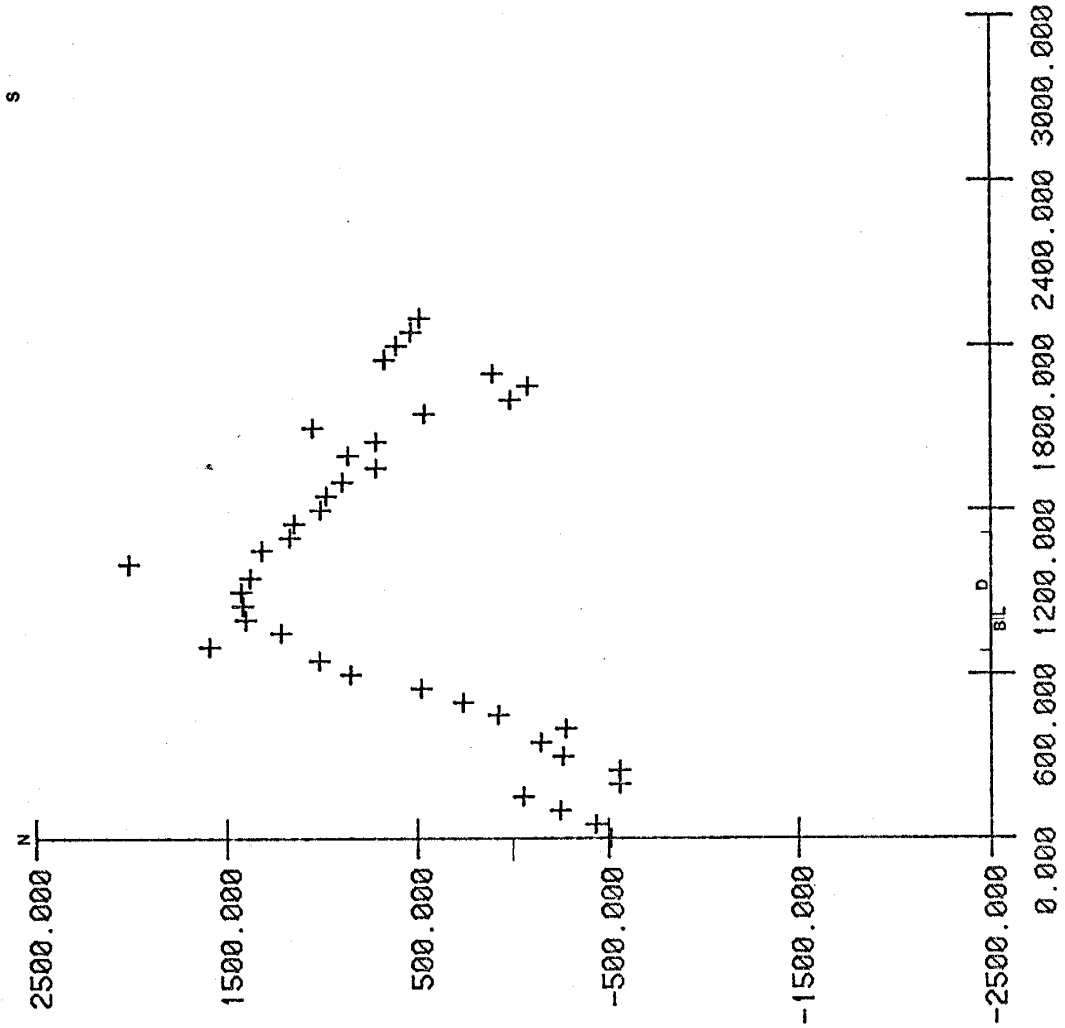
P37

s



S

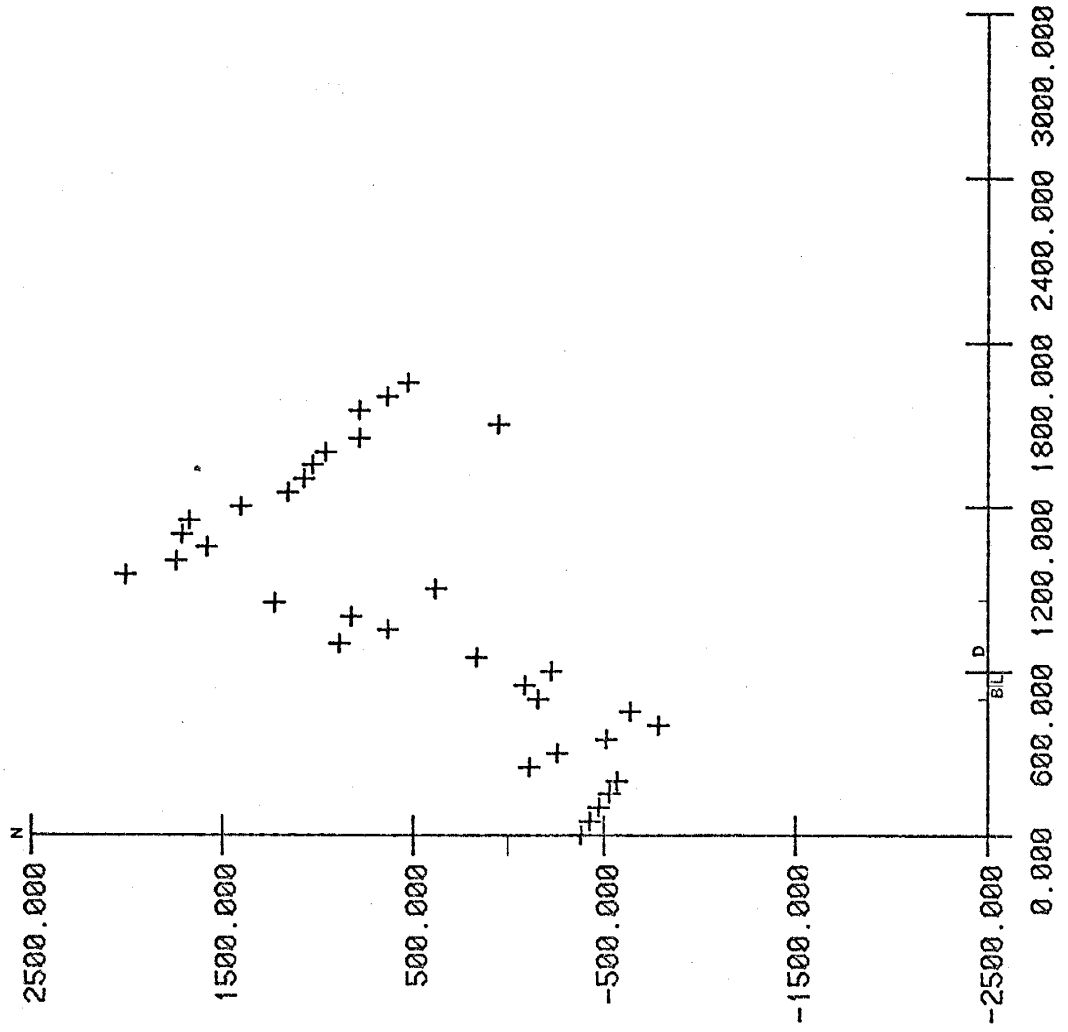




P39

S

s



P40

2500.000

1500.000

500.000

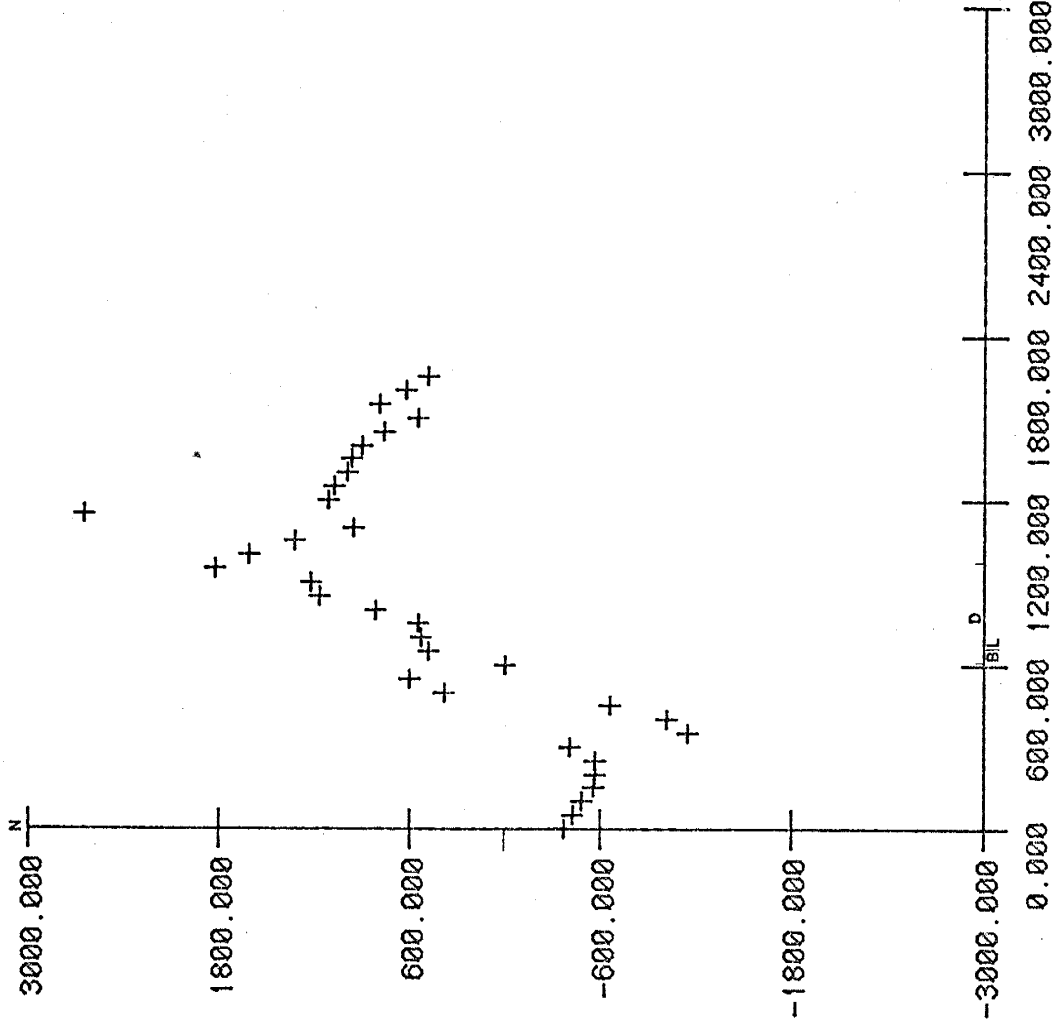
-500.000

-1500.000

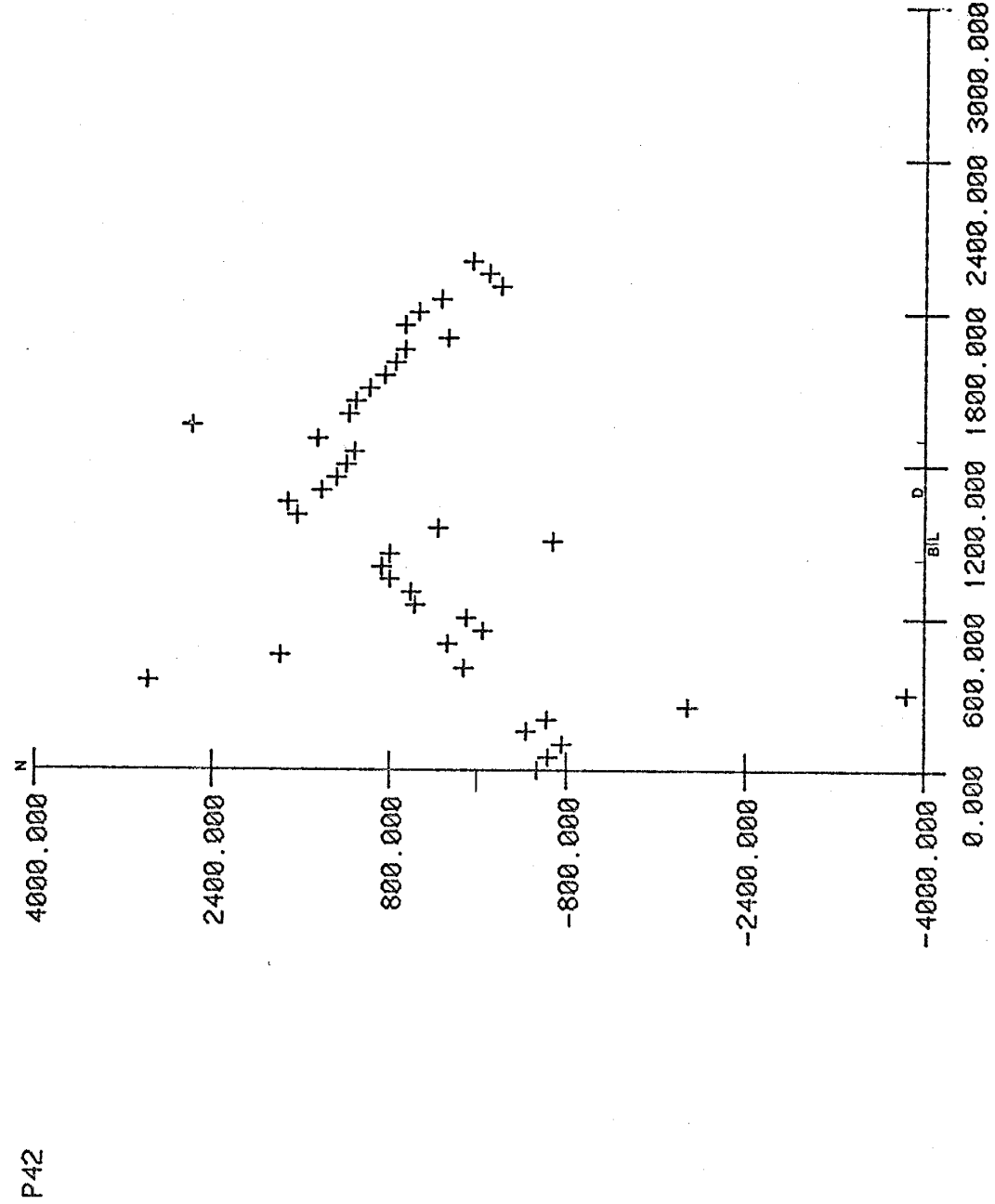
-2500.000

0.000 600.000 1200.000 1800.000 2400.000 3000.000

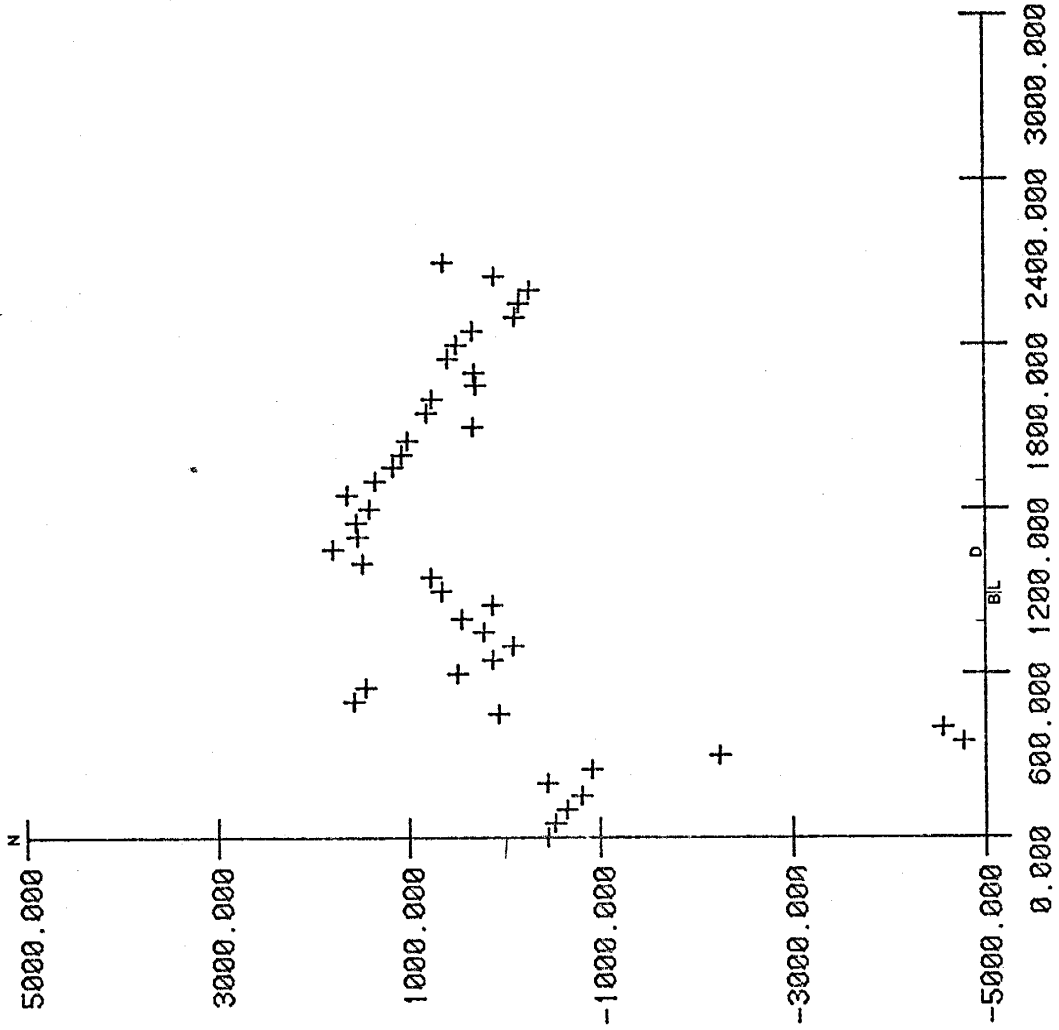
s



P41

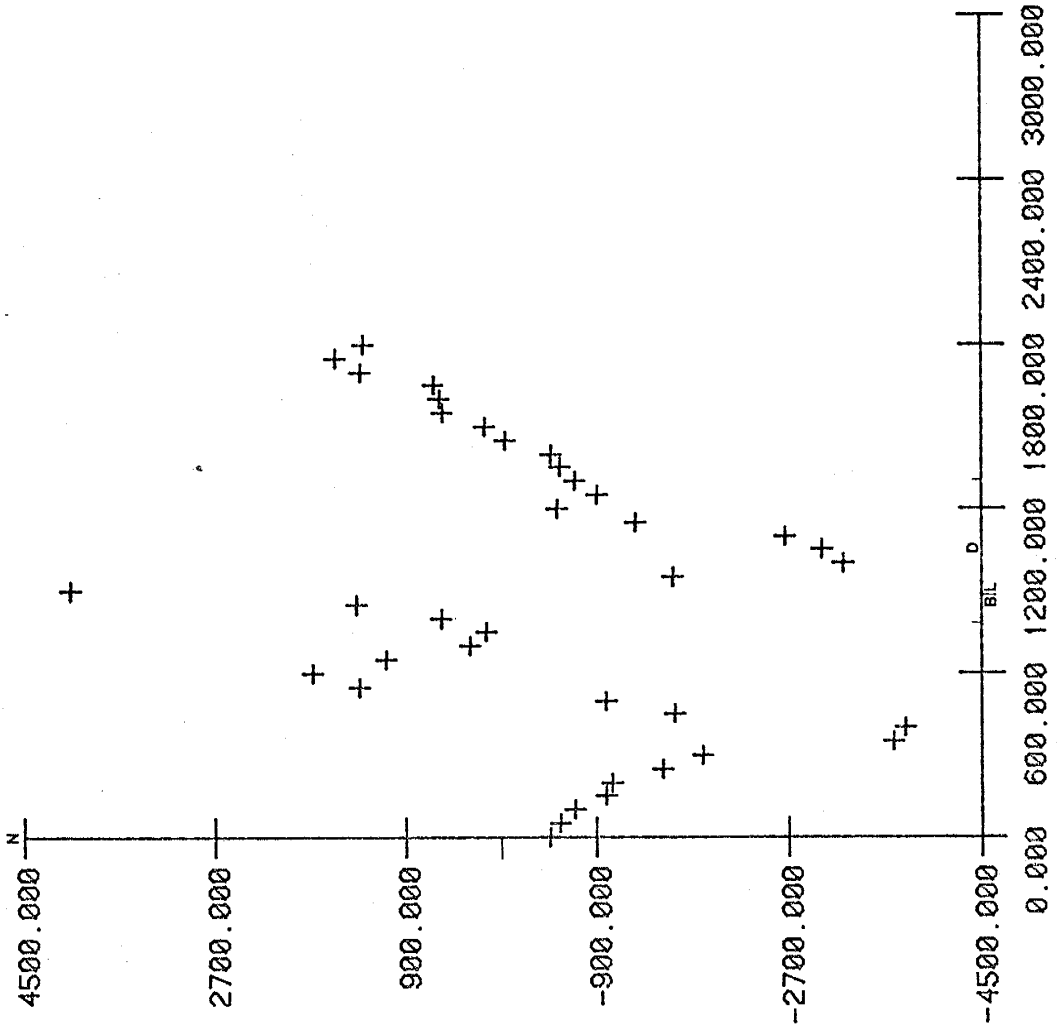


s



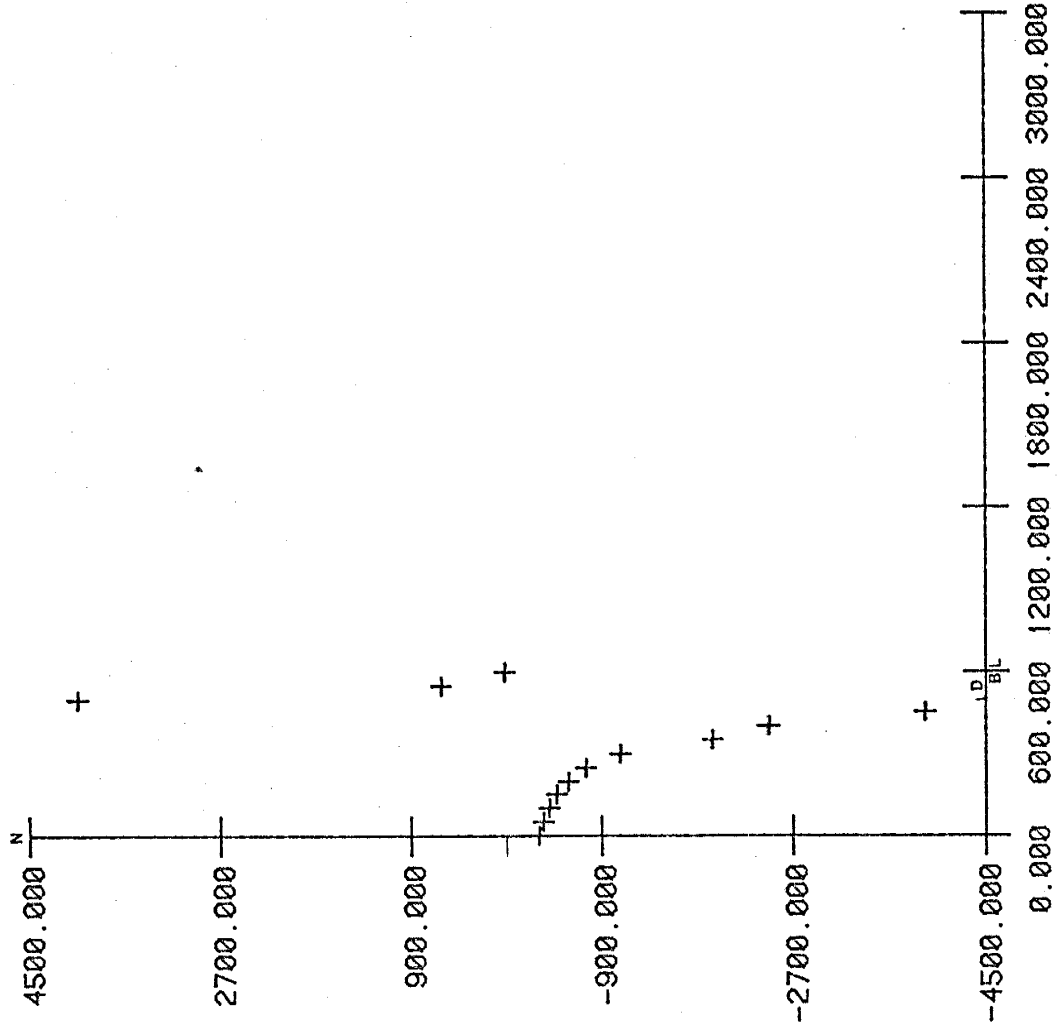
P43

s



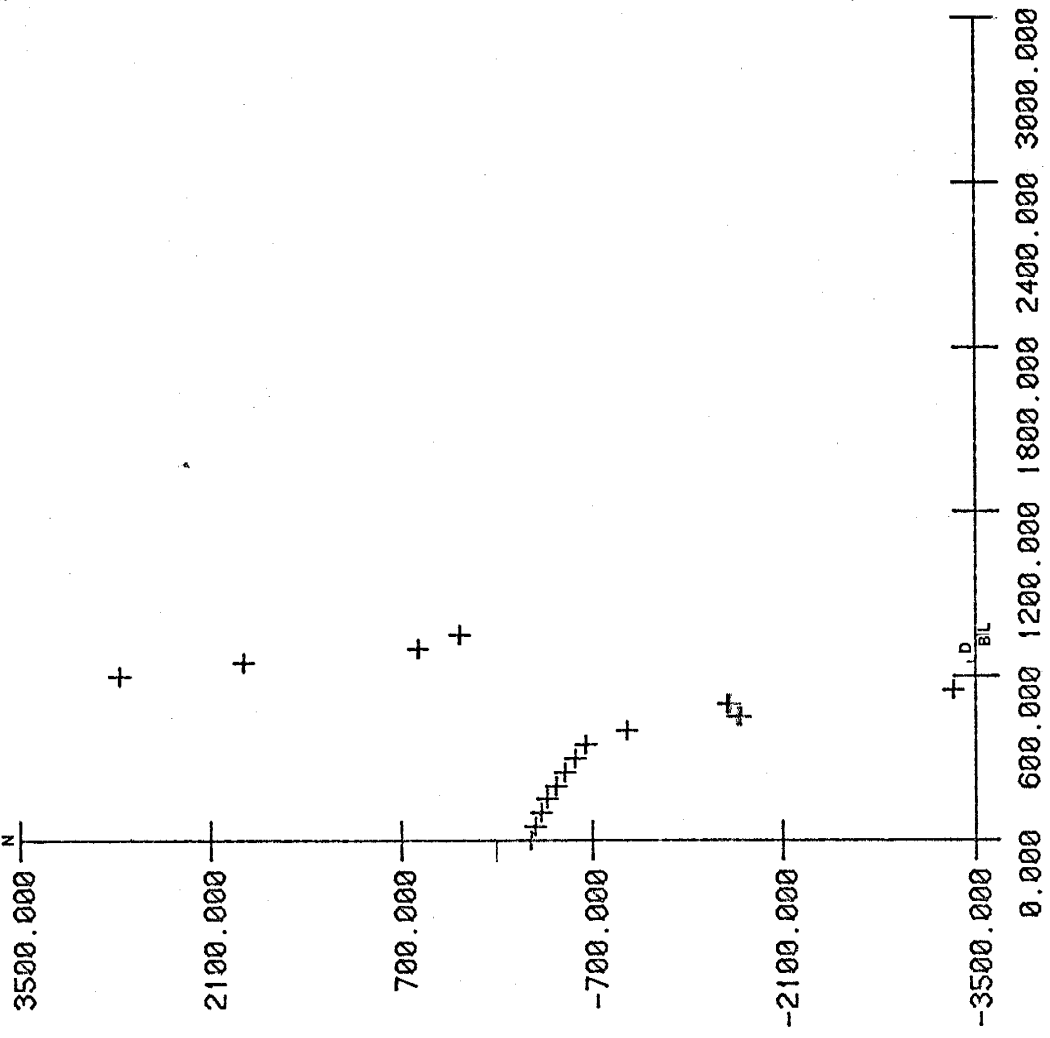
P44

S



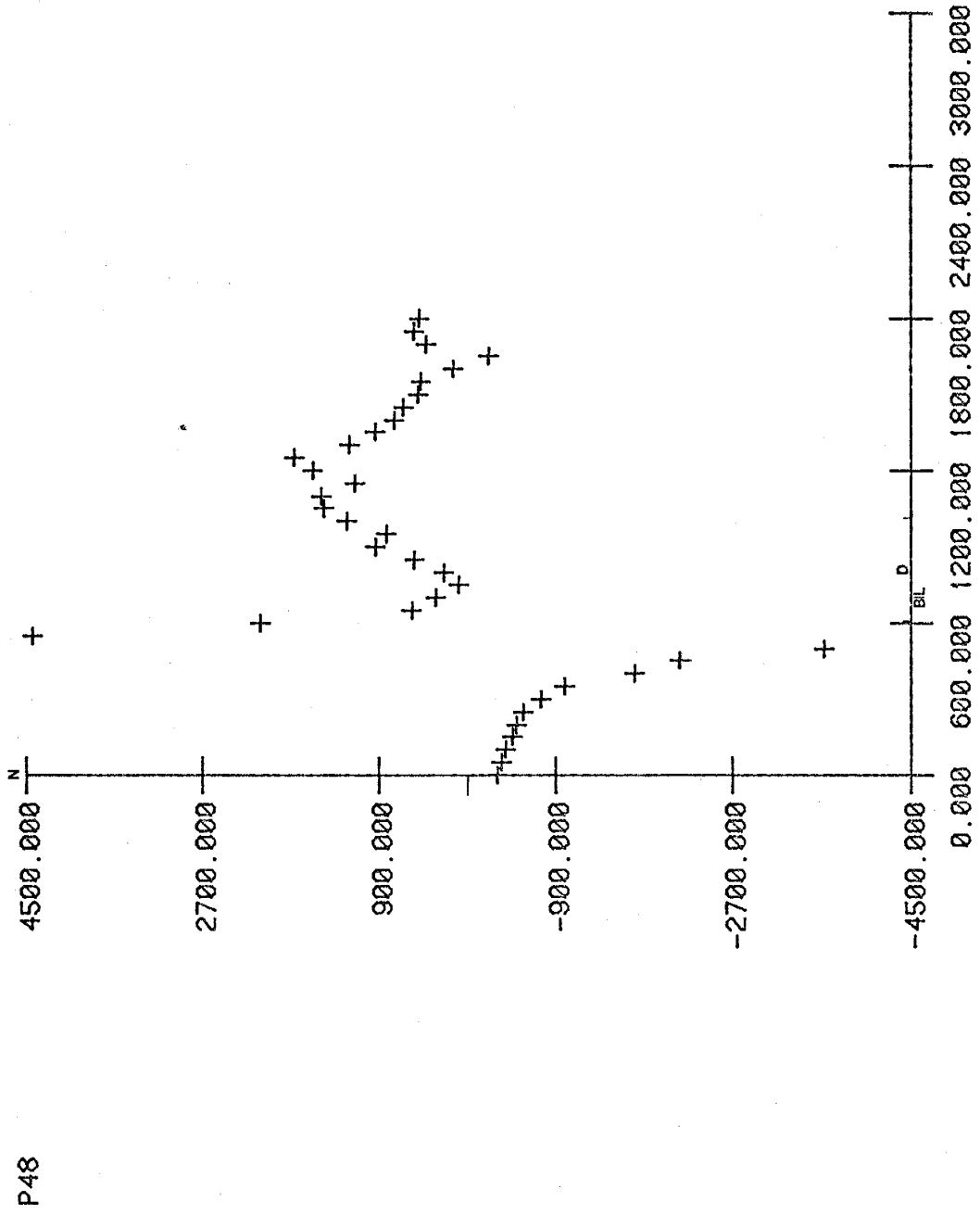
P45

s

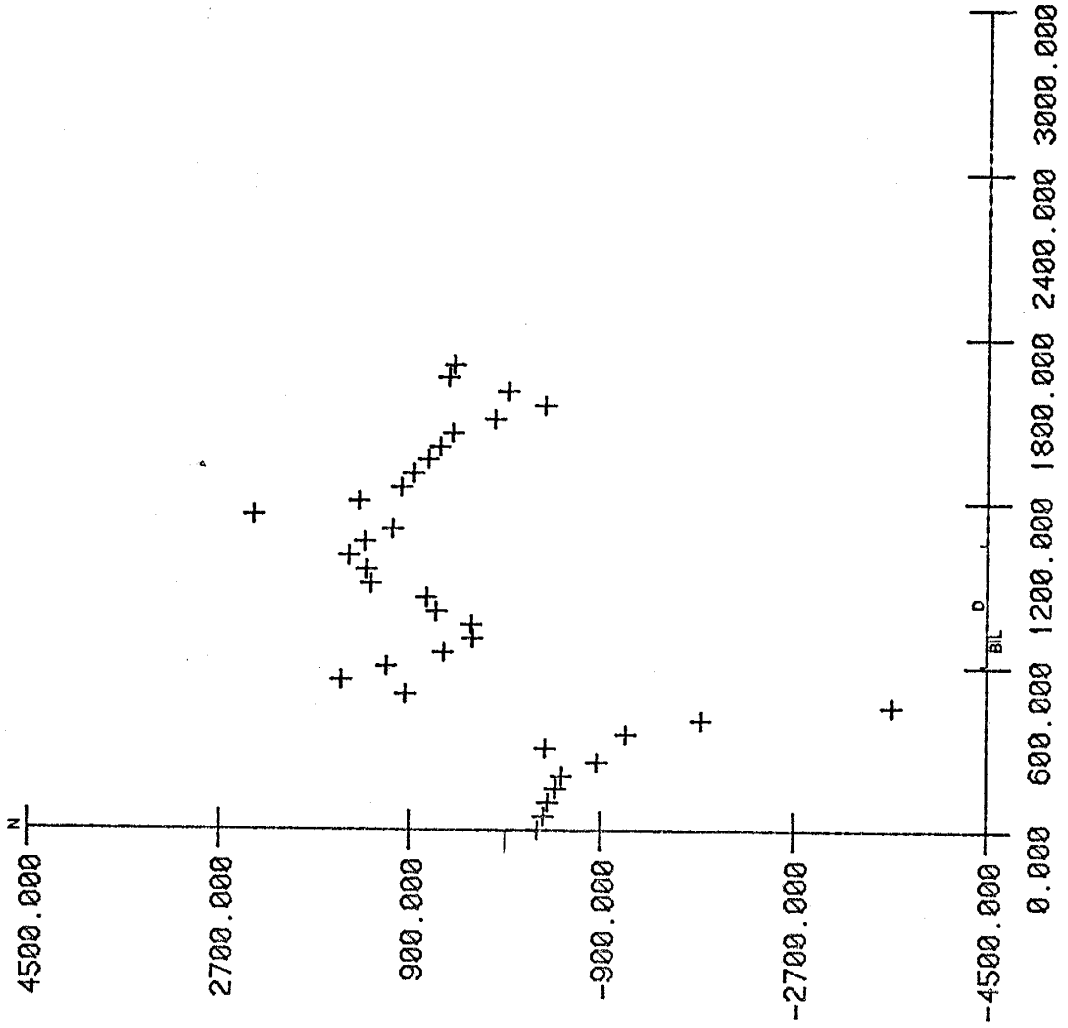


P47

S

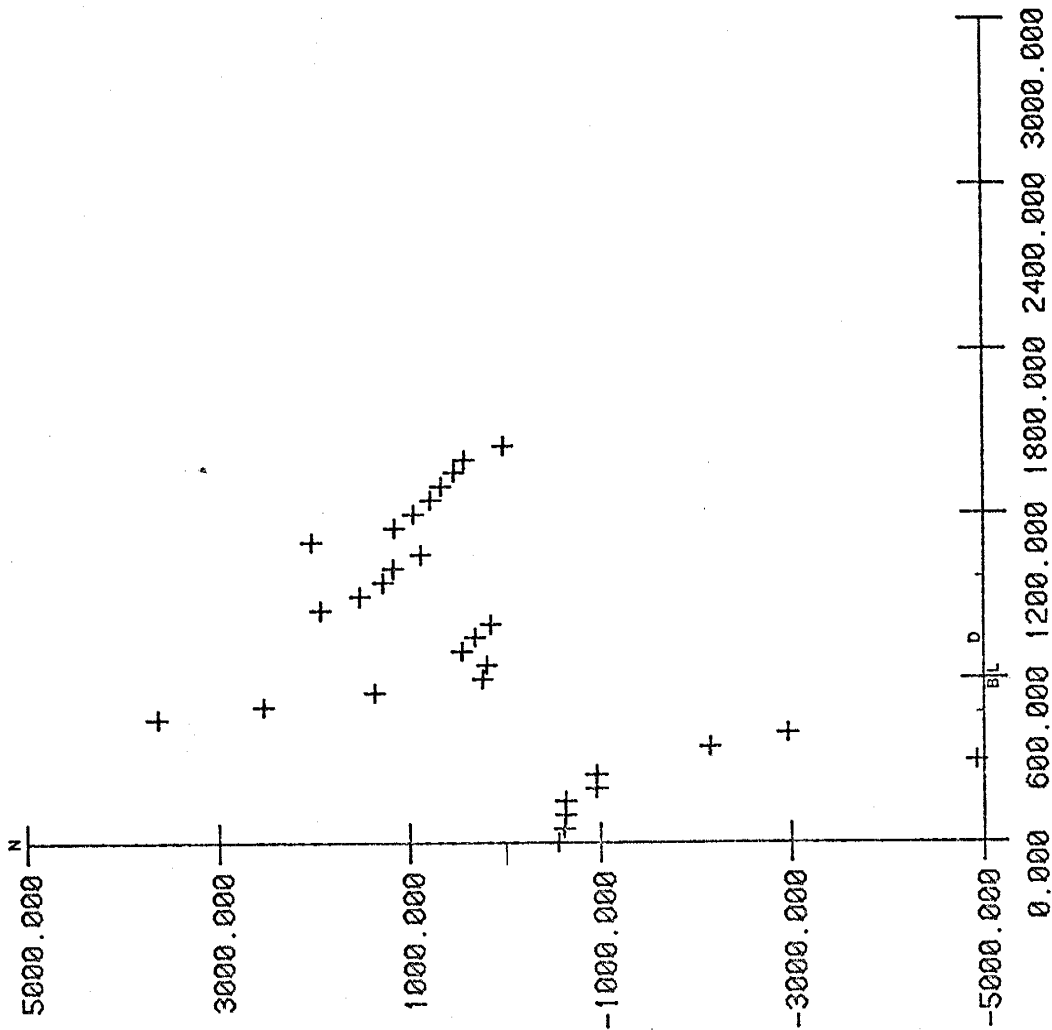


s



P49

5



P50

5000.000

3000.000

1000.000

-1000.000

-3000.000

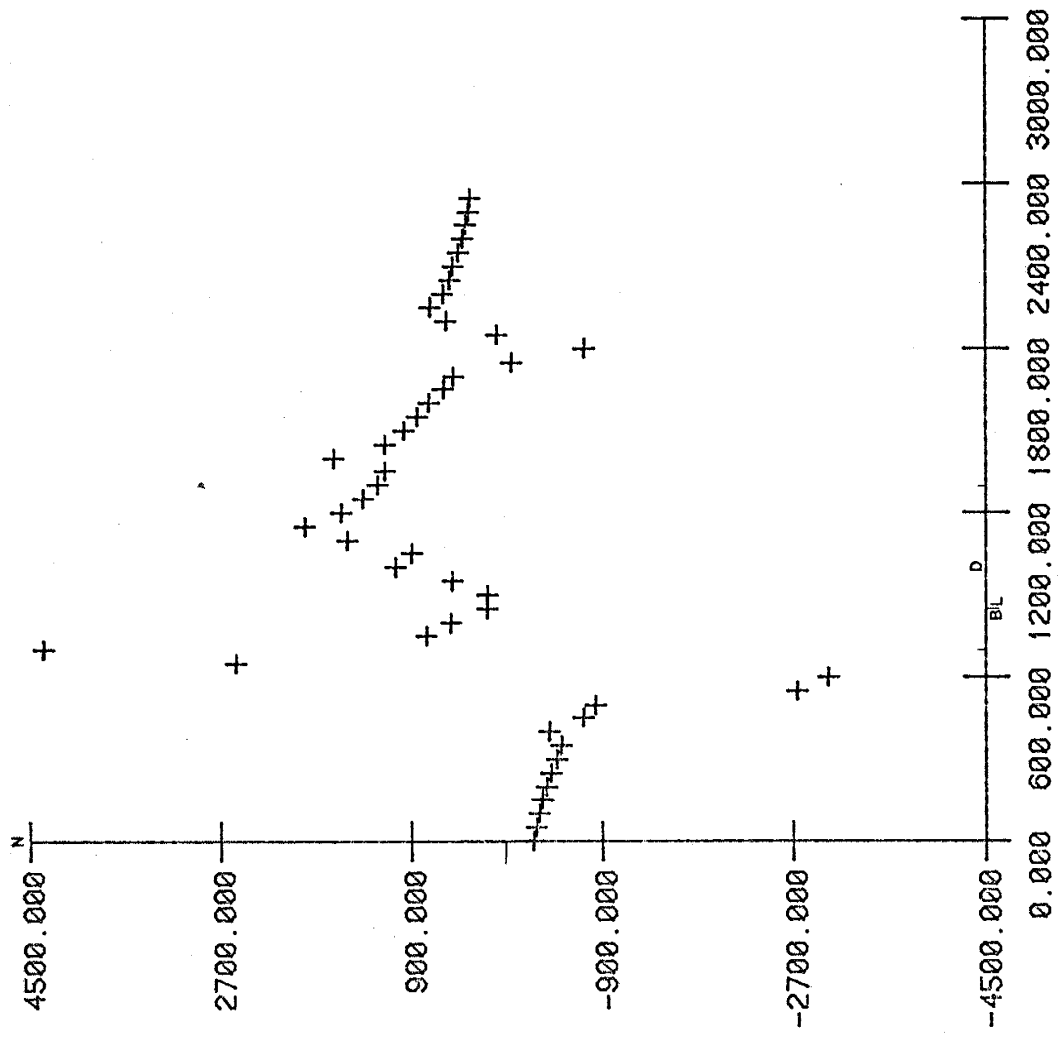
-5000.000

N

0
1000
2000
3000

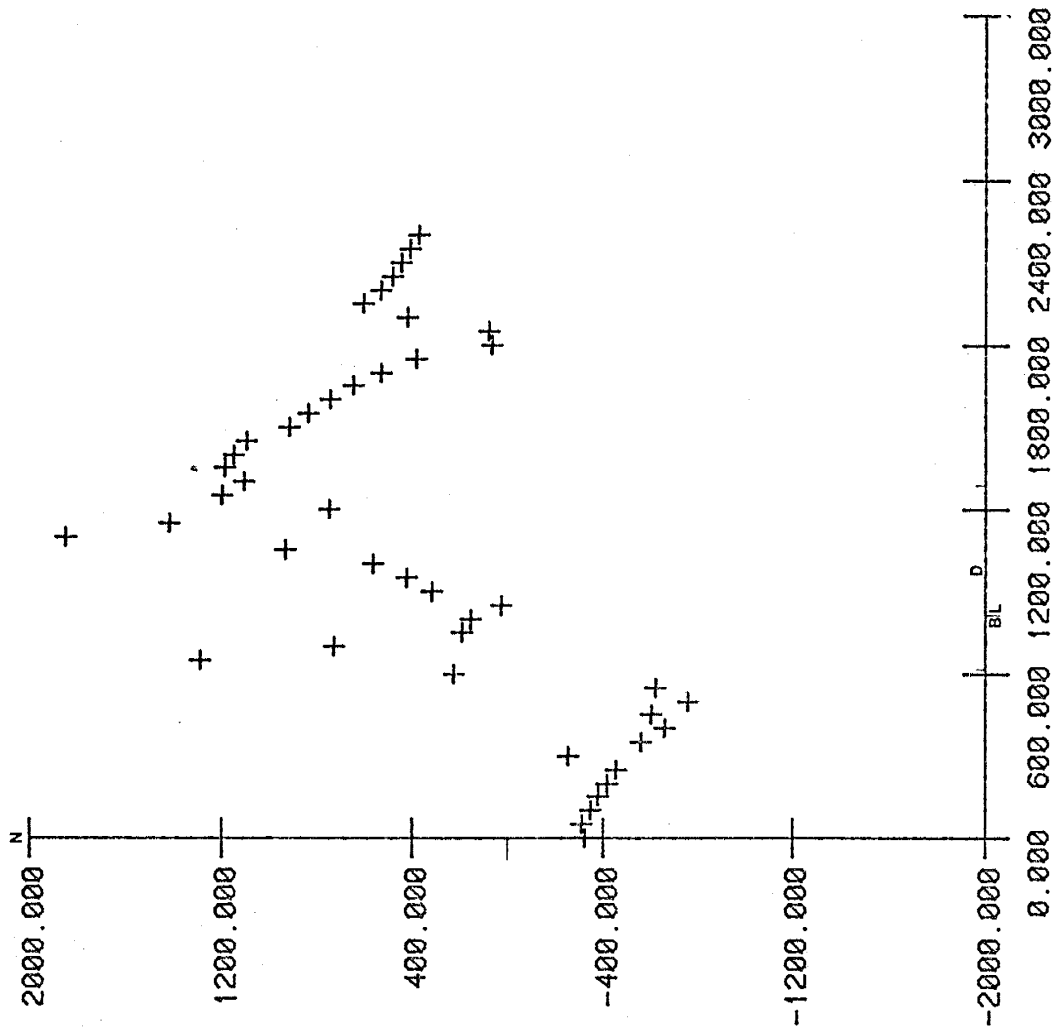
0.000 600.000 1200.000 1800.000 2400.000 3000.000

S



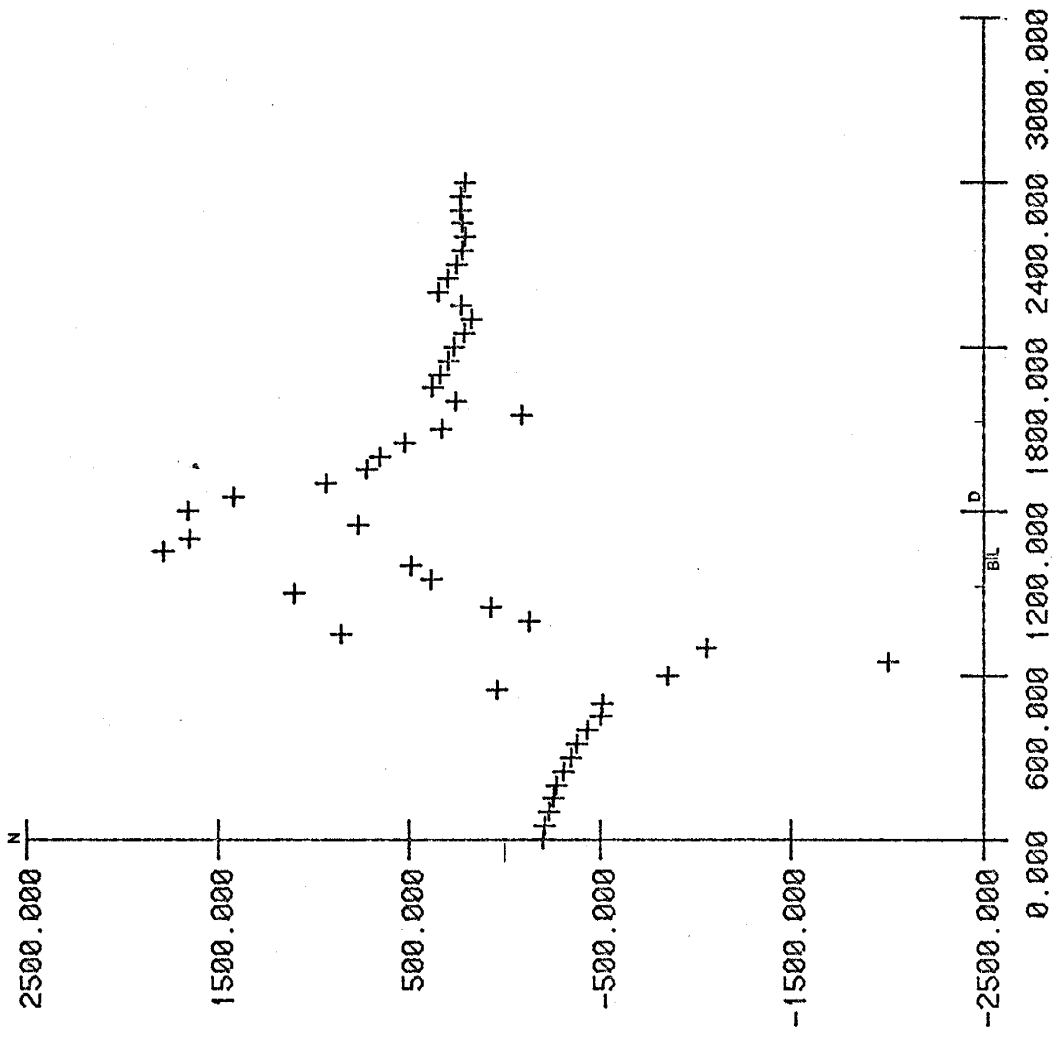
P51

S



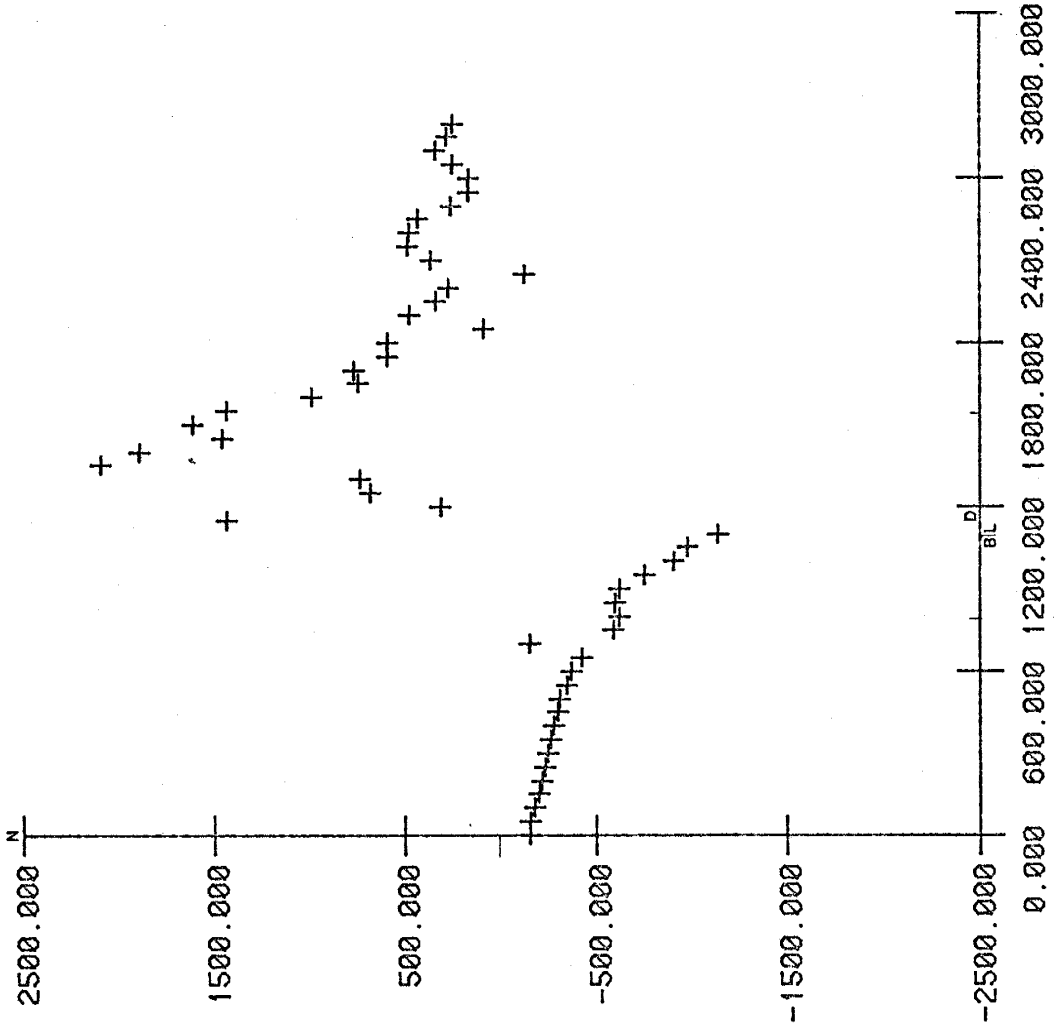
P52

s



P53

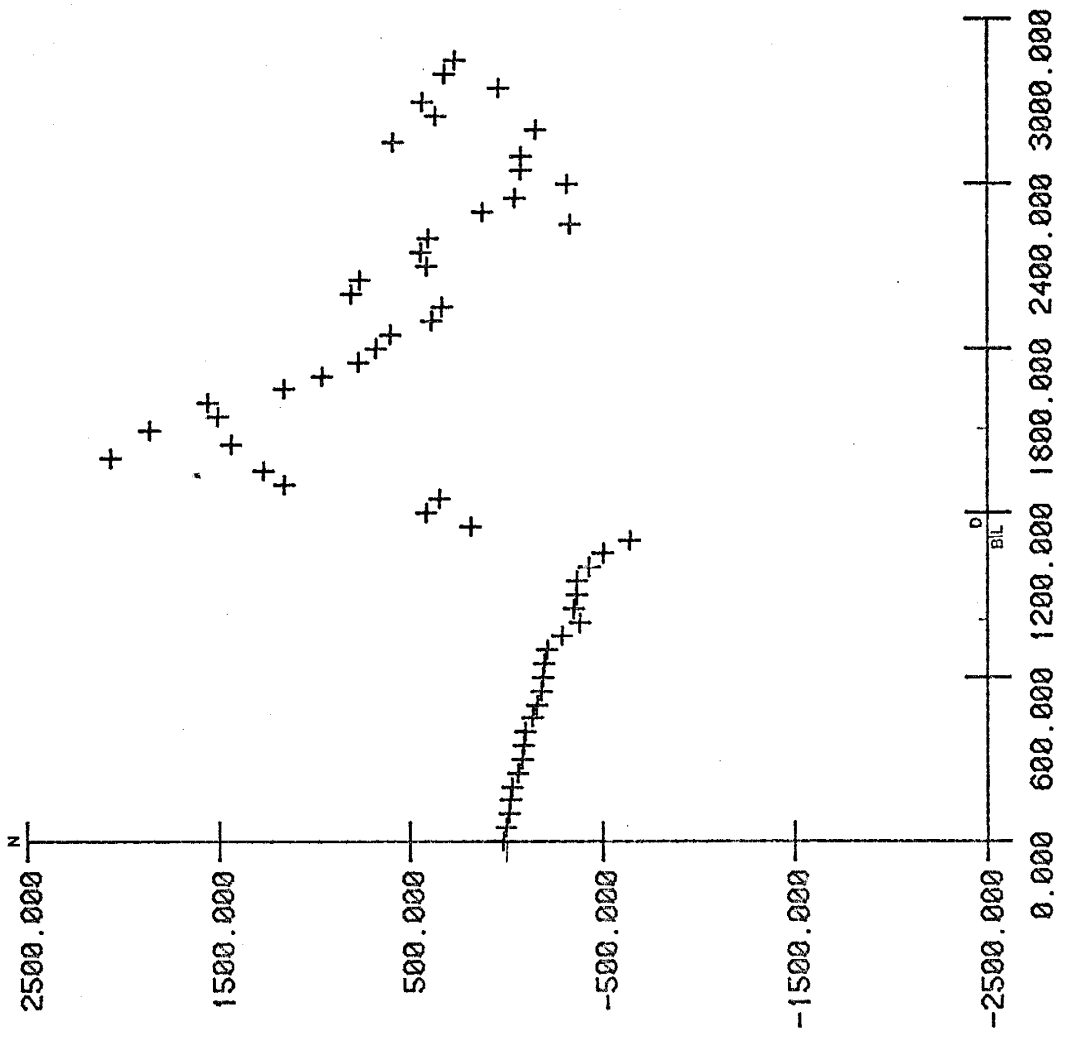
s



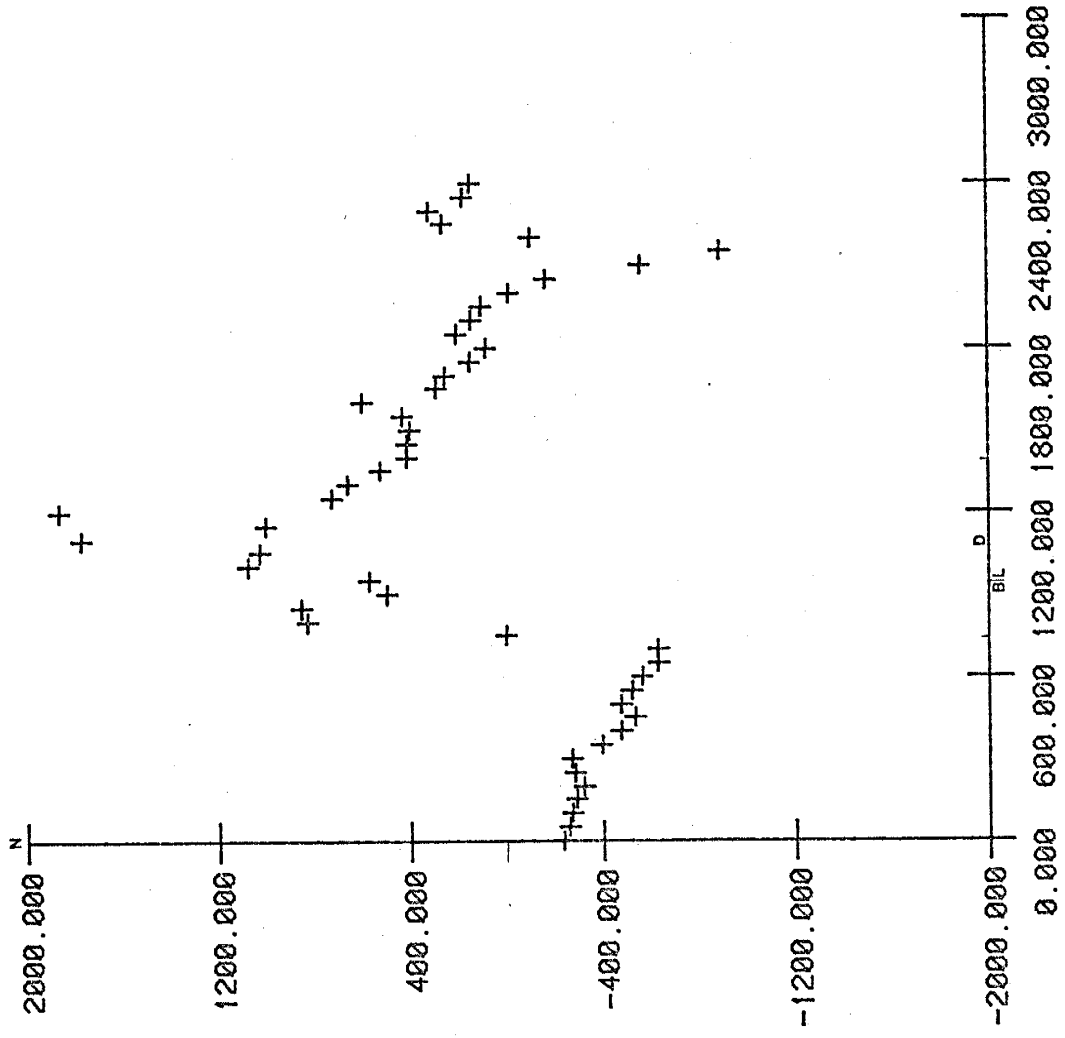
P54

P55

s

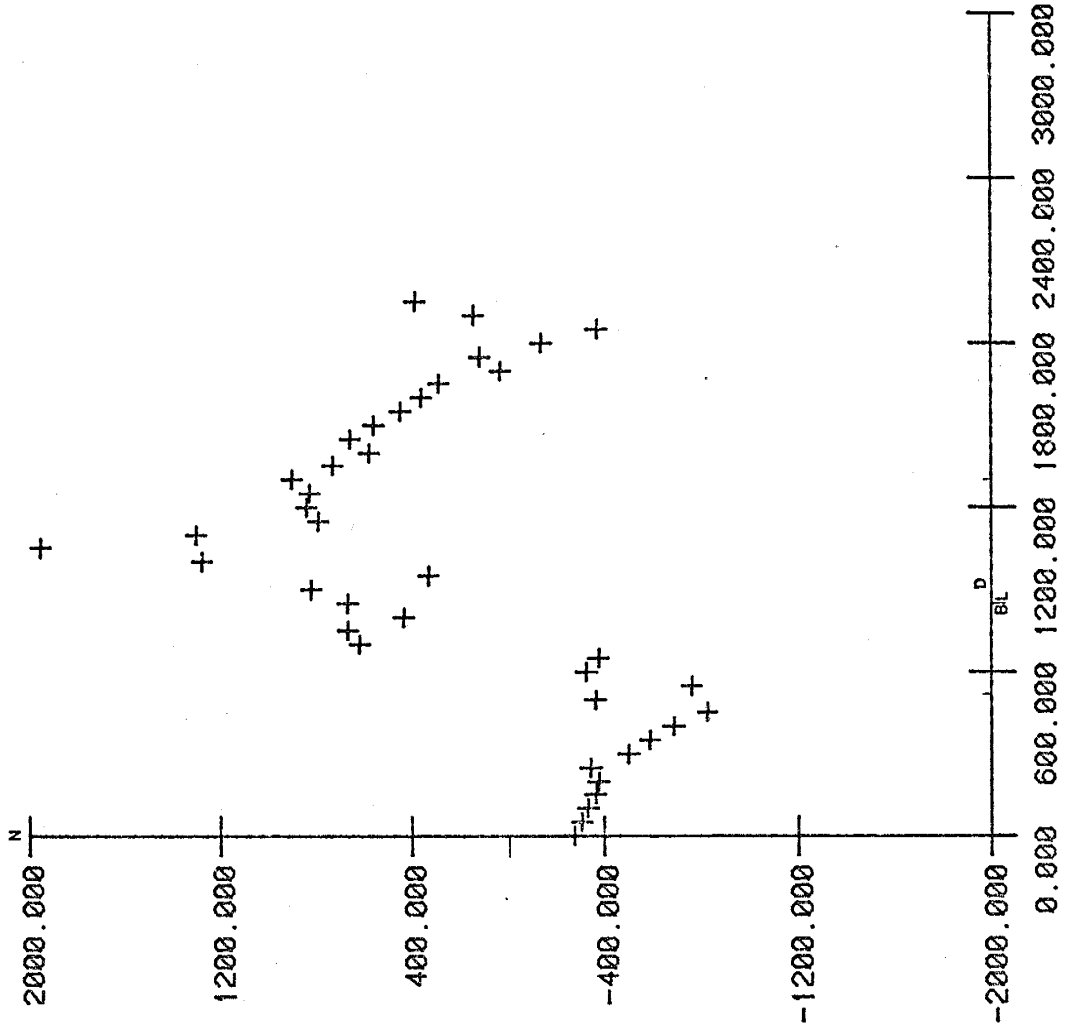


S

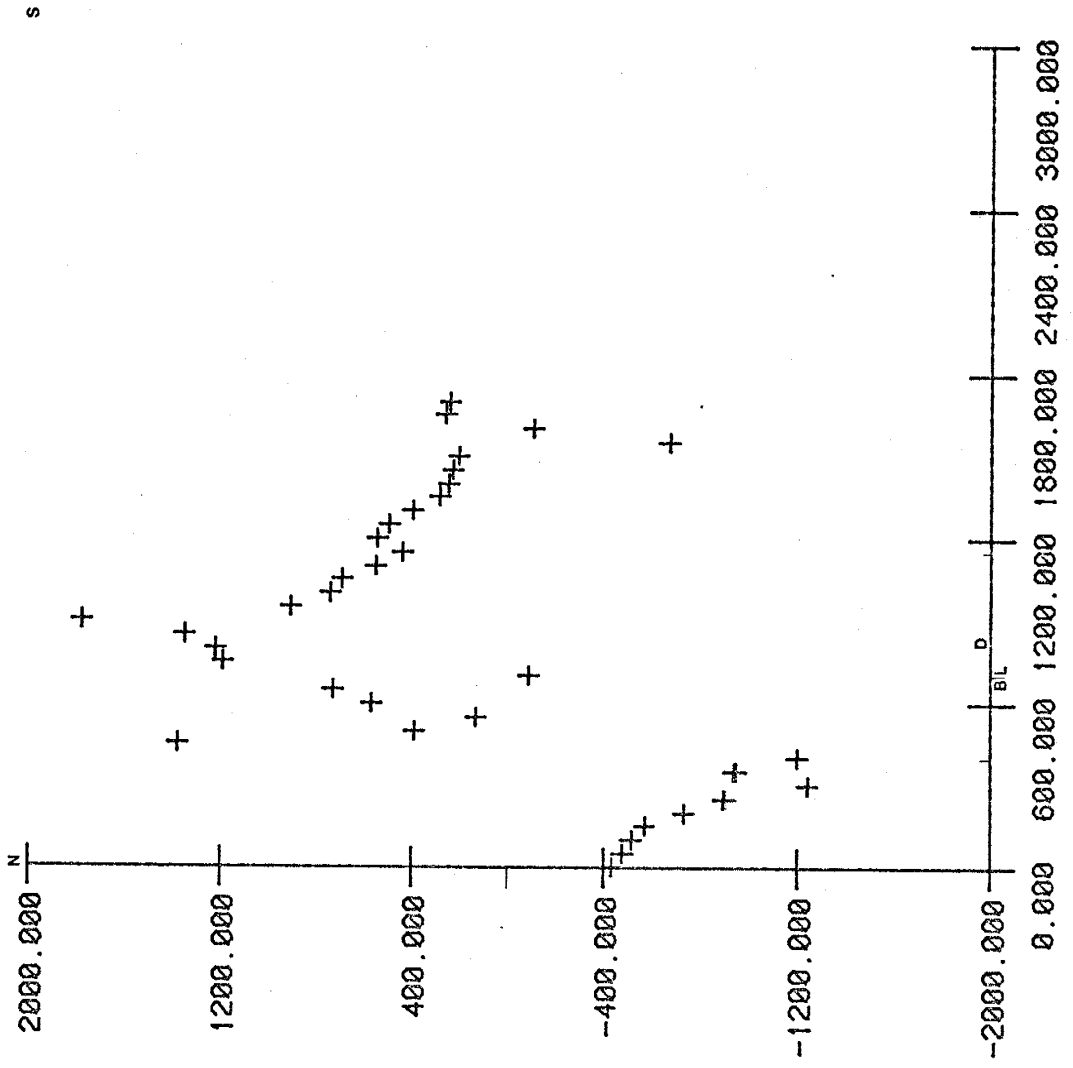


P56

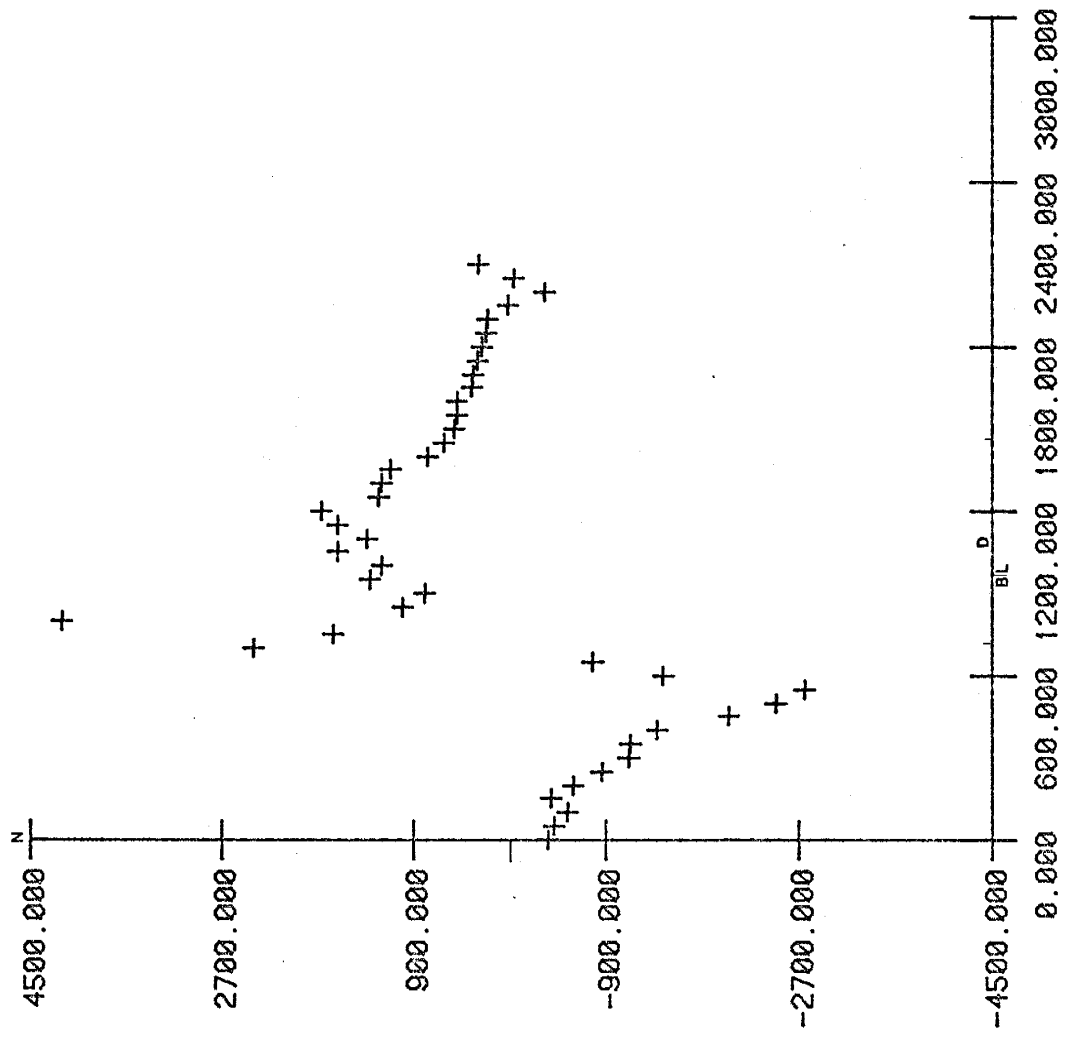
s



P57

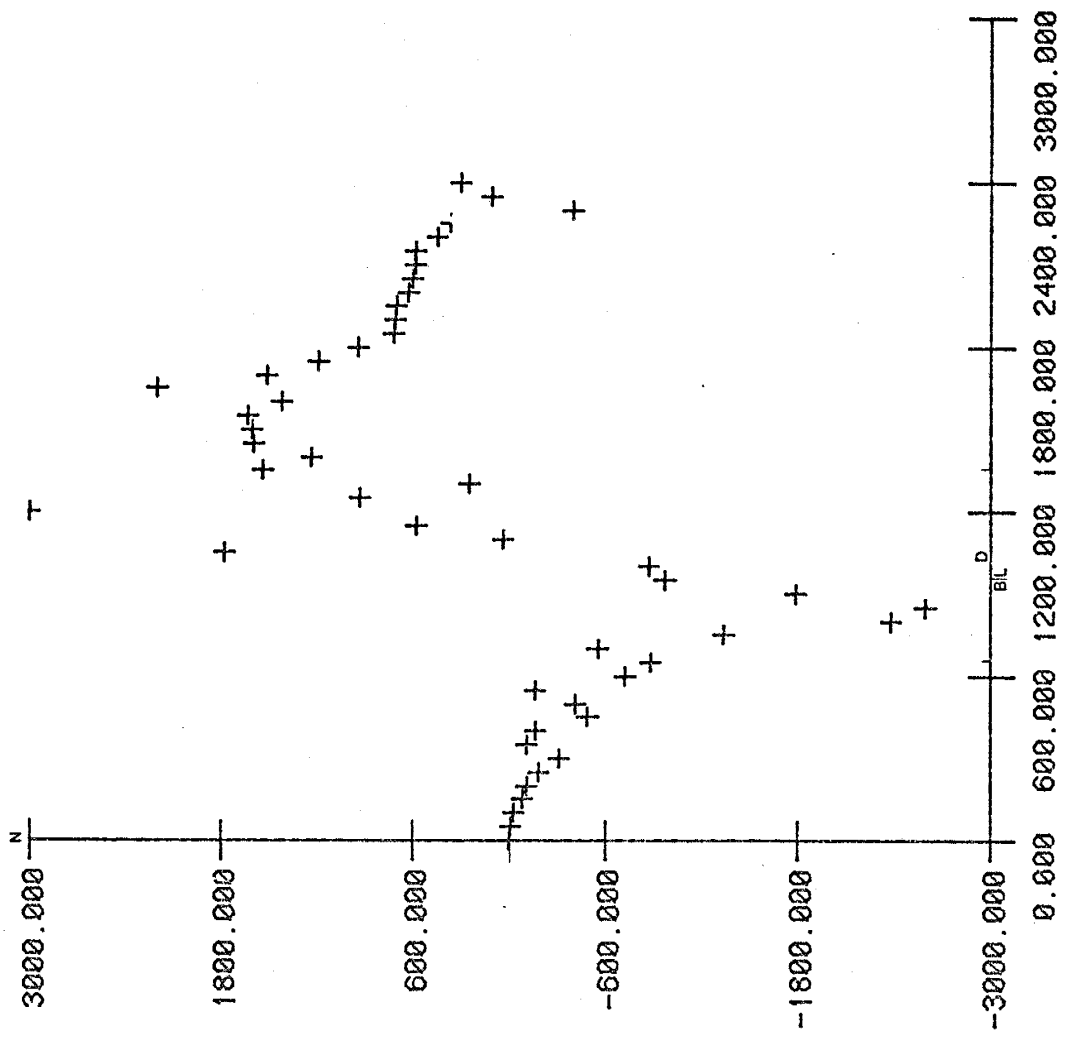


S



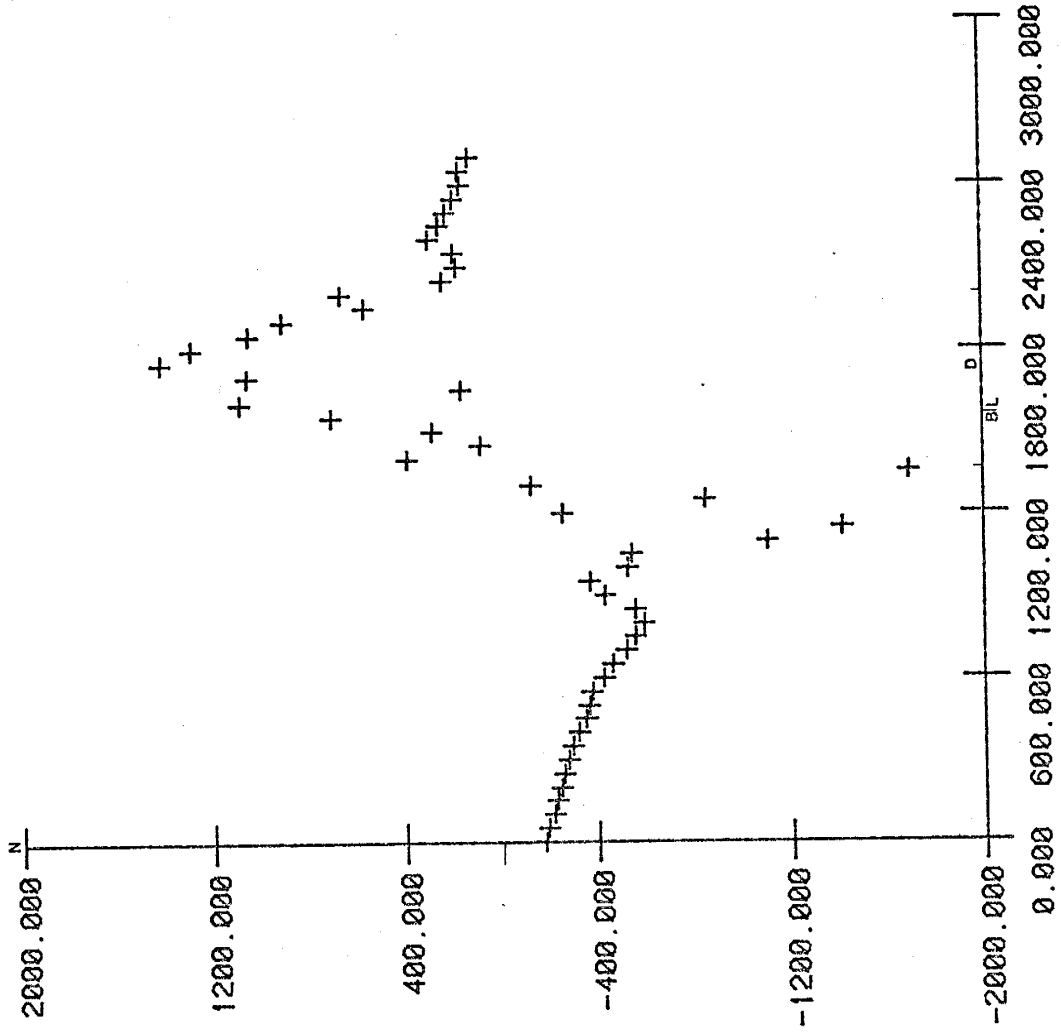
P59

S



P60

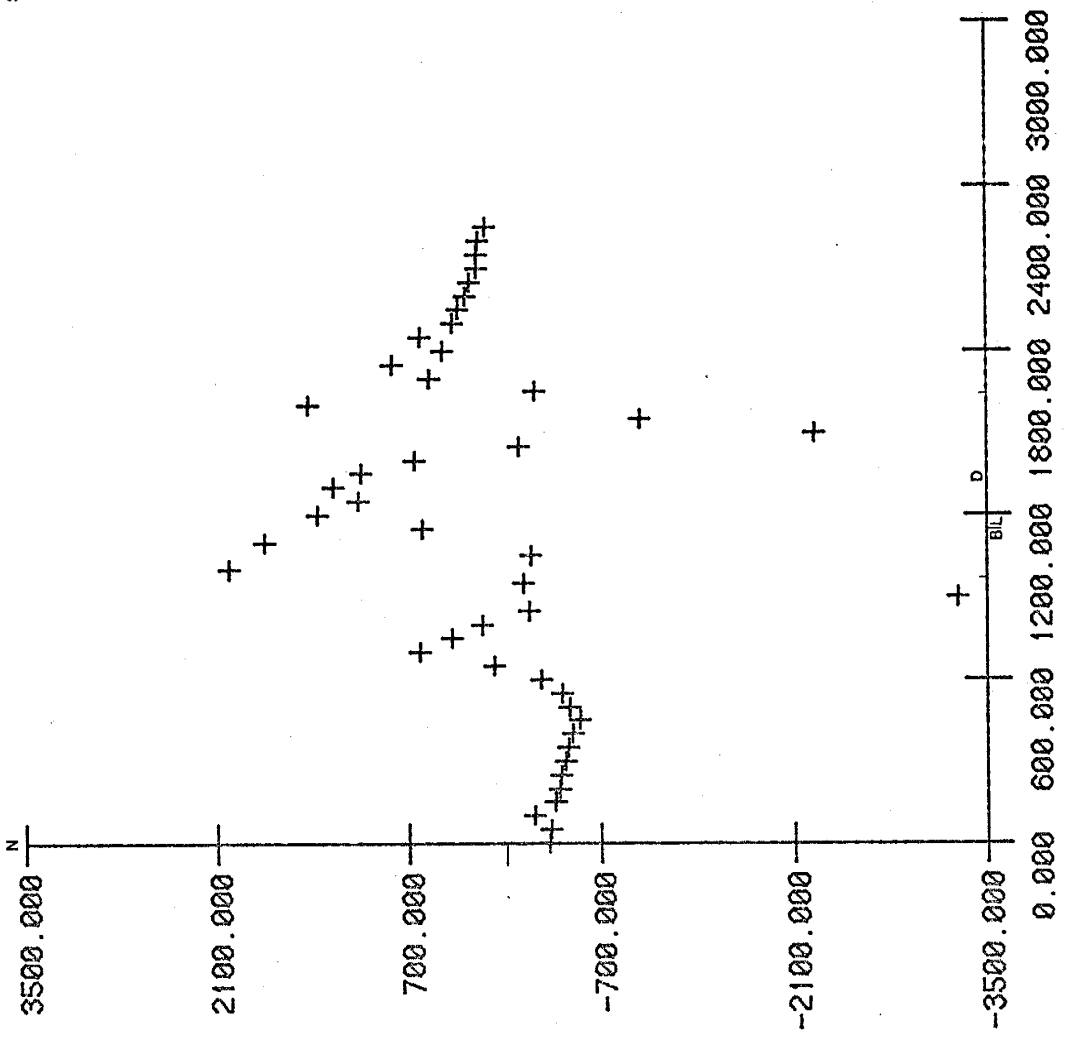
5



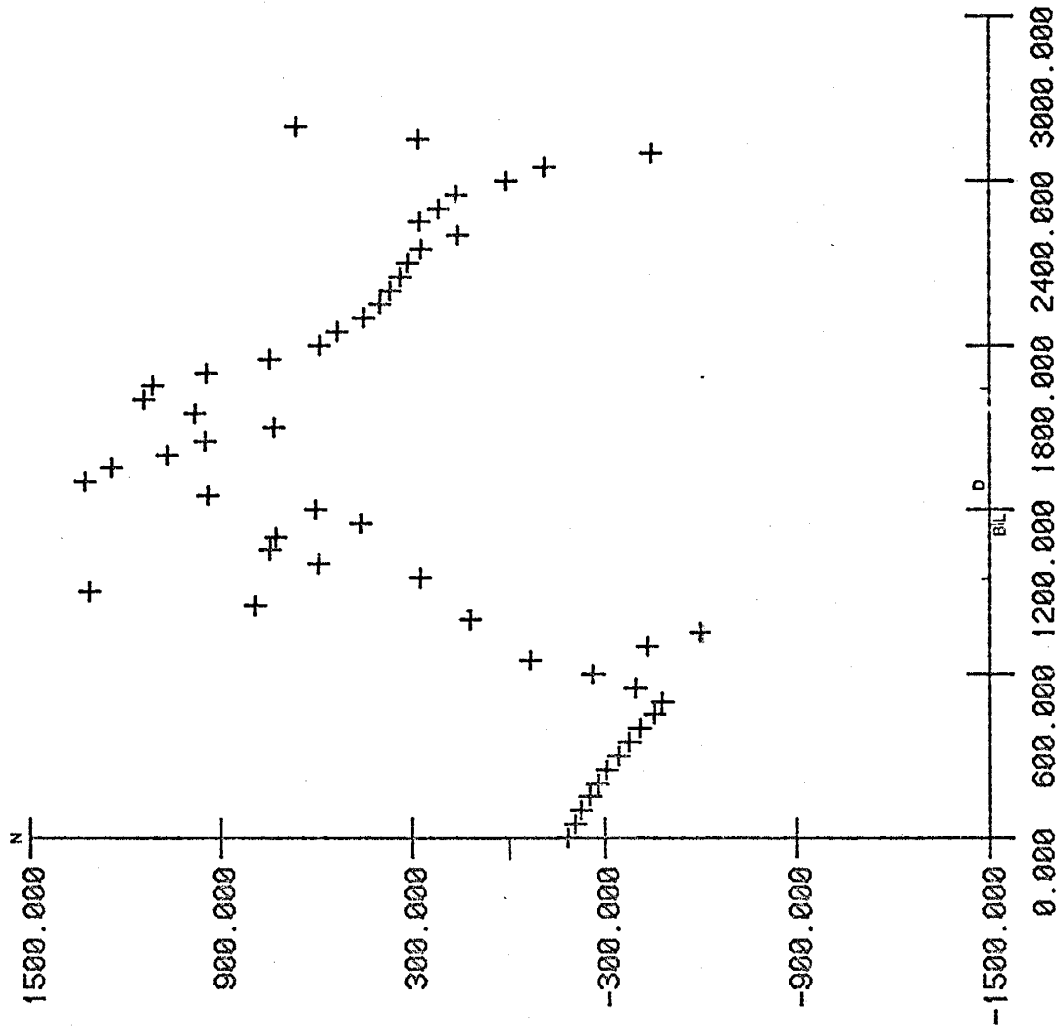
P61

P62

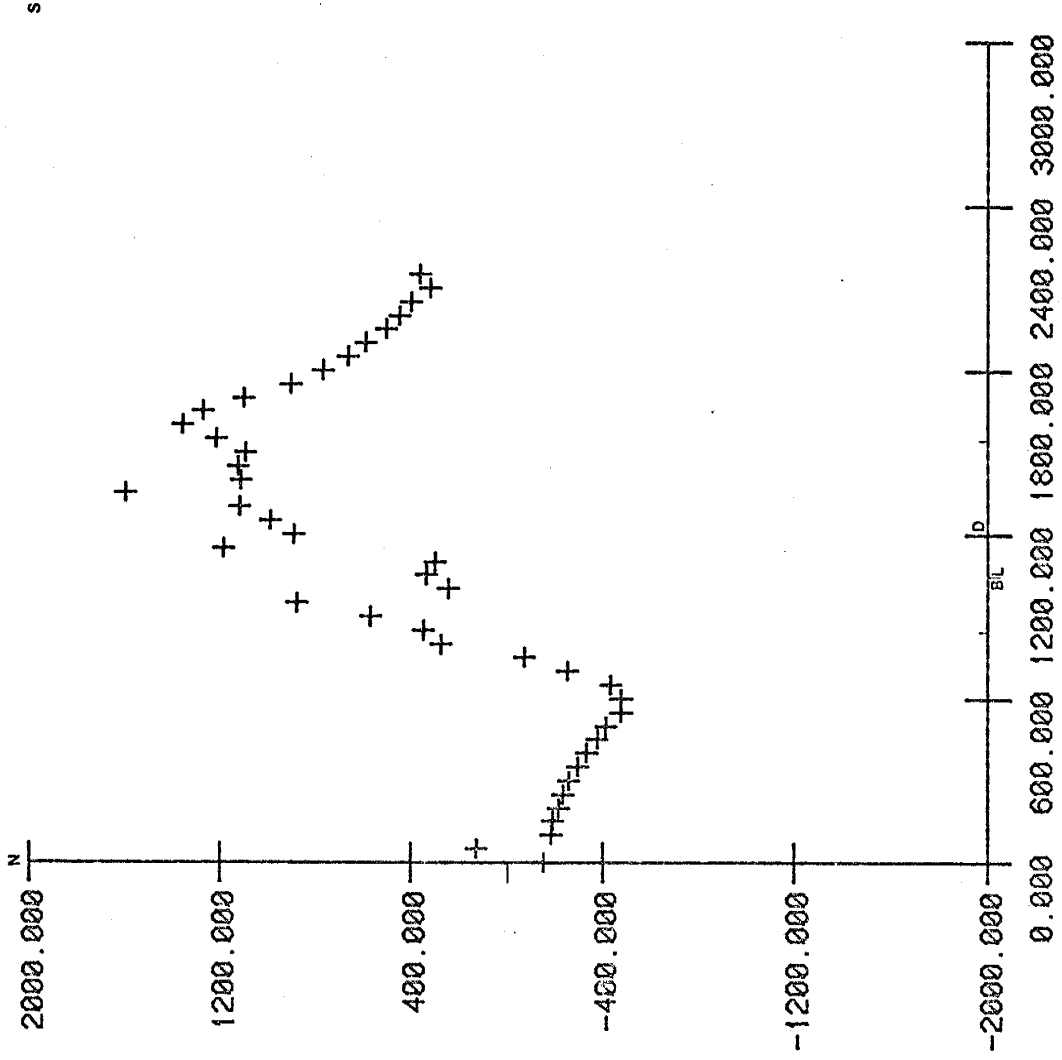
S



s

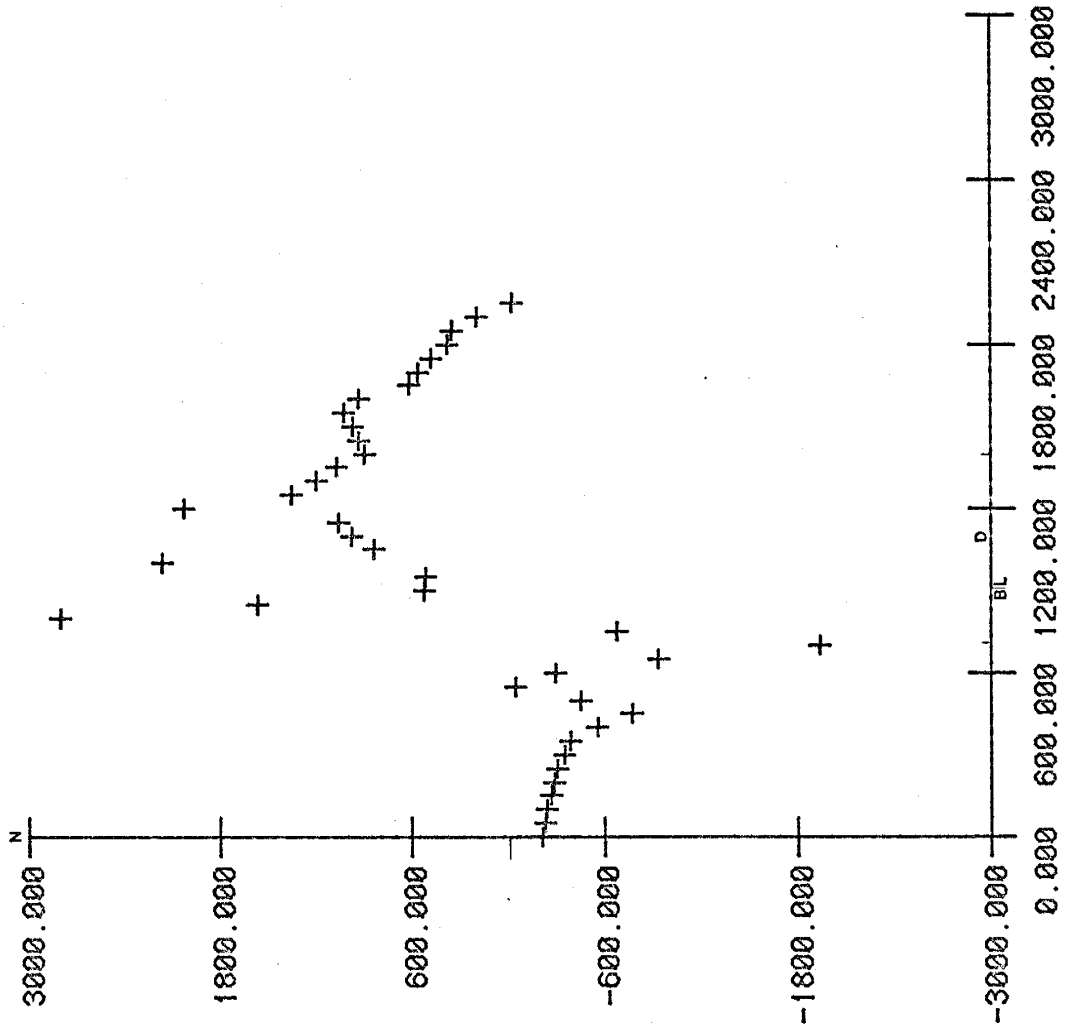


P63



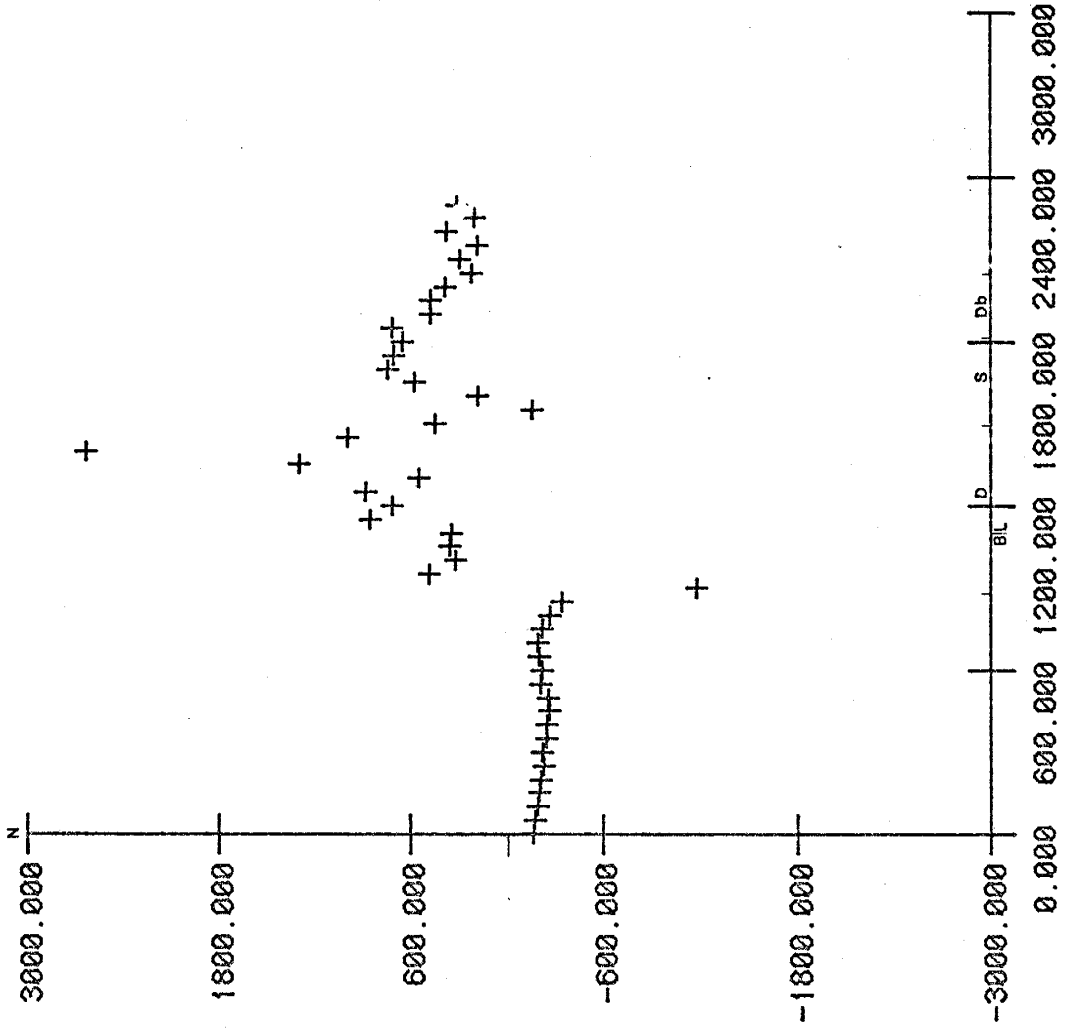
S

9

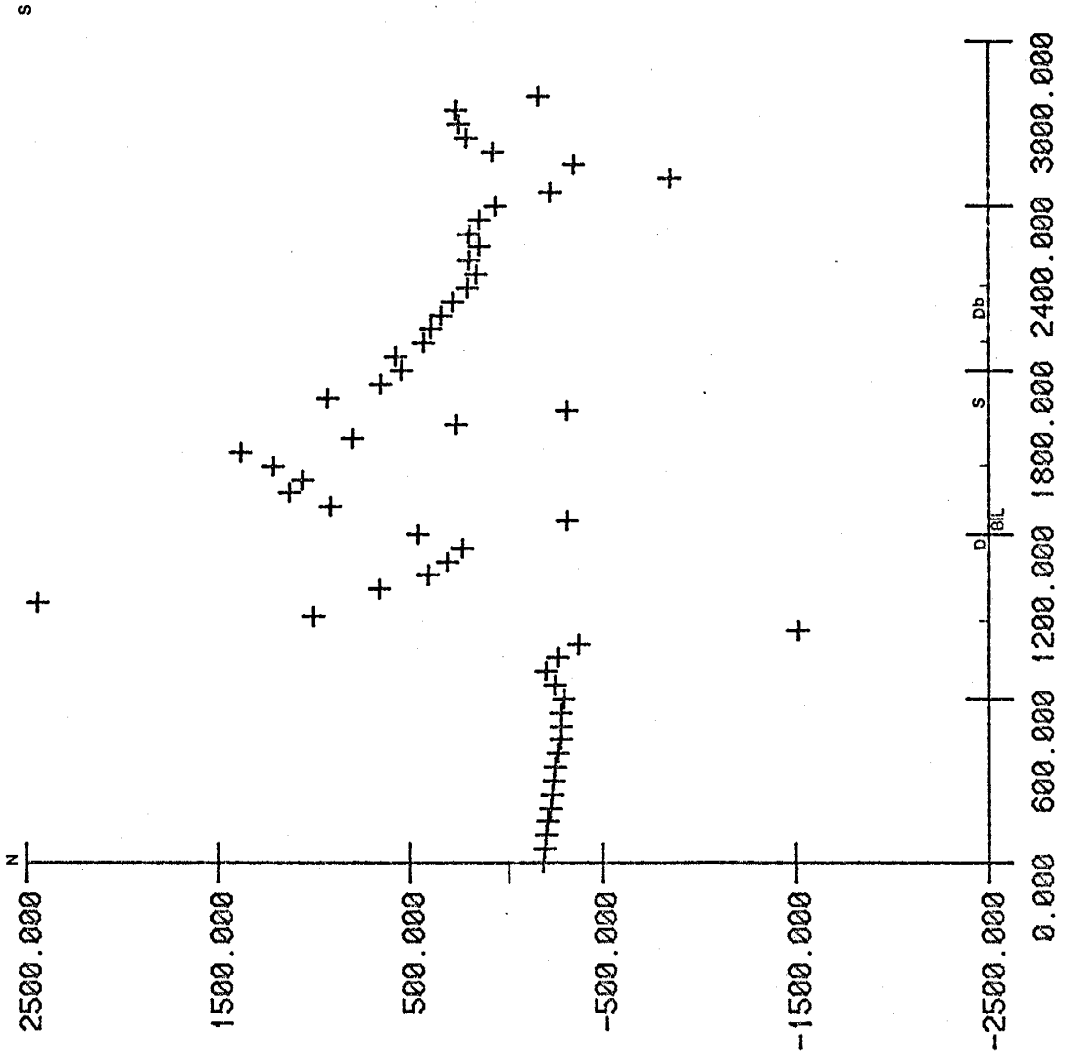


P65

S



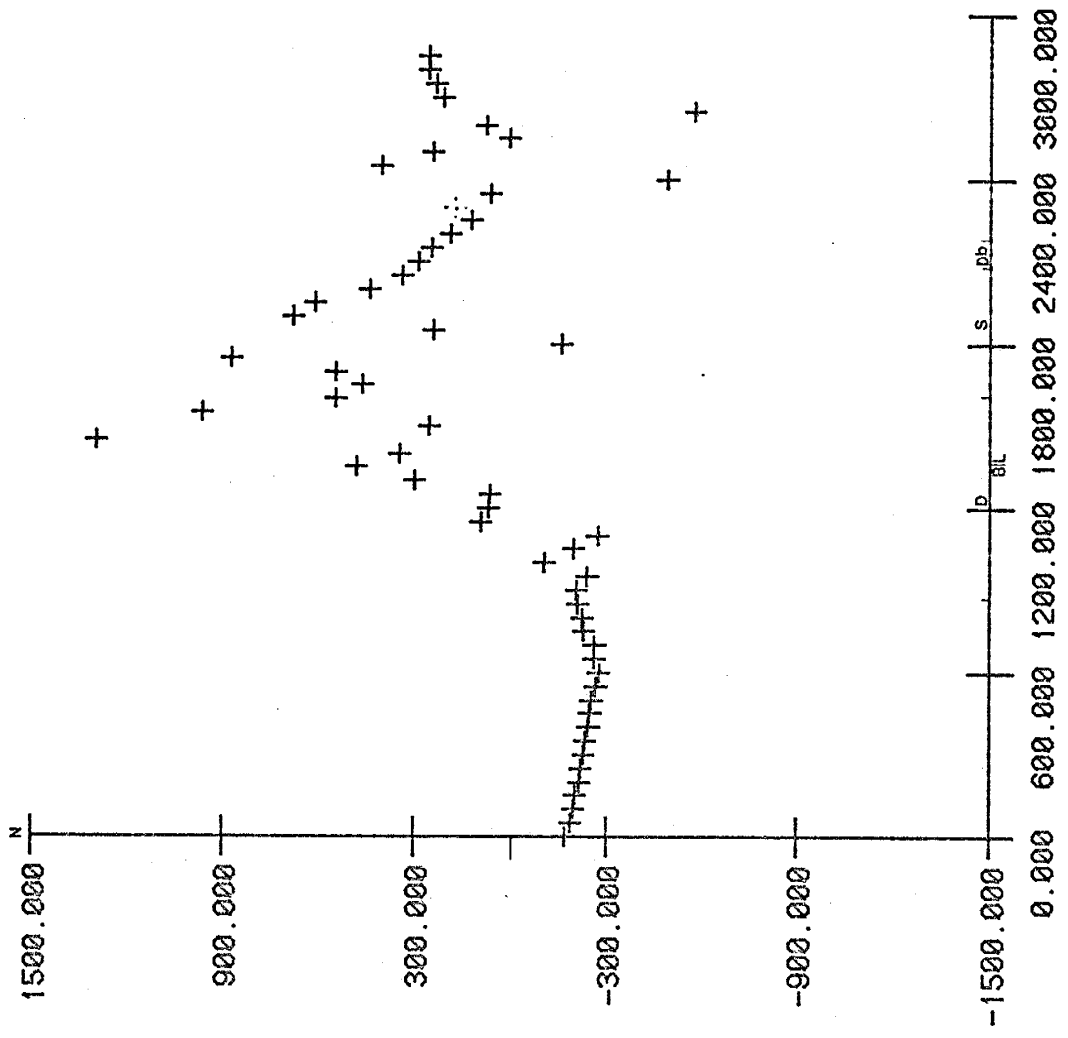
P66



P67

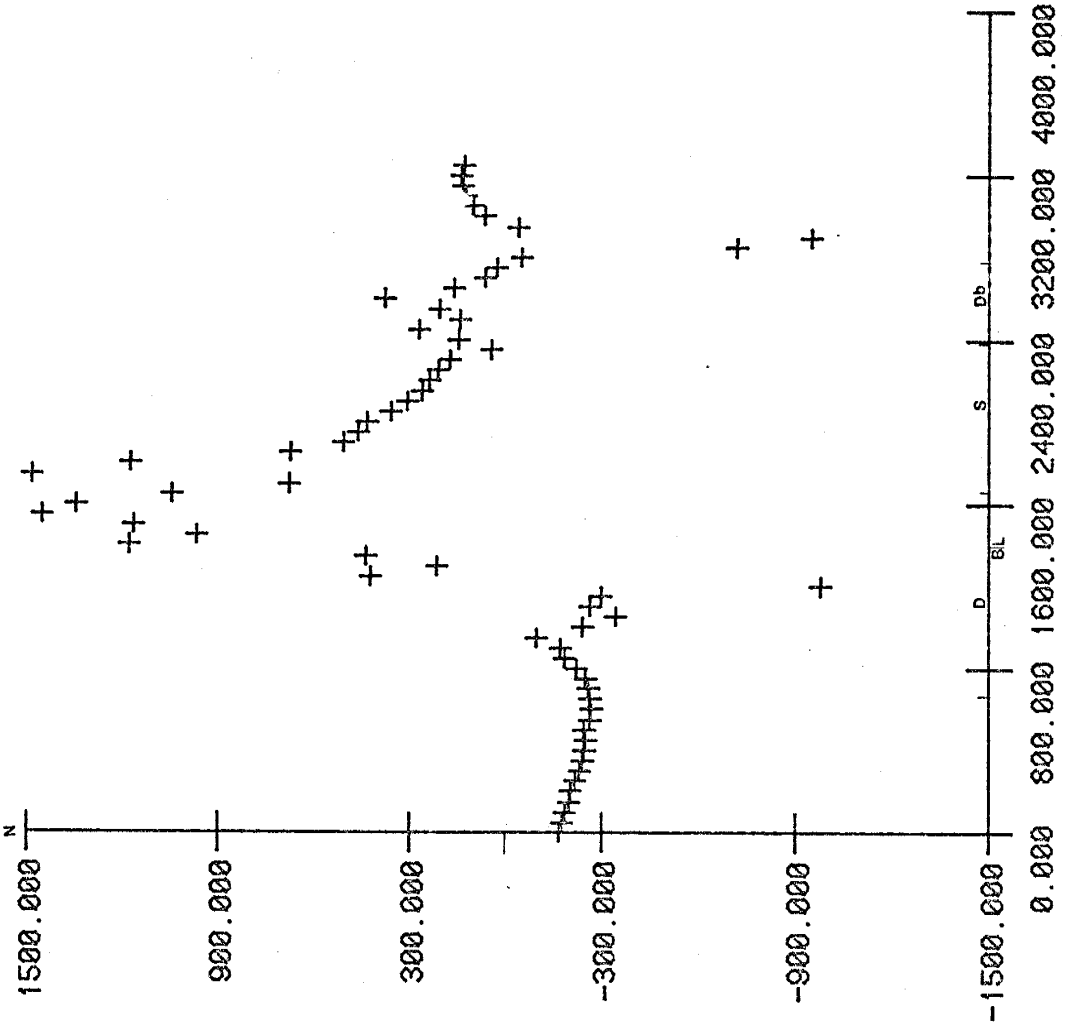
S

s



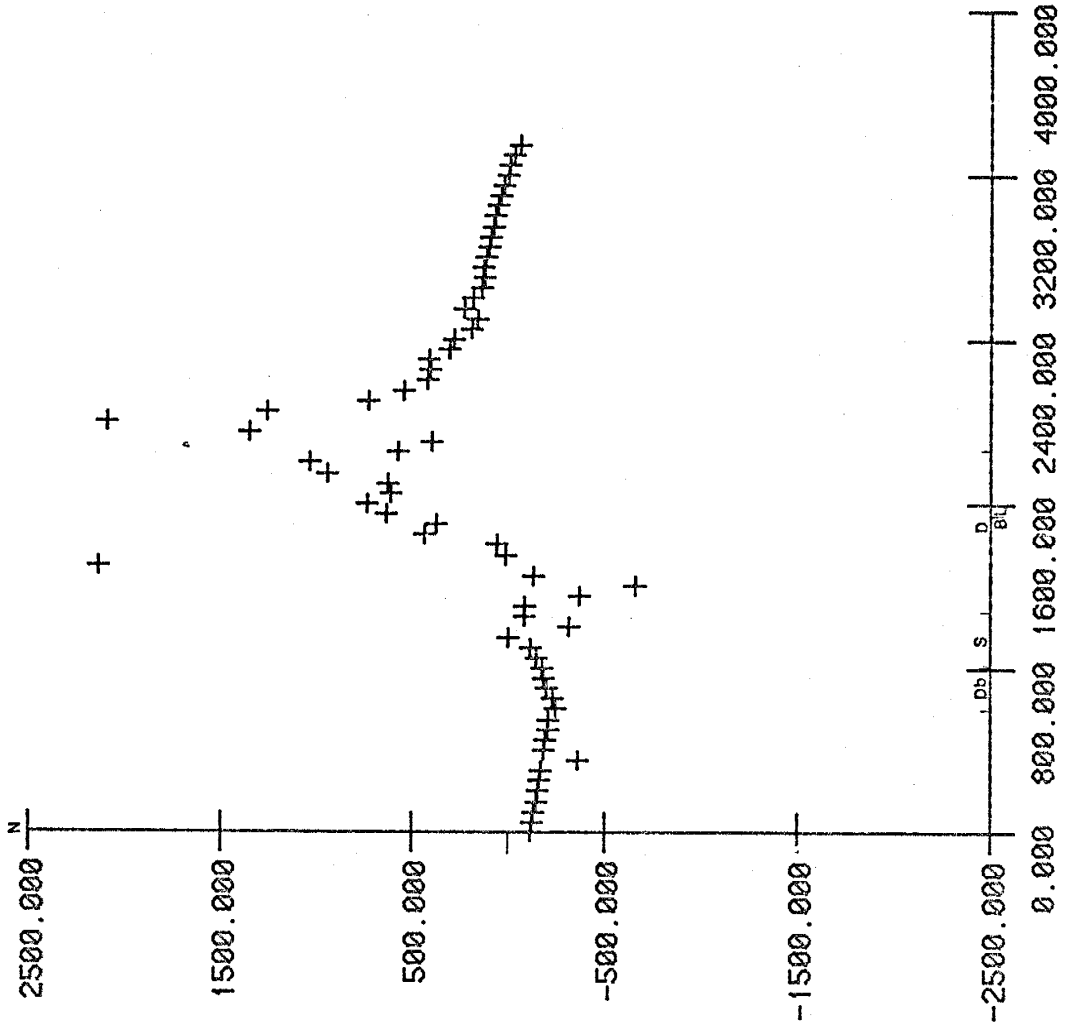
P68

s



P69

S



P71

2500.000 N

1500.000

500.000

-500.000

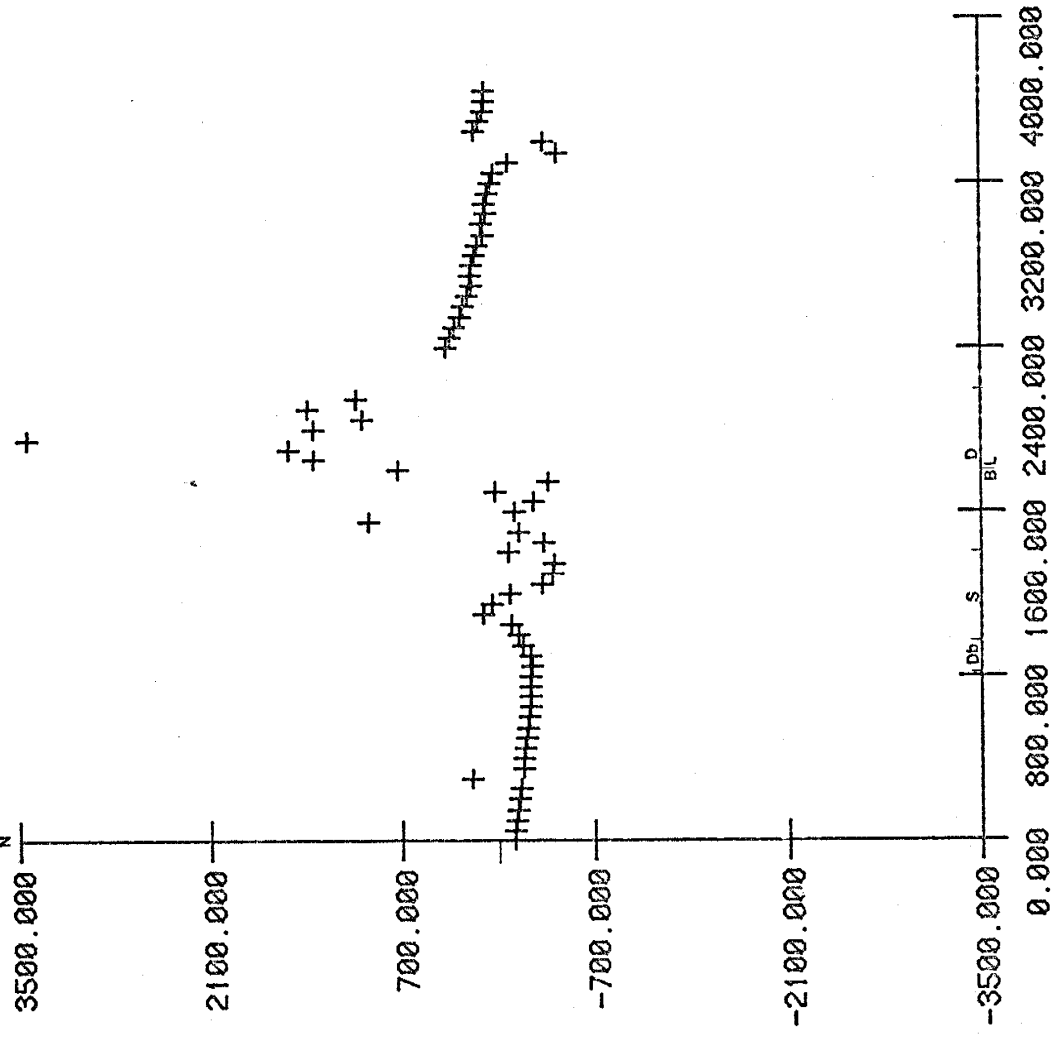
-1500.000

-2500.000

0.000 S D B

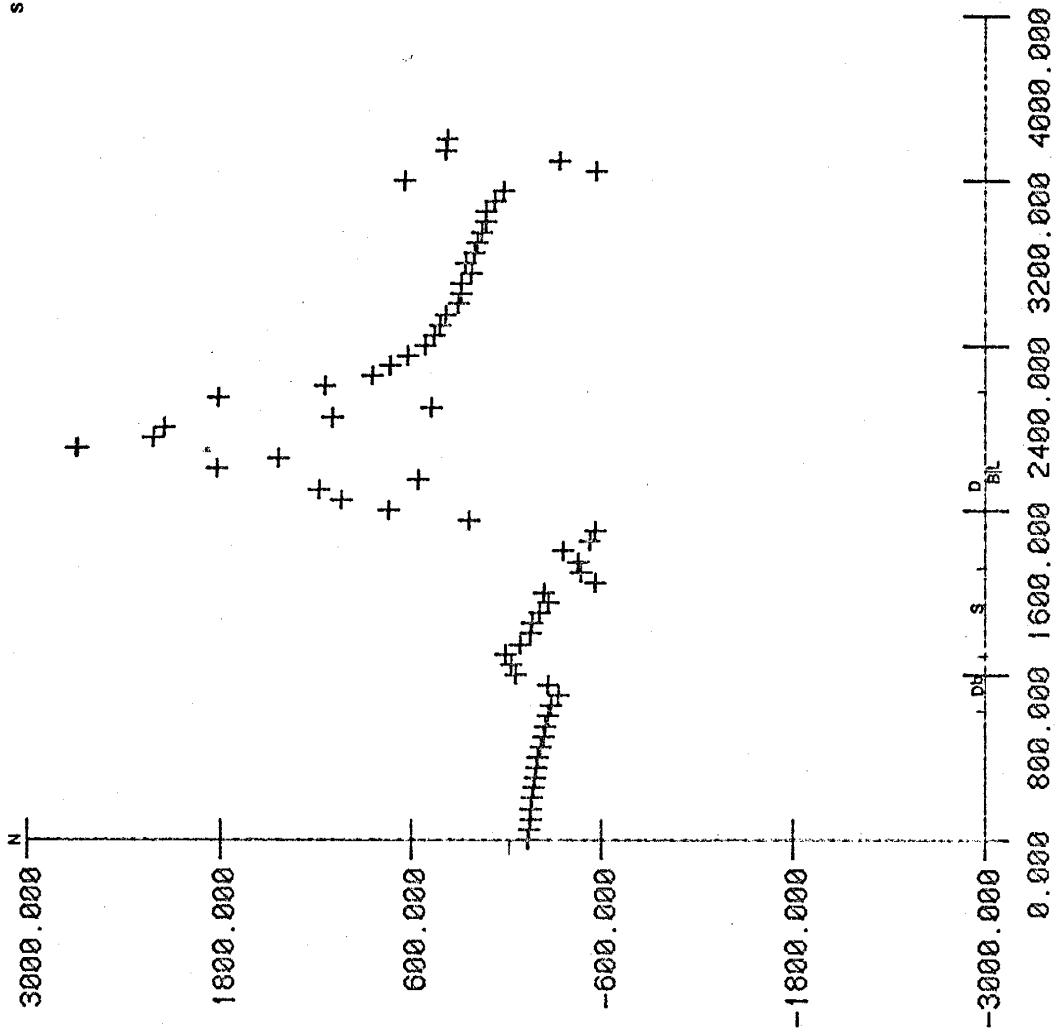
800.000 1600.000 2400.000 3200.000 4000.000

S



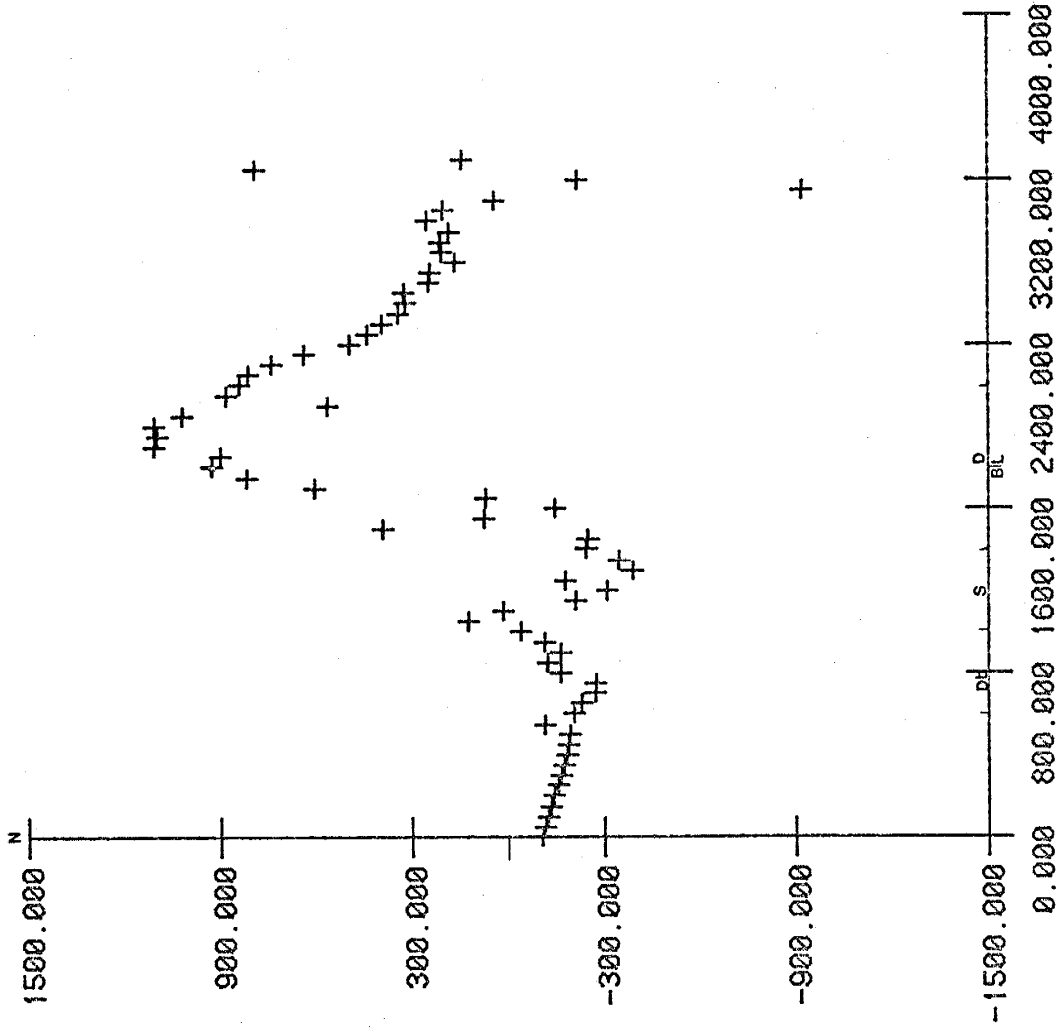
P72

s

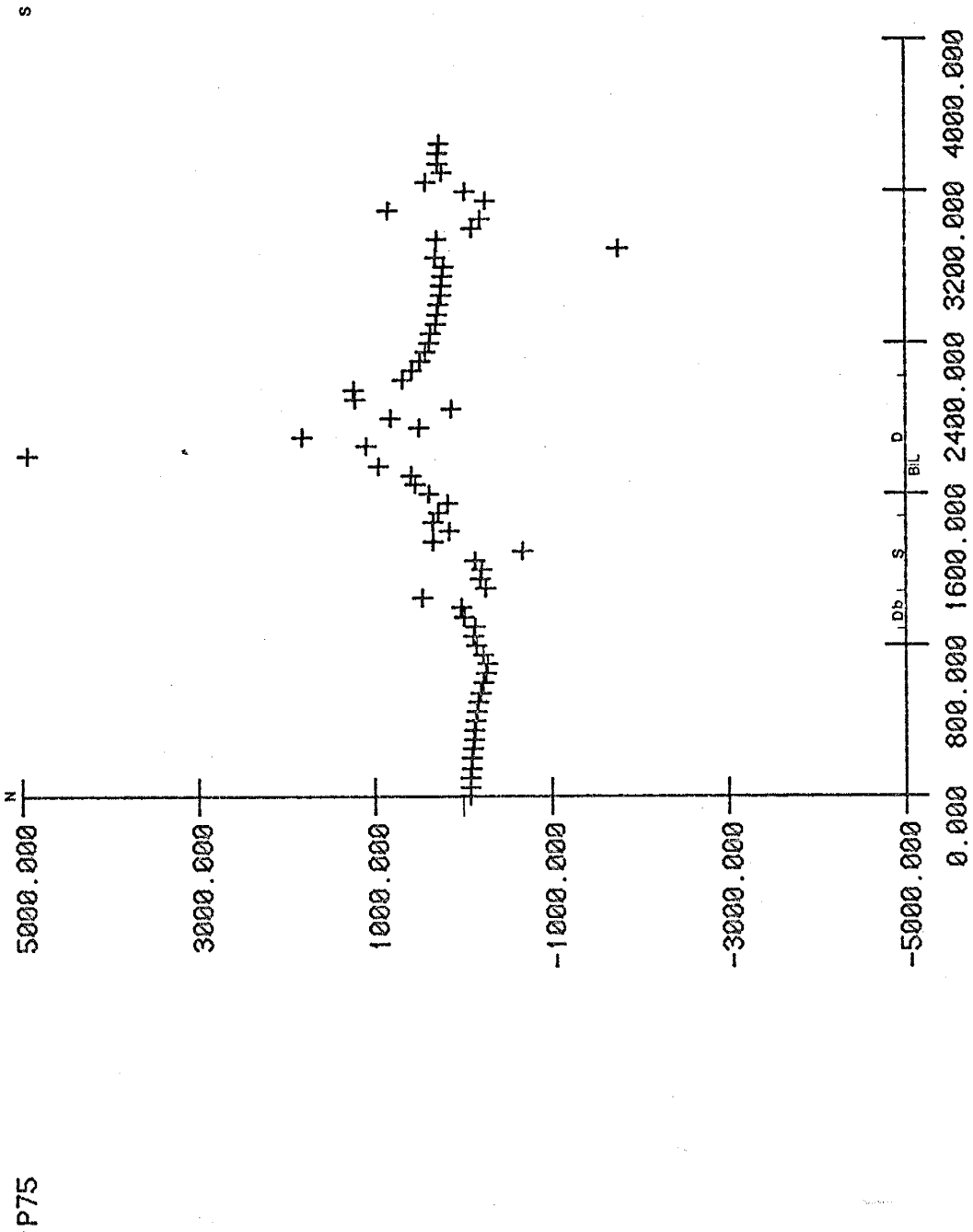


P73

S

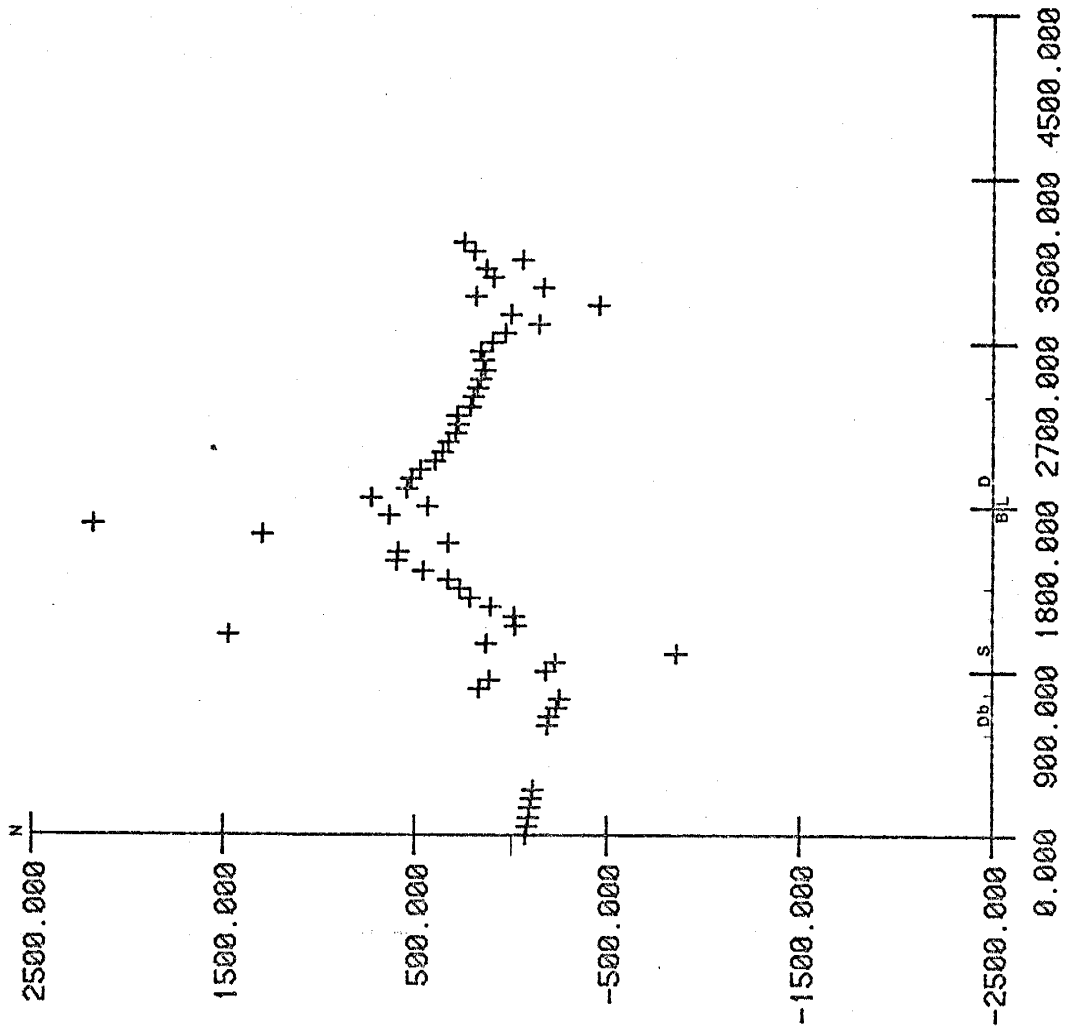


P74

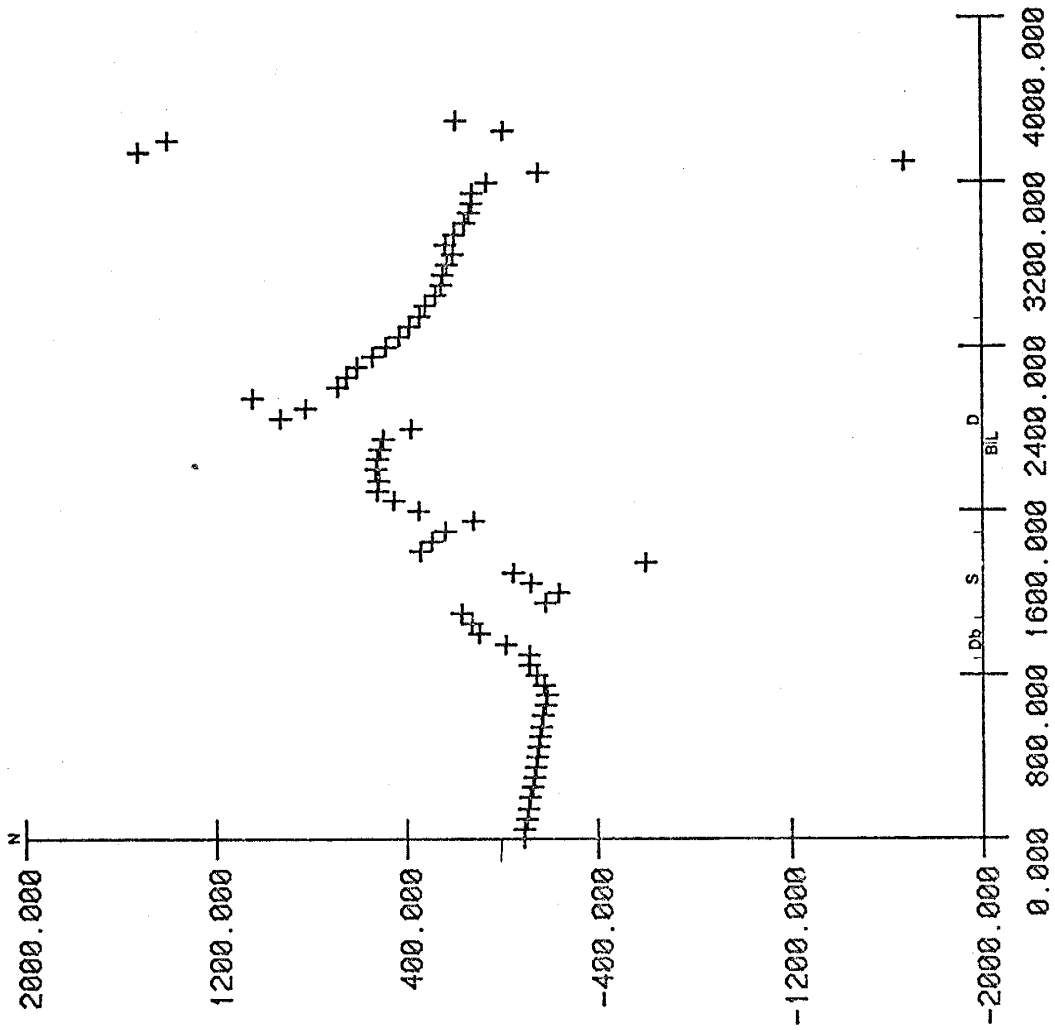


S

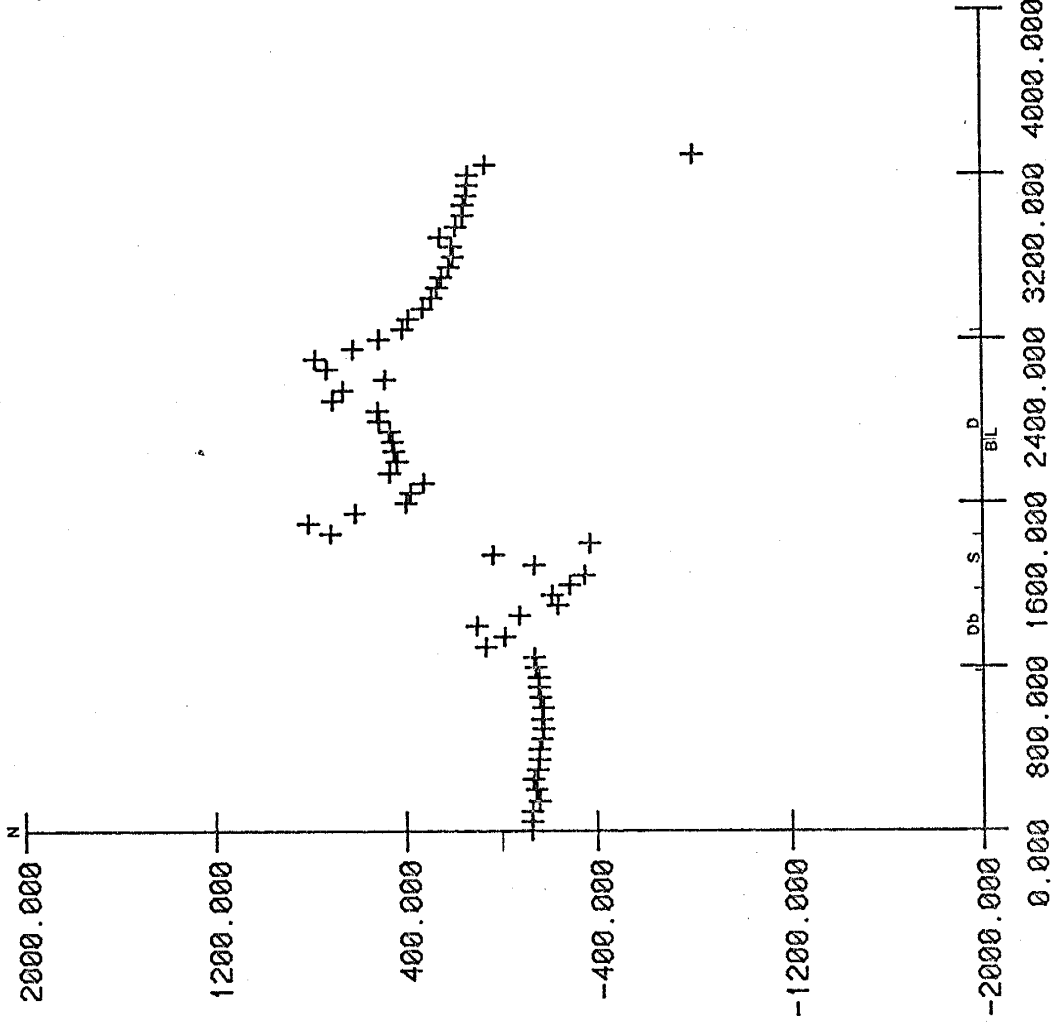
P76



s

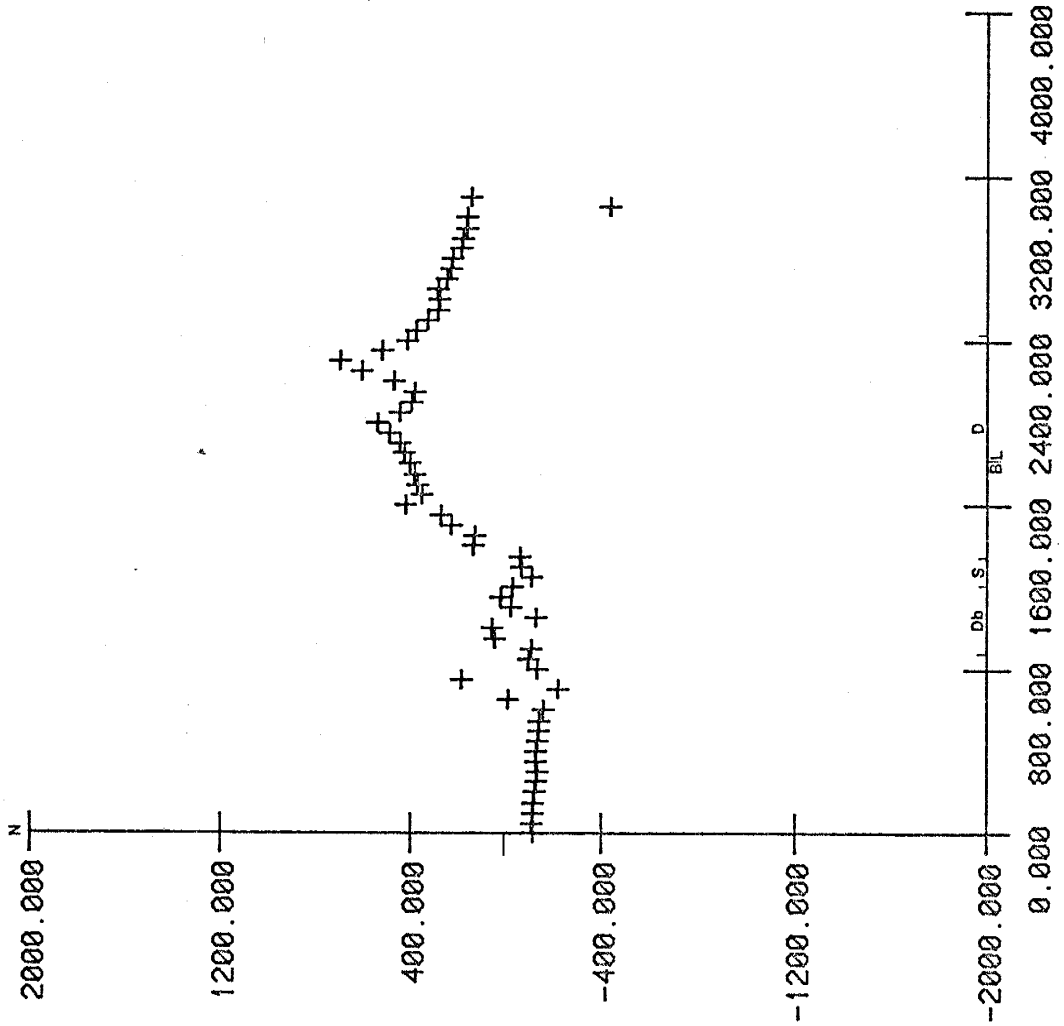


s



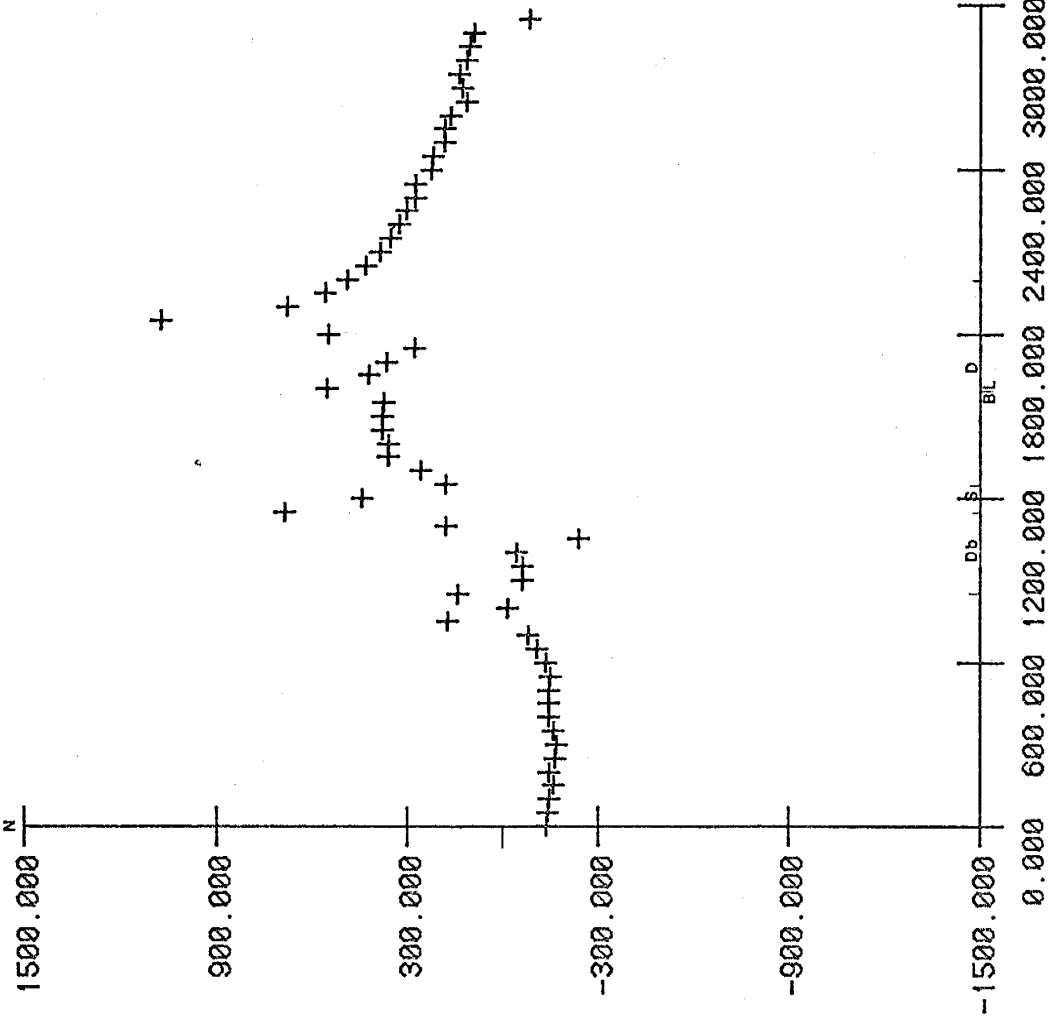
P78

S



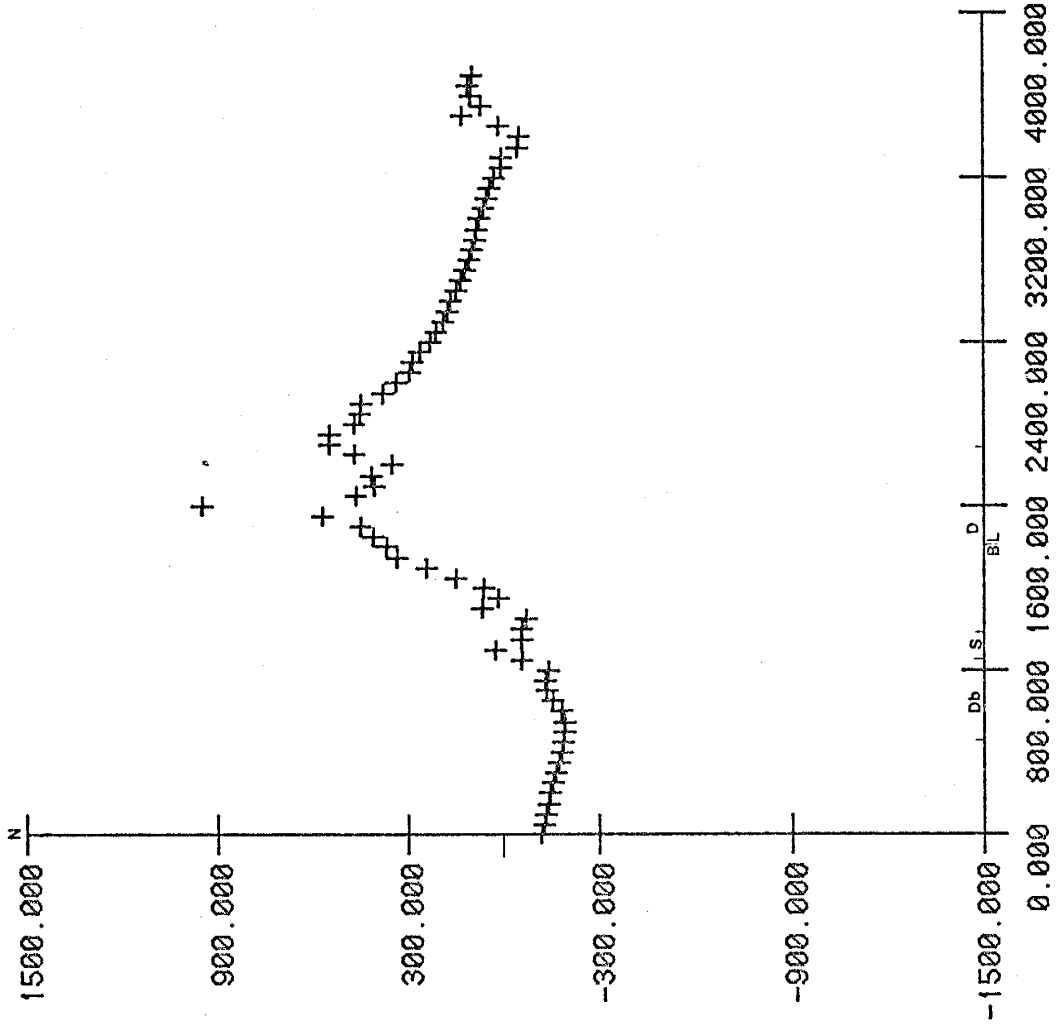
P79

S



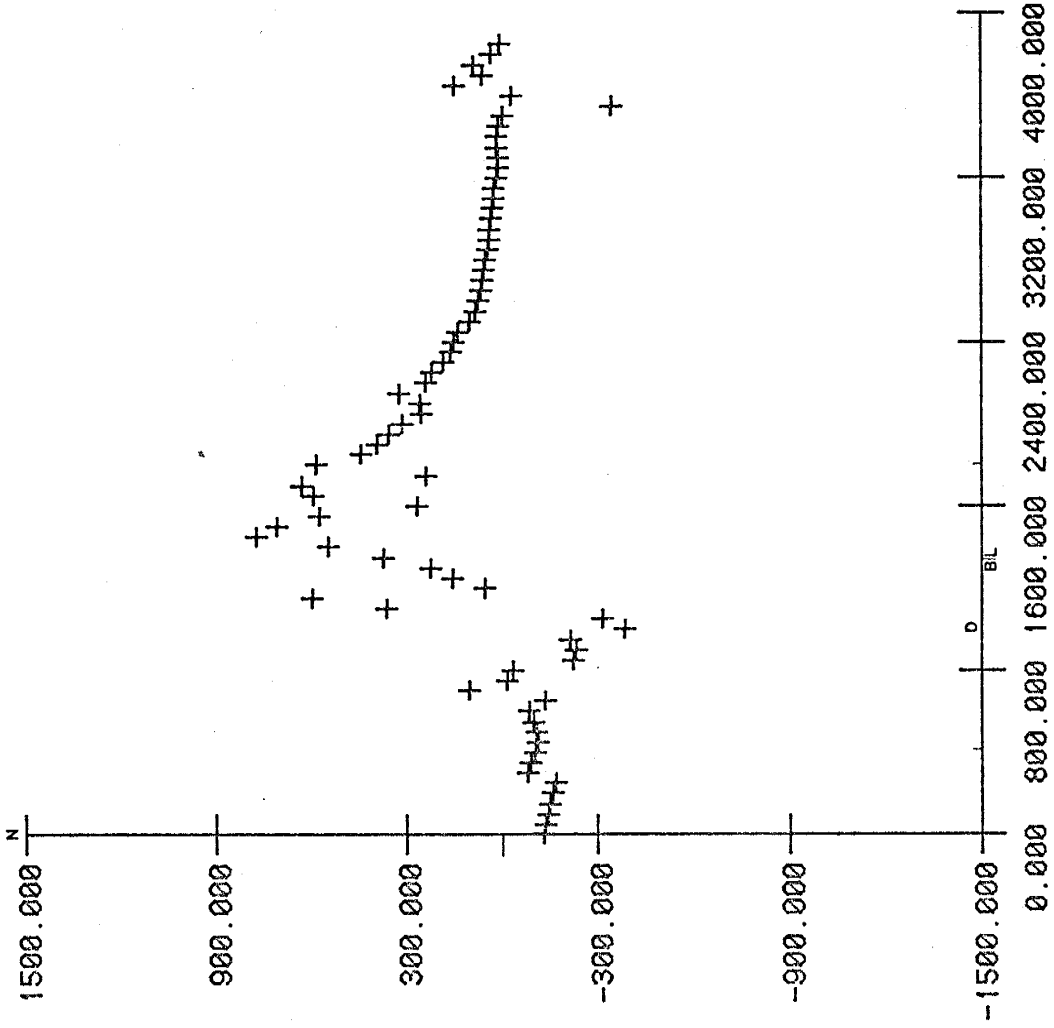
P80

S



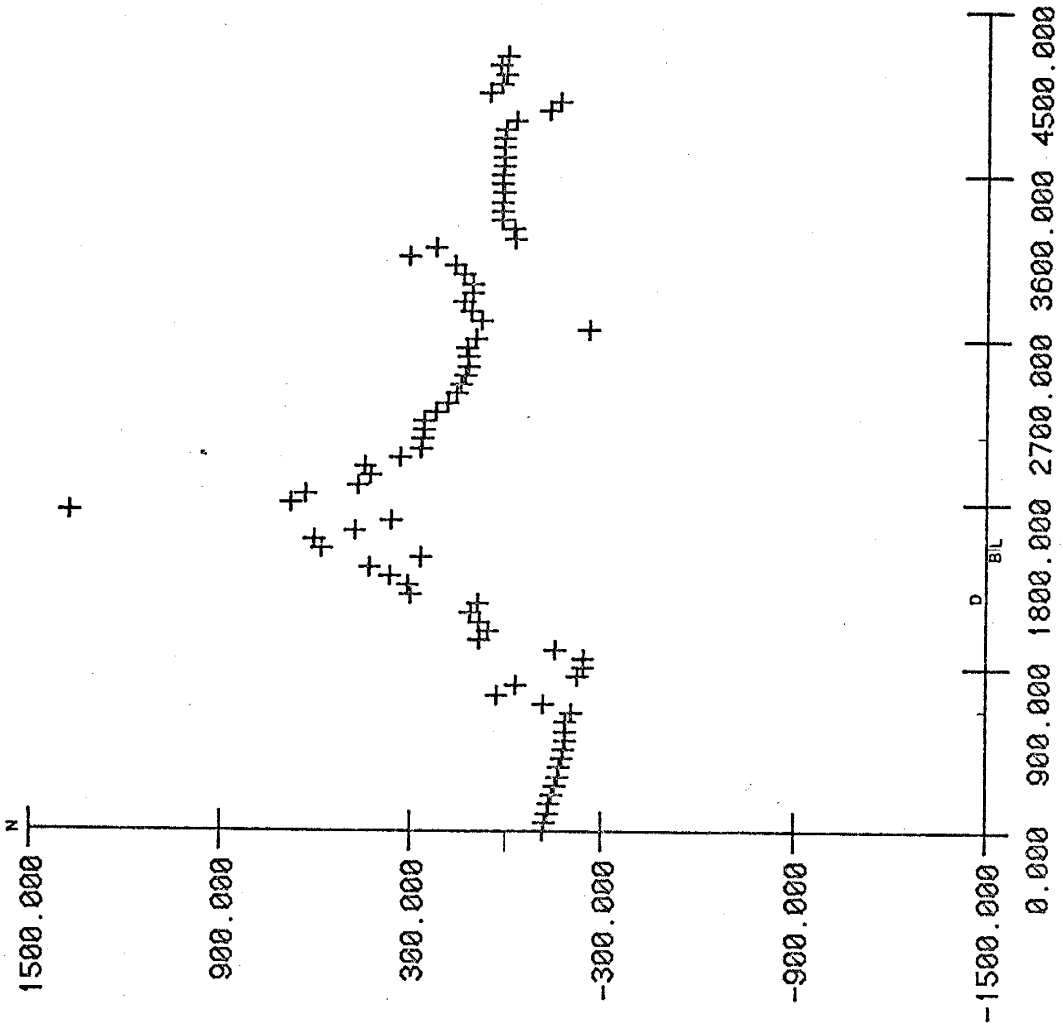
P81

S



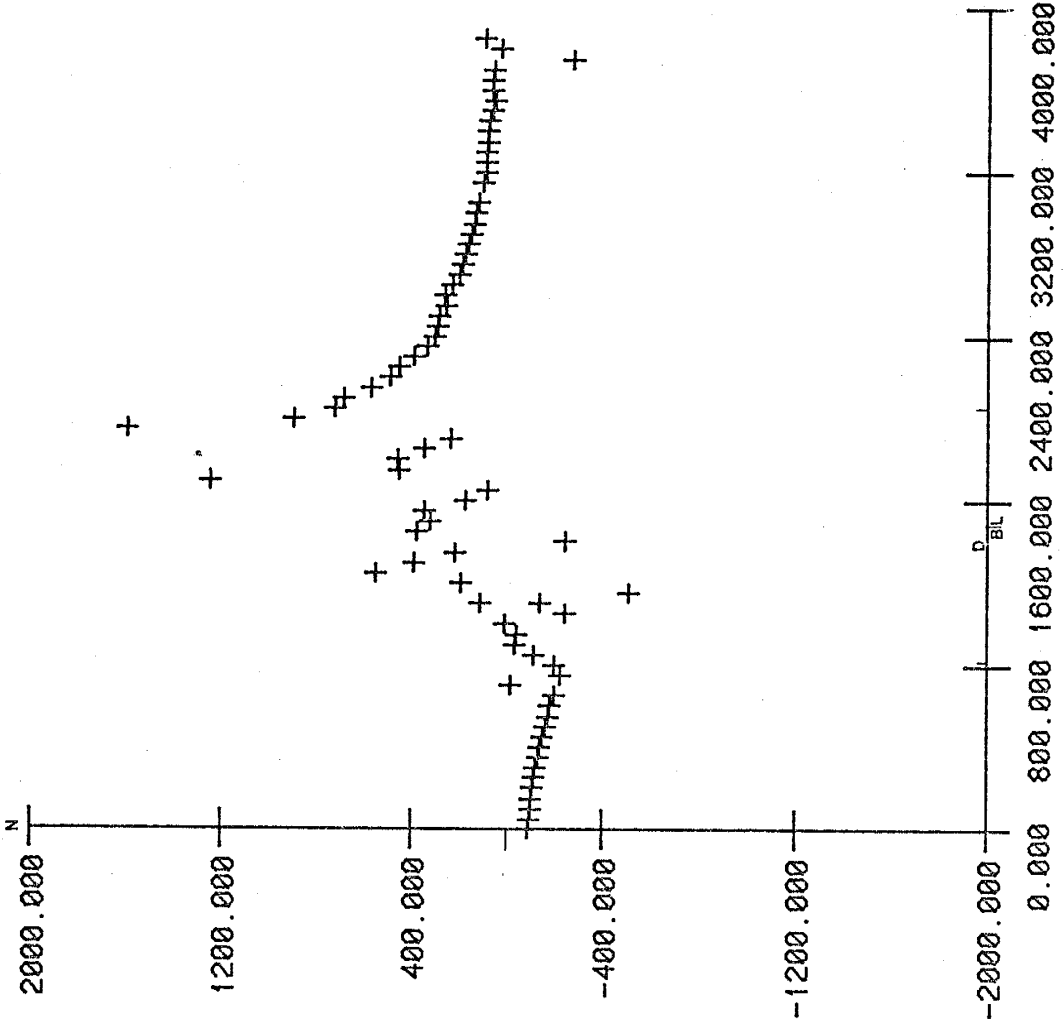
P82

s



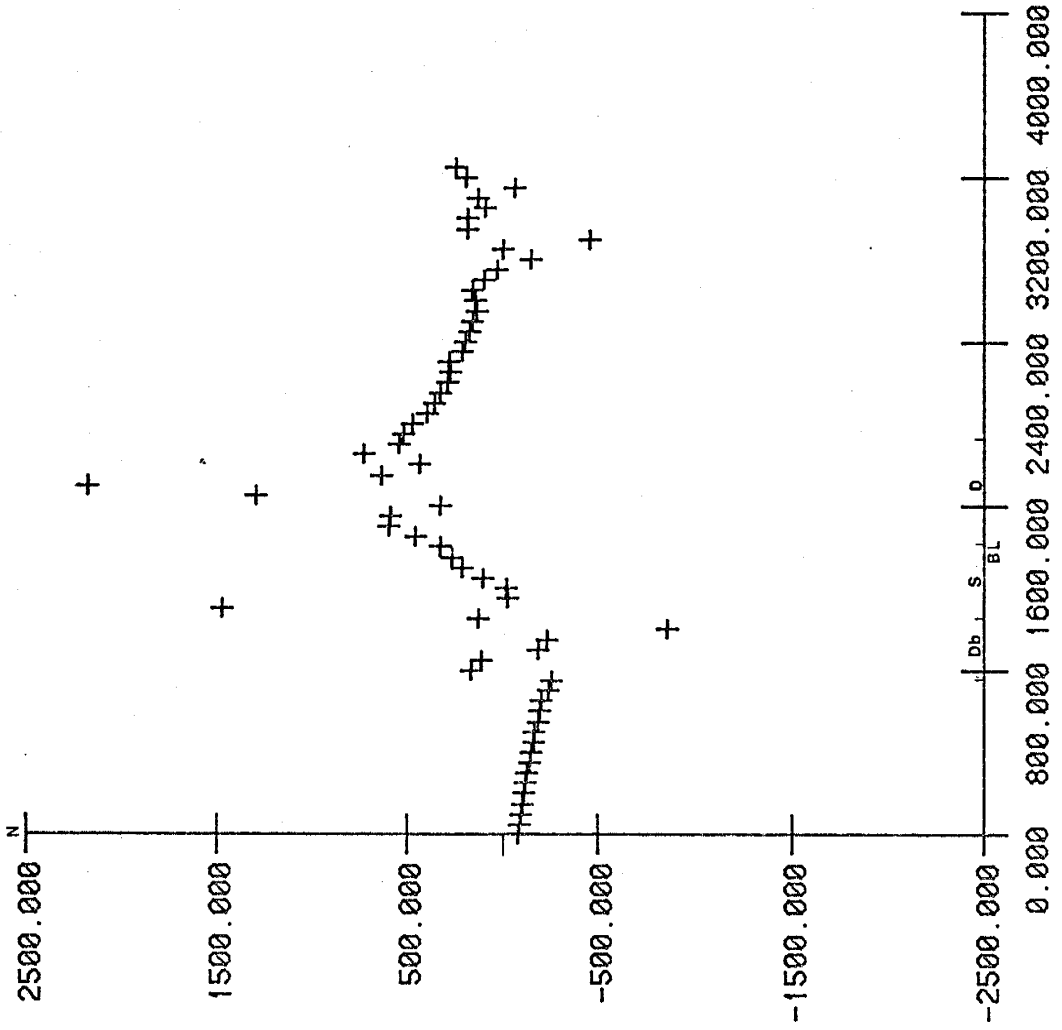
P83

s



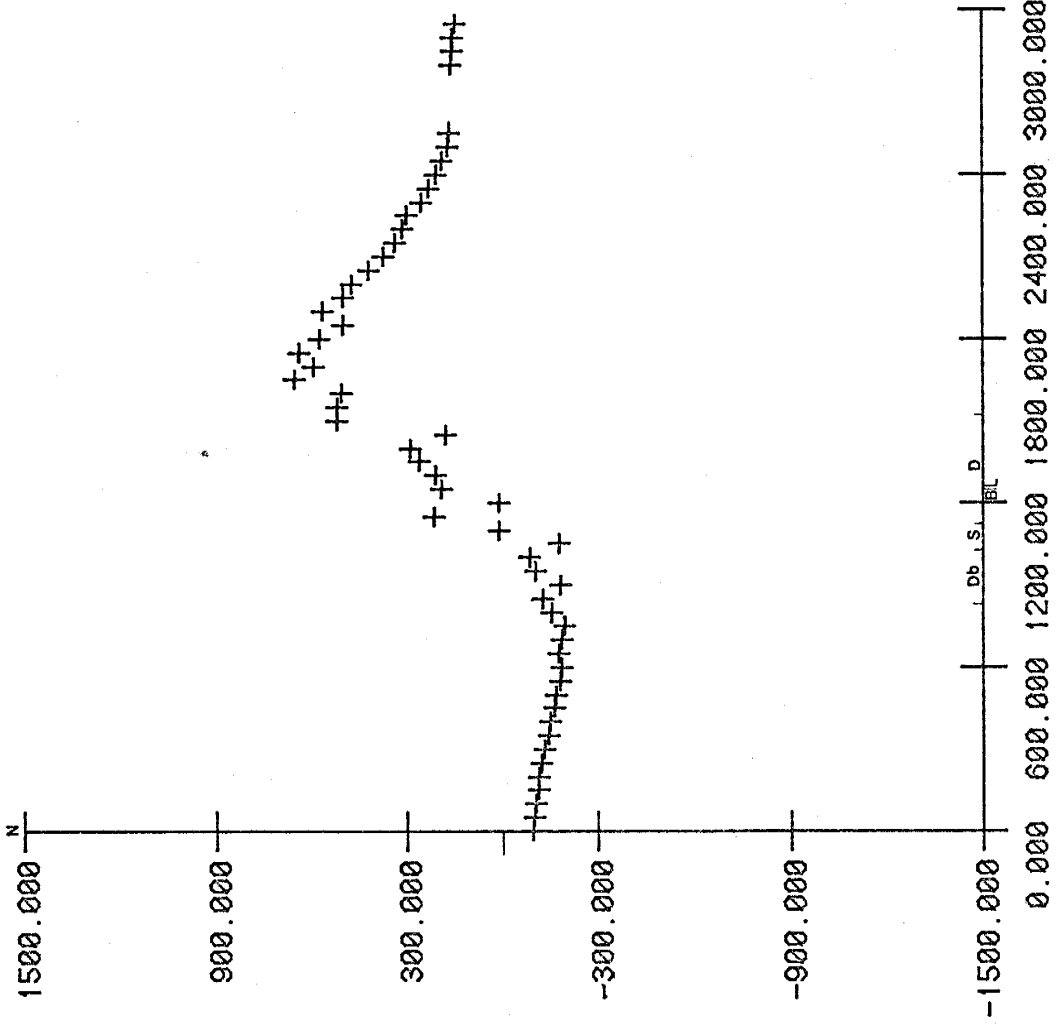
P84

s



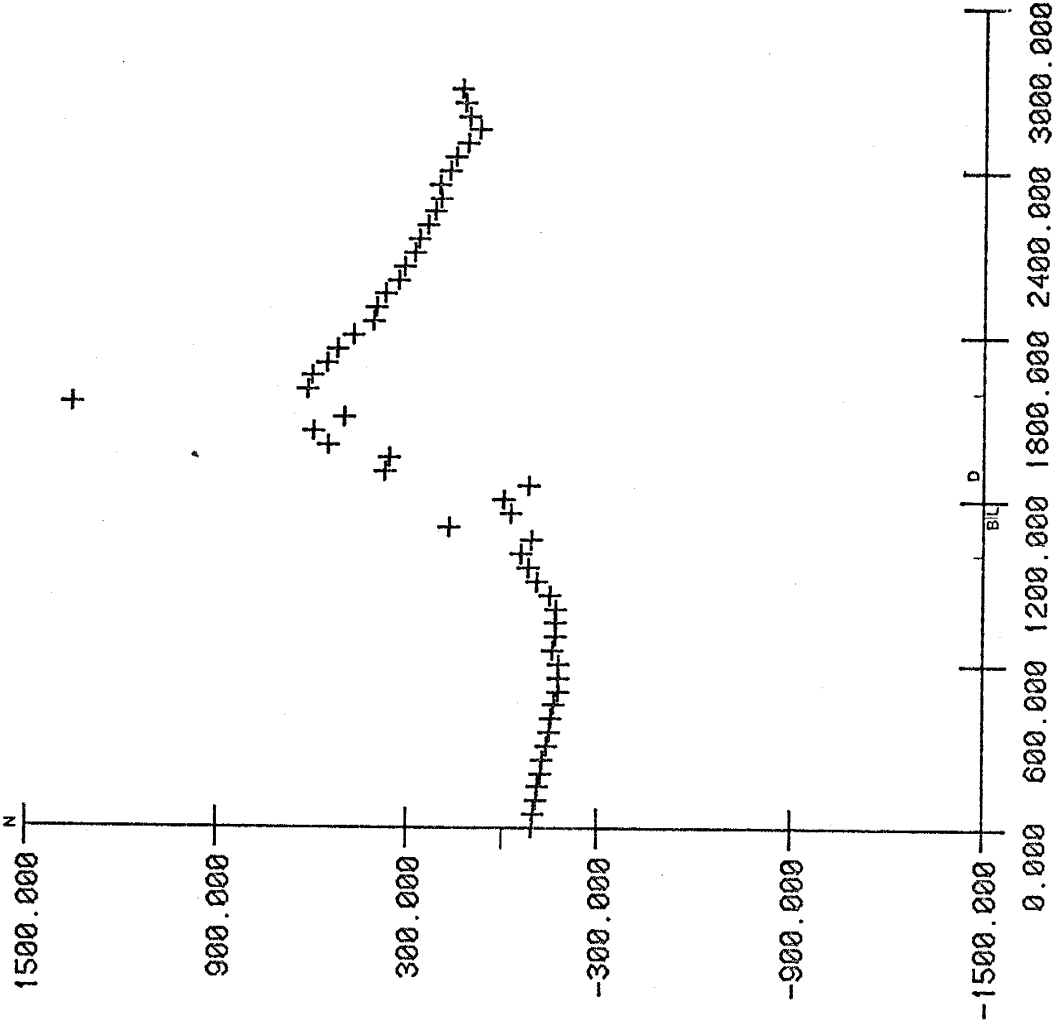
P85

S



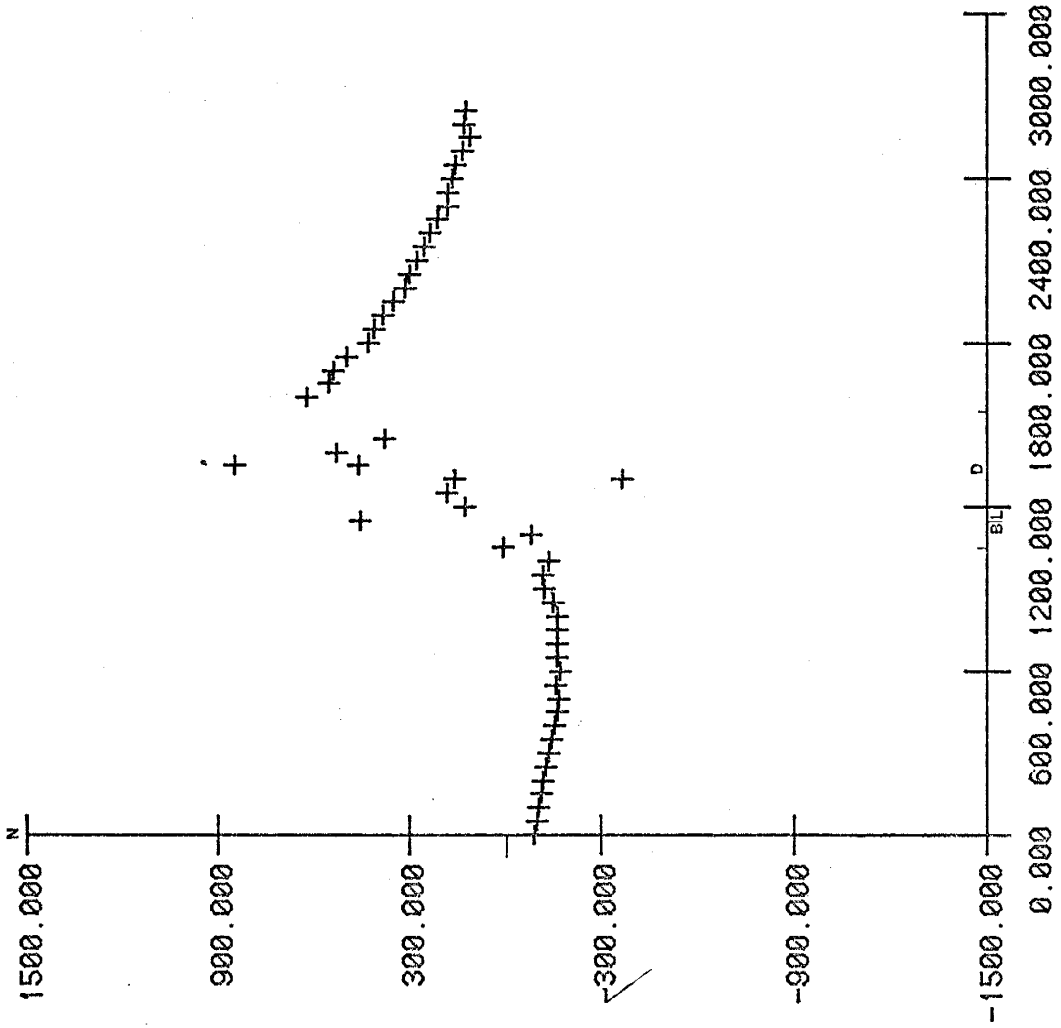
P86

S



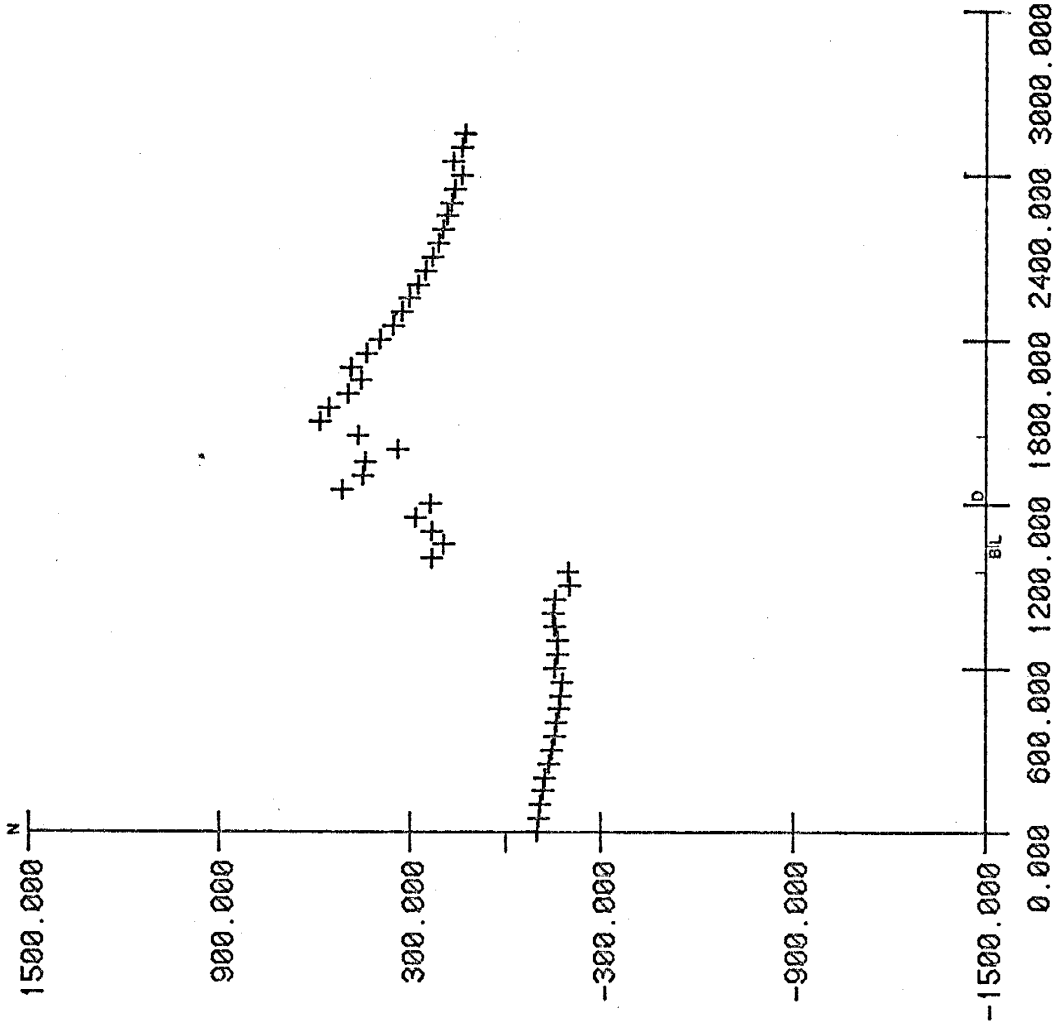
P87

s



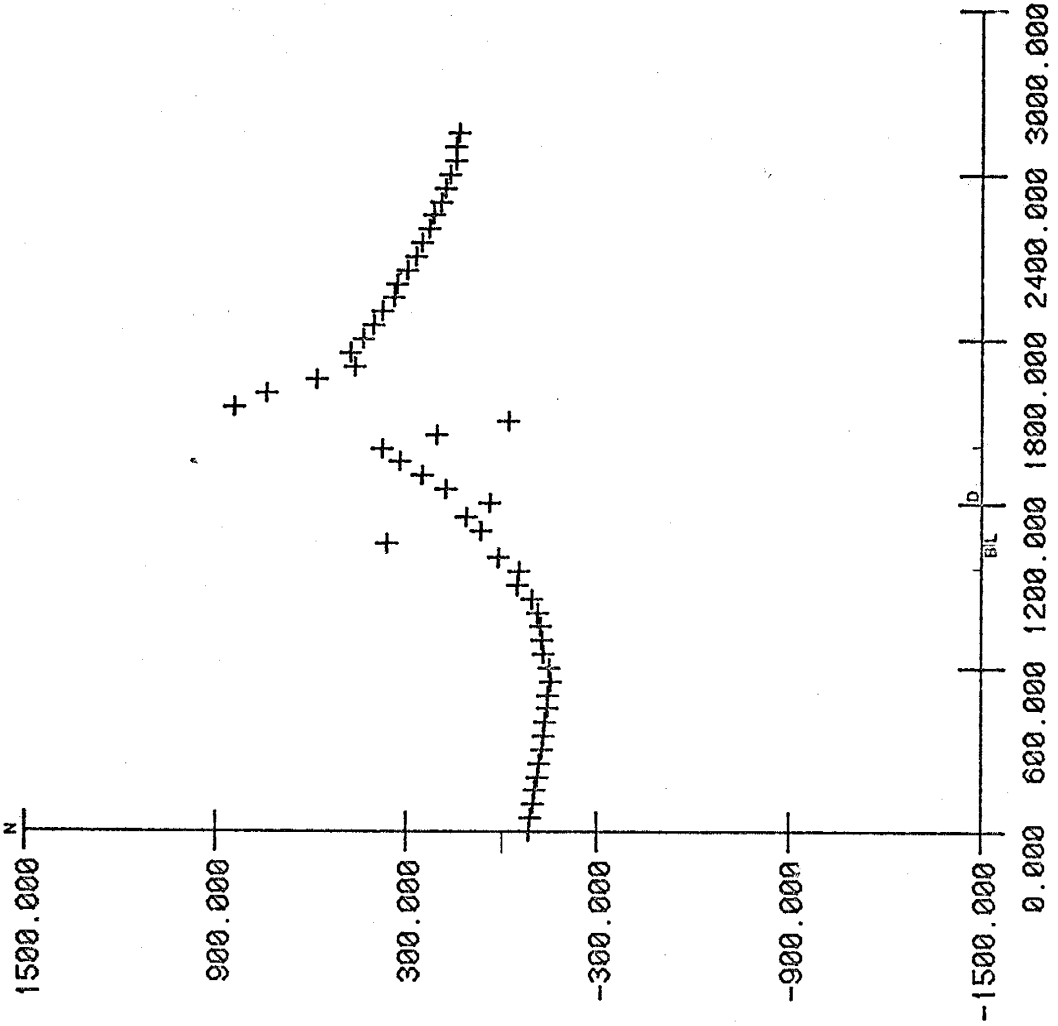
P88

s



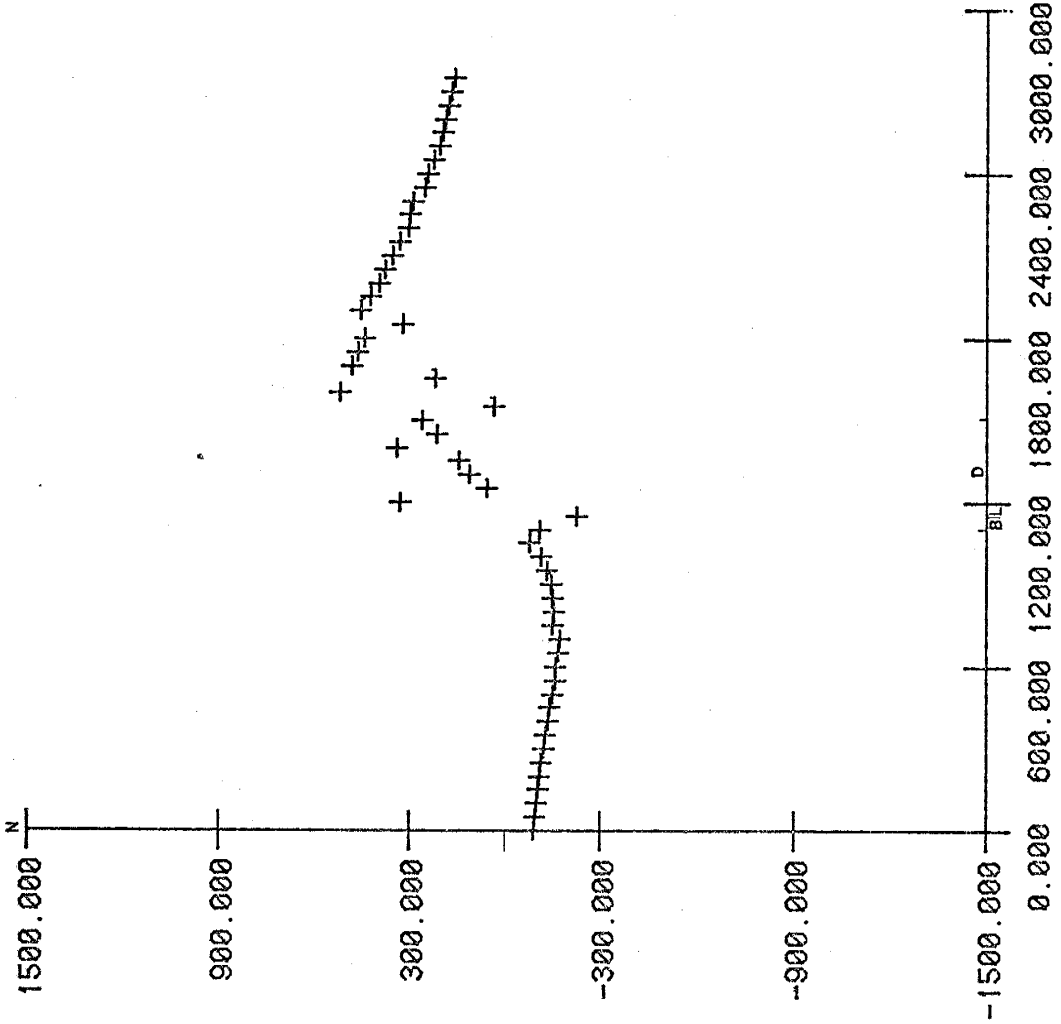
P89

s



P90

s



P91

1500.000

900.000

300.000

-300.000

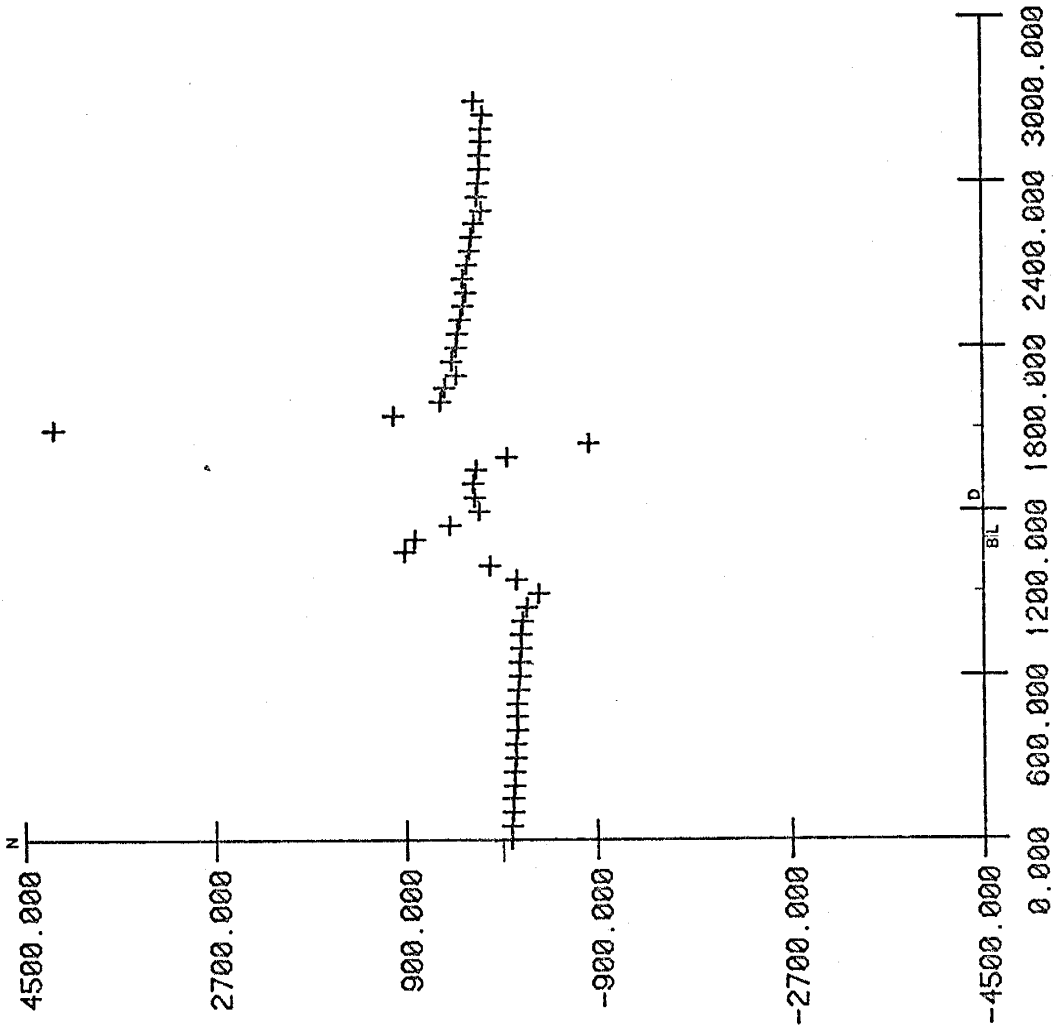
-900.000

-1500.000

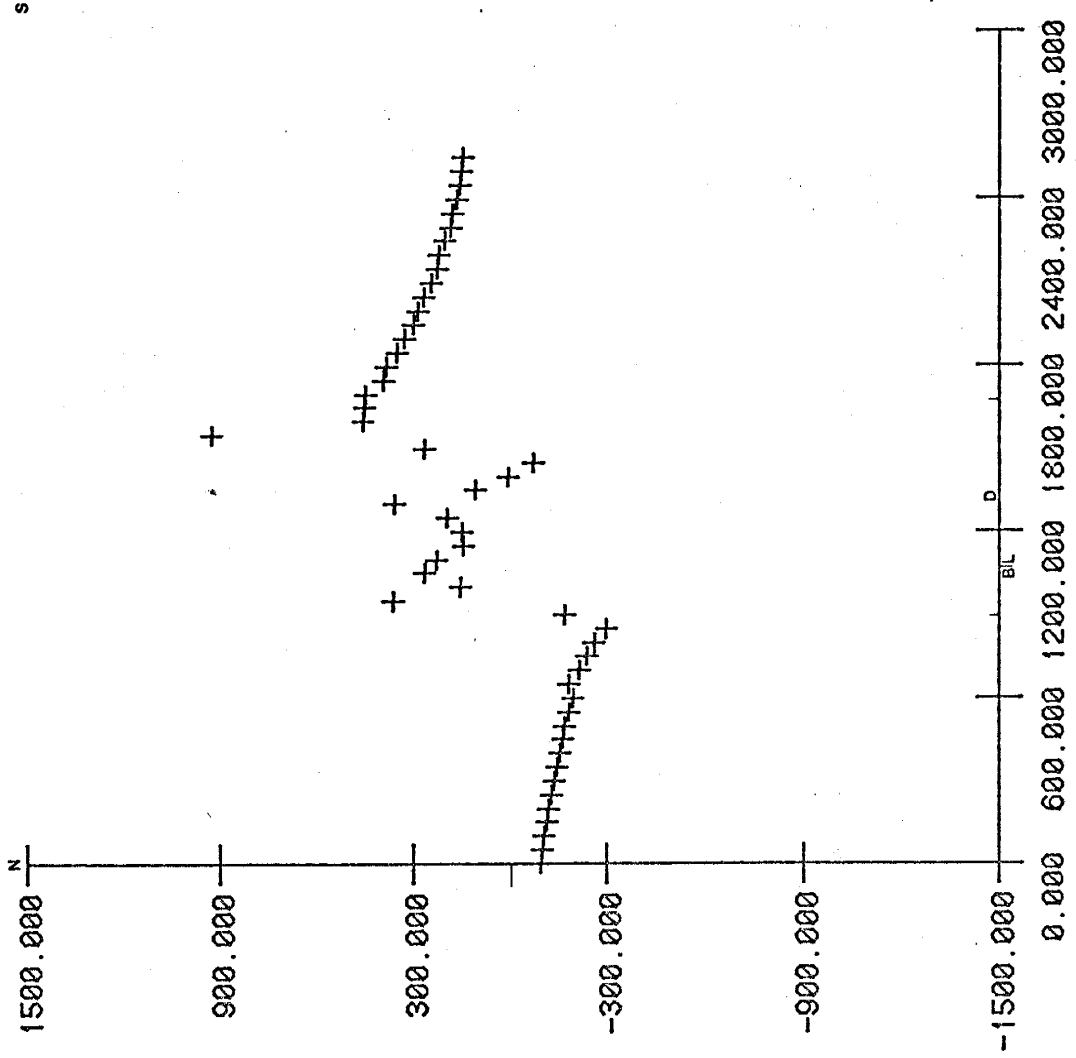
0.000 600.000 1200.000 1800.000 2400.000 3000.000

N

s



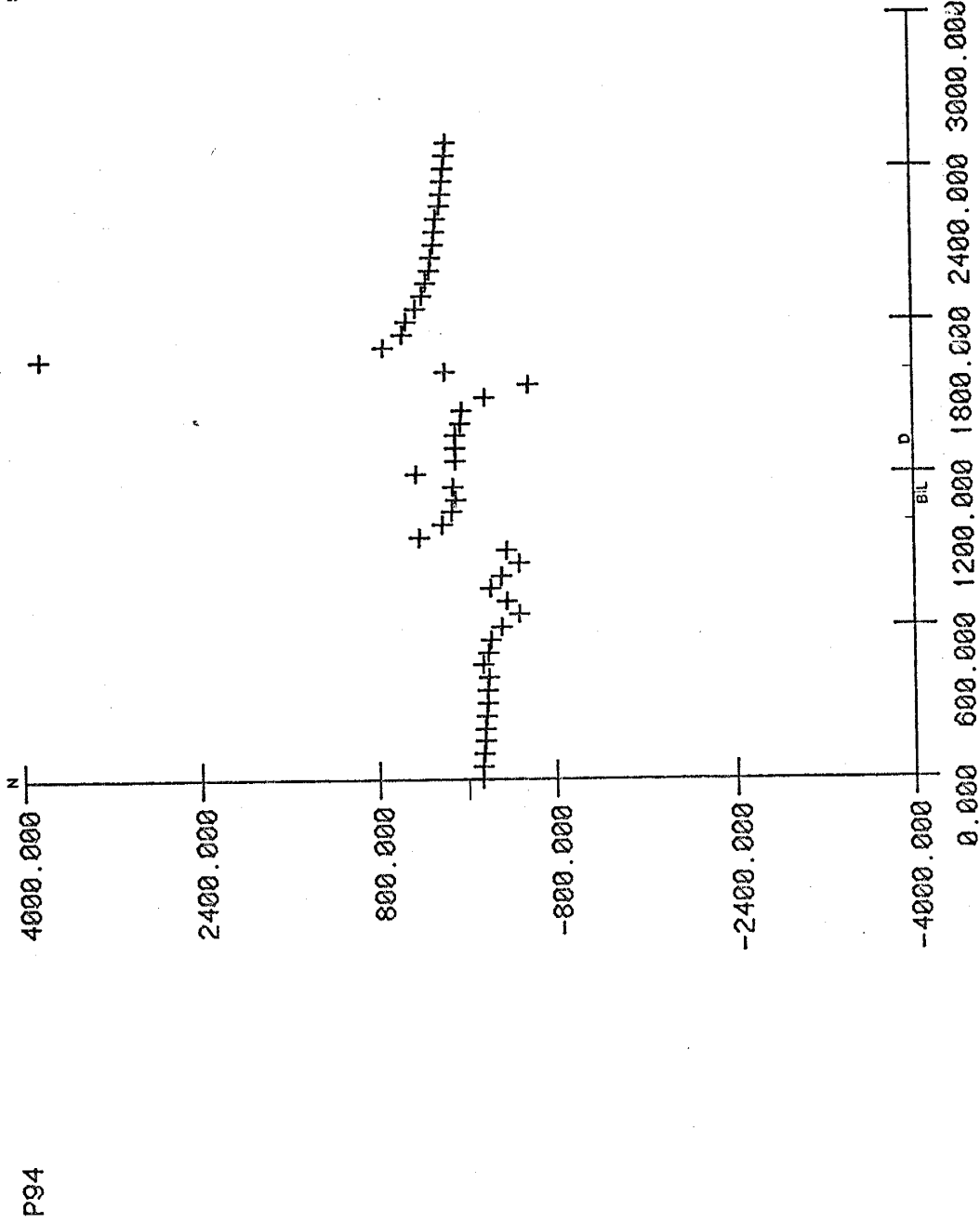
P92



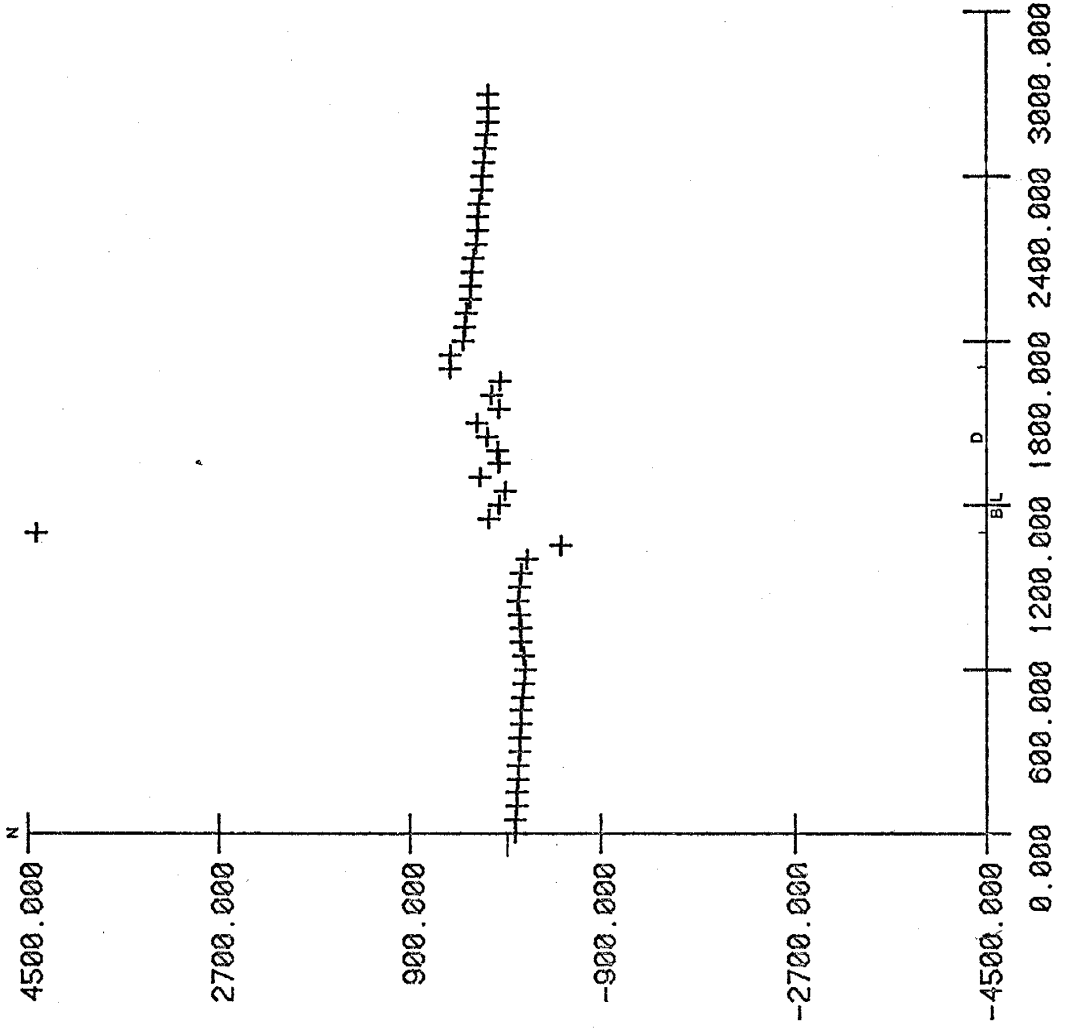
P93

S

s

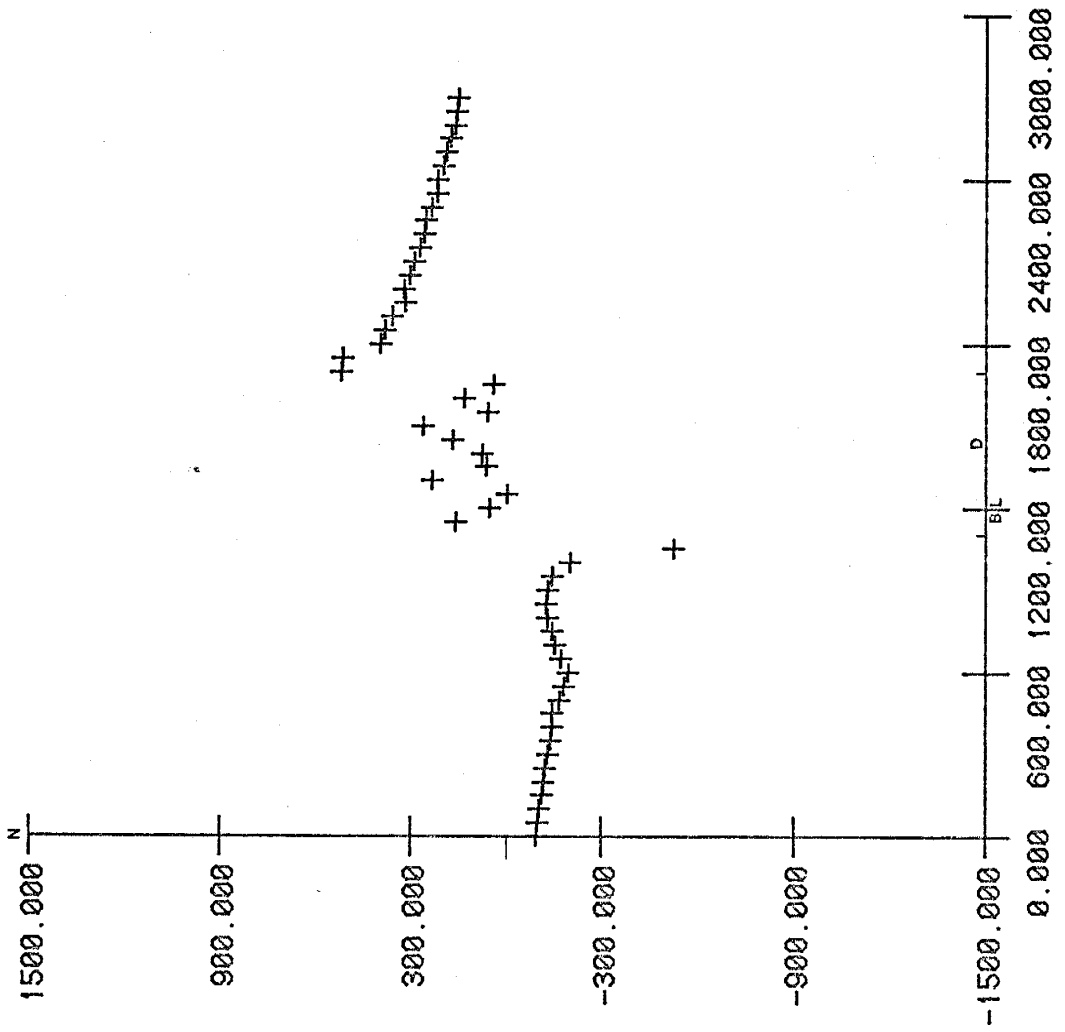


S



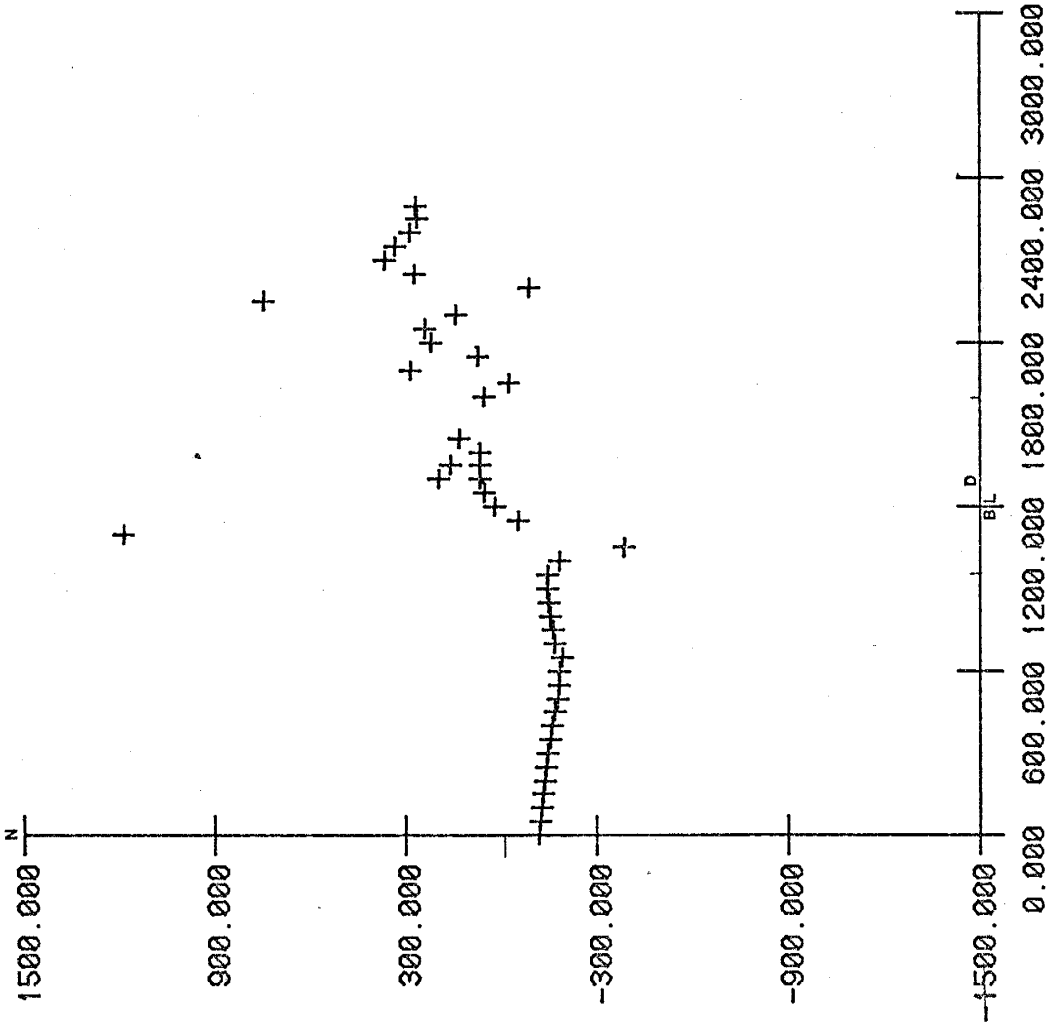
P95A

s



| -

S



P96

P97

1500.000 N

S

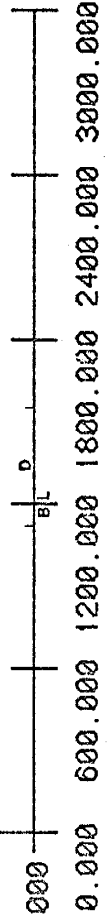
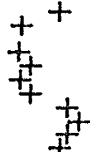
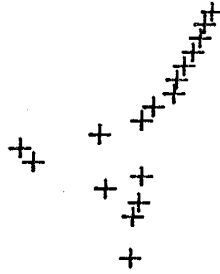
900.000

300.000

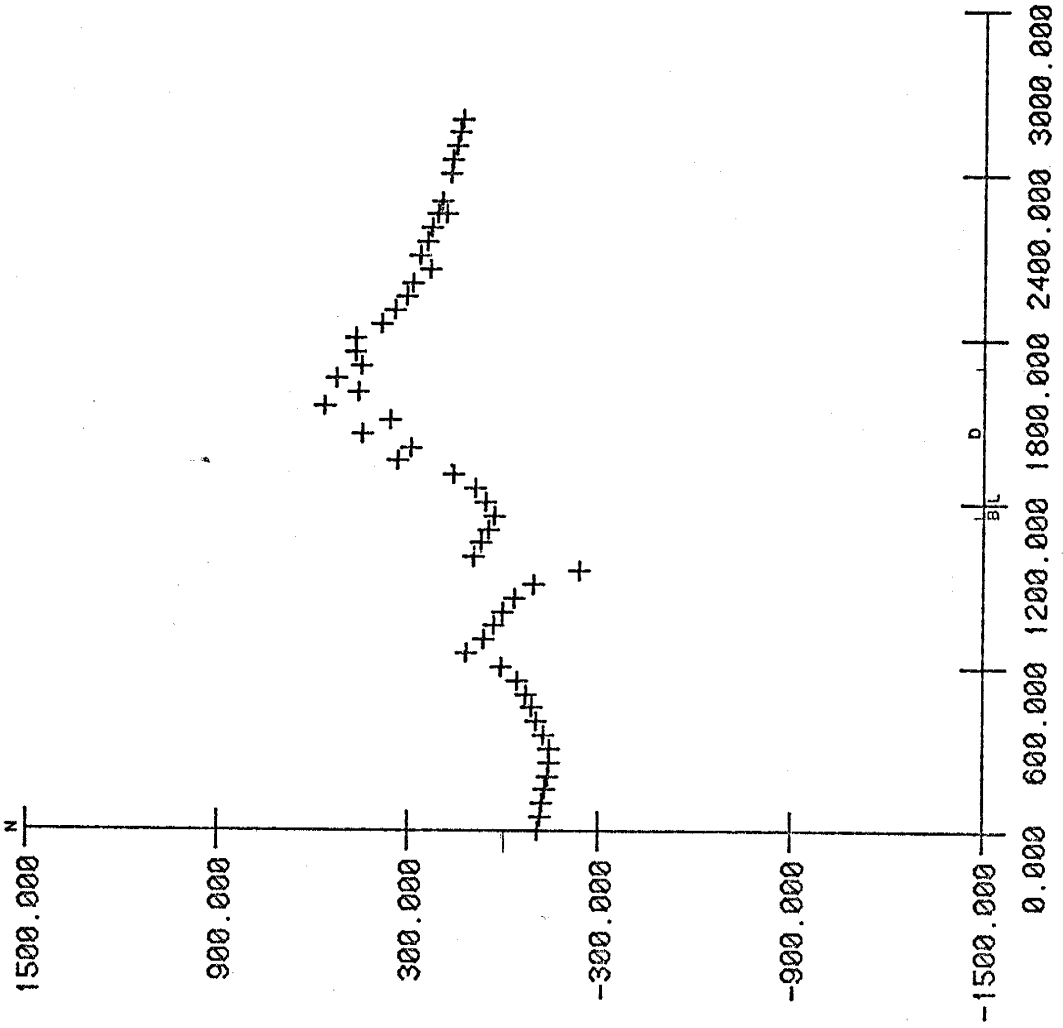
-300.000

-900.000

-1500.000

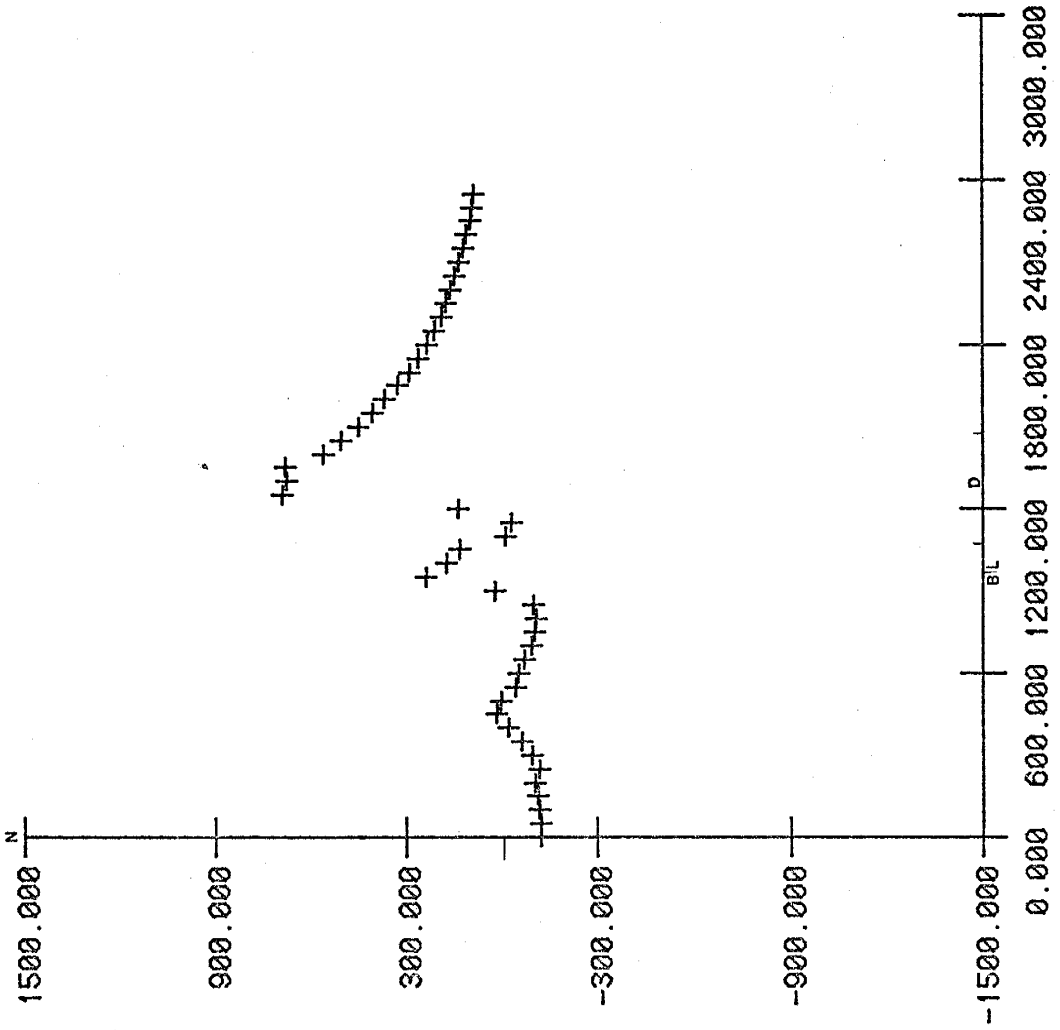


s



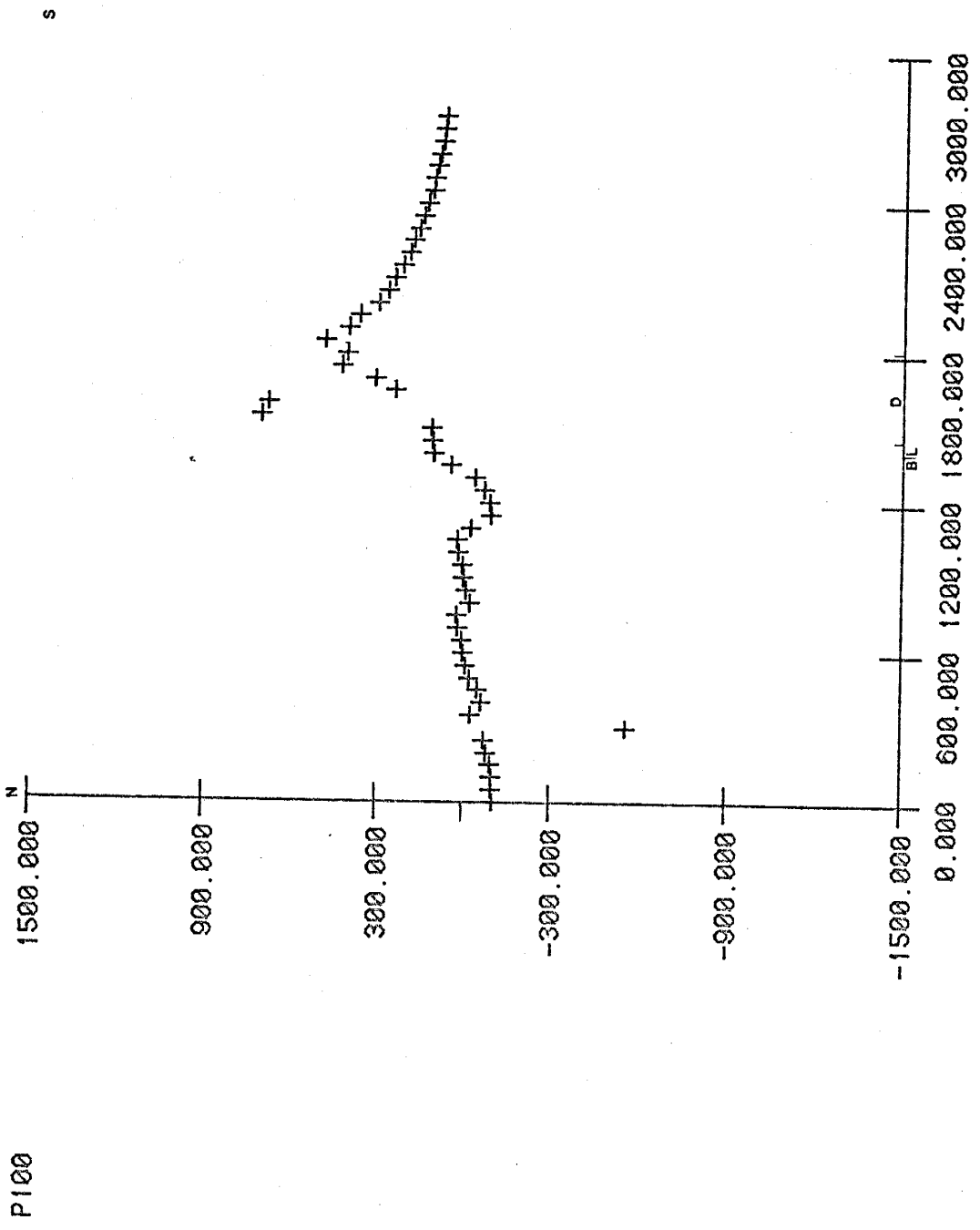
P98

S



P99

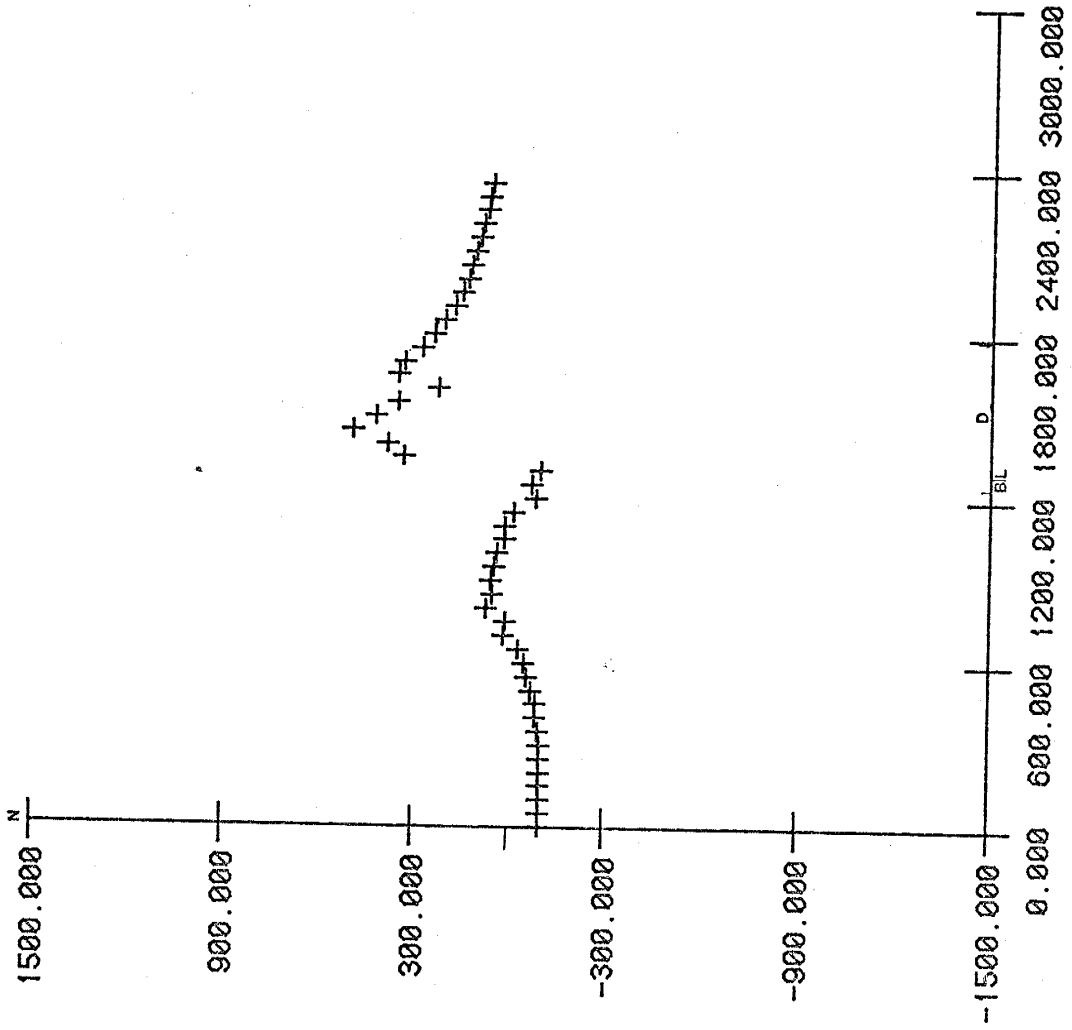




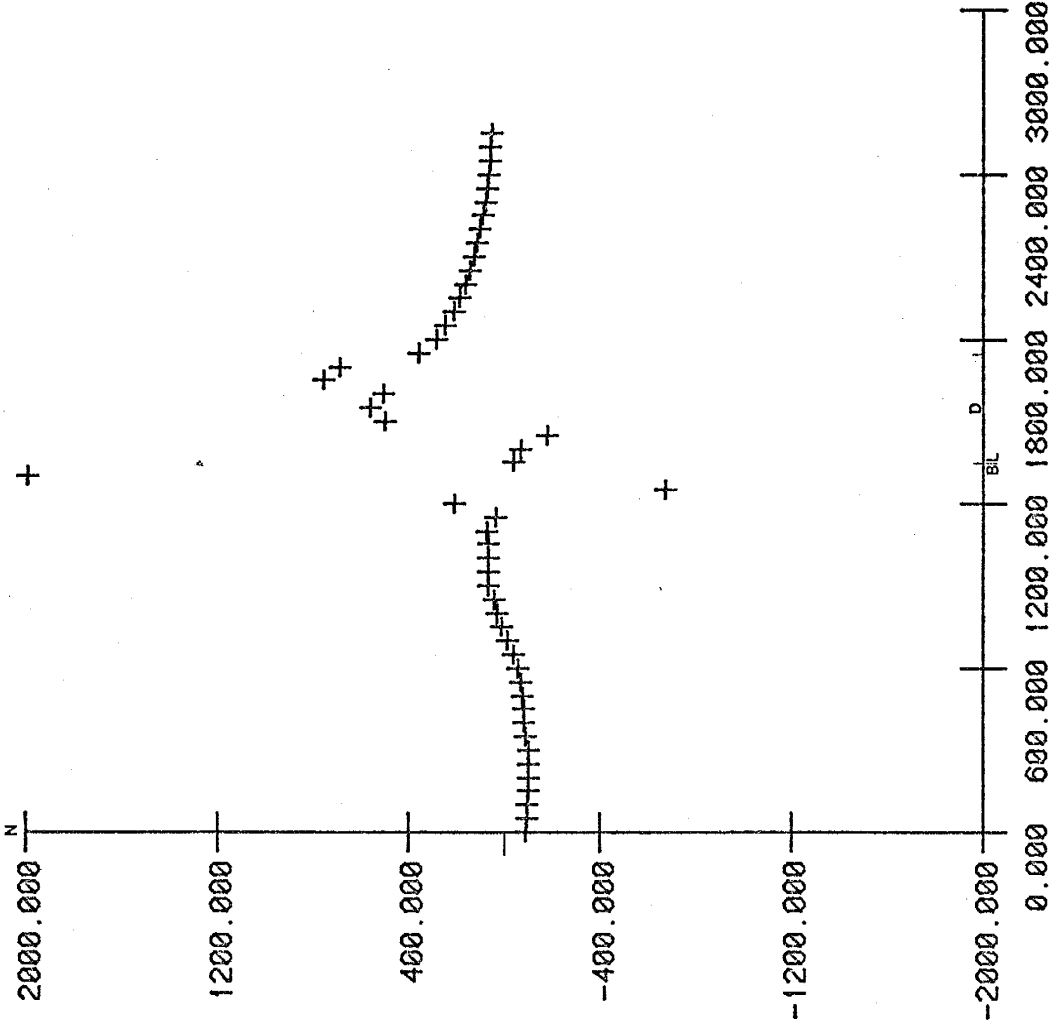
S

P101

S

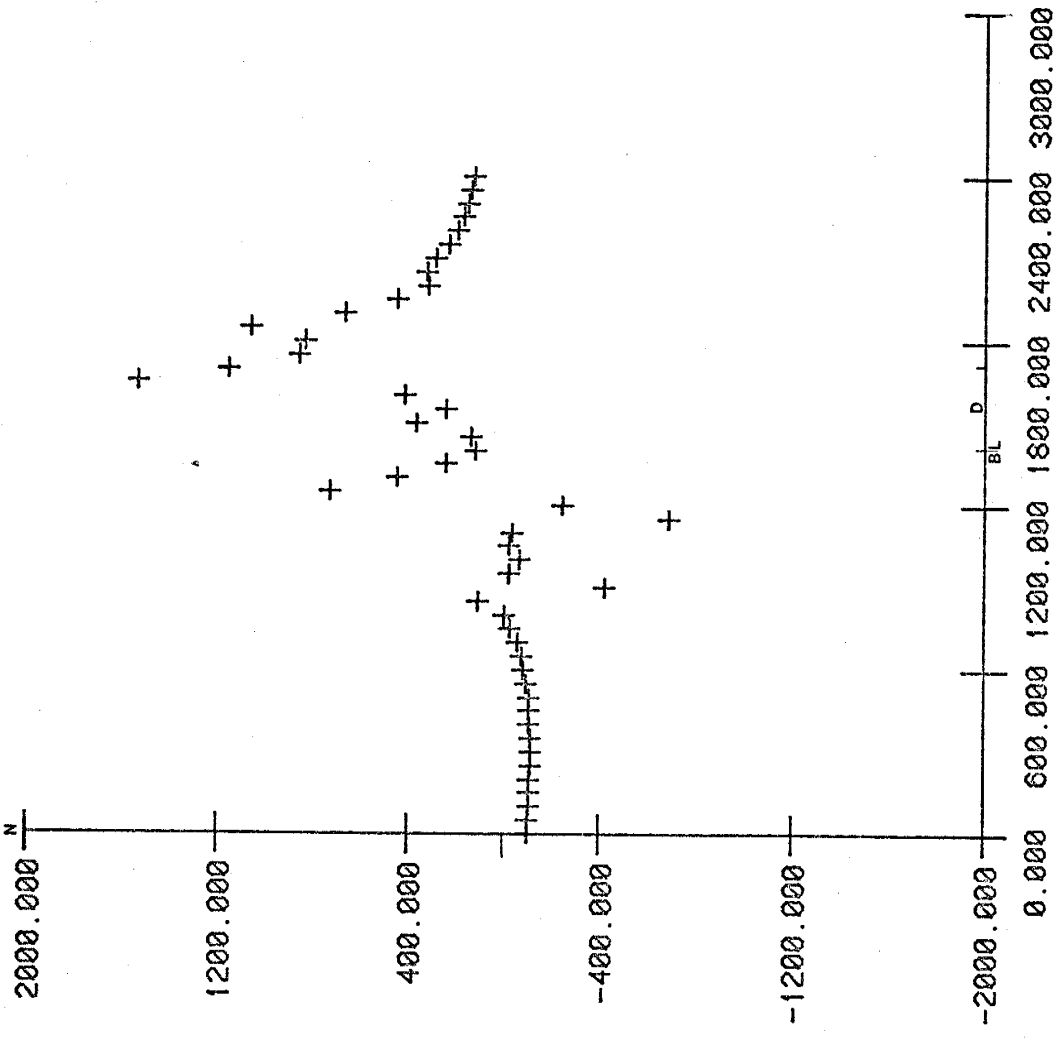


S



P102

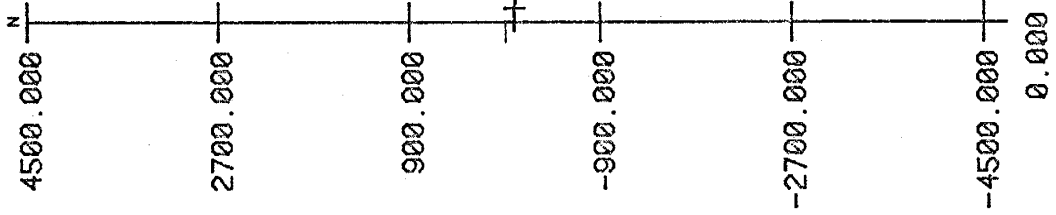
s



P103

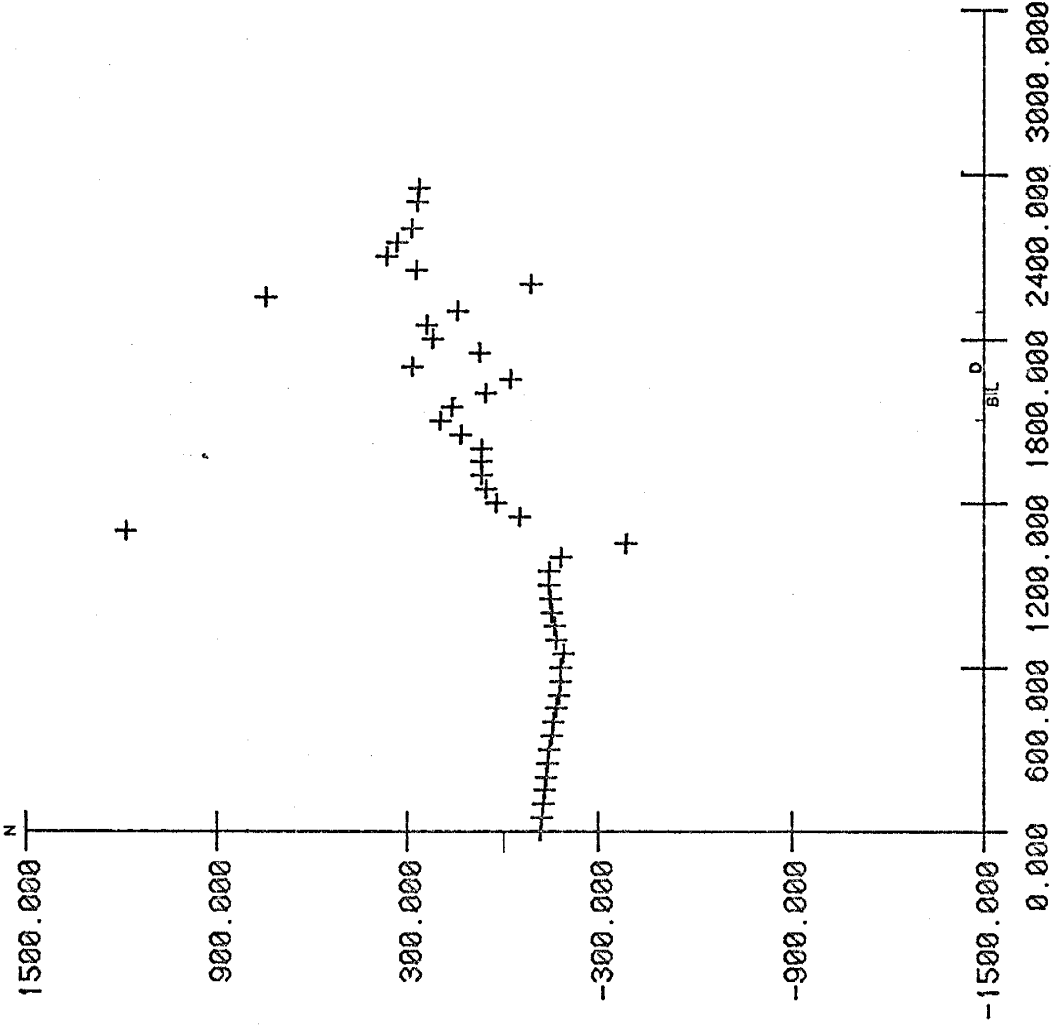
S

+



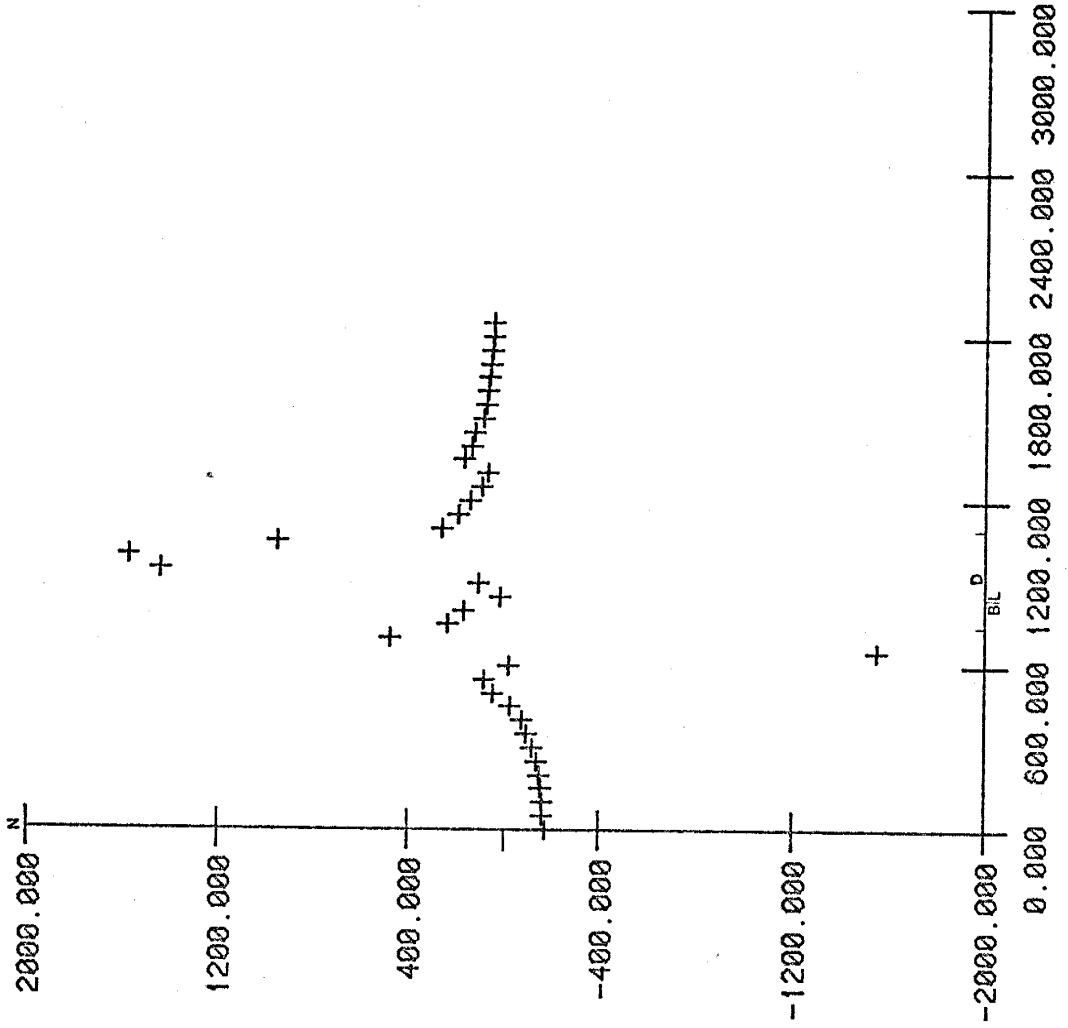
P104

S



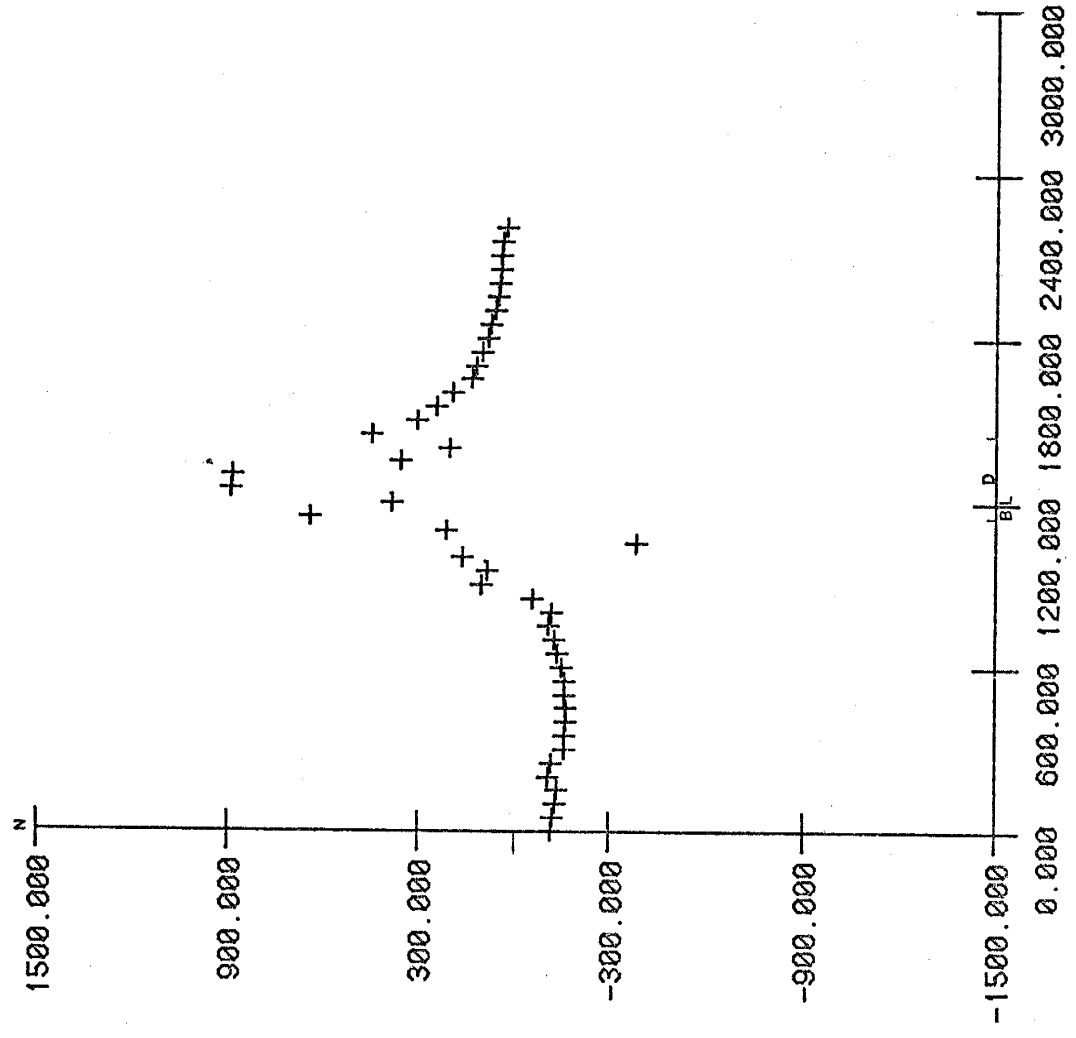
P105

P106 2000.000 N 9



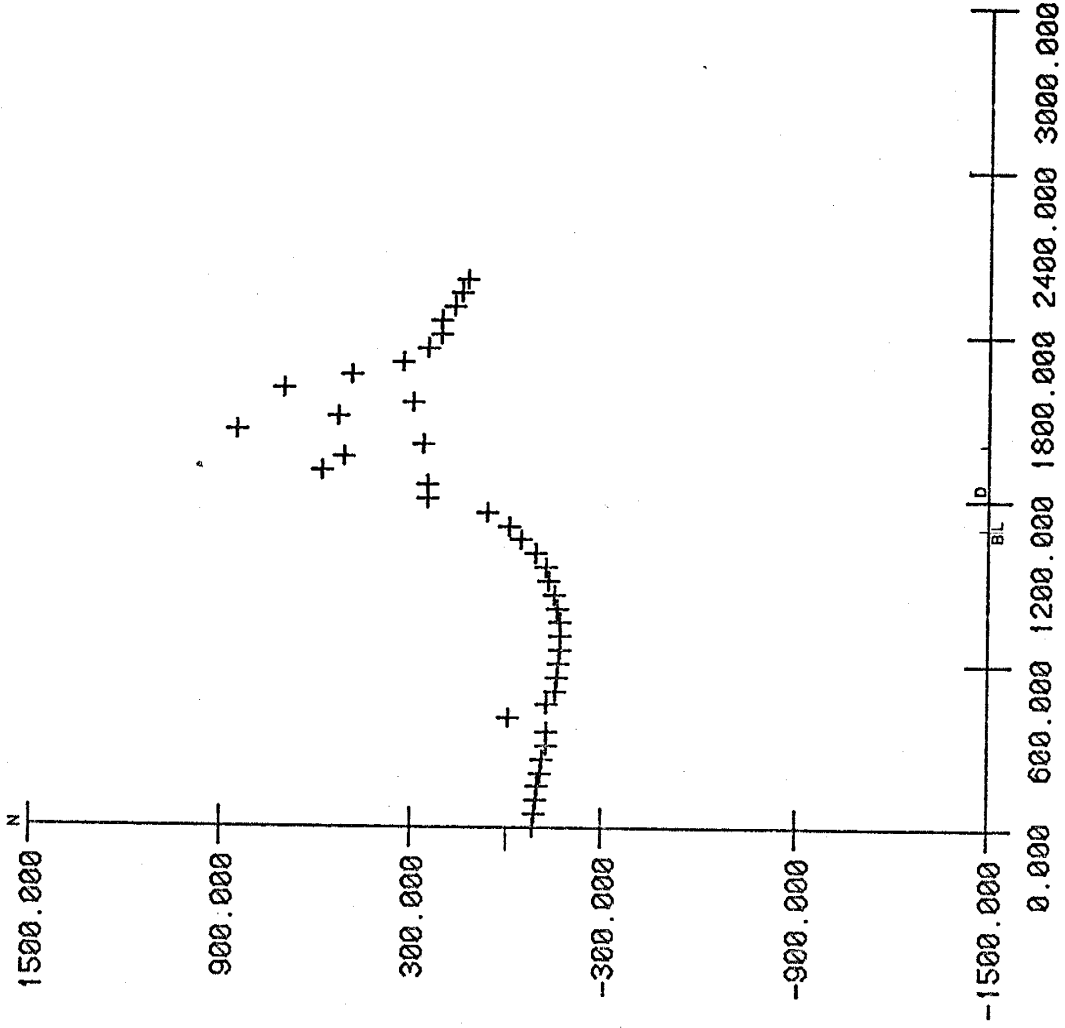
S

P107

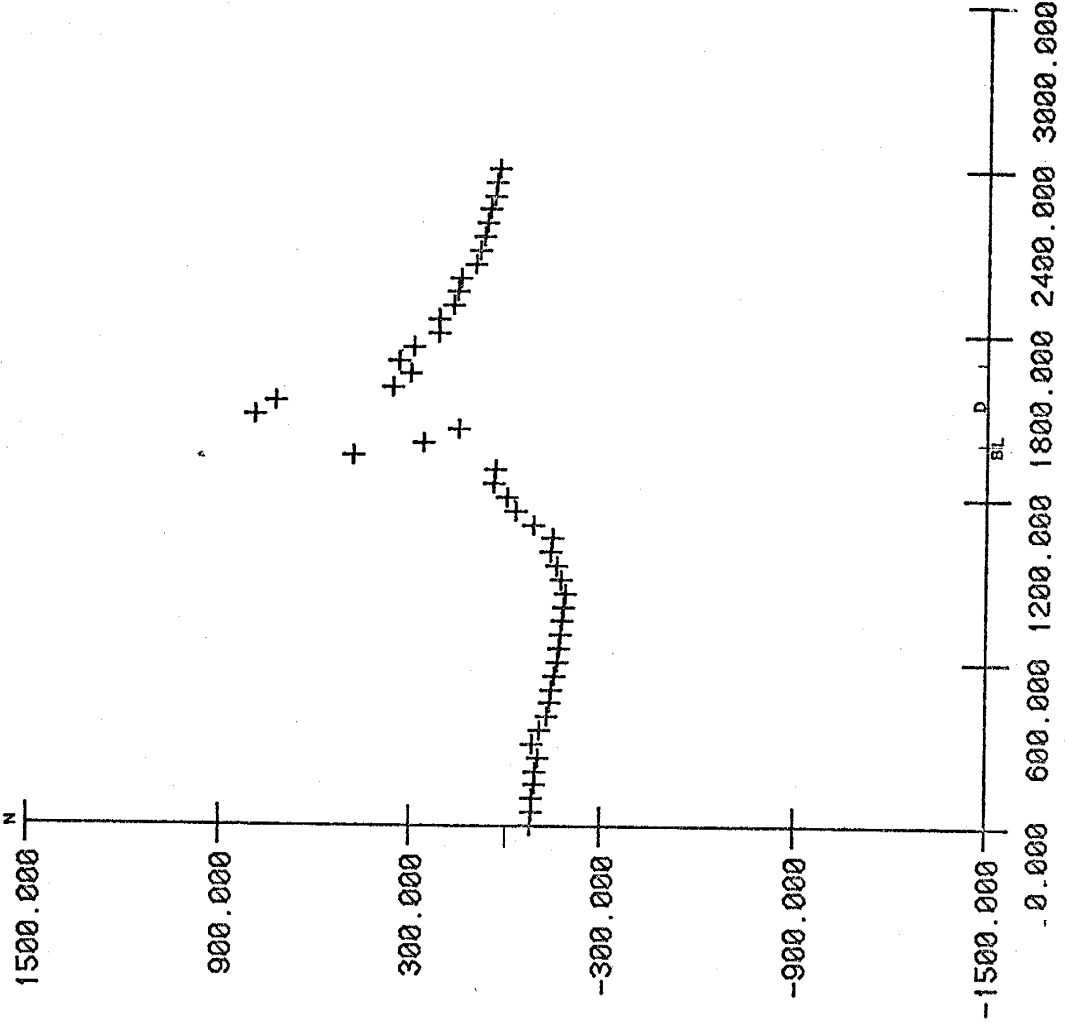


P108.

S

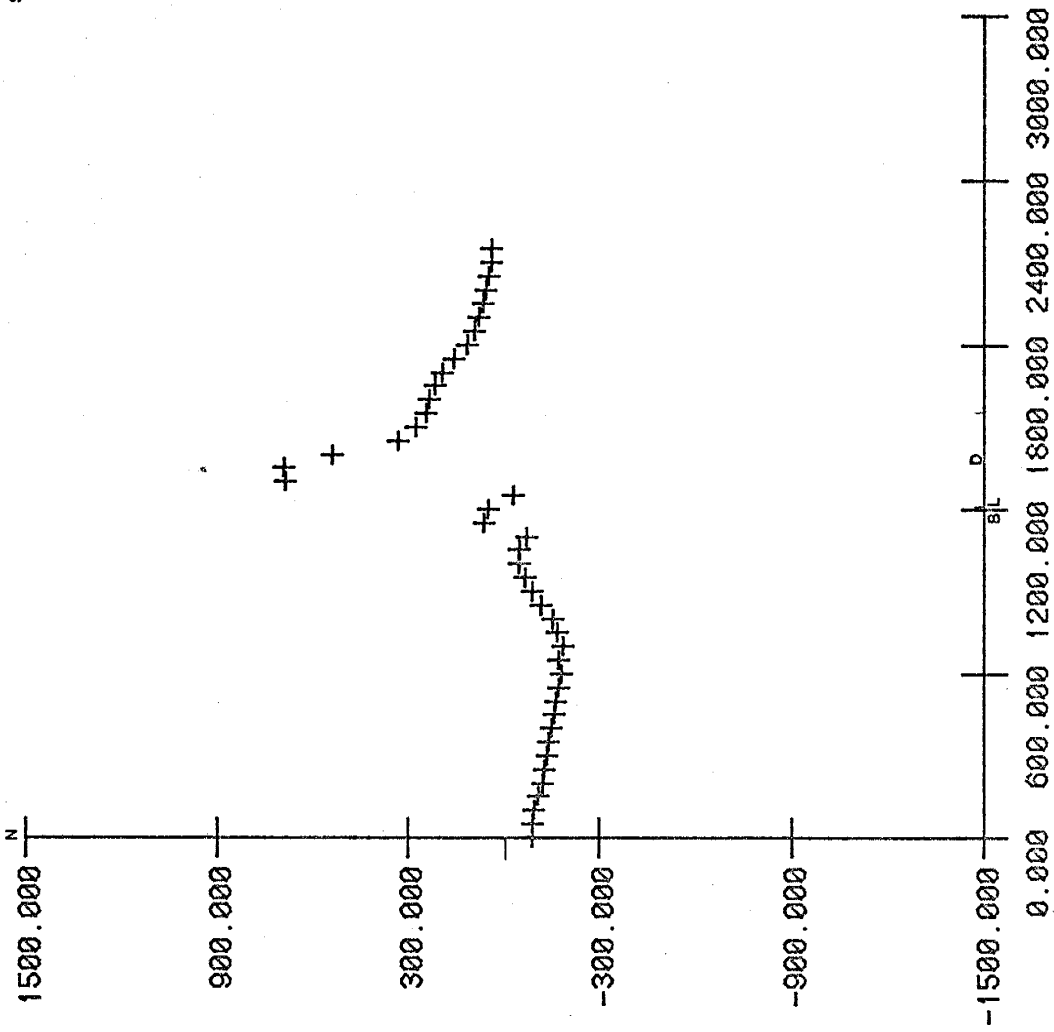


s



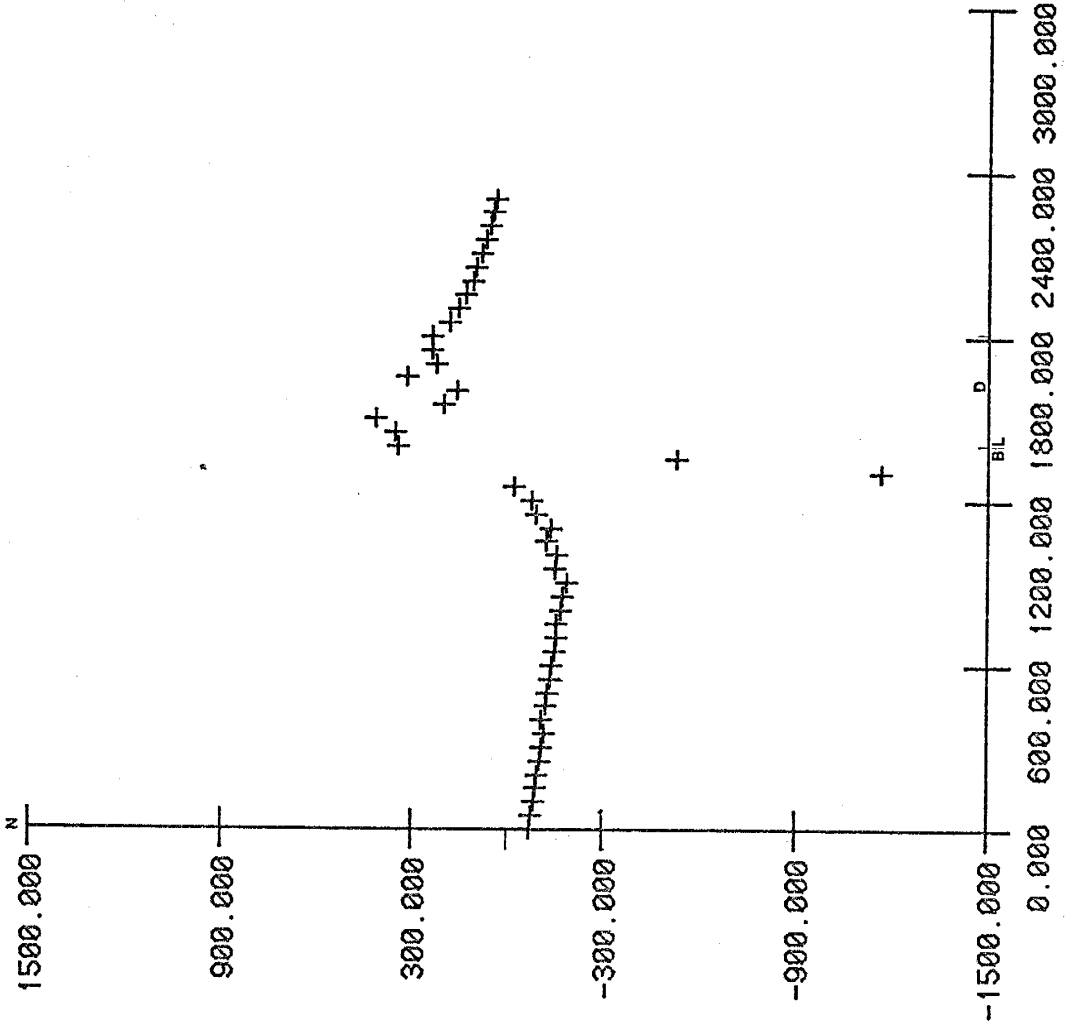
P109

s

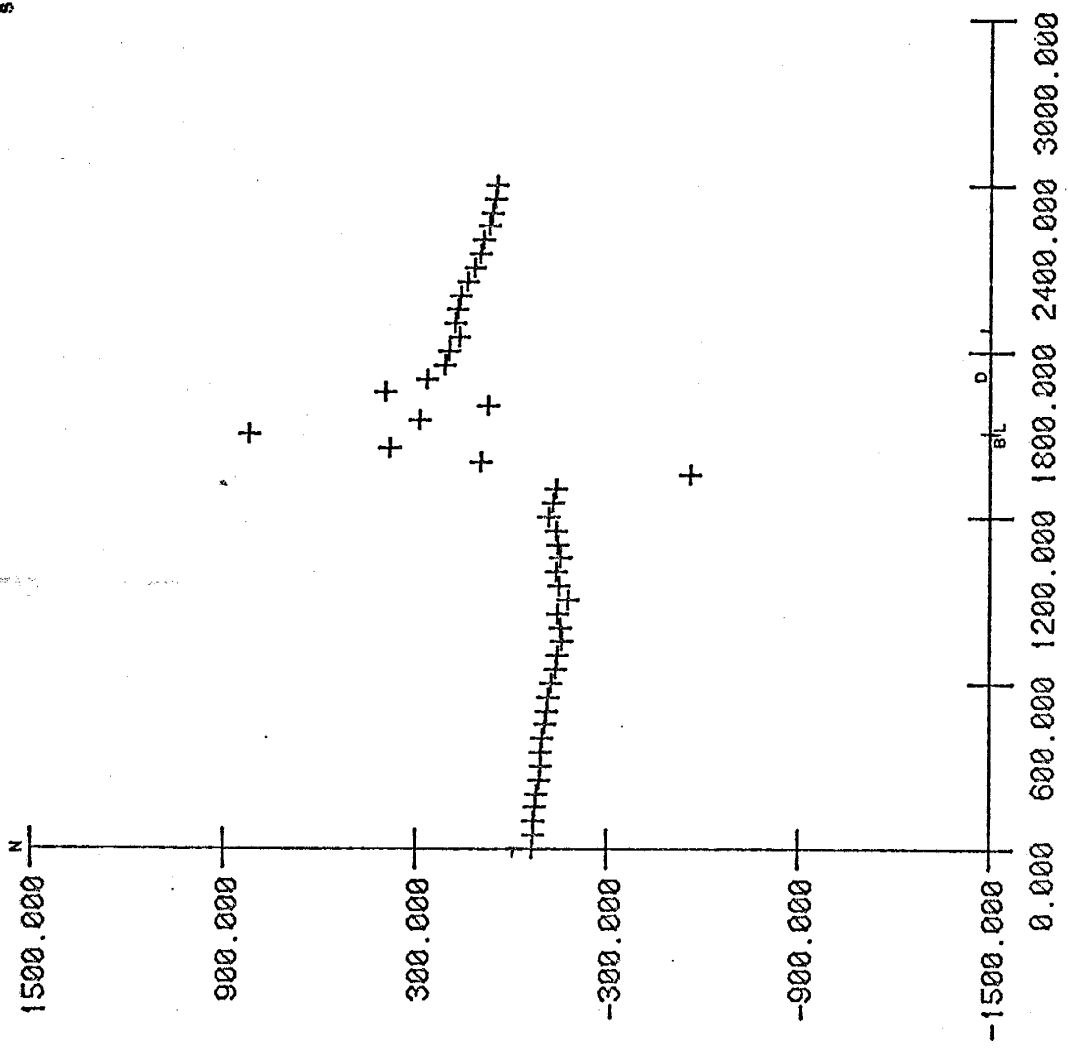


P110

S

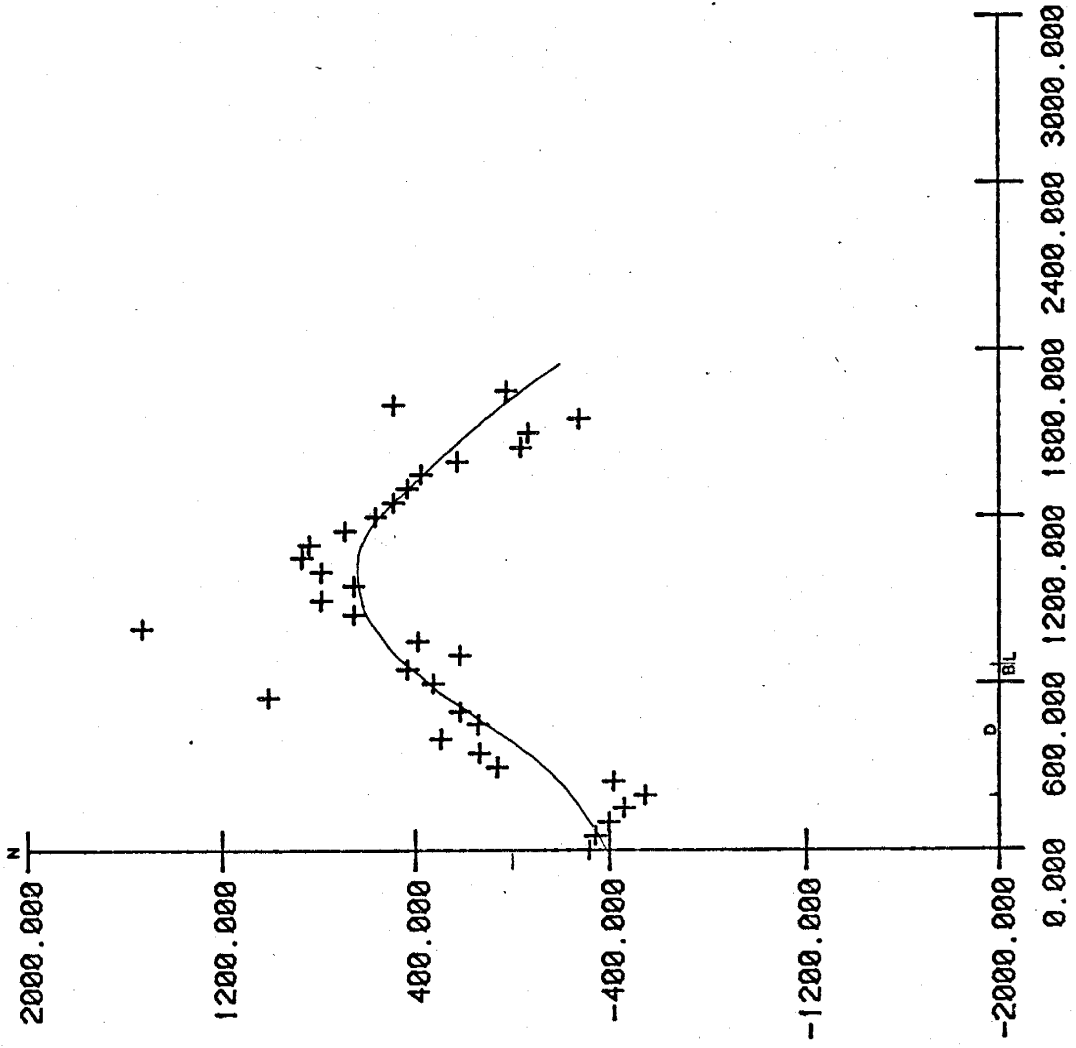


8

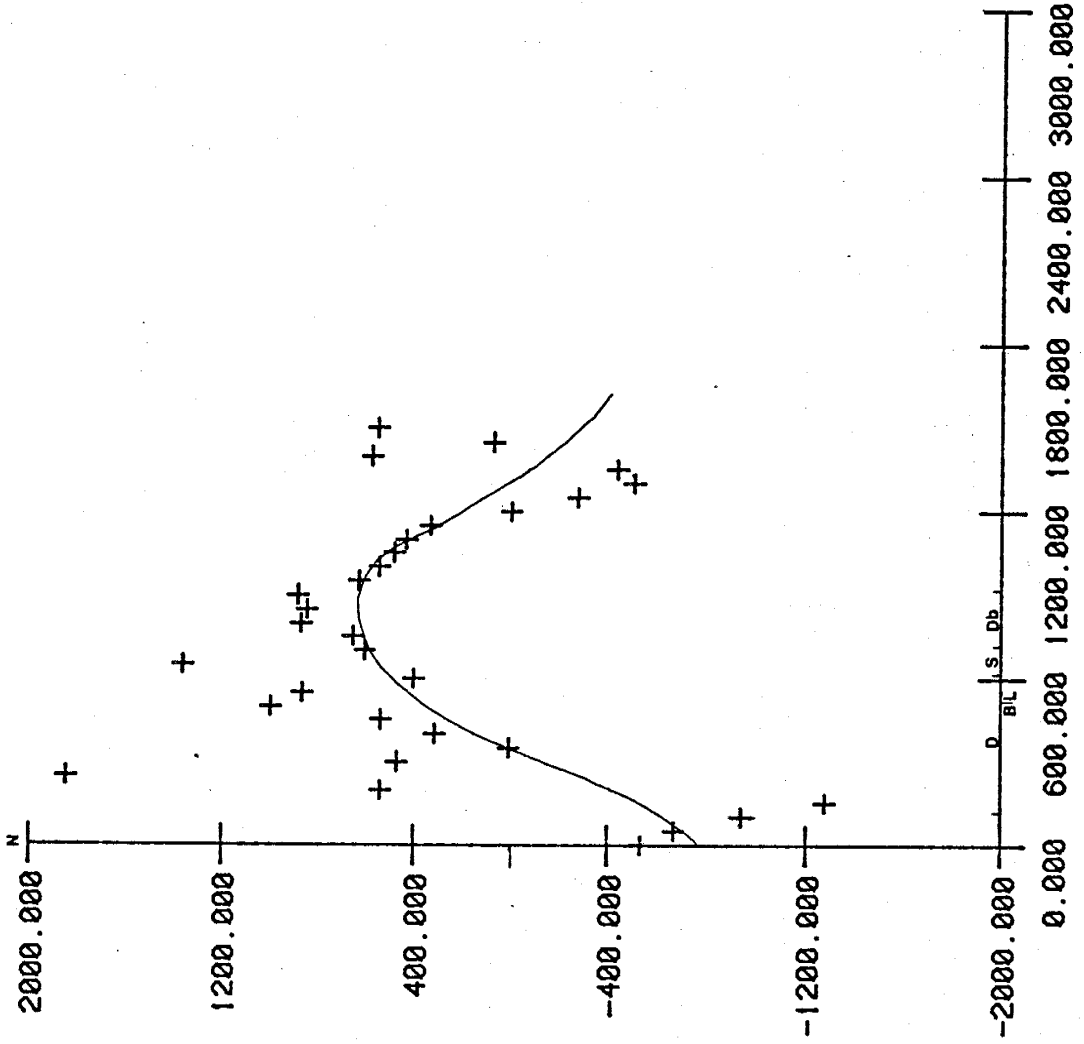


P112

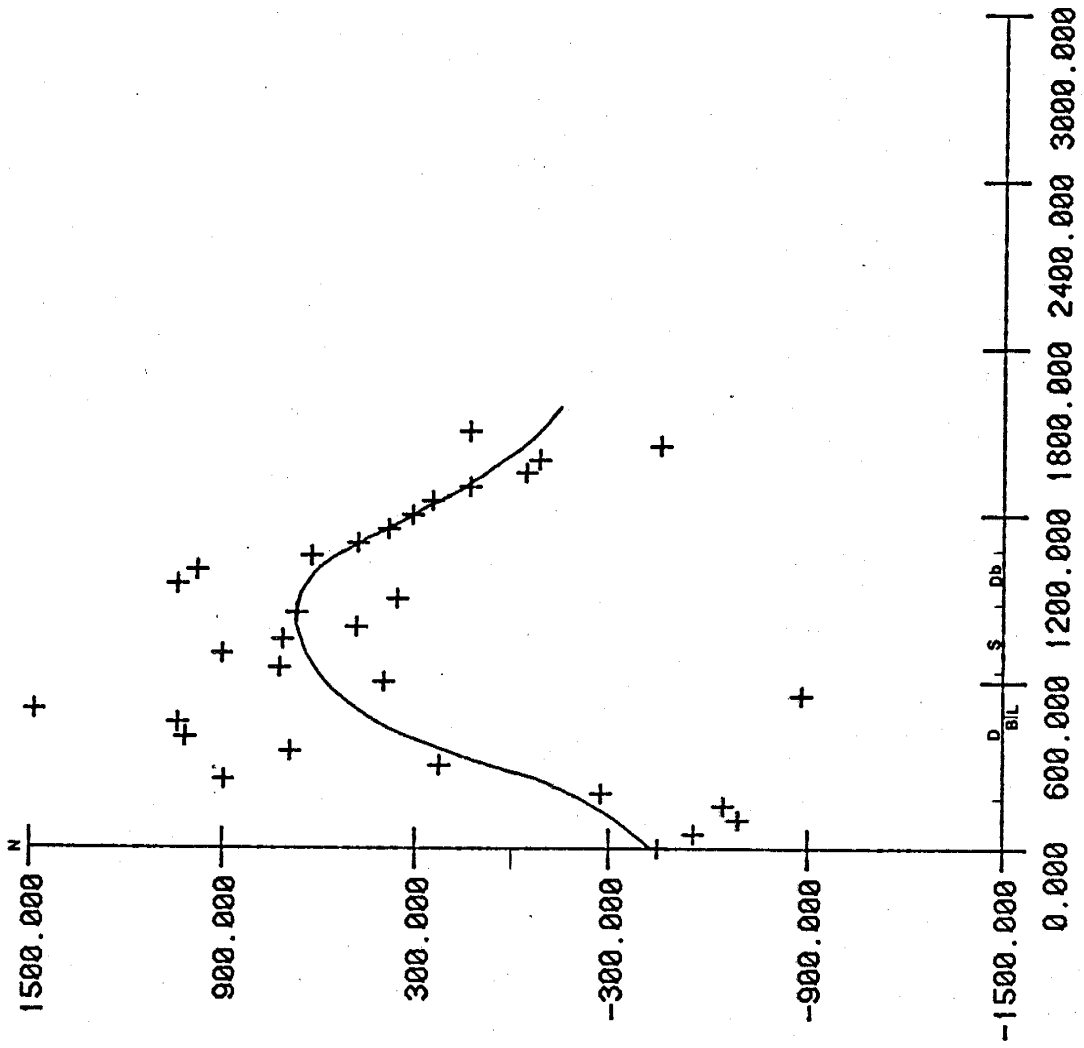
s



8

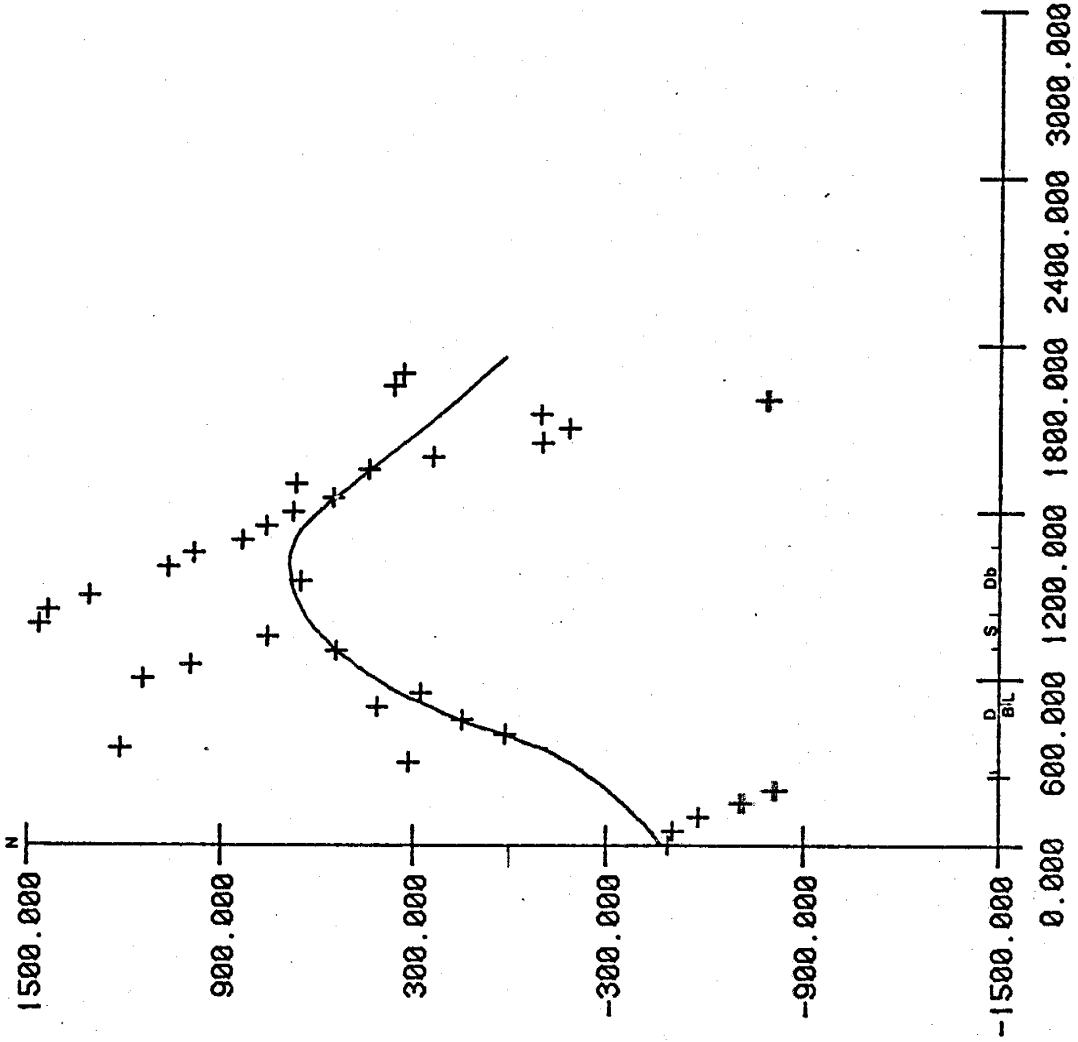


S



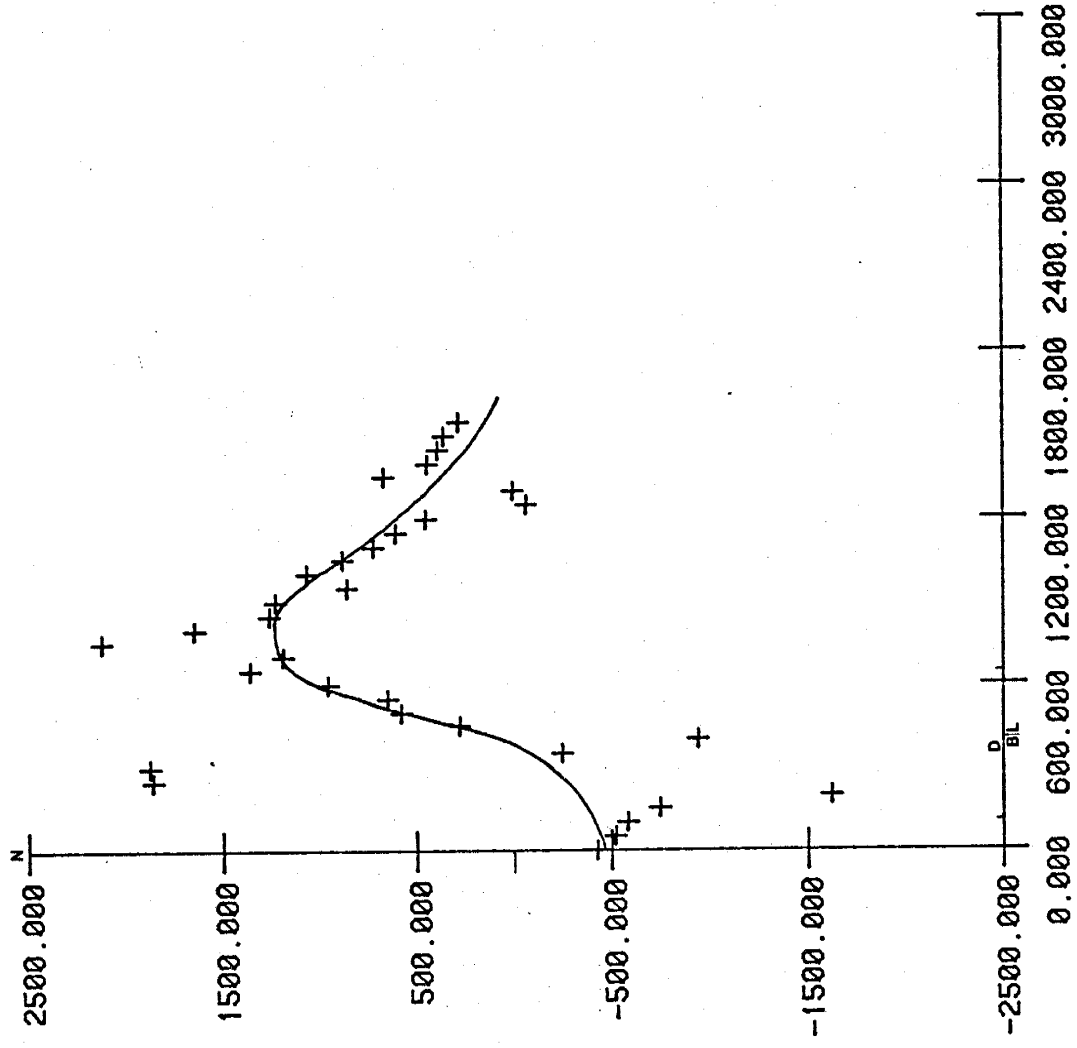
P13

8



P14

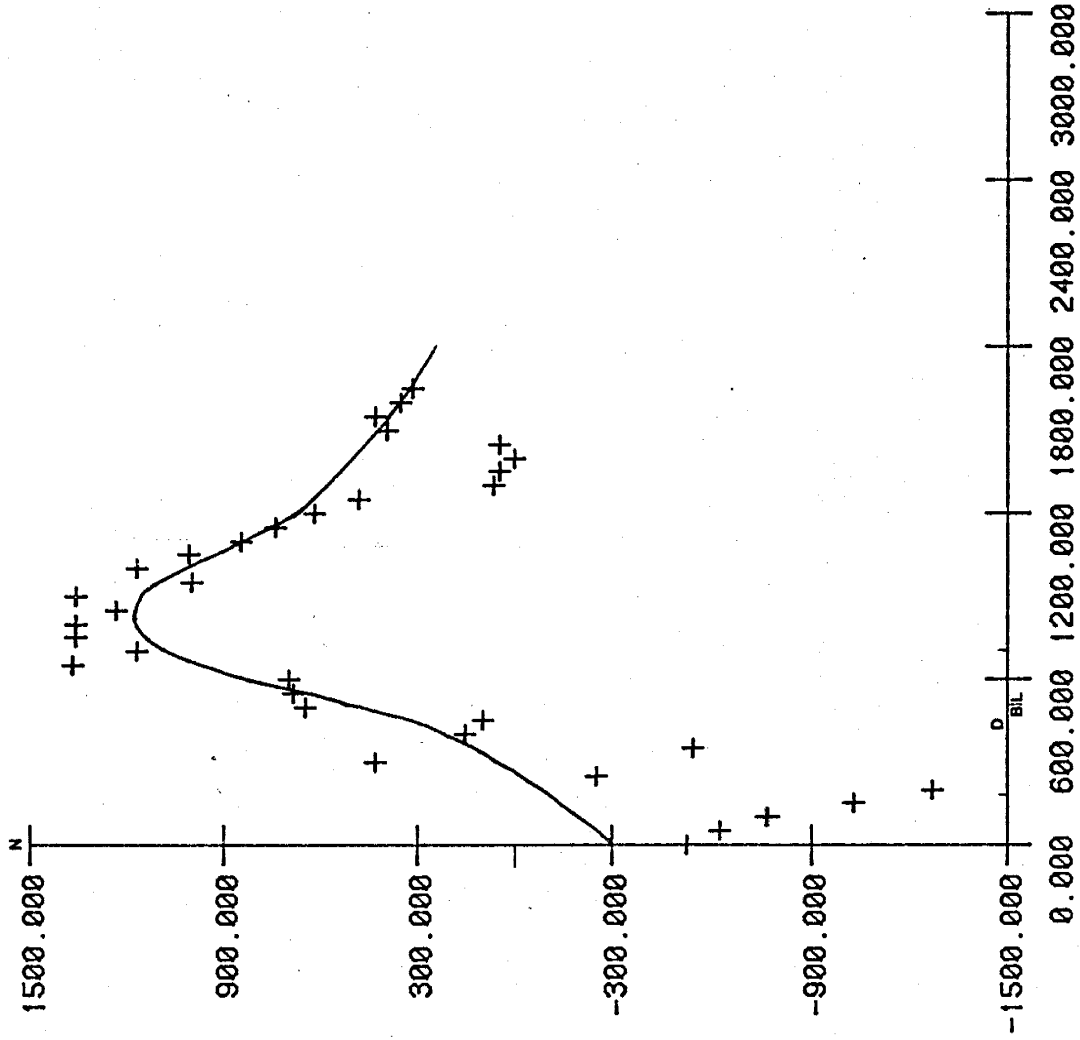
s



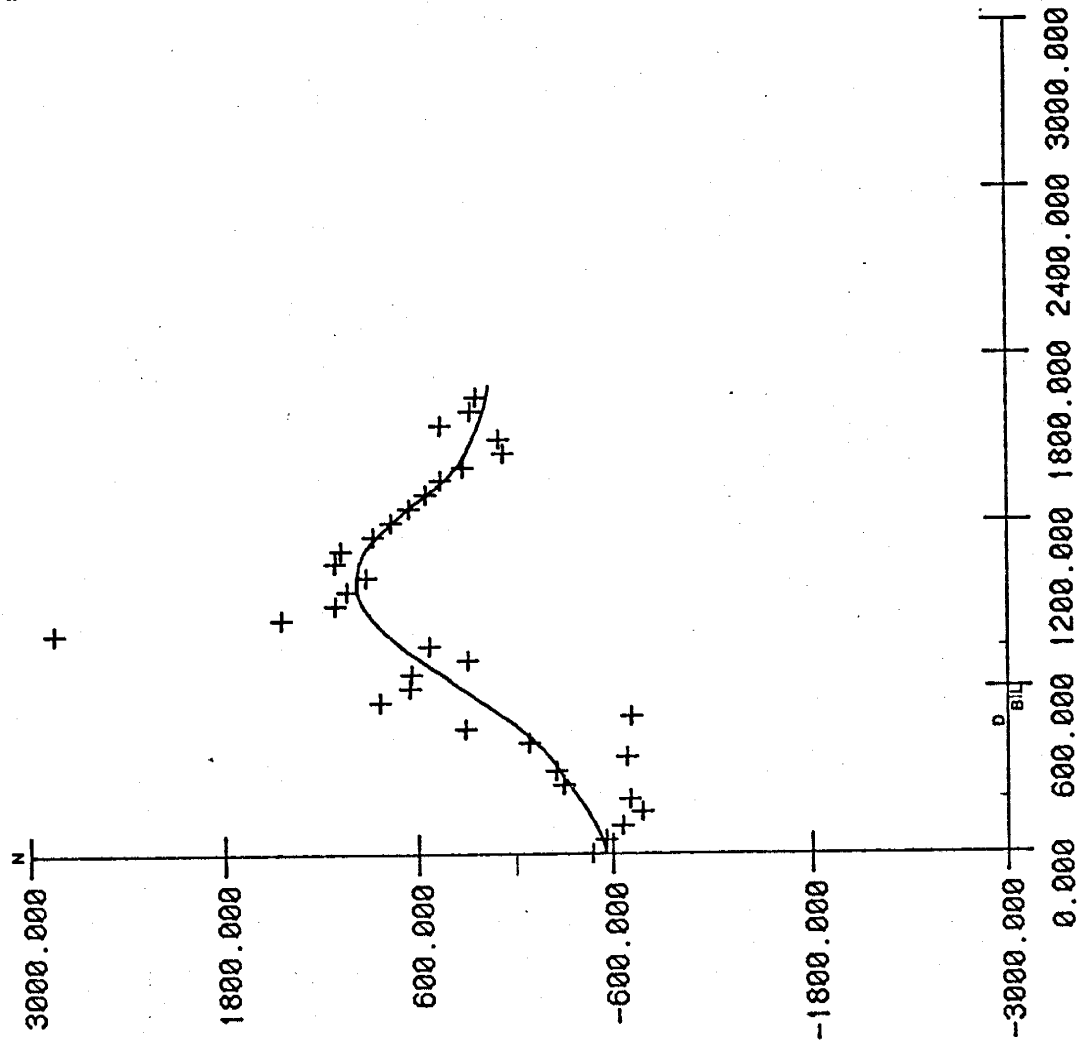
P15

P16

s

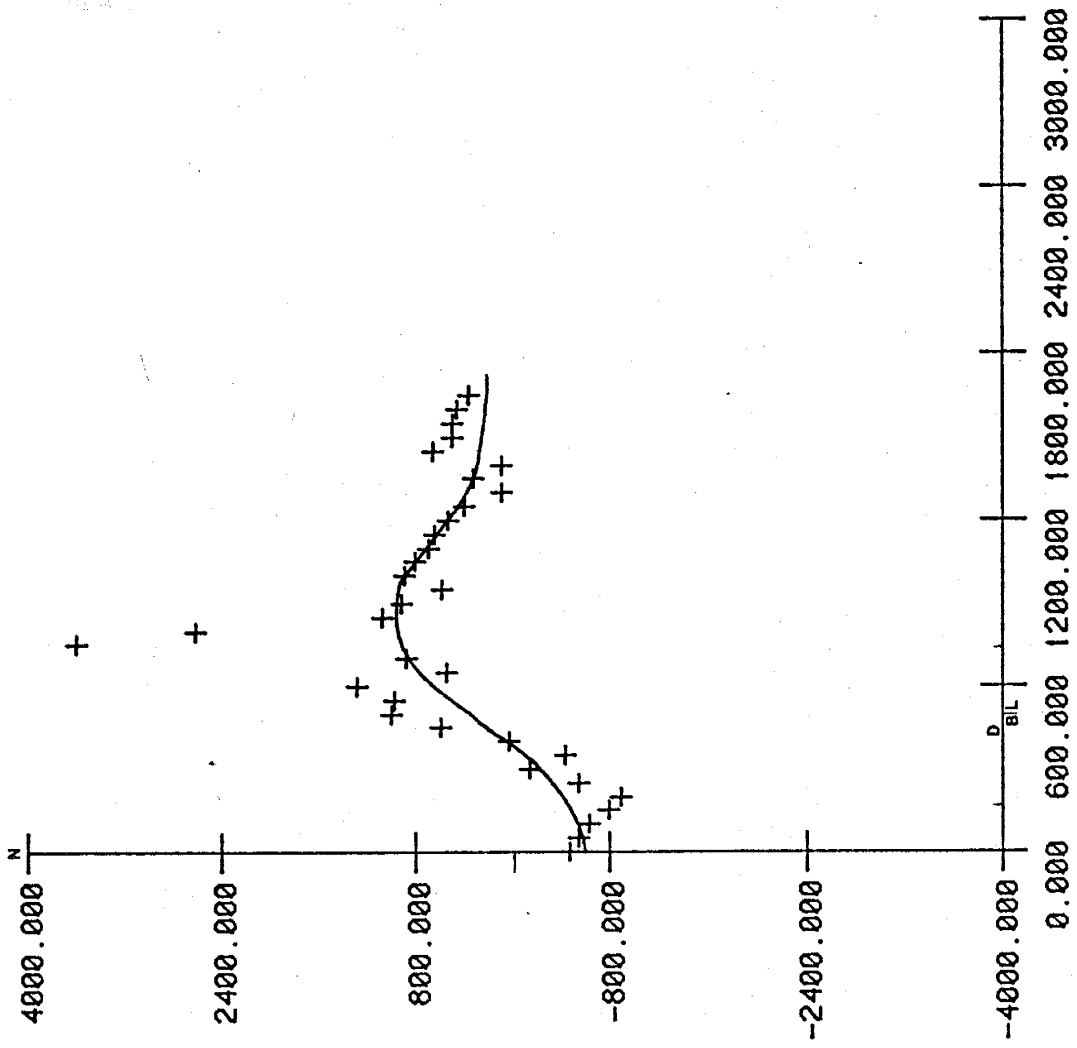


s



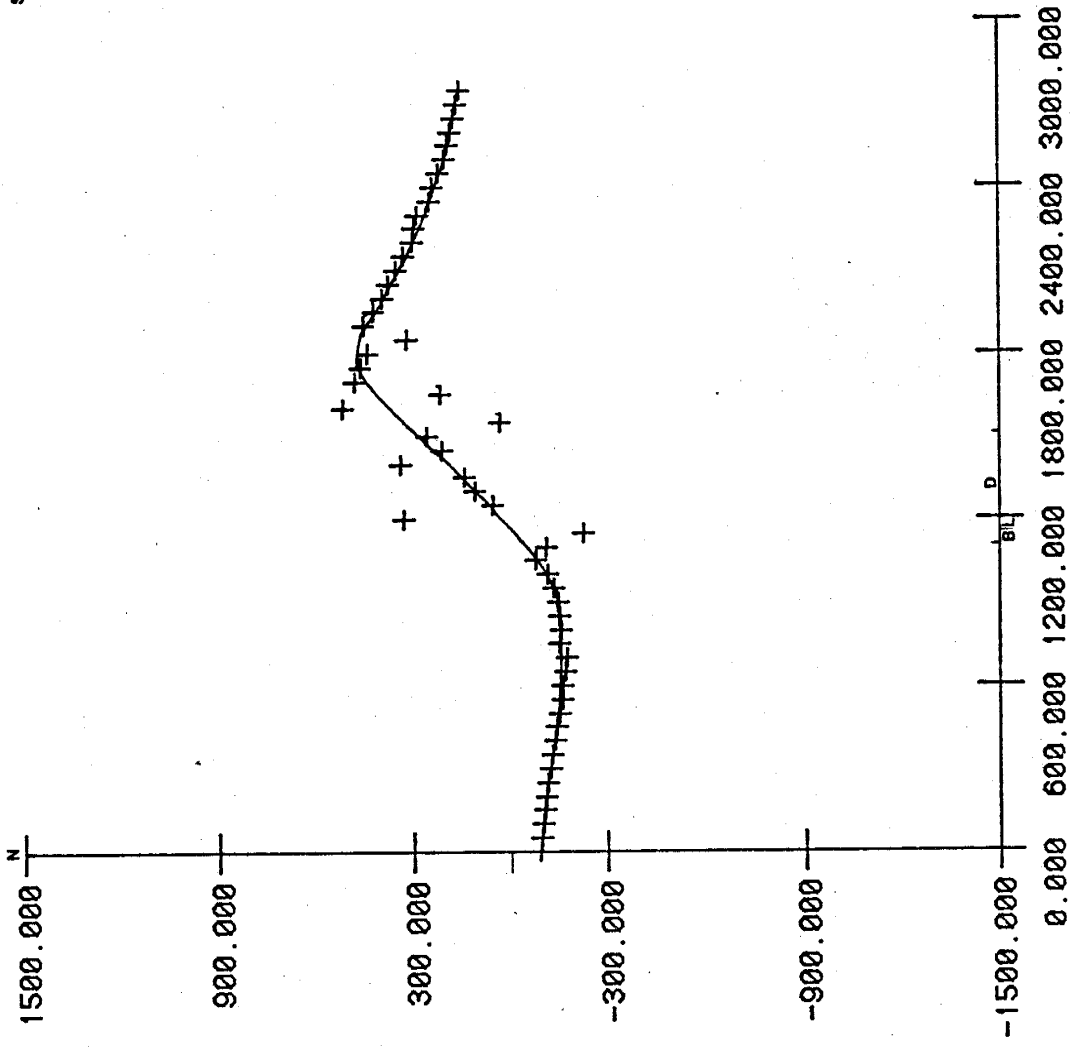
P17

8



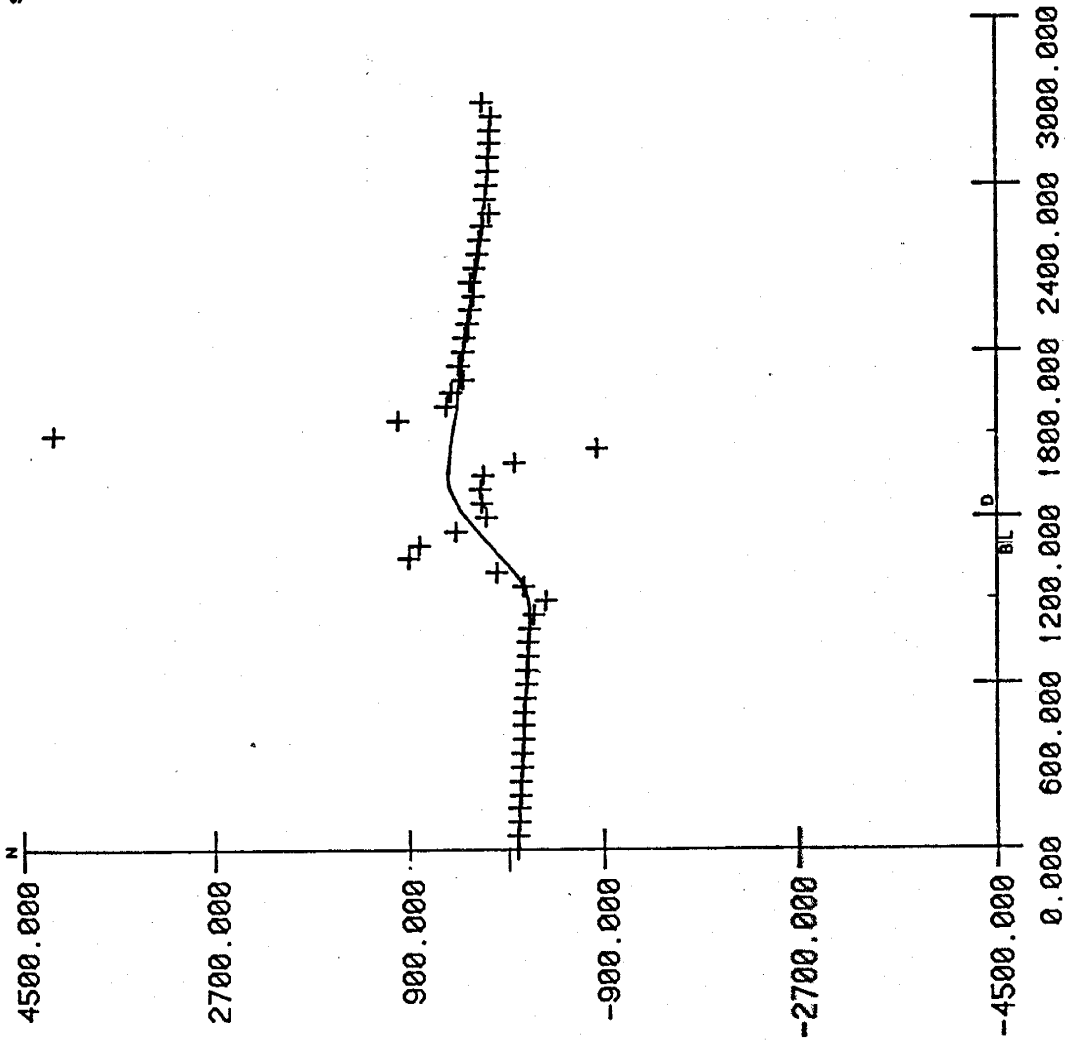
P18

S



P91

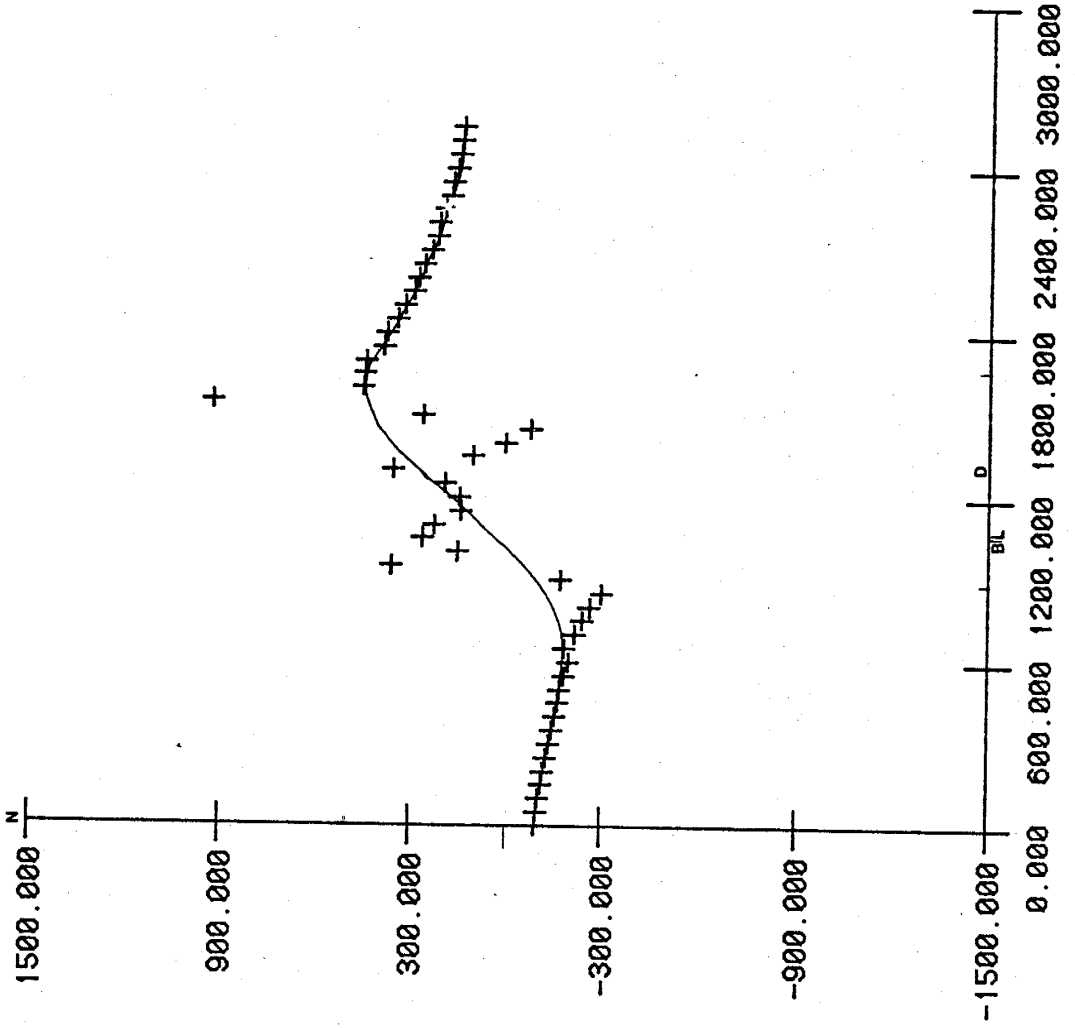
s



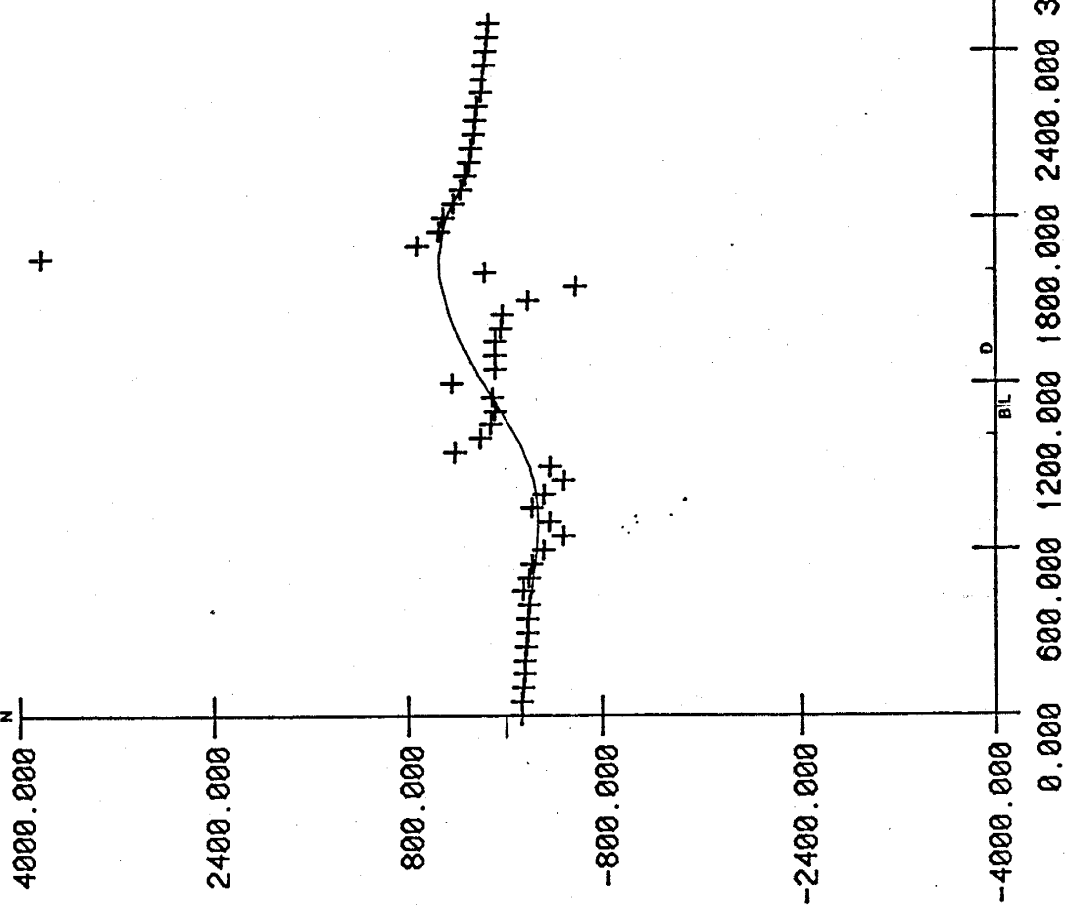
P92

P93

s

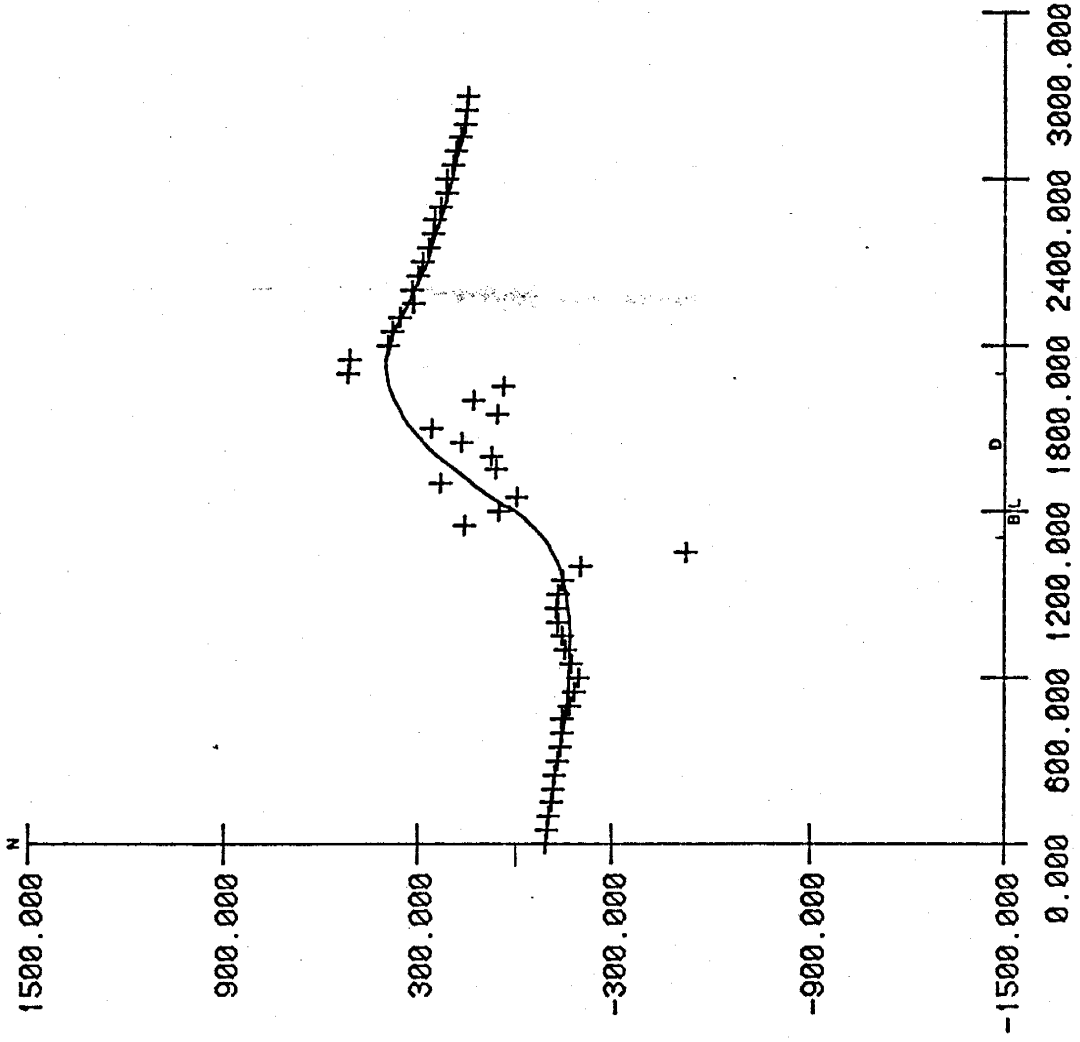


s

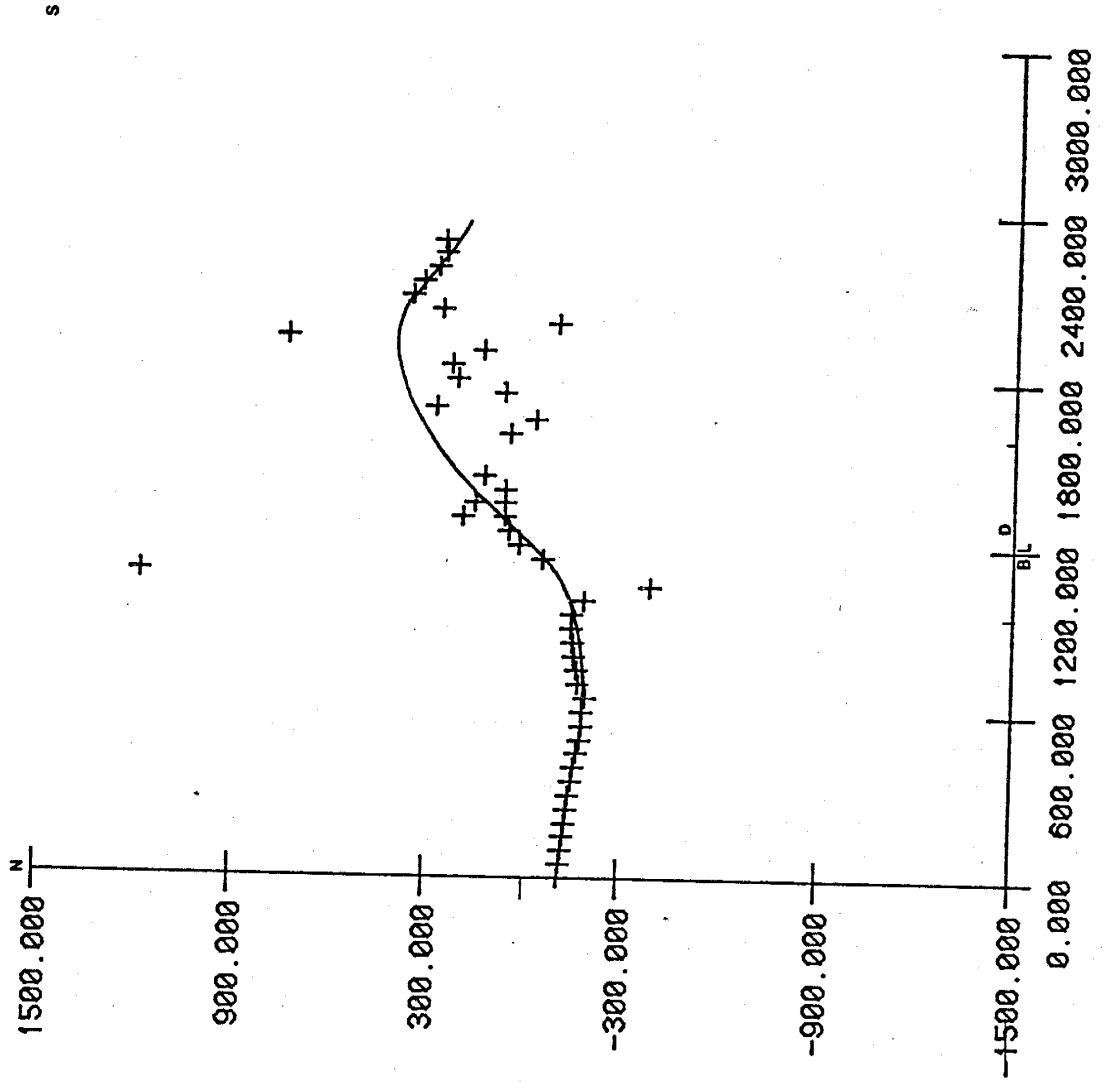


P94

s



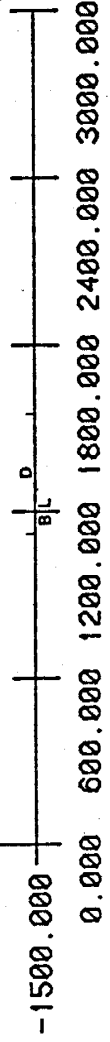
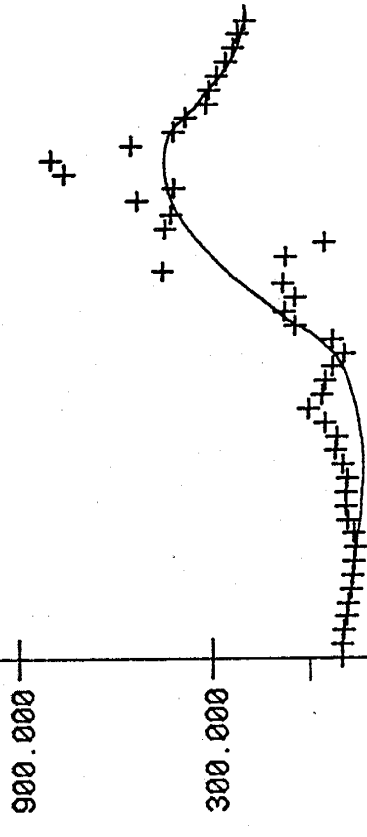
P95_B



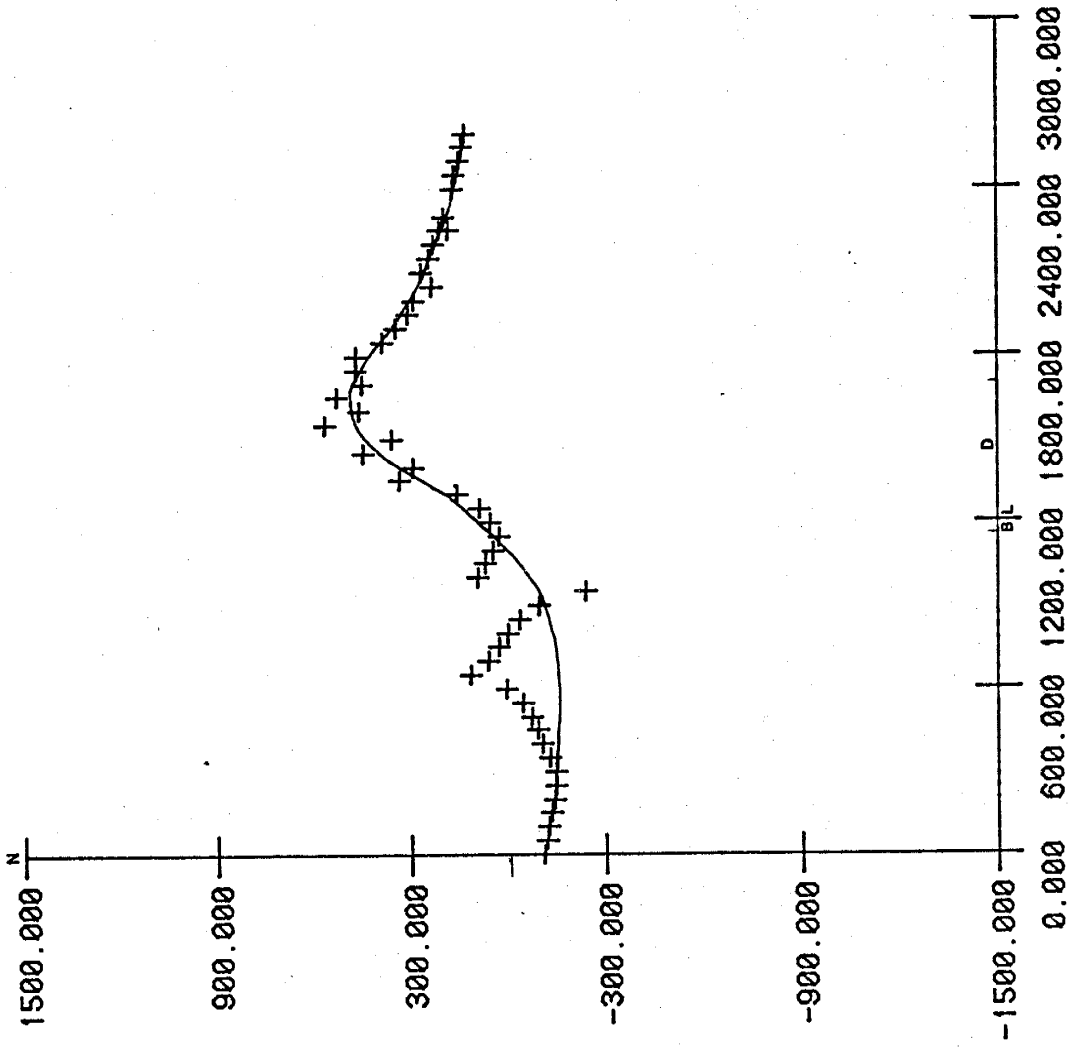
P97

1500.000 N

S

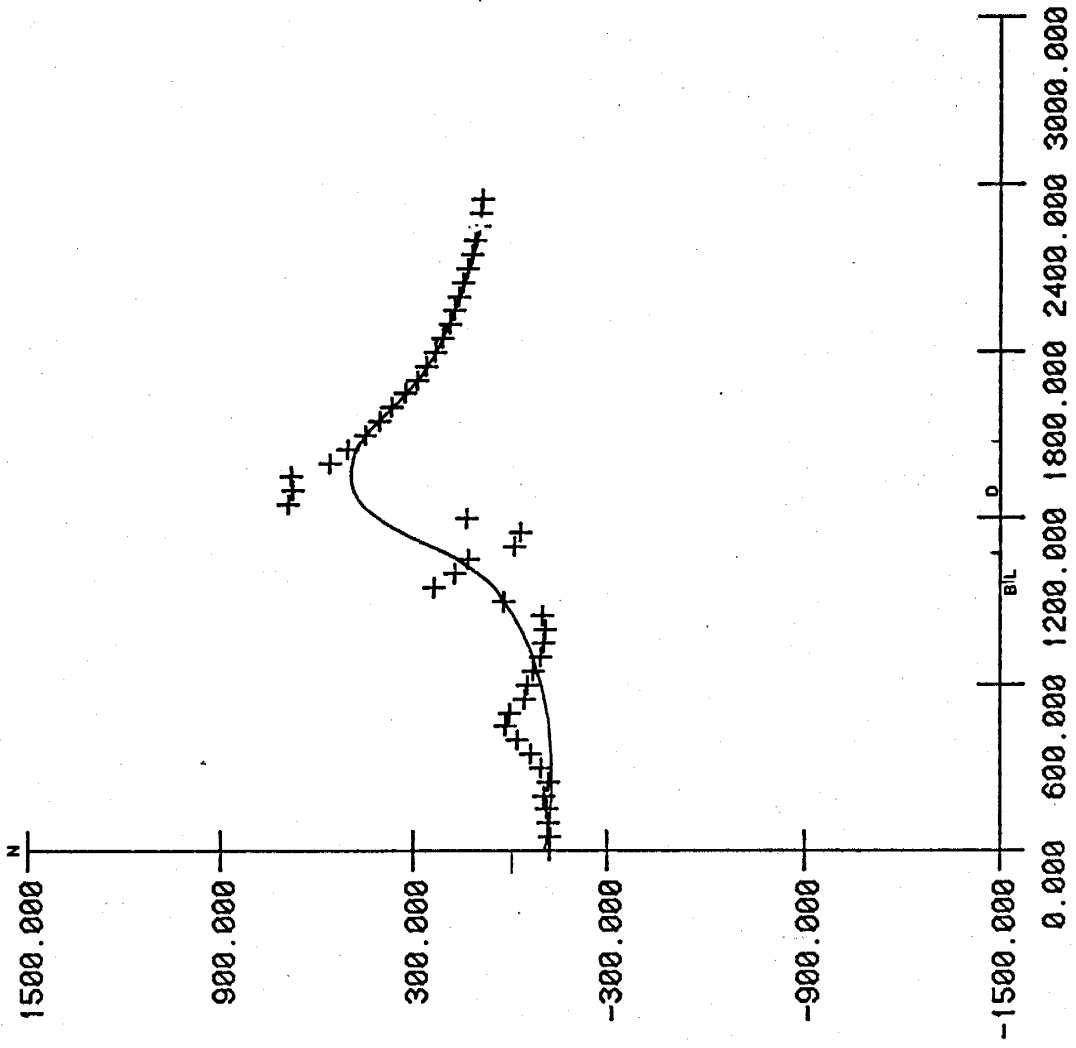


s



P98

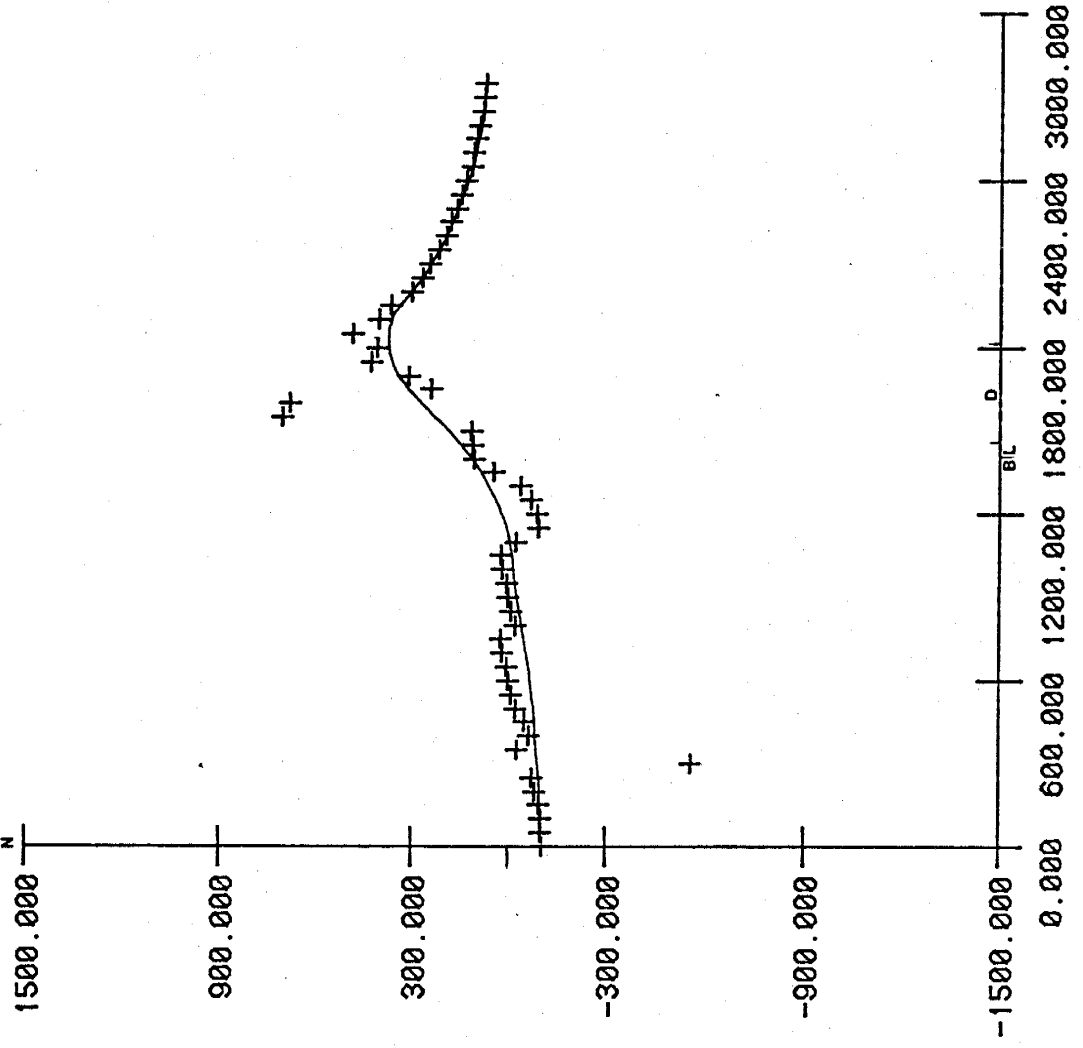
s

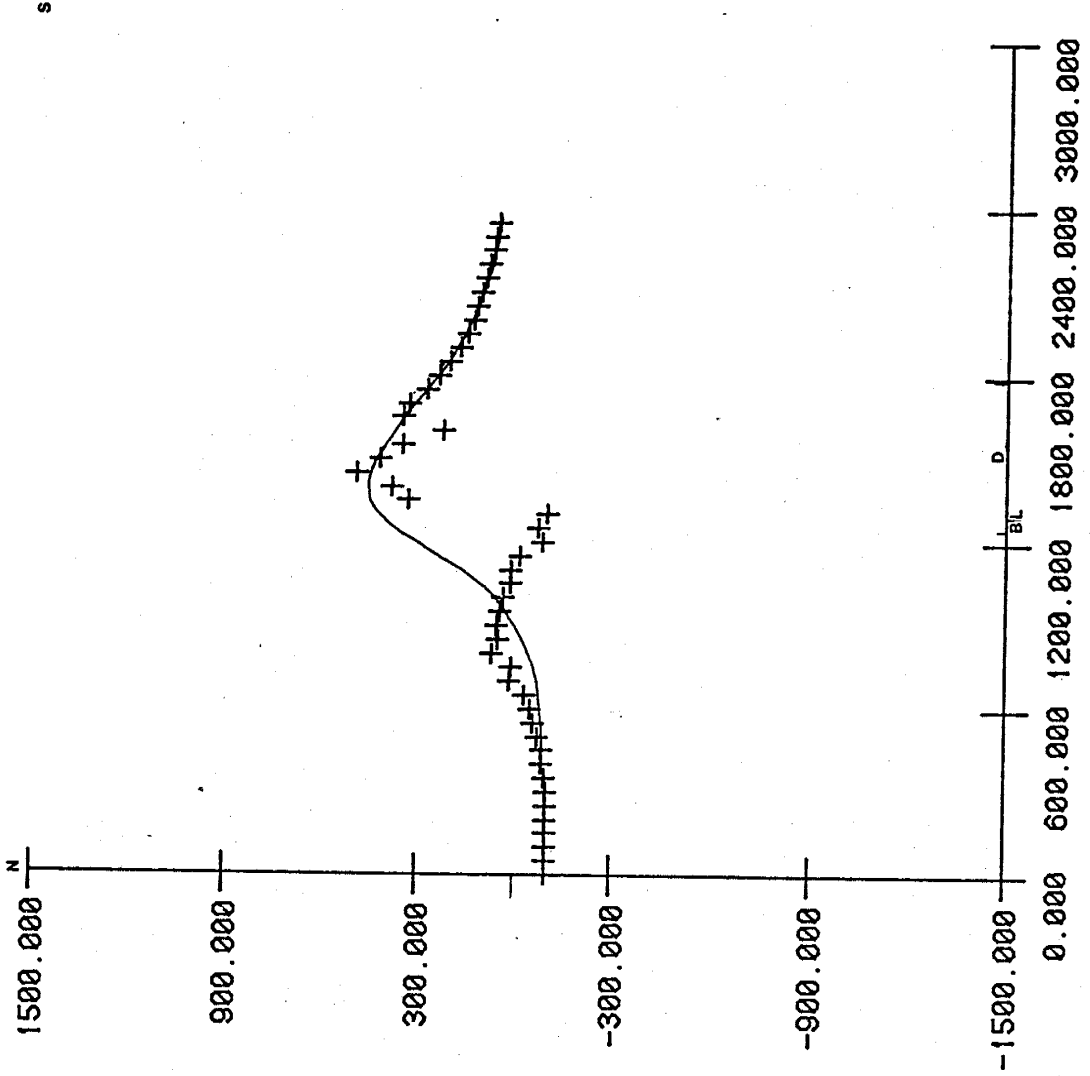


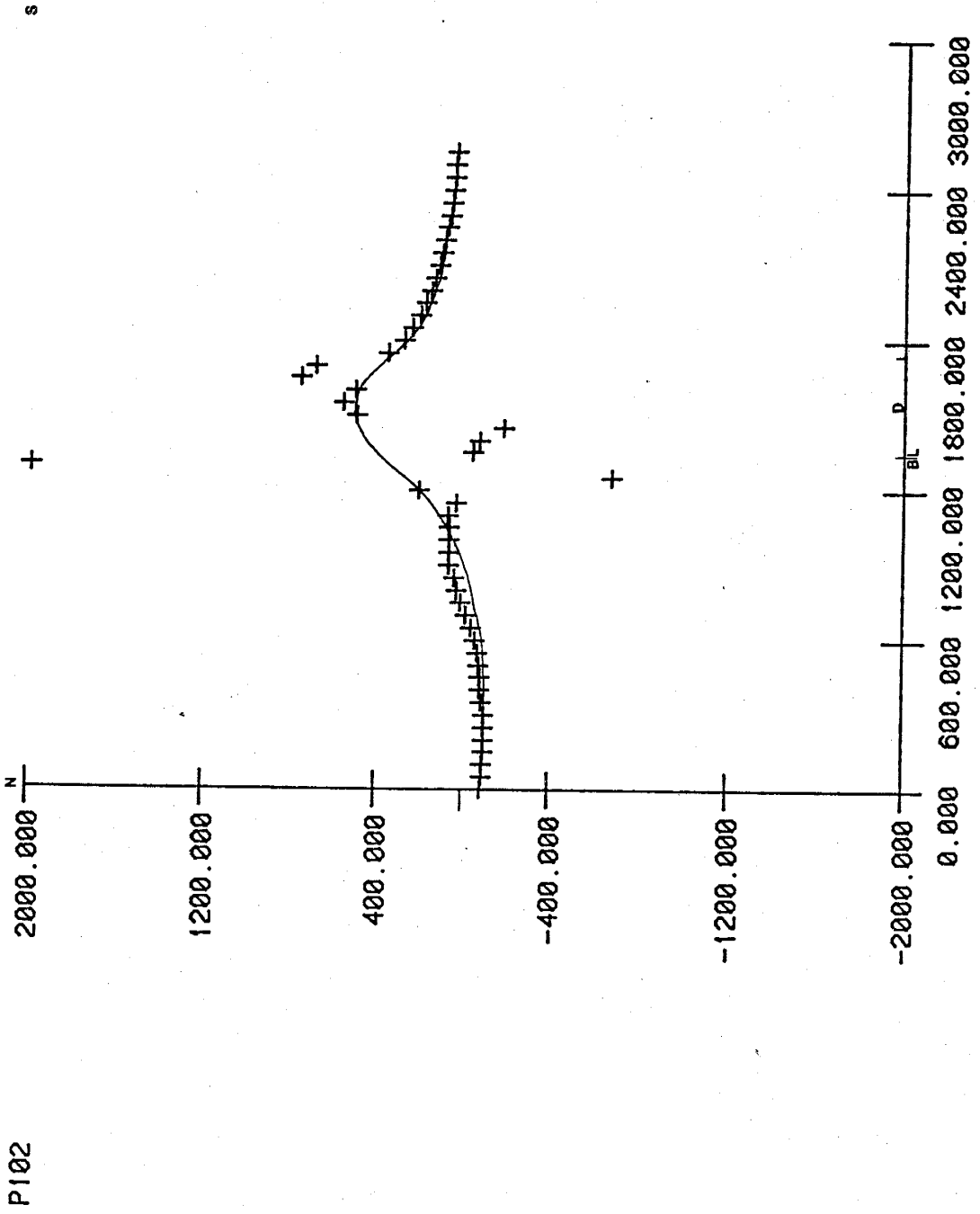
P99

|

s

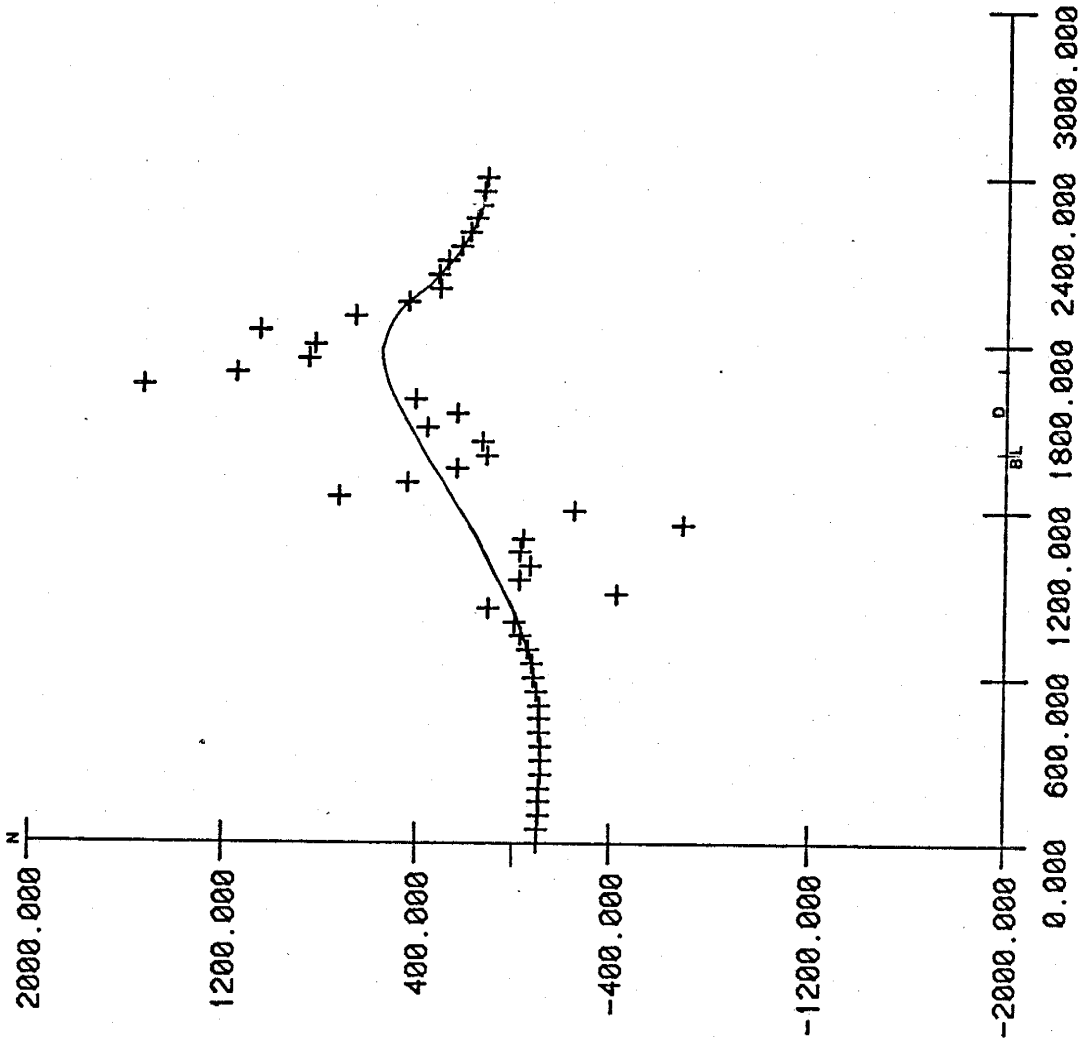


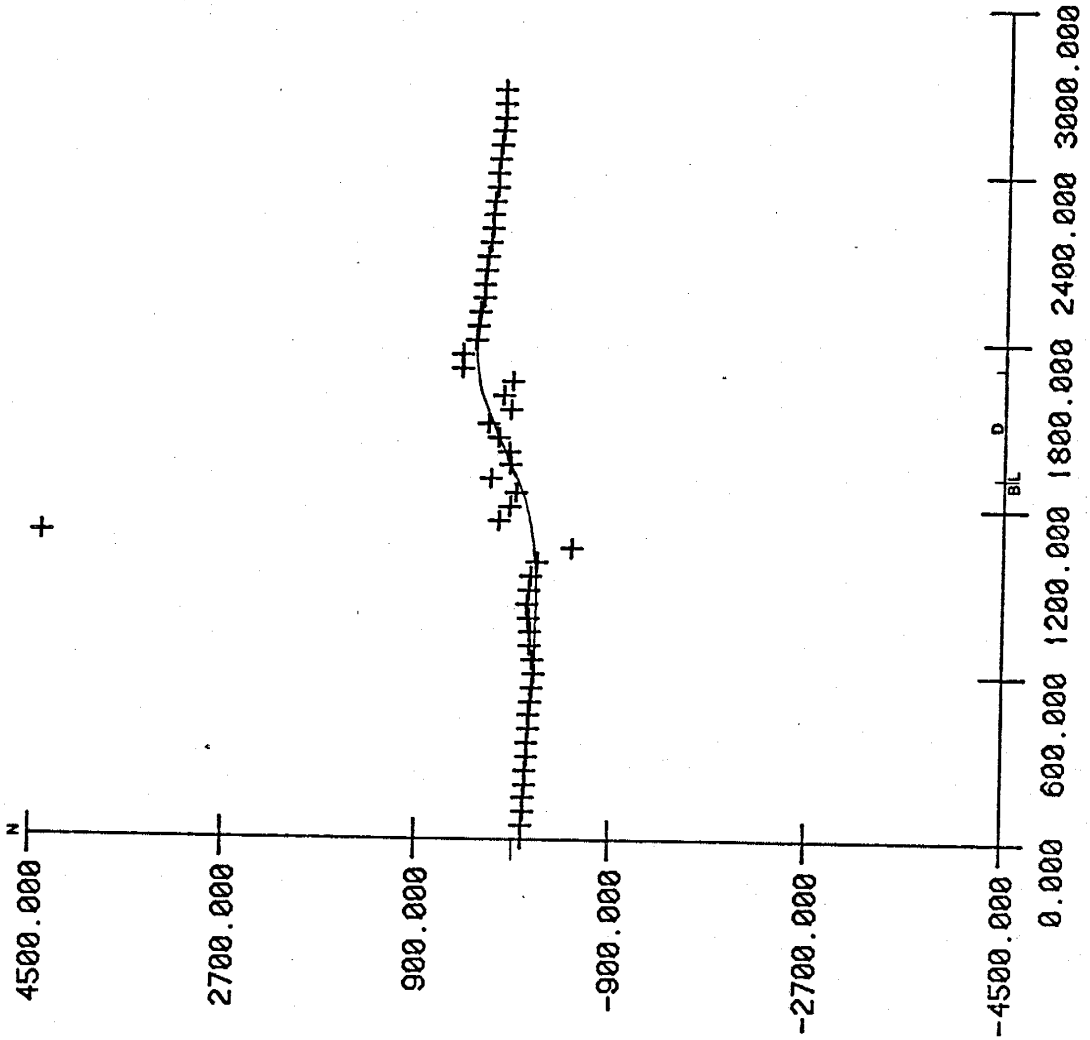


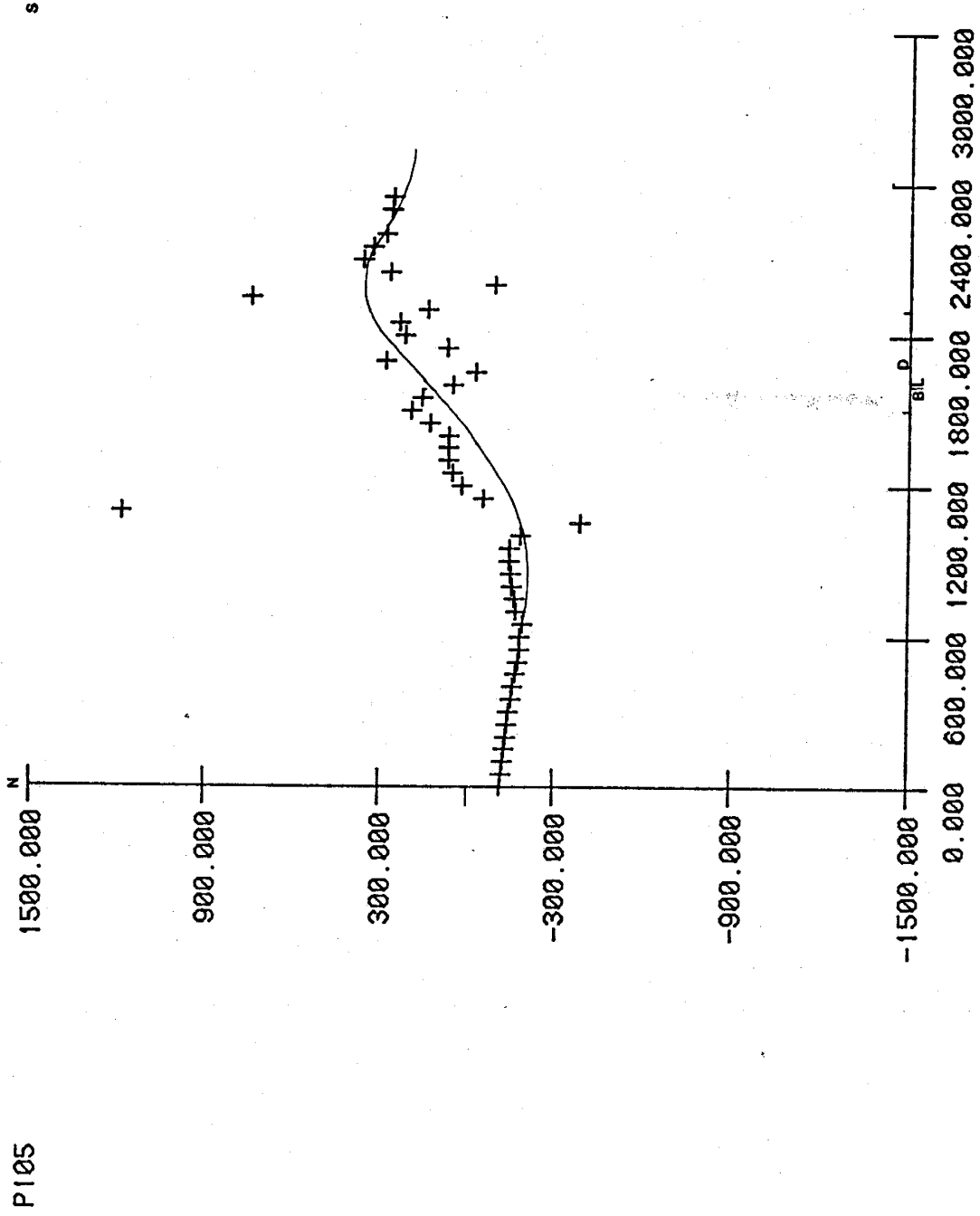


P103

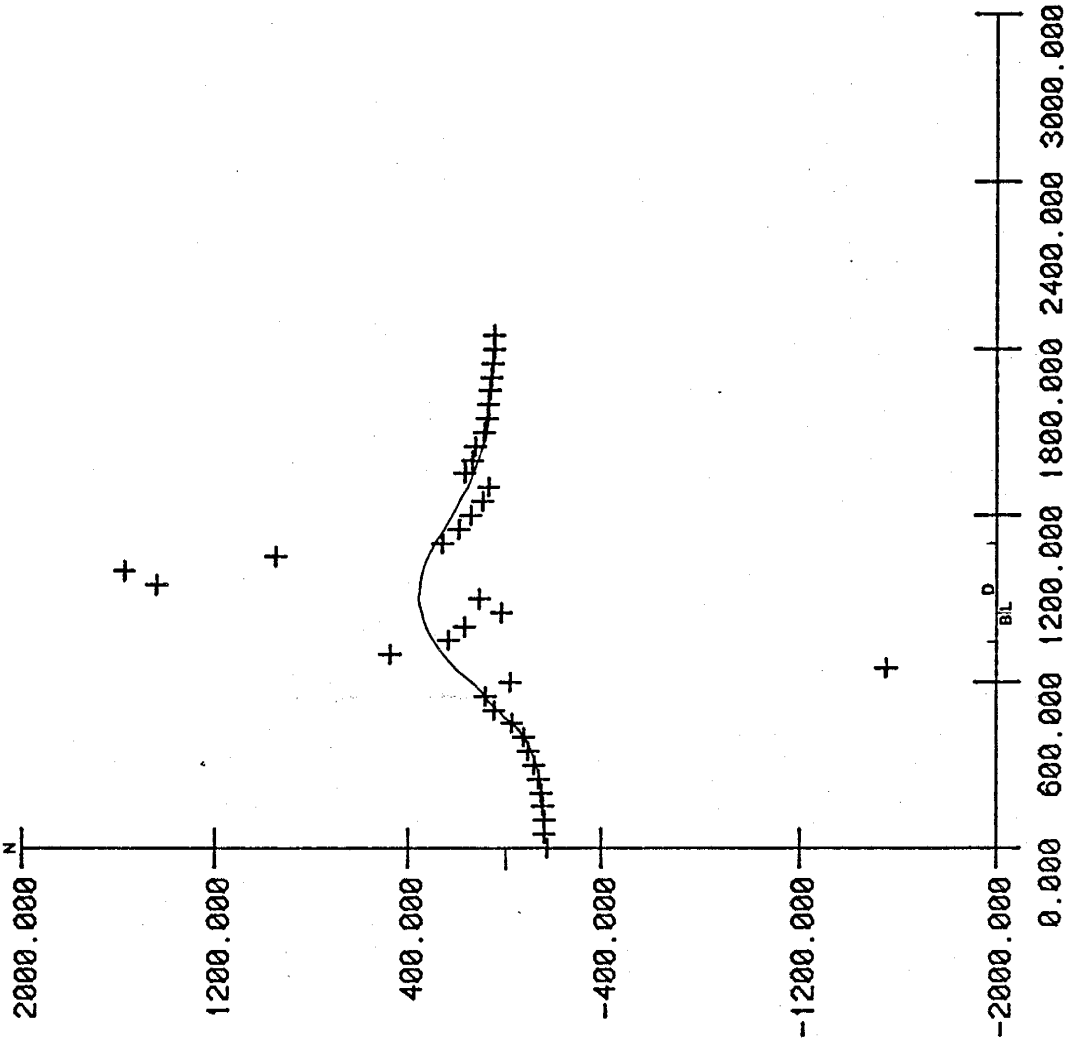
s







s

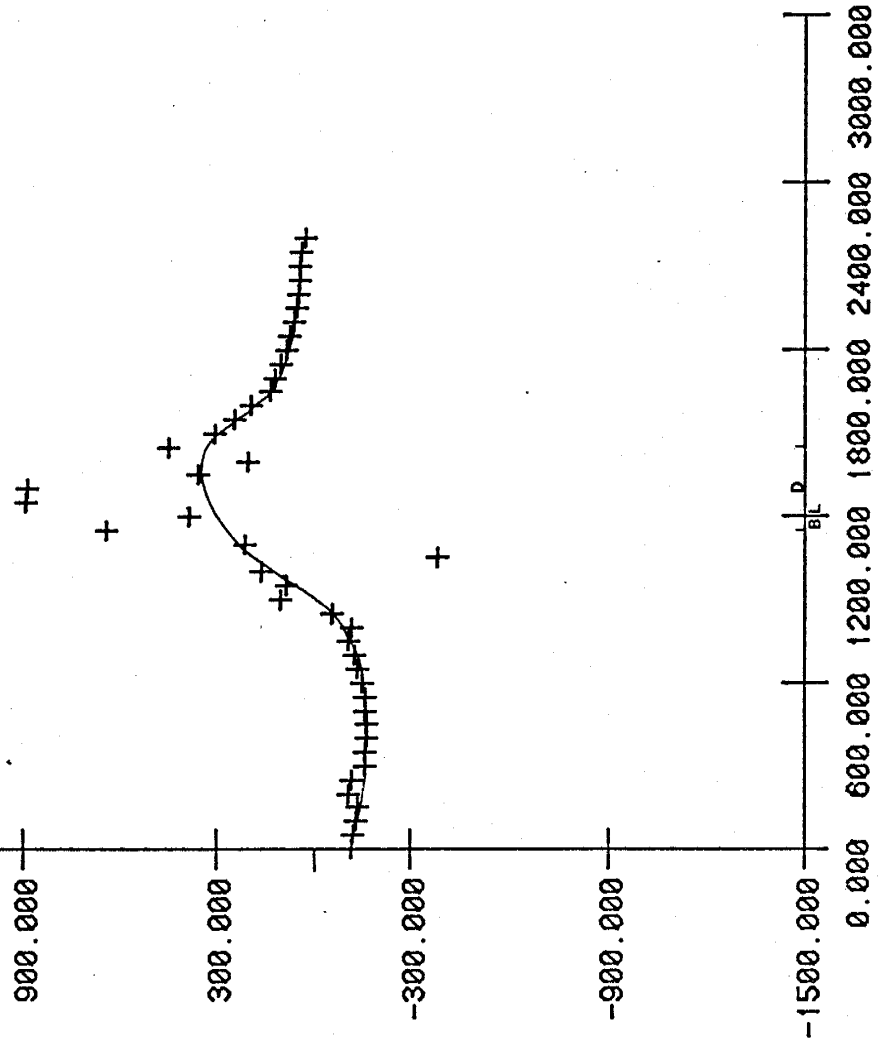


P106

P107

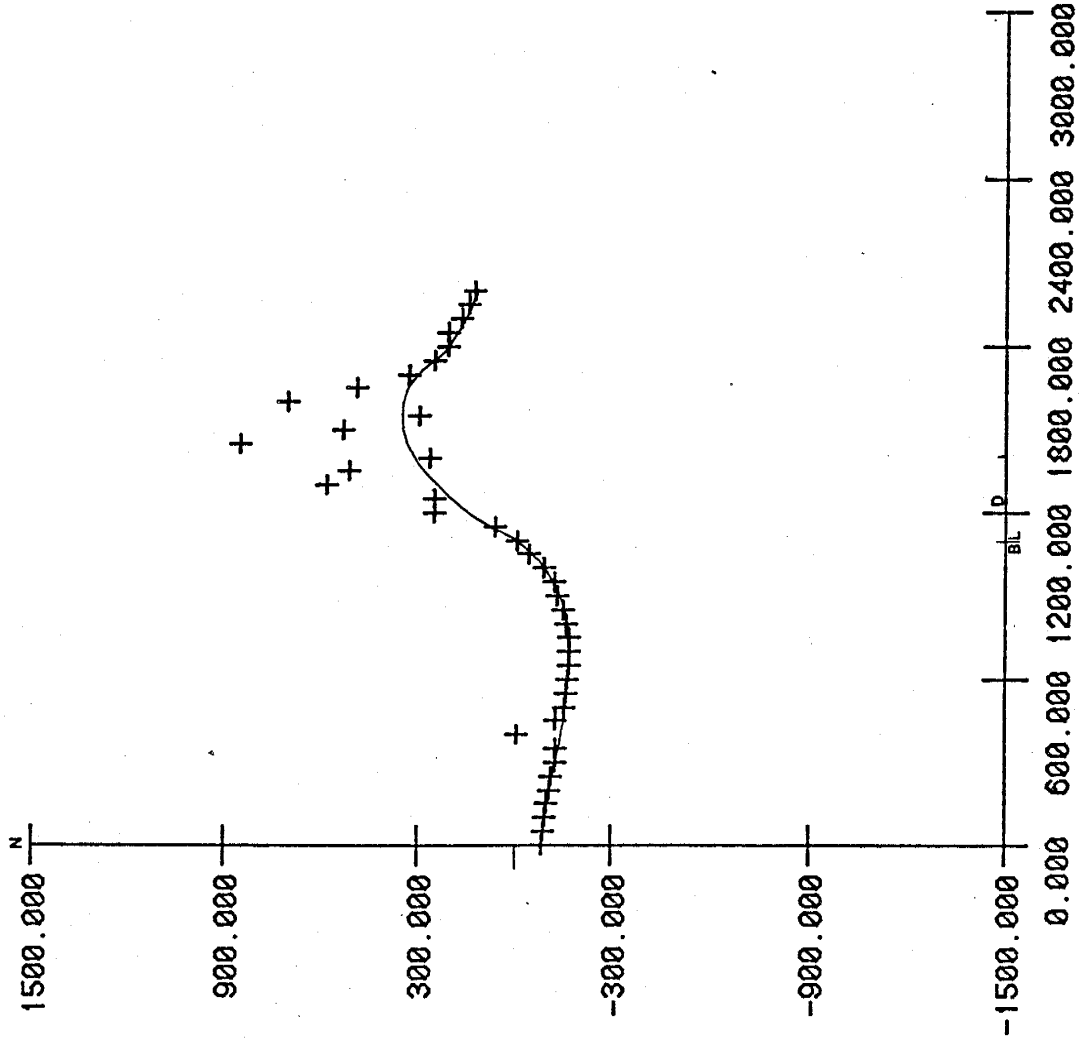
1500.000 N

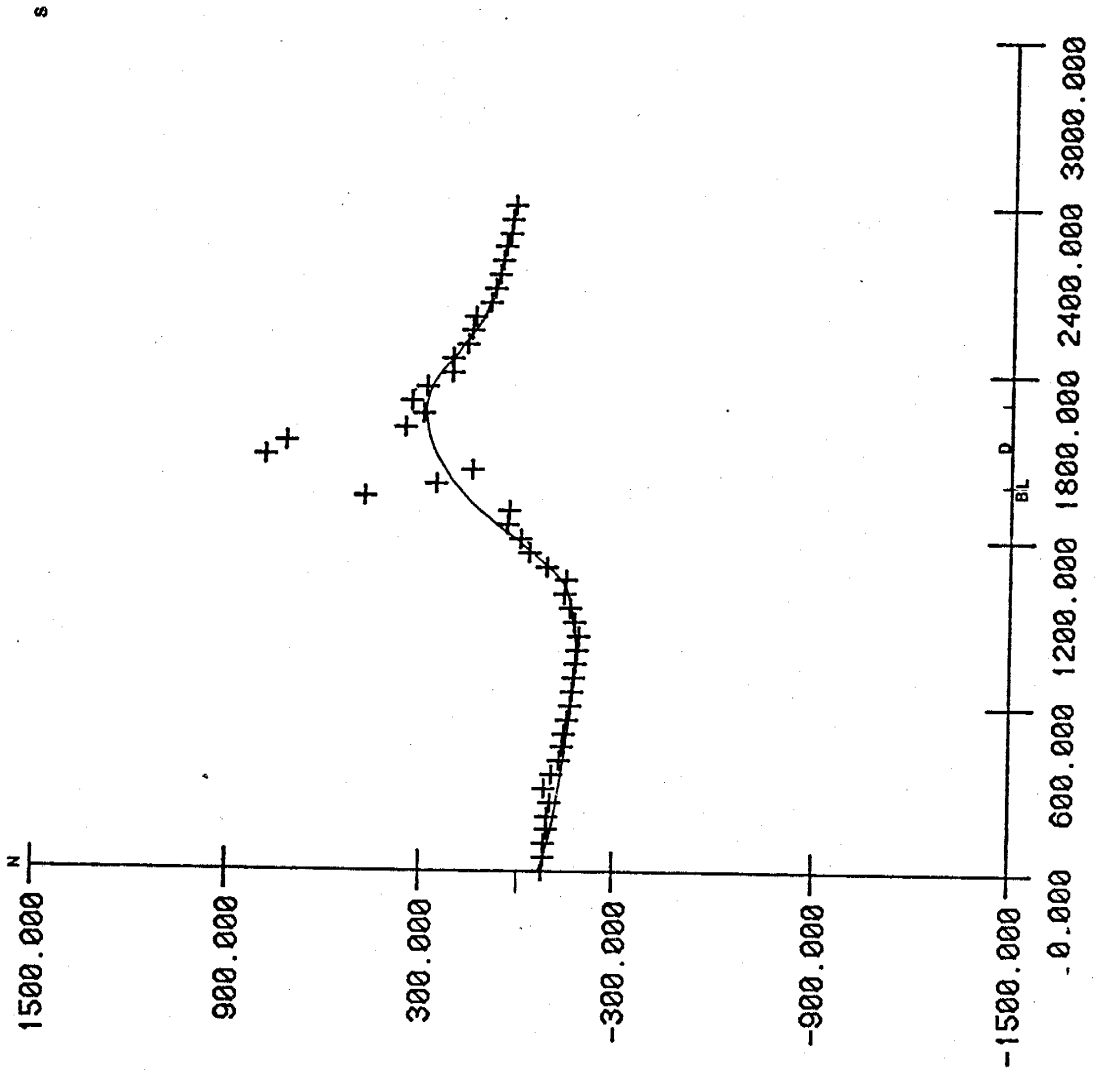
s



P108

S





s

S

1500.000 N

P110

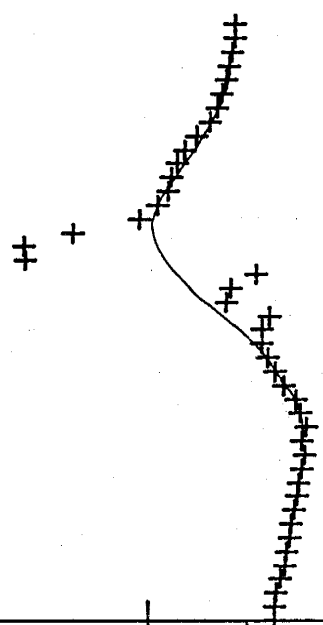
900.000

300.000

-300.000

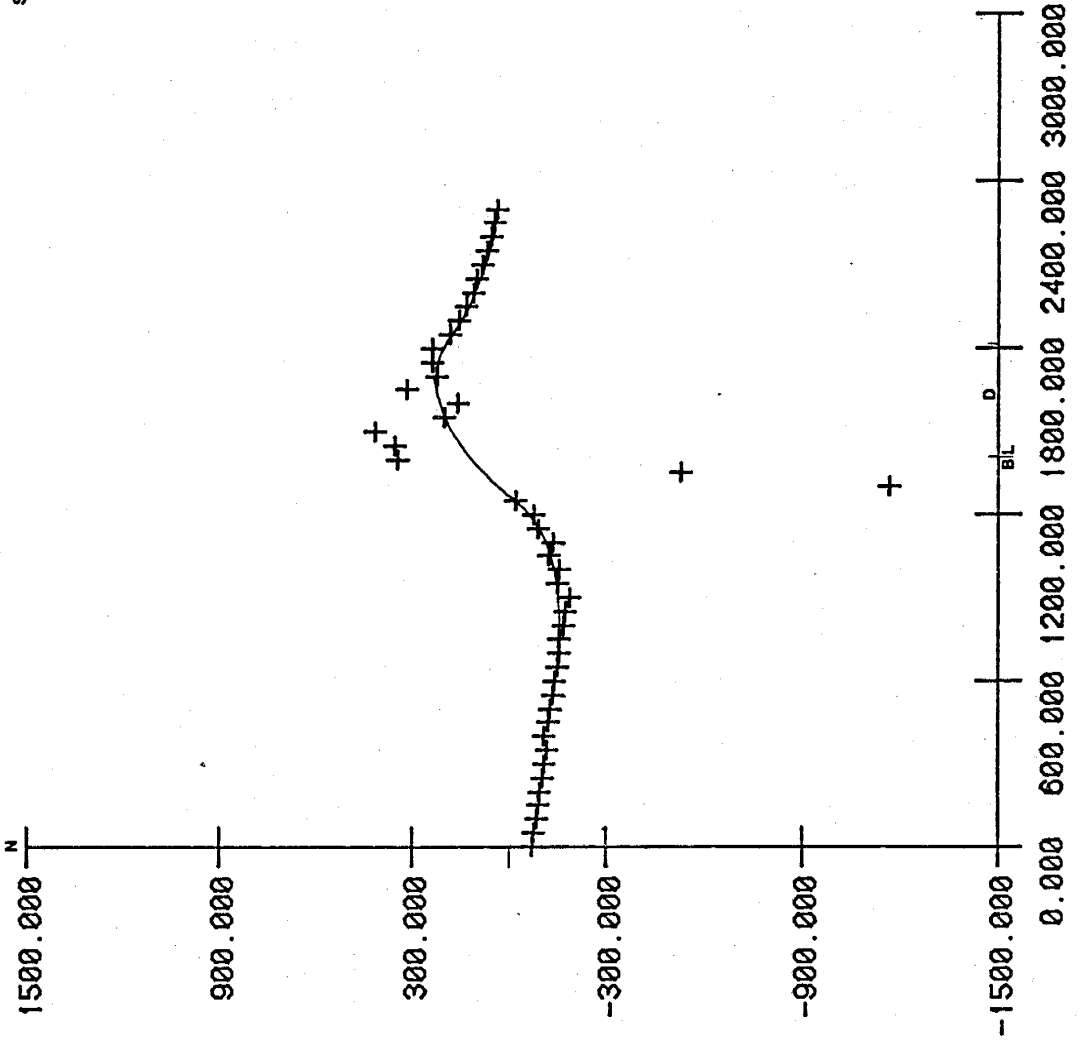
-900.000

-1500.000

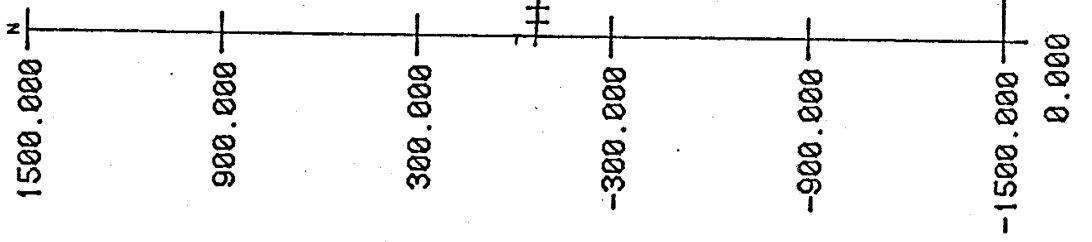


0.000 600.000 1200.000 1800.000 2400.000 3000.000

S



P112



(200)

APPENDIX II

Preliminary Feasibility Study of
the Jones Camp Deposit

Introduction

The purpose of this study is to provide a basis for making a sound financial decision on the continuation of the Jones Camp Project. The study should be considered the first of several made in the course of the project. As further information on reserves, operating costs, financing, government regulations, etc. becomes available, new studies will provide a more accurate picture of the project's potential.

This study has been approached from the position of an outside investor interested in acquiring the mining rights after the initial costs of land acquisition and exploration have been absorbed by the promoter.

Property Status

The property is currently controlled by AWECO Corporation of Dallas, Texas. AWECO has leased 42 claims from Carl Dotson of Socorro, New Mexico, while staking 74 of its own. Under agreement with Dotson, 29 of AWECO's claims overlay Dotson's for assessment purposes. A royalty of \$1/ton of ore sold from Dotson's claims is liable to AWECO. An advanced royalty of \$70,000 has been paid to Dotson by AWECO. Negotiations of a mining lease were completed in December of 1979 for Diversified

Mortgage and Investment Co. of Hemet, California to begin development of the property. Southwest Mineral Corporation is the likely name for the operating company.

A school section (sec. 16, T5S, R7E) lies in the western portion of the property. A lease agreement with the state of New Mexico would be required before mining from this section.

Mining Methods and Assumptions

Open-pit was selected as the best mining method for the deposit. Pits with 45° slopes and depths of 100 feet were used to calculate mining costs. A strip ratio of 11.44:1 (tons overburden:ton ore) is calculated by assuming an average ore thickness of 6', pit depth of 100', ore factor of 10 cu. ft./ton ore and overburden factor of 14.57 cu. ft./ton. Future geotechnics analysis of the property may show that pit slopes up to 60° can be sustained, which would reduce the strip ration to 6.60:1

Ore Reserves and Grade

Ore reserve calculations indicate probable reserves of approximately 1.70 million tons of 60% magnetite to the 100

foot depth. Inferred ore may add several times this amount.

Mine Life

Based on a mill output of 435 tons per day (276 days/yr, one 10 hour shift/day) an estimated recovery factor of 90% and a dilution factor of 10%, the mine has an expected life of approximately 10 years.

Financing

Approximately 3 million dollars would be required to bring the project from the initial preproduction stage through the first month of cash flow. 1.5 million is to be borrowed at 18% (prime + 2.5 pts.) The loan will be fully amortized over 60 months.

Cost Estimates

Costs are estimated in a variety of manners. Table 1 summarizes the various costs. Most of the operating costs are adapted from a financial proforma supplied by a potential investor. All federal, state, and local taxes are calculated in accordance with 1979 regulations.

Table no. 1, Summary of Operating & Capital Costs

Item	\$/year	\$/ton
Direct operating costs:		
Mining		
Labor (mine & mill)	564,000	4.70
Equipment		
D-8 bulldozers(3)	403,200	3.36
988B wheel loaders (2)	300,000	2.50
769C cat. ore trucks(4)	490,800	4.09
air-track drill(1)	39,600	0.33
misc. equipment	75,600	0.63*
development	180,000	1.50*
mine supplies	420,000	3.50*
Milling & pelletizing	480,000	4.00*
Trucking	630,000	5.25
Reclamation	60,000	0.50*
Royalties	1,200,000	10.00
Administrative	240,000	2.00*
Severance & property taxes	153,108	1.2759
Total operating costs	5,236,308	43.6359
Capital costs:		
Preproduction**	1,570,000*	
Mill & equipment	812,500*	
Mining equipment	1,630,000*	
Misc. equipment	140,000*	
Contingency @ %10	415,250	
Total	4,567,750	
* Order of magnitude estimate		
** See table 4 for breakdown		

Economic Analysis

To study the project's profitability, two ROI's (return on investment) are calculated using the discounted cash flow return on investment (DCFROI) method (Park, 1973). One is computed for a 5 year pay off period (Table 2) of capital expenditures, and one for a 10 year period (Table 3). Calculations of the payback periods on the original 3 million dollar investment are made at an 18% discount rate and with no discount rate.

Inflation

To eliminate the effect of inflation, it is assumed that any increase in operating costs or capital expenditures related to inflation is offset by a corresponding increase in the price of pelletized ore.

Depreciation

Depreciation is calculated by the straight line method. An additional 20% first-year depreciation allowable under IRS regulations, is also taken.

Table 2. Discounted Cash Flow Return of Investment Analysis

Cash Flow Year	\$/ton	1 \$/yr	2 \$/yr	3 \$/yr	4 \$/yr	5 \$/yr	6 \$/yr	7 \$/yr	8-12 \$/5 yrs.
Revenue	62.0		7,440,000	7,440,000	7,440,000	7,440,000	7,440,000	7,440,000	37,200,000
Mine & Mill Labor	4.70		564,000	564,000	564,000	564,000	564,000	564,000	2,820,000
Mining equipment	10.28		1,233,600	1,233,600	1,233,600	1,233,600	1,233,600	1,233,600	6,108,000
Milling & Pelletizing	4.00		480,000	480,000	480,000	480,000	480,000	480,000	2,400,000
Misc. equipment	0.63		75,600	75,600	75,600	75,600	75,600	75,600	372,000
Development	1.50	170,000	180,000	180,000	180,000	180,000	180,000	180,000	900,000
Mine supplies	3.50		420,000	420,000	420,000	420,000	420,000	420,000	2,100,000
Trucking	5.25		630,000	630,000	630,000	630,000	630,000	630,000	3,150,000
Reclamation	0.50		60,000	60,000	60,000	60,000	60,000	60,000	300,000
Administration	2.00	120,000	240,000	240,000	240,000	240,000	240,000	240,000	1,200,000
Royalties	10.00		1,200,000	1,200,000	1,200,000	1,200,000	1,200,000	1,200,000	6,000,000
Net after costs	19.64		2,356,800	2,356,800	2,356,800	2,356,800	2,356,800	2,356,800	11,784,000
Property tax	0.56		67,200	67,200	67,200	67,200	67,200	67,200	336,000
Severance taxes	0.7159		85,908	85,908	85,908	85,908	85,908	85,908	429,540
Interest			253,769	213,995	166,443	105,493	41,613		
Preproduction Devel.	0.775		93,000	93,000	93,000	93,000	93,000	93,000	465,000
Depreciation			1,218,447	315,892	315,892	315,892	315,892	315,892	1,579,460
Depletion			365,738	836,903	860,679	891,154	923,094	923,094	4,719,500
Net before income tax			365,738	836,903	860,679	891,154	923,094	923,094	4,719,500
N.M. income tax			18,287	41,845	43,034	44,558	46,155	46,155	235,975
Federal income tax			153,227	368,128	378,969	392,860	407,431	407,431	2,084,592
Net after taxes			194,174	426,930	438,676	453,730	469,508	469,508	2,398,933
Plus									
Investment tax credit			89,139		136,171				
Depreciation			1,218,447	315,892	315,892	315,892	315,892	315,892	1,579,460
Depletion			365,738	836,903	860,679	891,154	923,094	923,094	4,719,500
Operating cash flow			1,867,498	1,805,690	1,751,418	1,660,776	1,708,494	1,708,494	8,697,893
Capital expenditures		80,000	1,490,000	750,000	750,000	750,000	750,000	750,000	1,500,000
Working capital			500,000						
Net cash flow			-370,000	1,617,498	1,001,418	910,776	958,494	958,494	7,197,893
Present value @ 18%			1,370,761	758,180	609,494	469,768	418,967	418,967	1,967,783
Present value @ 40.29%			1,152,957	536,384	362,680	235,120	176,375	176,375	555,111

Based on annual production of 120,000 tons

Table 3, Discounted Cash Flow Return of Investment Analysis

Cash Flow Year	1	2	3	4	5	6	7	8-12
	\$/yr	\$/yr	\$/yr	\$/yr	\$/yr	\$/yr	\$/yr	\$/5 yrs.
Revenue			7,440,000	7,440,000	7,440,000	7,440,000	7,440,000	37,200,000
Mine & Mill Labor			564,000	564,000	564,000	564,000	564,000	2,820,000
Mining equipment			1,233,600	1,233,600	1,233,600	1,233,600	1,233,600	6,108,000
Milling & Pelletizing			480,000	480,000	480,000	480,000	480,000	2,400,000
Misc. equipment			75,600	75,600	75,600	75,600	75,600	378,000
Development	170,000	400,000	180,000	180,000	180,000	180,000	180,000	900,000
Mine supplies			420,000	420,000	420,000	420,000	420,000	2,100,000
Trucking			630,000	630,000	630,000	630,000	630,000	3,150,000
Reclamation			60,000	60,000	60,000	60,000	60,000	300,000
Administration			240,000	240,000	240,000	240,000	240,000	1,200,000
Royalties			1,200,000	1,200,000	1,200,000	1,200,000	1,200,000	6,000,000
Net after costs			2,356,800	2,356,800	2,356,800	2,356,800	2,356,800	11,784,000
Property tax			67,200	67,200	67,200	67,200	67,200	336,000
Severance taxes			85,908	85,908	85,908	85,908	85,908	429,540
Interest			253,769	213,995	166,443	105,493	41,613	
Preproduction Devel.			93,000	93,000	93,000	93,000	93,000	465,000
Depreciation			1,218,447	315,892	315,892	315,892	315,892	1,579,460
Depletion			365,738	836,903	860,679	891,154	923,094	4,719,500
Net before income tax			365,738	836,903	860,679	891,154	923,094	4,719,500
N.M. income tax			18,287	41,845	43,034	44,558	46,155	235,975
Federal income tax			153,227	368,128	378,969	392,860	407,431	2,084,592
Net after taxes			194,174	426,930	438,676	453,730	469,508	2,398,933
Plus								
Investment tax credit			89,139	225,965	136,171			
Depreciation			1,218,447	315,892	315,892	315,892	315,892	1,579,460
Depletion			365,738	836,903	860,679	819,154	923,094	4,719,500
Operating cash flow			1,867,498	1,805,690	1,751,418	1,660,776	1,708,494	8,697,893
Capital expenditures	80,000	1,490,000	1,050,000	1,050,000	1,050,000	1,050,000	1,050,000	
Working capital			500,000					
Net cash flow			-370,000	-2,130,000	701,418	610,776	658,494	8,697,893
Present value @ 18%			1,317,498	542,725	426,905	315,031	287,834	2,371,857
Present value @ 33.37%			987,846	424,837	295,662	193,036	156,044	942,573

Based on yearly production of 120,000 tons

Marketing

A market for the pelletized iron is assured with the Colorado Fuel and Iron Company, Pueblo, Colorado. A price of \$62 per ton would be paid for the minimum delivery of 10,000 tons per month of pelletized ore.

Information from Mineral Industry Report (U. S. Bureau of Mines, July 1979) indicates that the price of pelletized iron ore is keeping pace with current inflation rates (Fig. 1).

Results

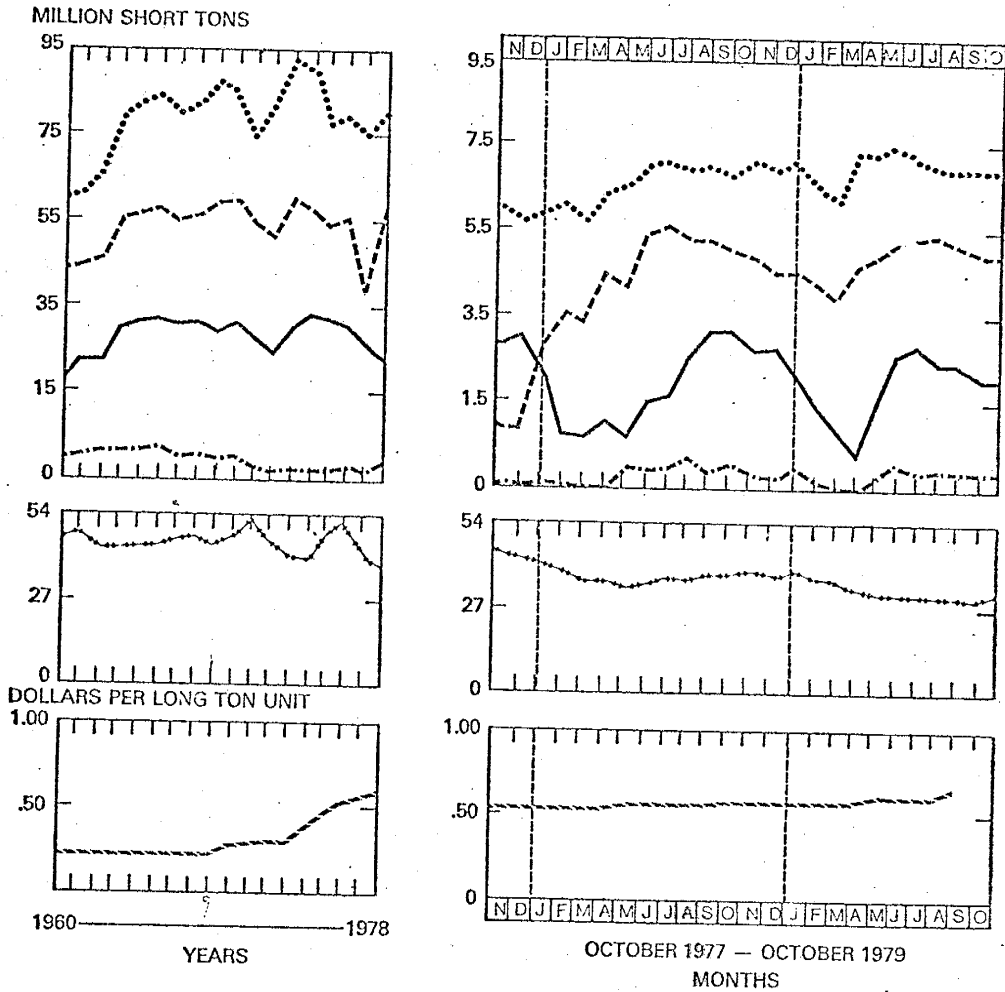
	10 year pay off period of capital expenditures	5 year pay off period of capital expenditures
ROI	0.4029121	.3337078
Payback period of original investment @ 18% discount	3.56 years	5.48 years
Payback period of original investment with no discount	2.33 years	3.37 years

Discussion

Results of the DCFROI and payback period analysis indicate that the Jones Camp Project could be profitable.

Before proceeding any further, a note of warning is in order. The results of any study are limited by the accuracy of the data used. Some of the costs and equipment estimates used in this analysis are only order of magnitude figures. These estimates and any calculations

Figure 1 Iron Ore Market Data (U.S. Bureau of Mines, 1979)



made with them should not be stretched beyond their intended limits of accuracy. Thus this study, although providing hard numbers as to what the profitability of the project may be, should only be used to help decide whether or not the project is to be continued. Future feasibility studies with more detailed information, will give closer estimates of the project's profitability.

During the DCFROI analysis, several factors were recognized that would significantly affect the operation. These include capital expenditures, royalty payments, increased operating costs, and inflation.

By altering the capital expenditure pay out period from 5 years to one of 10 years, the attractiveness of the investment improves.

Royalty payments are unusually high (16.1% of gross) for a mining operation. By reducing royalties 50%, the ROI increases approximately 3.5 points. If future studies show the project to be submarginal, negotiations to reduce royalty payments would be in order.

The effect of rising equipment requirements will also affect the projects profitability. Geologic mapping has shown the ore bodies to be distributed along the 8 mile length of the property. Such a distribution is likely to require additional equipment to meet production goals, since production cannot be concentrated

in a single opening.

Inflation should be another consideration to any potential investors. Contracts for ore delivery should include an escalator clause to adjust prices to match inflated costs.

Careful monitoring of all these factors could significantly improve the ROI.

Conclusions

Results of the feasibility study show that continuation of the Jones Camp project is justified.

Development steps and their approximate costs are given in figures 2 & 3, and table 4. Future expenditures should be made with the understanding that the next feasibility study may show the project to be unprofitable.

The success of this operation will depend largely on the hiring of a qualified project manager with a proven track record in small mining operations.

Fig. 2 Preproduction Flow Diagram

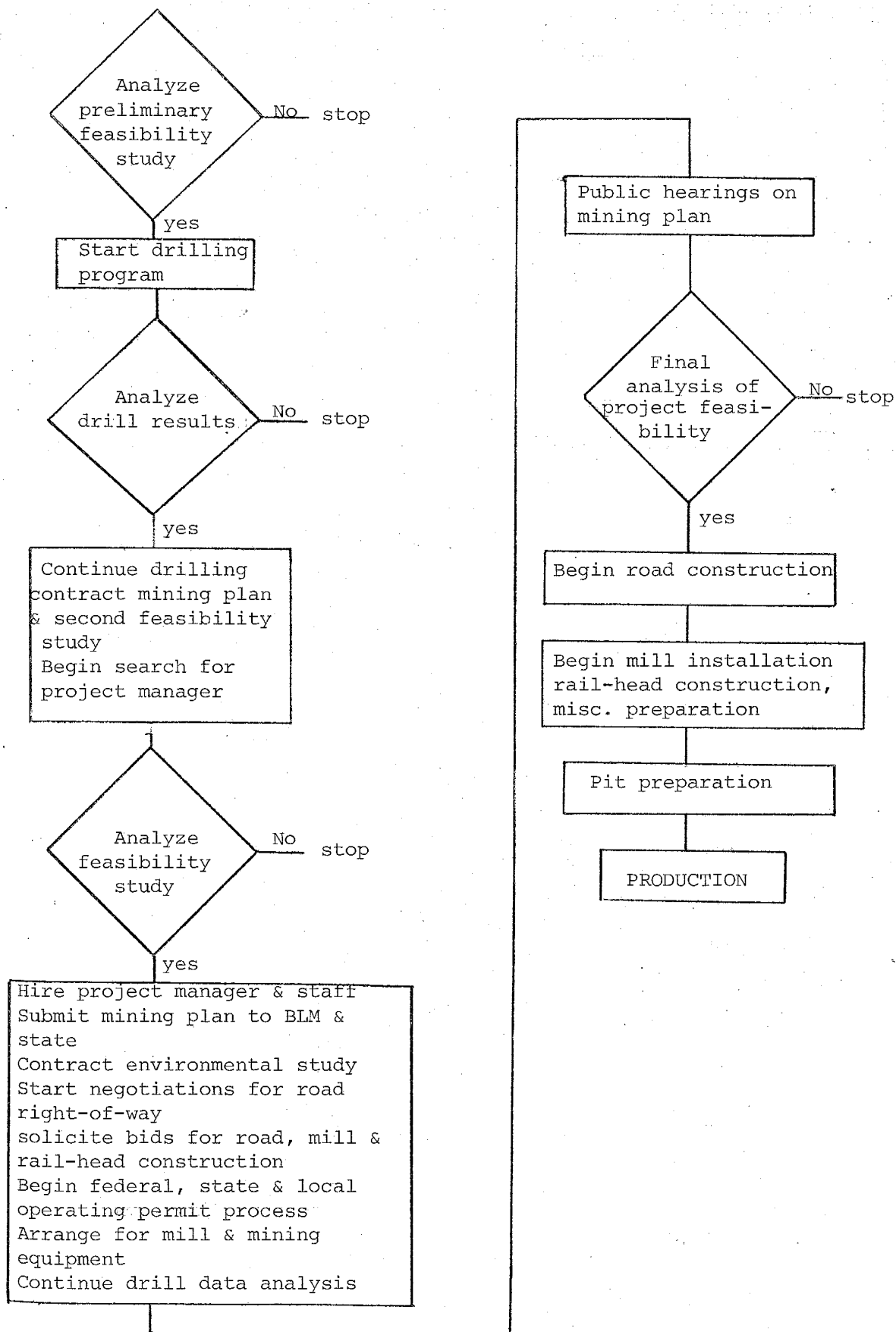


Fig. 3 Preproduction Time Schedule

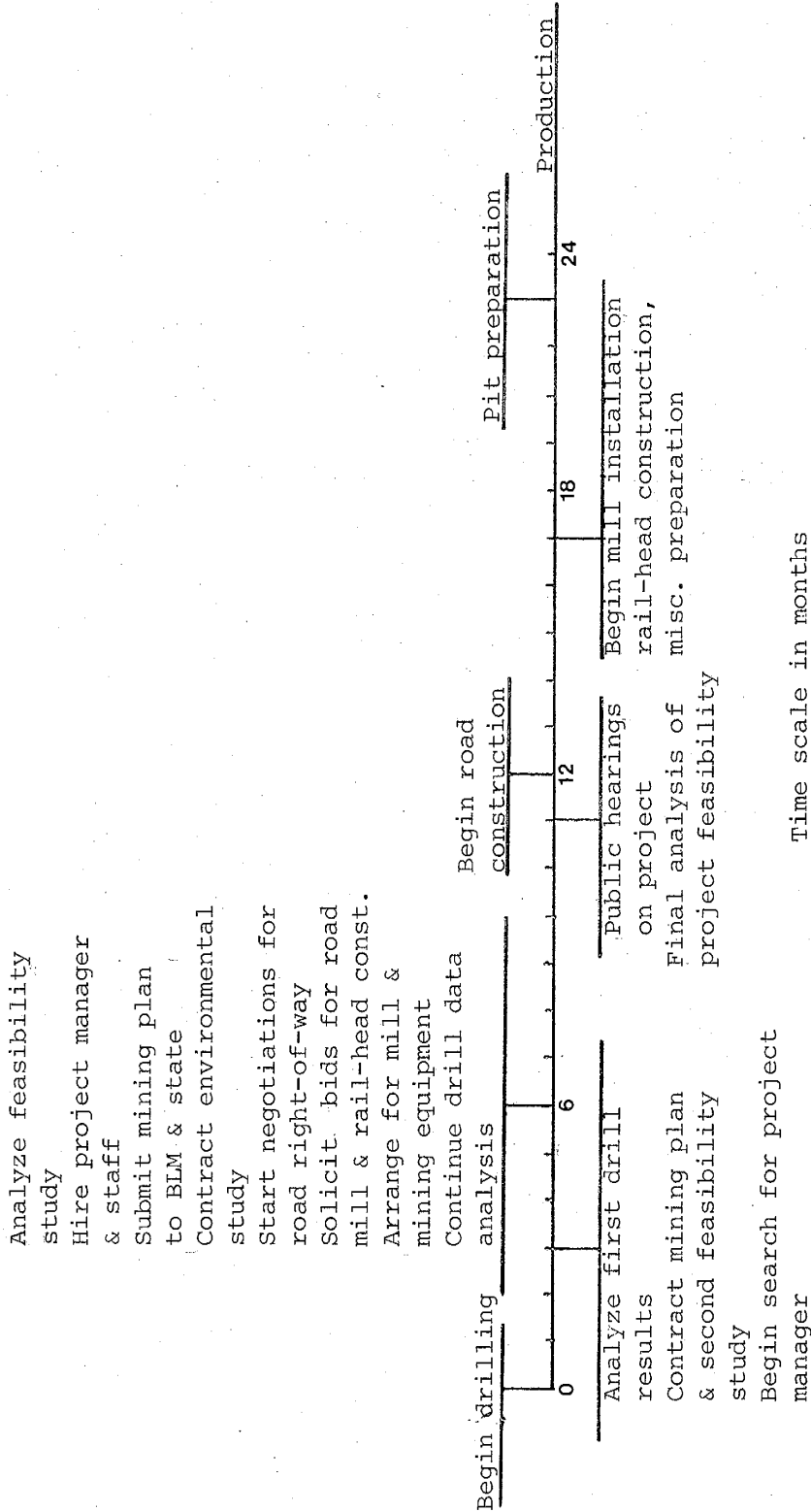


Table 4, Detailed Preproduction Cost Breakdown

Item	Capital Cost	
	1st year (\$)	2nd year (\$)
Studies	50,000*	20,000*
Road right-of-way		25,000*
Road construction		1,200,000*
Mill & rail site construction		40,000*
Office purchase	20,000*	
Mill & equipment payments		60,000*
Contingency	10,000	145,000
Total	80,000	1,490,000 =
		1,570,000

Item	Deductable Development costs	
	1st year (\$)	2nd year (\$)
Geologist	5000	20,000
Office & staff	120,000*	240,000*
Drilling	125,000	125,000
Mill & railsite construction		100,000*
Pit development		100,000*
Contingency	40,000	55,000
Total	290,000	640,000 =
		930,000

Total Preproduction Cost 2,500,000

* order of magnitude estimate

- B) Mining equipment @ \$10.28/ton
 - 1) 3 D-8 cats @ \$48.69/hr = \$3.36/ton
 - 2) 2 988B wheel loaders @ \$54.36/hr = \$2.50/ton
 - 3) 4 769C cat. oretrucks @ \$44.46/hr = \$4.09/ton
 - 4) 1 air track devel. drill (4 hrs. per day)
@ \$35.82/hr. = \$0.33/ton

\$10.28/ton

- C) Miscellaneous equipment @ \$.63/ton
 - 1) F-250 service vehicle
 - 2) F-250 4x4 utility truck
 - 3) Ford Bronco
 - 4) Backhoe
 - 5) Water truck
 - 6) Misc. mine & safety equipment
 - 7) Two-way radios

- D) Trucking from mill to rail-head
 - 1) contract for 8, 20 ton trucks
 - a) \$1.40/loaded mile and \$0.50/unloaded mile = \$5.25/ton

- E) Milling & pelletizing
 - 1) estimated @ \$4/ton
 - a) includes supplies & operating costs

- F) Reclamation
 - 1) estimated @ \$.50/ton

- G) Development work
 - 1) includes: drilling, removal of top soil, surveying, etc.
 - a) estimated @ \$1.50/ton

- H) Royalties
 - 1) set @ \$10/ton by promoter

- I) Administrative
 - 1) includes: office staff & rent, utilities, phone, office supplies, licenses & fees, insurance, etc.
 - a) estimated @ \$2.00/ton

- J) Mining, milling & pelletizing equipment
 - 1) bought on time @ monthly payments
estimated @ \$49,410 for 5 years or \$24,705 for 10 years

- K) Mine supplies & contingency
 - 1) estimated @ \$3.50/ton

- L) Taxes
 - 1) New Mexico State severance tax
 - a) calculated to be \$0.7159/ton
 - 1) based on \$62/ton for pelletized ore and \$22/ton for raw ore
 - 2) Property tax
 - a) calculated to be \$0.56/ton
 - 1) based on \$26.861/\$1000 assessed value
- M) Loan
 - 1) \$1.5 million
 - a) amortized over 60 months
 - b) 18% interest rate (prime + 2.5 pts.)
 - c) monthly payments of \$38,090.14

Depreciable Basis Calculation

Preproduction	\$ 1,510,000
Mining equipment	1,630,000
Mill & pelletizer	812,500
Misc. equipment	150,000
contingency @ 10%	410,250
Depreciable basis	\$4,512,750

Salvage value @ 10% = \$451,275

APPENDIX III

Thin Section Descriptions

Table of Contents	Page
Sedimentary rocks	219 - 222
Igneous rocks	222 - 226

Sample: L-0

Location: Torres member (upper contact) of the Yeso Formation

Porosity: 0%

Allochemical material:

- 1) unidentified fossil material (3%); medium-grained, well-sorted, subrounded

Interstitial material:

- 1) pseudospar (96%); intergranular material

Diagenetic changes:

- 1) neomorphism (aggrading)
- 2) precipitation of spar in fossil fragments

Mineralization: Magnetite replacing carbonate. At the sediment or contact there is an interfacial zone of magnetite and carbonate. Along the outer fringe of this zone there are a number of medium-grained rhombs which resemble dolomite crystals.

Rock name: gray mineralized fossiliferous sparite

Sample: L-4A

Location: Torres member (upper contact) of the Yeso Formation

Porosity: 10%

Allochemical material:

- 1) Unidentified fossil fragments (1%); medium-grained, well-sorted, subrounded

Interstitial material:

- 1) pseudospar (59%); intergranular
- 2) microspar (40%); intergranular

Diagenetic changes:

- 1) Neomorphism (aggrading)

Mineralization:

- 1) very fine grained-anhedral magnetite crystals (1%) scattered through specimen

Rock name: gray, mineralized fossiliferous sparite

Sample: L-8

Location: Joyita member of the Yeso Formation

Porosity: 19%*

Allochemical materials: 0%

Interstitial material:

- 1) pseudospar (50%)
- 2) microspar (30%)
- 3) authigenic feld. (<1%)

Diagenetic changes:

- 1) precipitation of spar in pore spaces
- 2) precipitation of feldspar in pore spaces
- 3) neomorphism (aggrading)

Rock name: gray, sparite

*Gypsum present in the hand specimen was plucked during thin section preparation. A visual estimate of the samples porosity is 10-15%.

Sample: L-11

Location: Torres member of the Yeso Formation

Porosity: 14.5%

Allochemical material:

- 1) unidentified fossil fragments (11.5%); medium-grained well-sorted, subrounded

Interstitial material

- 1) microspar (83%); intergranular
- 2) pseudospar (1%); poikilotopic crystals
- 3) authigenic feldspar (<1%); intergranular

Diagenetic changes:

- 1) precipitation of spar in pore spaces
- 2) precipitation of feldspar in pore spaces
- 3) neomorphism (aggrading)

Rock name: gray biosparite

Sample: S-7

Location: Torres member of the Yeso Formation

Porosity: 10%

Granular material:

- 1) quartz (59%); fine-grained, moderately sorted, subrounded
- 2) feldspar (17%); very fine-grained, moderately-sorted, rounded

Grain contacts: line

Cement: silica

Mineralization:

- 1) actinolite-tremolite (13%); fine-grained, anhedral crystals replacing both quartz and feldspar
- 2) hematite and magnetite (1%); microcrystalline material rimming feldspar.

Rock name: buff, fine-grained siliceous subarkose

Sample: S-12a

Location: Torres member of the Yeso Formation

Porosity: 6%

Granular material:

- 1) quartz (34%); very fine-grained, moderately-sorted, subrounded
- 2) feldspar (16%); very fine-grained moderately-sorted, subrounded

Grain contacts: point

Mineralization:

- 1) epidote (23%); very fine-grained, anhedral crystals
- 2) magnetite (21%); microcrystalline material, replacing epidote and detrital constituents.

Rock name: buff, very fine-grained, mineralized subarkose

Sample: S-12b

Location: Torres member of the Yeso Formation

Porosity: 0%

Granular material:

- 1) quartz (26%); very fine-grained poorly-sorted, subrounded
- 2) feldspar (9%); very fine-grained, poorly-sorted, subrounded

Cement: magnetite

Mineralization:

- 1) Magnetite and hematite (59%); microcrystalline material replacing both feldspar and quartz
- 2) epidote (6%); very fine-grained subhedral crystals replacing feldspar and quartz

Rock name: buff, very fine-grained mineralized subarkose

Sample: Db-2a

Essential minerals:

- 1) plagioclase (andesine), 56%; fine-grained, euhedral laths
- 2) alkali feldspar, 3%

Varietal minerals:

- 1) pyroxene (1%); fine-grained, anhedral crystals
- 2) biotite (<1%); fine-grained, subhedral crystals

Accessory minerals:

- 1) magnetite (<1%); fine-grained subhedral crystals
- 2) apatite (<1%); fine-grained prismatic crystals

Secondary minerals:

- 1) actinolite-tremolite (23%); fine-grained fibrous masses
- 2) magnetite (15%); fine-grained rods and anhedral blebs
- 3) sericite (1%)
- 4) biotite (<1%)
- 5) carbonate (<<1%)
- 6) kaolinite (<<1%)

Textures: plagioclase laths rimmed by alkali feldspar surround ferro-magnesian minerals forming an ophitic texture

Alteration: Feldspars have altered to sericite and kaolinite. Pyroxenes have been replaced by actinolite-tremolite. Some of the pyroxene has also probably altered to magnetite and carbonate

Mineralization: Magnetite replaces both feldspars and ferromagnesian minerals

Rock name: Green holocrystalline, hypidiomorphic fine-grained pyroxene syenodiorite

Sample: Db-5b

Essential minerals:

- 1) plagioclase (oligoclase?), 43%; fine-grained subhedral crystals
- 2) alkali feldspar (30%); fine-grained anhedral crystals

Varietal minerals:

- 1) pyroxene (2%); fine-grained subhedral crystals
- 2) biotite (7%); fine-grained subhedral crystals

Accessory minerals:

- 1) magnetite (<1%); fine-grained, subhedral
- 2) apatite (<1%); fine-grained, euhedral prismatic crystals

Secondary minerals:

- 1) magnetite (5%); fine-grained rods and blebs
- 2) Sericite (5%)
- 3) uralite (4%); fine-grained masses of prismatic crystals
- 4) carbonate (3%); fine-grained, anhedral crystals
- 5) chlorite (<<1%)
- 6) muscovite (<<1%)
- 7) kaolinite (<<1%)

Textures: equant plagioclase and alkali-feldspar crystals are intergrown with and surround ferromagnesian minerals in a subophitic texture

Alteration: Sericite and kaolinite are present in feldspars, pyroxenes are replaced by uralite, and some have altered to magnetite and carbonate. Biotite is rimmed by chlorite.

Mineralization: Magnetite rods and blebs replace feldspars and ferromagnesian minerals

Rock name: green, holocrystalline, hypidiomorphic granular, medium-grained, pyroxene syenodiorite

Sample: Db-6

Essential minerals:

- 1) plagioclase (oligoclase) (63%); normally zoned, medium-grained phenocrysts and fine-grained laths
- 2) alkali-feldspar (7%); rims around plagioclase laths and fine-grained anhedral crystals

Varietal minerals:

- 1) hornblende (20%); fine-grained, subhedral crystals

Accessory minerals:

- 1) apatite (1%); fine-grained prismatic euhedral rods

Secondary minerals:

- 1) sericite (4%)
- 2) magnetite (4%); fine-grained rods and blebs
- 3) kaolinite (<<1%)

Textures: plagioclase phenocrysts are in a ground mass of intergrown plagioclase laths and alkali-feldspar crystals surrounding ferromagnesian minerals

Alteration: Sericite and kaolinite are concentrated in the calcic portion of plagioclase crystals

Mineralization: magnetite rods and blebs replace feldspars and hornblende

Rock name: gray, holobrystalline, hypidiomorphic porphyritic phaneritic, fine-grained, hornblende, syenodiorite

Sample: Db-9a

Essential minerals:

- 1) plagioclase (andesine?) (32%); normally zoned medium-grained phenocrysts and fine-grained laths
- 2) alkali-feldspar (21%); fine-grained anhedral crystals and rims around plagioclase laths
- 3) quartz (1%); fine-grained anhedral crystals

Varietal minerals:

- 1) biotite (<1%); fine-grained subhedral crystals

Accessory mineral:

- 1) apatite (<<1%); fine-grained prismatic euhedral crystals

Secondary minerals:

- 1) actinolite-tremolite (20%); fine-grained masses of prismatic crystals
- 2) sericite (9%)
- 3) magnetite (9%); fine-grained rods and blebs
- 4) carbonate (7%); veinlets (.05mm) and fine-grained anhedral crystals

Textures: plagioclase phenocrysts in a ground mass of plagioclase laths rimmed by alkali-feldspar intergrown with, and surrounding quartz, alkali-feldspar, and ferromagnesian crystals

Alteration: Sericite is present in cores of plagioclase laths. Pyroxenes have altered to magnetite and carbonate. Actinolite and tremolite also replace pyroxenes

Mineralization: Carbonate forms veinlets cutting sample, and magnetite rods and blebs cross cut carbonate veinlets and replace silicates

Rock name: green, holocrystalline, hypidiomorphic, porphyritic phaneritic, fine-grained, quartz-bearing pyroxene syenodiorite

Sample: Db-9b

Essential minerals:

- 1) plagioclase (oligoclase?) (40%); fine-grained laths
- 2) alkali-feldspar (22%); fine-grained anhedral grains and rims around plagioclase laths
- 3) quartz (<1%); fine-grained, anhedral crystals

Varietal minerals:

- 1) pyroxene (<<1%); medium-grained, subhedral phenocrysts and fine-grained anhedral crystals

Accessory minerals:

- 1) apatite (<<1%); fine-grained, prismatic, euhedral crystals

Secondary minerals:

- 1) actinolite-tremolite (16%); fine-grained fibrous masses

- 2) sericite (15%)
- 3) magnetite (4%); fine-grained rods, blebs and subhedral crystals
- 4) carbonate (3%); forms veinlets (.05 mm) cutting sample

Textures: pyroxene phenocrysts are in a groundmass of plagioclase laths rimmed by alkali-feldspar, which is intergrown with and surrounding pyroxene, alkali-feldspar and quartz

Alteration: Sericite and kaolinite are present in feldspars.
Actinolite-tremolite have replaced pyroxenes

Mineralization: Magnetite rods and blebs replace silicates, and carbonate veinlets cut the sample

Rock name: gray holocrystalline, inequigranular, porphyritic phaneritic, fine-grained, quartz-bearing pyroxene syenodiorite

Sample: Db-11

Essential minerals:

- 1) plagioclase (oligoclase?) (33%); fine-grained laths and microlites
- 2) alkali-feldspar (25%); rims around plagioclase crystals

Varietal minerals:

- 1) pyroxene (<1%); fine-grained anhedral crystals

Accessory minerals:

- 1) apatite (2%); fine-grained prismatic euhedral crystals

Secondary minerals:

- 1) uralite (31%); fine-grained prismatic masses
- 2) magnetite (7%); fine-grained rods and blebs
- 3) sericite (1%)
- 4) carbonate (<1%), veinlets (.02 mm)

Textures: plagioclase laths in a groundmass of intergrown, plagioclase, microlites, alkali-feldspar, and pyroxenes

Alteration: Sericite is present in feldspars, and uralite has replaced pyroxenes

Mineralization: Magnetite replaces feldspars and silicates, and carbonate veinlets cut sample

Rock name: dark gray, holocrystalline, inequigranular, fine-grained, pyroxene syenodiorite

This dissertation is accepted on behalf of the faculty of the
Institute by the following committee:

Clay T. Smith

Adviser

George J. Carter

Allen P. Seaford

5/23/80

Date